Contribution à la modélisation mathématique et numérique pour des modèles d'écoulement non-linéaires dispersifs en eaux peu profondes

Debyaoui Mohamed Ali

UNIVERSITÉ DE TOULON

جامعة صفاقس
Université de Sfax

École doctorale 548 - Mer et Sciences
École doctorale des sciences fondamentales de FSS-Sfax

THÈSE présentée par :

Mohamed Ali DEBYAOUI

Pour obtenir le grade de

DOCTEUR DES UNIVERSITÉS DE TOULON ET DE SFAX

Spécialité : MATHÉMATIQUES

Contribution à la modélisation mathématique et numérique pour des modèles d'écoulement non-linéaires dispersifs en eaux peu profondes

Préparée dans le cadre d'une cotutelle entre

L'UNIVERSITÉ DE TOULON ET L'UNIVERSITÉ DE SFAX -TUNISIE

Soutenue le **11 décembre 2020** devant le jury composé de :

M. CHAABANE Slim	Professeur, Université de Sfax	Examinateur
M. DAMAK Mondher	Professeur, Université de Sfax	Directeur de thèse
M. ERSOY Mehmet	Maître de conférences, Université de Toulon	Co-encadrant de thèse
M. GALUSINSKI Cédric	Professeur, Université de Toulon	Directeur de thèse
M. GERBI Stéphane	Maître de conférences, Université Savoie Mont Blanc	Président
M. LANNES David	Professeur, Université de Bordeaux	Rapporteur
Mme LUCAS Carine	Maître de conférences, Université d'Orléans	Examinateur
M. MARCHE Fabien	Maître de conférences, Université de Montpellier	Rapporteur

À la mémoire de mon père et mon grand frère : Mouldi et Ilyes.
À ma famille : Khira, Hanen, Ikbel, Fedya et Maher.

Remerciements

Tout d'abord, je voudrais remercier mes directeurs de thèse Mehmet Ersoy, Cédric Galusinski et Mondher Damak, sans leur aide, aucune de ces lignes n'aurait pu être écrite.

Mehmet et Cédric ont été non seulement mes directeurs de thèse mais aussi ma deuxième famille en France, ils m'ont rassuré dans les périodes de doute et m'ont aidé de bien des façons à résister et à poursuivre mon chemin, qui n'était pas du tout facile. Ils ont été mes enseignants de Master 2. Pendant ces cinq années, ils m'ont enseigné non seulement les mathématiques, mais aussi comment être un mathématicien. Ils ont toujours répondu patiemment à mes questions naïves et m'ont guidé pas à pas dans mes recherches.

Mondher m'a donné l'opportunité de venir poursuivre mes études en France, je lui en serais reconnaissant. J'ai la chance d'être encadré par eux, je voudrais leur faire part de ma profonde gratitude.

Je tiens à exprimer ma gratitude à David Lannes et Fabien Marche qui ont rapporté cette thèse. Leurs commentaires enthousiastes et leurs critiques constructives de ce manuscrit ont été très encourageants.

Je tiens également à remercier Stéphane Gerbi, Slim Chaabane et Carine Lucas qui m'ont fait l'honneur de faire partie de mon jury.

Je tiens à remercier tous les professeurs de Toulon qui m'ont appris ce que je sais. Merci à Guy Bouchitté qui a encadré mon TER en M2.

Ma gratitude va également à tous mes collègues de l'IMATH, en particulier à Gloria Faccanoni, qui a participé à mon comité de suivi de thèse pendant deux ans et m'a donné des conseils constructifs, à Catherine Le Poupon avec qui j'ai enseigné la mécanique statique pendant trois ans, à Christelle Boyer qui a soutenu mes voyages aux conférences universitaires et à Soufiane qui m'a aidé de temps en temps à résoudre des problèmes informatiques. Et merci à mes amis de IMATH, en particulier Ahmed, David, Houssam, Hadjer, Yssouf, Soufiane, Jean-Baptiste, Mohamed et Abdallah.

Merci à ma famille qui a sacrifié tant de choses si précieuses pour que cette journée soit merveilleuse.

Enfin, je tiens à remercier les professeurs Kheireddine Benhissi, Mouldi Daoudi, Mme Safia Khalfi, qui ont toujours été présents et au premier rang pour m'aider, je leur en serais reconnaissant.

Merci ma mère, pour avoir toujours été là pour moi !

"Un jour, ta douleur sera ta force.
Alors fais-y face. Tu y arriveras !"

Roger Garaudy

Contribution à la modélisation mathématique et numérique pour des modèles d'écoulement non-linéaires dispersifs en eaux peu profondes

Résumé

Cette thèse porte sur la modélisation et l'analyse mathématique de modèles asymptotiques utilisés en océanographie et décrivant la propagation des ondes longues. L'objectif de cette thèse est de construire et de justifier de nouveaux modèles asymptotiques en tenant compte de la variation de la topographie et de la section transversale. Pour ce faire, plusieurs hypothèses sont formulées sur la profondeur de l'eau et les déformations de la section transversale. La première partie de cette thèse consiste à dériver et à étudier les caractéristiques linéaires de dispersion et de shoaling des modèles asymptotiques. Dans la deuxième partie, un modèle unidimensionnel des ondes longues moyenné par section, est développé. Des équations tridimensionnelles du mouvement des fluides non visqueux et incompressibles sont d'abord intégrées sur une section transversale du canal, ce qui donne les équations de type SGN. Le nouveau modèle est donc adéquat pour décrire des ondes fortement non linéaires et faiblement dispersives le long d'un canal de section transversale arbitraire et non uniforme. Plus précisément, le nouveau modèle étend le modèle de Saint-Venant moyenné par section et généralise les équations de Serre-Green-Naghdi à toute section. Ce nouveau modèle a été reformulé d'une manière plus appropriée pour la résolution numérique en conservant le même ordre de précision que l'original et en améliorant ses propriétés de dispersion. Enfin, nous présentons quelques simulations numériques pour étudier l'influence du changement de section sur la propagation d'une onde solitaire. La dernière partie de cette thèse est consacrée à la simulation numérique du modèle SGN avec une nouvelle reformulation.

Mots clés : Équations aux dérivées partielles, Modélisation mathématique des écoulements à surface libre, Écoulement en canal ouvert, Fluide incompressible, Analyse asymptotique, Lagrangien, Dispersif, Non-Linéaire, Volumes Finis, Saint-Venant, Boussinesq, Serre-Green-Naghdi.

Contribution to mathematical and numerical modeling for non-linear dispersive shallow water flow models

Abstract

This work focuses on the modeling and mathematical analysis of asymptotic models used in oceanography describing long wave propagation. This thesis aims to derive and justify new asymptotic models taking into account the variation in topography and cross-section. To do so, several hypotheses are formulated on water depth and cross-sectional deformations. The first part of this thesis consists in deriving and studying the linear dispersion and shoaling characteristics of the asymptotic models. In the second part, a one-dimensional model of section-averaged long waves is developed. Three-dimensional equations of motion of non-viscous and incompressible fluids are first integrated over a cross-section of the channel, resulting in the SGN-type equations. Therefore, the new model is adequate to describe fully non-linear and weakly dispersive waves along a channel of an arbitrary and non-uniform cross-section. Specifically, the new model extends the Saint-Venant model to cross-section mean and generalizes the Serre-Green-Naghdi equations to any cross-section. This new model has been reformulated in a way more appropriate for numerical resolution by maintaining the same order of accuracy as the original and improving its properties of dispersion. Finally, we present some numerical simulations to study the influence of the change of section on the propagation of a solitary wave. The last part of this thesis is devoted to the numerical simulation of the SGN model with a new reformulation.

Keywords: Partial differential equations, Mathematical modeling of free surface flows, Open channel flow, Incompressible Fluid, Asymptotic Analysis, Lagrangian, Dispersive, Non-Linear, Finit Volumes, Saint-Venant, Boussinesq, Serre-Green-Naghdi.

Contents

Notations

Notations concerning the physical settings

- $\sigma(x,z) = \beta(x,z) - \alpha(x,z)$: width of the section at z with $\beta(x,z)$ (resp. $\alpha(x,z)$) is the right (resp. left) boundary point at elevation z
- $d(x,y)$: definition of the boundary of the channel/river cross-section as a function of y
- $d^*(x) = d(x,y^*(x)) = \min_y d(x,y)$: z-coordinate of the deepest point of the cross-section
- $\varphi(x,z) = \begin{cases} \alpha(x,z) \text{ if } & \varphi(x,z) < y^*(x) \\ \beta(x,z) \text{ otherwise.} \end{cases}$: definition of the boundary of the channel/river cross-section as a function of z
- $\Omega(t,x)$: fluid cross-section
- $\eta(t,x,y)$: z-coordinate of the free surface level
- $h(t,x,y) = \eta(t,x,y) - d(x,y)$: local height of water in $\Omega(t,x)$
- $A(t,x) = |\Omega(t,x)|$: wet area
- $\boldsymbol{n}_{\text{fs}}$: outward normal vector to the free surface boundary Γ_{fs} of $\Omega(t,x)$
- $\boldsymbol{n}_{\text{wb}}$: outward normal vector to the wet boundary Γ_{wb} of $\Omega(t,x)$

Notations concerning the asymptotic parameters

- H_2: characteristic water depth
- H_1: characteristic scale of the channel width
- h_1 : characteristic wave-length in the transversal direction.
- L: characteristic wave-length in the longitudinal direction
- $\mu_1 = \dfrac{h_1^2}{L^2}$: dispersive parameter in the transversal direction
- $\mu_2 = \dfrac{H_2^2}{L^2}$: usual dispersive parameter

Notations concerning the model

- $\Omega_{\text{eq}}(t,x)$: fluid cross-section (flat free surface approximation of $\Omega(t,x)$)
- $\eta_{\text{eq}}(t,x)$: z-coordinate of the free surface level
- h_{eq} : local height of water in $\Omega_{\text{eq}}(t,x)$
- A_{eq} : wet area of $\Omega_{\text{eq}}(t,x)$
- Q_{eq} : discharge
- P_{h} : hydrostatic pressure
- P_{nh}: non hydrostatic pressure

Other notations

- $\langle X \rangle(t,x,z)$: width-average of the function $(t,x,y,z) \mapsto X(t,x,y,z)$
- $\overline{u}(t,x)$: $\Omega(t,x)$-averaged velocity
- $\bar{u}_{\text{eq}}(t,x)$: $\Omega_{\text{eq}}(t,x)$-averaged velocity
- $X_q(t,x,z) := X\left(t,x,q(x,z),z\right)$ where $q=\alpha$ or $q=\beta$
- $f_b(t,x) = f_\alpha(t,x,d^*(x))$
- $S(x,z) = \displaystyle\int_{d^*(x)}^{z} \sigma(x,s)\, ds$
- $\mathcal{S}(u,x,z) = \dfrac{1}{\sigma(x,z)} \dfrac{\partial}{\partial x}\left(uS(x,z)\right)$
- $\nabla_{k_1,k_2}(X)$: gradient of a function X with respect to the variable k_1 and k_2
- $\text{div}_{k_1,k_2}[\boldsymbol{X}]$: divergence of a vector function $\boldsymbol{X}$ with respect to the variable k_1 and k_2

Bold characters are used for vectors notations.
For almost all computations, we assume that x and t are fixed.

Numerical analysis notation

- $x_{1/2}$: upstream node of mesh (upstream interface)
- $x_{N/2}$: downstream node of mesh (downstream interface)
- $x_{i+\frac{1}{2}}$: internal mesh node
- $m_i = \left(x_{i-\frac{1}{2}}, x_{i+\frac{1}{2}}\right)$: mesh

- $x_i = \dfrac{x_{i-\frac{1}{2}} + x_{i+\frac{1}{2}}}{2}$: centre of mesh
- $(\Delta x)_i$: variable mesh-step
- Δx : constant mesh-step
- Δt^n : time step

Définition 0.0.1.
The phase velocity is the speed of propagation of a particle on the free surface:

$$C_p = \frac{\omega}{k}. \tag{1}$$

ω is the frequency of the wave and k is the wave number of the wave.

Définition 0.0.2.
The group speed is the speed of propagation of a wave packet:

$$C_g = \frac{d\omega}{dk}. \tag{2}$$

List of Figures

Part I

Introduction

Chapter 1

Introduction

1.1 Contexte et motivation

La modélisation des écoulements en eau peu profonde est d'une importance majeure dans l'étude de la dynamique des fluides et plus particulièrement en océanographie; étude des mers, océans, leurs limites et leurs interactions avec l'air, la topographie y compris les organismes vivants. Plus particulièrement, la modélisation de l'hydrologie des bassins versants et des rivières occupe une place centrale dans les sciences de l'environnement, notamment en ce qui concerne la disponibilité de l'eau, les réseaux d'égouts urbains, les risques d'inondation et en particulier pour les tsunamis. Les vagues pénètrent dans les rivières beaucoup plus rapidement à l'intérieur des terres que l'inondation côtière ne le fait sur le sol, et peuvent provoquer des inondations dans les zones de basse altitude situées à plusieurs kilomètres des côtes [90]. La modélisation de ces processus et la prévision du mouvement de l'eau est une tâche difficile à laquelle des efforts considérables ont été consacrés [49, 94].

L'un des modèles les plus utilisés pour décrire le mouvement des cours d'eau est le modèle à surface libre moyenné par section [34, 15, 39] qui est une généralisation du système bien connu *Saint-Venant* (introduit par Adhémar Jean Claude Barré de Saint-Venant au 19ème siècle [31, 46]) :

$$\begin{cases} \dfrac{\partial}{\partial t}A + \dfrac{\partial}{\partial x}Q & = & 0\,, \\ \dfrac{\partial}{\partial t}Q + \dfrac{\partial}{\partial x}\left(\dfrac{Q^2}{A} + I_1(x,A)\right) & = & I_2(x,A)\,. \end{cases} \tag{1.1}$$

Dans ces équations, A est l'aire mouillée, Q est le débit d'eau, I_1 est la pression hydrostatique et I_2 est le terme source de la pression hydrostatique qui tient compte de la variation de la section. Le modèle (1.1) est l'approximation du premier ordre en eau peu profonde des équations de Navier-Stokes ou d'Euler moyennées par section, sous des hypothèses appropriées sur les échelles horizontale et verticale (voir, par exemple, [48, 34]).

Grâce à la structure hyperbolique de ces équations, les transitions brusques entre deux états d'écoulement différents donnent lieu à une solution discontinue, tant au niveau de la surface de l'eau que de la vitesse. Ces solutions discontinues appelées chocs sont bien adaptées à la rupture brusque des vagues avec des rouleaux turbulents pour les grandes transitions du nombre de Froude. Cependant, pour des transitions faibles ou modérées, le front de vague qui avance peut être suivi d'un train d'ondulations à surface libre, parfois appelées "whelps". Ce phénomène, appelé ondes de choc dispersives, est induite par une distribution de pression non hydrostatique [75]. En conséquence, les ondes se répandent dans l'espace au fur et à mesure de leur évolution dans le temps, c'est-à-dire que des ondes de différentes longueurs d'onde se déplacent à des vitesses différentes. C'est ce qu'on appelle l'effet dispersif. Par conséquent, les ressauts undulaires ne sont pas reproductibles avec le système de surface libre non dispersive et une pression non hydrostatique est nécessaire.

Les équations dispersives ont été introduites pour la première fois par Boussinesq [17] en 1872 pour justifier mathématiquement l'existence d'ondes solitaires observées par les expériences de Russell en 1834. Ces équations entrent dans le cadre des équations des eaux peu profondes. Elles peuvent être obtenues par approximation asymptotique du second ordre des équations d'Euler moyennées en profondeur par rapport à un paramètre

μ. Ici, $\mu = \left(\frac{H}{L}\right)^2$ est un paramètre d'aspect-ratio, où H représente une profondeur d'eau caractéristique et L est une échelle horizontale caractéristique. Les équations de type Boussinesq, qui sont faiblement non linéaires et faiblement dispersives, sont définies par un petit paramètre de non-linéarité supplémentaire $\varepsilon = \frac{a}{H} = O(\mu) \ll 1$ où a est l'ordre de l'amplitude de la surface libre. Ces équations pour un fond plat, par exemple en 1D, sont données par

$$\left\{ \begin{array}{lcl} \frac{\partial}{\partial t}\xi + \frac{\partial}{\partial x}(h\overline{u}) & = & O(\mu^2) \\ \frac{\partial}{\partial t}\overline{u} + \varepsilon\overline{u}\frac{\partial}{\partial x}\overline{u} + \nabla\xi + \mu\mathbb{D} & = & O(\mu^2) \end{array} \right. \tag{1.2}$$

où h est la profondeur de l'eau, ξ est l'élévation de la surface libre et $\overline{u}$ est la vitesse moyenne en profondeur. Le terme $\mathbb{D}$ représente le terme dispersif.

En 1877, l'équation de KdV a été découverte par Boussinesq [17] et a ensuite été dérivée par Korteweg et Gustav de Vries (KdV) [55]. Cette équation décrit approximativement l'évolution de longues vagues unidimensionnelles dans de nombreux contextes physiques, y compris des vagues en eau peu profonde au comportement faiblement non linéaire. Cette équation peut également être obtenue dans le cas d'ondes unidirectionnelles pour lesquelles le cadre théorique permet de calculer une solution analytique telle que la propagation d'une onde solitaire 1D sur fond plat (voir par exemple Boussinesq [17, 55, 7]). Nous avons également l'équation de Benjamin, Bona et Mahony (BBM) qui est une amélioration de l'équation KdV [10].

Cependant, dans la pratique et surtout dans les applications du génie côtier, la dynamique des vagues littorales étant souvent variable - dépendante du fond, dispersive et non linéaire, les équations de type Boussinesq ne sont pas appropriées. En 1967, Peregrine [77] a introduit les premières équations de type Boussinesq bidimensionnelles faiblement non linéaires pour les fonds non plats. Witting [93] a proposé une méthode basée sur le développement de Padé pour améliorer les caractériqtiques de dispersion des équations de type Boussinesq. A partir de cette méthode, plusieurs équations d'ordre $O(\mu^2)$ avec une caractéristique de dispersion améliorée ont été proposées, voir par exemple [69, 71]. En 1953, une équation unidimensionnelle, fortement non linéaire ($\varepsilon = O(1)$) et faiblement dispersive pour fond plat a été dérivée par Serre [86], indépendamment de Su et Gardner [89] avec

$$\mathbb{D}(v) = \frac{1}{h}\frac{\partial}{\partial x}\left(\frac{h^3}{3}\mathcal{D}(v)\right) \tag{1.3}$$

où

$$\mathcal{D}(v) = \left(\frac{\partial}{\partial x}v\right)^2 - \frac{\partial}{\partial x}\frac{\partial}{\partial t}v - v\partial_x^2 v \ . \tag{1.4}$$

Ce modèle a ensuite été étendu aux fonds non plats par Seabra-Santos [85], voir aussi [25]. Enfin, Green et Naghdi [50] ont dérivé les équations dispersives bidimensionnelles entièrement non linéaires pour les fonds irréguliers qui sont l'extension des équations de Serre. Dans la littérature, ce système est souvent appelé équations de SGN. D'autres extensions intéressantes sont également présentées dans [91, 60, 61, 80] basées soit sur les équations d'Euler, soit sur les équations d'ondes de surface ou les principes variationnels. Tous les modèles dispersifs précédents sont obtenus par réduction 3D-2D ou

2D-1D, mais, à notre connaissance, la réduction 3D-1D n'a jamais été réalisée auparavant.

Mes travaux de thèse s'inscrivent dans cette optique de modélisation mathématique et numérique des écoulements à surface libre. Ainsi, le principal objectif est de dériver à partir des équations d'Euler tridimensionnelles incompressibles et irrotationnelles avec des conditions aux limites appropriées, des modèles similaire à (1.2)–(1.4) via la moyenne de section sous l'hypothèse d'eau peu profonde qui tient en compte la variation de la topographie et de la géométrie.

1.2 Descriptif des travaux de thèse

L'objectif de cette thèse est de proposer de nouveaux modèles dispersifs en eau peu profonde pour prendre en compte l'influence de la topographie et de la section transversale sur les ondes de surface. La réalisation de cet objectif est divisée en trois étapes:

- Une étape de **modélisation**, où les méthodes de construction des modèles sont présentées en détail.

- Une étape d'**analyse mathématique linéaire** des caractéristiques de la dispersion et de shoaling afin d'optimiser les modèles.

- La dernière étape est la **simulation numérique** où ces modèles sont implémentés et des cas de tests numériques prenants en compte la variation de la section et de la bathymétrie ont été réalisés.

Dans le premier chapitre, nous présentons la dérivation formelle des modèles réduits par approximation en eaux peu profondes. Ces modèles réduits sont généralement obtenus à partir des équations de Navier Stokes, Euler irrotationnel ou les équations d'ondes de surface. Dans ce type d'écoulement, le profil suivant la profondeur est faiblement parabolique et fonction du paramètre $\mu = \frac{H^2}{L^2}$. Cette propriété " écoulement par tranches " ou encore " motion by slices " est celle qui permet de négliger les variations des profils de vitesses verticaux par rapport aux profils des vitesses horizontaux. En outre, cela justifie la réduction du problème à n dimensions à n-1 dimensions et par conséquent l'approximation des équations de la mécanique des fluides initiales par ces équations réduites. Dans le cadre des équations de Navier-Stokes, le fluide est supposé faiblement visqueux et les équations sont munies de conditions aux limites de Navier avec friction (traduisant les effets de rugosité de la topographie) et de non-pénétration (de la topographie), et d'une condition de pression atmosphérique à la surface libre. La propriété " motion by slices " est induite par les forces de friction, voir par exemple [46, 39].

Dans le cadre des équations d'Euler, le fluide est supposé incompressible et irrotationnel. Les équations d'Euler sont munies des conditions aux limites à la surface libre de condition cinématique et d'une condition d'imperméabilité de la topographie.

Comme dans le cadre des équations de Navier-Stokes, par développement asymptotique, le modèle réduit de Saint-Venant est obtenu. Dans cette approche la propriété " motion by slices " est issue de la contrainte d'irrotationnalité. S'affranchir de cette condition ne permettrait donc pas de retrouver cet aspect avec la limite faible profondeur qui permet d'obtenir les équations de Saint-Venant (au moins formellement). Cette propriété est cruciale pour établir les modèles réduits.
Ces modèles asymptotiques peuvent également être dérivés via un principe variationnel tel que la méthode de relaxation [37, 26] ou le Lagrangien augmenté [43]. Les premières formulations variationnelles ont été proposé par Lagrange [56] pour dériver les équations de la dynamique des fluides parfait. Le premier principe pour les écoulements à surface libre a été proposé par Riabuchinsky [79] et le principe variationnel pour un écoulement sur un plan a été proposé bien plus tard par Luke (voir [67]). D'autres variantes ont été proposées ultérieurement, voir, par exemple, [37] pour un Lagrangien "relaxé" et [43] pour un Lagrangien "augmenté". Les termes de relaxation permettent au principe variationnel "relaxé" de se donner de la liberté dans la construction de modèles. Le Lagrangien "augmenté" permet d'étudier des variations du Lagrangien en imposant une condition d'équilibre (sous forme de pénalisation) à la surface libre. Cette approche permet ainsi de construire des variantes de modèles SGN dispersives mais à l'instar de [43], les équations obtenues forment un système hyperbolique à 4 équations. Dans ce chapitre, nous considérons le principe variationnel classique pour dériver certains modèles asymptotiques en eaux peu profondes, à savoir les équations de Saint-Venant non dispersives et les équations dispersives de Boussinesq et de Serre-Green Naghdi.

En faisant intervenir des paramètres supplémentaires tels que la non-linéarités de la houle $\varepsilon = \dfrac{A}{H}$ où A est une amplitude caractéristique des ondes, couplées au paramètre d'aspect-ratio (appelé aussi paramètre de dispersion) $\mu = \dfrac{H^2}{L^2}$, on obtient une classe de modèle non-linéaire ou faiblement non- linéaire avec caractère dispersif ou non dispersif. En particulier, c'est suite à l'étude de l'existence d'ondes solitaires que Boussinesq [17] montra que la dispersion est nécessaire pour contrebalancer la non-linéarité du modèle de Saint-Venant afin de propager un soliton (i.e. une onde solitaire se propageant dans un milieu non-linéaire et dispersif sans se déformer). Il démontra ainsi la nécessité de la présence de termes dispersifs dans les équations pour établir l'existence de ces solitons observables dans de nombreux phénomènes physiques (hydrodynamique, optique, acoustiques, etc). Il dériva ainsi, probablement, le premier modèle faiblement non-linéaire et faiblement dispersif. Le modèle de Saint-Venant décrit ci-dessus est un modèle non-linéaire et non dispersif. L'emploi de multiparamètres asymptotiques est à la base de la dérivation de nombreux modèles de type "couche mince" Korteweg-de Vries [55], Boussinesq [17], Serre[86], Green and Naghdi [50], etc. à partir des équations d'Euler. Notons également que Lannes et Bonneton [60] ont proposé une méthode générale pour dériver les équations réduites (faiblement) non-lineaires et (faiblement) dispersif à partir des équations d'ondes de surface à l'aide de l'opérateur de Dirichlet-Neumann. De nouveau la contrainte d'irrotationnalité est nécessaire comme nous l'avons cité plus haut.

Le deuxième chapitre de cette thèse est consacrée à la reformulation des modèles asymptotiques en introduisant des opérateurs linéaires pour éviter le calcul direct des dérivées partielles d'ordre 3. Le problème reformulé est en général plus adapté pour

construire un schéma numérique robuste de volume fini pour sa résolution. De plus, ce problème reformulé permet de construire un modèle équivalant à (1.6) pour lequel on peut améliorer les caractéristiques linéaires du modèle, en ajoutant quelques termes d'ordre $O(\mu_2^2)$ à l'équation de conservation de la quantité de mouvement sans affecter la précision du modèle. Les propriétés linéaires couramment utilisées sont la vitesse de phase, la vitesse du groupe, le gradient de shoaling et la cinématique des ondes [69, 68]. Les effets non linéaires sont évaluées en analysant le transfert d'énergie entre les composants [71]. Dans [35], Dingemans propose une séquence d'étapes dans laquelle les modèles de type Boussinesq peuvent être analysés et améliorés :

- le comportement linéaire des fréquences
- le comportement linéaire de shoaling

Des améliorations significatives peuvent être obtenues à la fois pour les propriétés linéaires telles que la dispersion de fréquence linéaire, le shoaling linéaire, le profil de vitesse, et pour les propriétés non linéaires tels que la dispersion d'amplitude [21].
Il est observé que pour la fréquence de dispersion des équations de SGN, voir aussi (1.6), convergent vers la théorie de Stokes du premier ordre. Cependant, les caractéristiques de dispersion du système (1.6) peuvent être améliorés (voir par exemple [14, 24]). Elle peut être réalisée en ajoutant des termes d'ordre $O(\mu_2)$ et/ou en paramétrant la vitesse à une certaine profondeur $z = \theta$ au lieu de $z = d$ ([71]), et/ou en considérant une vitesse modifiée (voir [24]). Tous ces modèles introduisent des paramètres pour lesquels plus la valeur de n est élevée, plus les améliorations des propriétés dispersives sont importantes. Par exemple, en suivant la méthode BBM [12], nous pouvons ajouter des termes artificiels dans l'équation du moment pour améliorer le comportement linéaire dans les équations

$$\begin{cases} \partial_t \eta + \boldsymbol{\nabla} \cdot [(\eta + d)\bar{\boldsymbol{u}}] = 0 \\ \partial_t \bar{\boldsymbol{u}} + \boldsymbol{\nabla}[\frac{1}{2}\bar{\boldsymbol{u}}^2 + g\eta] + \mathcal{D}(\boldsymbol{u}, \eta, \alpha) = 0 \end{cases} \tag{1.5}$$

où α est un coefficient libre, pour améliorer les propriétés dispersives linéaires. Ce modèle a été développé dans [71, 69, 68, 70] (voir [45] pour une analyse de la légère différence entre ces méthodes).

Le troisième chapitre propose un nouveau modèle dispersif en eau peu profonde prenant en compte l'influence de la topographie et de la section transversale sur les ondes de surface. Il s'agit d'une extension du modèle du type Serre-Green-Naghdi au cas d'une section variable.
Nous présentons ici, brièvement, la stratégie permettant de dériver le modèle dispersif non linéaire moyenné sur la section. Nous introduisons d'abord le problème sans dimension en introduisant le paramètre dispersif classique μ_2. Nous introduisons également un paramètre dispersif μ_1 mais dans le sens transversal. Dans ce travail, nous supposons que $\mu_1 < \mu_2$ pour obtenir le modèle dispersif moyenné par section par rapport à μ_2 comme on le fait habituellement. En raison de la structure des équations, nous ne pouvons pas obtenir le modèle par une moyennisation sur section directe. Nous devons d'abord développer des développements asymptotiques appropriés en deux étapes, brièvement résumées ci-dessous :

- Première étape : les équations d'Euler sont moyennées en largeur pour obtenir le développement asymptotique suivante de la vitesse horizontale du fluide

$$u(t,x,y,z) = \langle u\rangle(t,x,z) + O(\mu_1)$$

où $\langle u\rangle$ est la vitesse moyenne en largeur.

- Deuxième étape : les équations d'Euler moyennées en largeur permettant d'obtenir le développement asymptotique de la vitesse horizontale moyenne en largeur du fluide

$$\langle u\rangle(t,x,z) = \overline{u}(t,x) + \mu_2 f(\overline{u}(t,x),\Omega(t,x)) + O(\mu_2^2)$$

où $\bar{u}$ est la vitesse moyenne de la section pour une fonction f donnée.

Ainsi, le développement asymptotique de u jusqu'à l'ordre $O(\mu_2^2)$, le "*motion by slices*" (voir [46]), peut s'écrire comme suit :

$$u(t,x,y,z) = \overline{u}(t,x) + \mu_2 f(\overline{u}(t,x),\Omega(t,x)) + O(\mu_2^2)\ .$$

Enfin, en utilisant ces développements asymptotiques, nous sommes capables de faire la moyennisation sur section des équations d'Euler pour obtenir les nouvelles équations dispersives non linéaires unidimensionnelles

$$\begin{cases} \dfrac{\partial}{\partial t}A + \dfrac{\partial}{\partial x}Q = 0 \\ \dfrac{\partial}{\partial t}Q + \dfrac{\partial}{\partial x}\left(\dfrac{Q^2}{A} + I_1(x,A)\right) + \mu_2\dfrac{\partial}{\partial x}(G(x,A)\mathcal{D}(u)) = I_2(x,A) + \mathcal{G}(x,A,Q) \\ +O(\mu_2^2) \end{cases} \tag{1.6}$$

où A est l'aire mouillée, $Q = Au$ est le débit d'eau, u est la vitesse moyenne de section, I_1 (resp. I_2) est la pression hydrostatique (resp. source), $G(x,A)$ généralise $\dfrac{h^3}{3}$ dans (4.3), le terme $\mathcal{G}(x,A,Q)$ étend le terme source de fond irrégulier, $\mathcal{D}$ est le terme donné par (1.4).

La deuxième partie de ce chapitre est consacrée à la reformulation du problème (1.6) en introduisant un opérateur linéaire et un opérateur quadratique afin d'améliorer le modèle. Comme mentionné précédemment, différentes méthodes existent dans la littérature pour étudier les caractéristiques linéaires des modèles dispersifs. Comme la méthode BBM a montré de très bonnes corrections au niveau de la dispersion et le shoaling, nous la considérons dans ce chapitre. Elle est basée sur l'observation que:

$$\partial_t Q = -\frac{\partial}{\partial x}\left(\frac{Q^2}{A} + I_1(x,A)\right) - I_2(x,A) + O(\mu_2) \tag{1.7}$$

$$= \kappa\partial_t Q - (1-\kappa)\left[\frac{\partial}{\partial x}\left(\frac{Q^2}{A} + I_1(x,A)\right) - I_2(x,A)\right] + O(\mu_2) \tag{1.8}$$

avec κ un réel. Comme les termes ajoutés sont d'ordre $O(\mu_2)$, la précision du modèle n'est pas affecté.

En appliquant *l'astuce* BBM à (1.6), on obtient une famille d'équations SGN à un paramètre avec une dispersion améliorée sous la forme conservatrice :

$$\begin{cases} \dfrac{\partial}{\partial t}A + \dfrac{\partial}{\partial x}(Au) = 0 \\ \left(I_d - \mu_2\kappa\mathbb{L}[A,d,\sigma]\right)\left(\dfrac{\partial}{\partial t}(Au) + \dfrac{\partial}{\partial x}(Au^2) + \dfrac{(\kappa-1)}{\kappa}\left(\dfrac{\partial}{\partial x}I_1 - I_2\right)\right) \\ +\dfrac{1}{\kappa}\left(\dfrac{\partial}{\partial x}I_1 - I_2\right) + \mu_2 A\mathcal{Q}[A,d,\sigma](u) = O(\mu_2^2) \end{cases} \tag{1.9}$$

où I_d représente l'opérateur d'identité, $\sigma(x,z)$ est la largeur de la section à z donné, $d(x,y)$ désigne la limite de la section transversale du canal/de la rivière en fonction de y, $\mathbb{L}[A,d,\sigma]$ est un opérateur linéaire et $\mathcal{Q}[A,d,\sigma]$ est un opérateur quadratique.
Cette nouvelle formulation (1.9) ne contient aucune dérivée du troisième ordre, on peut donc s'attendre à des calculs numériques plus stables et plus robustes.

Dans la dernière partie de ce chapitre, nous nous intéressons uniquement au cas d'une section variable rectangulaire. Un schéma volumes finis d'ordre 1 équilibre pour le modèle dispersif reformulé (1.9) a été construit et quelques cas tests numériques ont été effectués. La construction d'un schéma bien équilibré peut être facilement réalisée en ne considérant que la partie hyperbolique des Eqs. (1.9), par exemple, par l'utilisation de la reconstruction hydrostatique (voir par exemple [4]).
Dans le premier cas test, la précision de la méthode et l'influence de la variation de section dans le cas de la propagation d'une onde solitaire ont été testé. Pour cela, on considère les solutions exactes d'ondes solitaires des équations de Green-Naghdi dans le cadre unidimensionnel sur un fond plat (voir [61]), données dans les variables avec dimensions, par

$$\begin{cases} \eta(t,x) = a\mathrm{sech}^2(k(x-ct)), \quad u(t,x) = c\left(\dfrac{\eta(t,x)}{\eta(t,x)+z_0}\right) \text{ with} \\ k = \dfrac{\sqrt{3a}}{2z_0\sqrt{z_0+a}} \text{ and } c = \sqrt{g(z_0+a)} \end{cases} \tag{1.10}$$

où z_0 est la profondeur du fluide et a est l'amplitude relative.

Précision: La propagation de l'onde solitaire (1.10) est initialement centrée à $x_0 = 10$ m avec une amplitude relative $a = 0.2$ m sur une profondeur d'eau constante $z_0 = 1$ m. Le domaine de calcul est $L_c = 100$ m et discrétisé par N cellules. L'onde solitaire se propage de gauche à droite. Dans ce test, puisque l'onde solitaire est initialement éloignée des limites du domaine, les conditions limites n'affectent pas le calcul, nous choisissons donc d'imposer des conditions limites sortie libre aux extrémités aval et amont. La solution exacte est calculée dans un canal de largeur $\sigma = 1$.

Dans ce qui suit, nous quantifions la précision numérique de notre schéma numérique en calculant la solution numérique pour ce cas particulier pour un nombre croissant de cellules N sur une durée $T = 20$ s. En commençant par un nombre de cellules $N = 100$, nous multiplions successivement le nombre de cellules par deux. Les erreurs relatives $E_{L^2}(\eta) = \dfrac{\|\eta - \eta_{\delta x}\|}{\|\eta\|}$ et $E_{L^2}(u) = \dfrac{\|u - u_{\delta x}\|}{\|u\|}$ sur la déformation de la surface de l'eau et la

vitesse moyenne présentée sont calculées à $t = 20$ s, en utilisant la norme discrète L_2 où (η, u) est la solution exacte et $(\eta_{\delta x}, u_{\delta x})$ est la solution numérique. Pour tous les N, nous comparons, dans la Fig. 1.1, $M^n := \max_{0\le i\le N+2}(h_i^n)$ de notre solution numérique fournie par Eqs. (1.9) avec l'exacte $M(t_n) := \max h(t_n, x)_{x\in[0,L_c]} = 2.2$ donnée par les (1.10). On peut facilement remarquer que la discrétisation du premier ordre n'est pas précise pour une simulation à long terme en raison de la dissipation numérique. Cependant, pour limiter la dissipation numérique du schéma numérique du premier ordre, on peut soit limiter le temps de simulation, soit considérer un très grand nombre de cellules. Il est cependant préférable d'augmenter l'ordre du schéma numérique mais ceci est laissé à un travail futur. Par conséquent, dans ce qui suit, nous considérons un temps de simulation plus court et un grand nombre de cellules, juste pour illustrer l'influence de la variation de la section du canal.

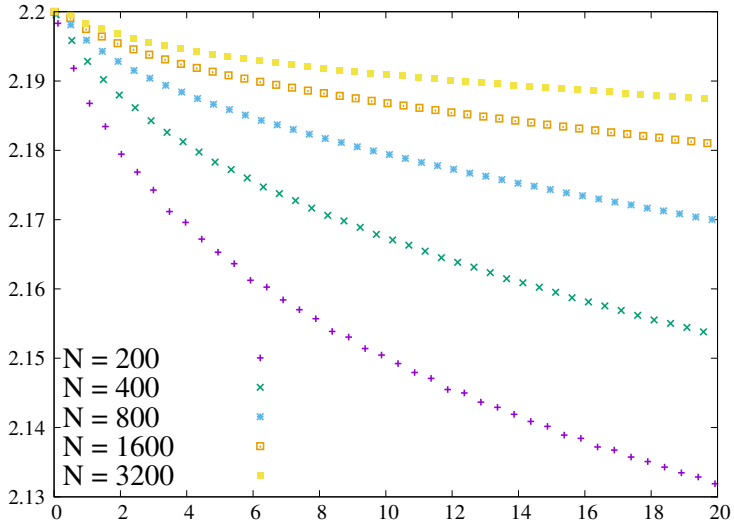

Figure 1.1: $M^n := \max_{0\le i\le N+2}(h_i^n)$

Influence de la variation de la section: Nous considérons à nouveau la propagation d'une onde solitaire initialement centrée en $x_0 = 10$ m d'amplitude relative $a = 0.2$ m, sur une profondeur d'eau constante $z_0 = 1$ m sur un domaine de calcul de $L_c = 50$ m et discrétisée avec des $N = 5000$ cellules. Commençant initialement par $(\eta(0, x), u(0, x))$ (voir Eqs. (1.10)), nous calculons la simulation numérique pour les canaux définis par

$$\sigma(x;\varepsilon) = \beta(x;\varepsilon) - \alpha(x;\varepsilon) \text{ with } \beta = \frac{1}{2} - \frac{\varepsilon}{2}\exp\left(-\varepsilon^2\left(x - L/2)^2\right)\right) \text{ et } \alpha = -\beta$$

avec $\epsilon = 0$, $\epsilon = 0,1$, $\epsilon = 0,2$, $\epsilon = 0,3$ et $\epsilon = 0,4$. Les résultats obtenus sont présentés dans la Fig 1.2. Dans la Fig.1.2(a), pour chaque géométrie, nous montrons l'évolution du maximum du niveau de l'eau $M^n := \max_{0\le i\le N+2}(h_i^n)$. Comme prévu, puisque la première partie de $x \le 25$ converge linéairement, le niveau de l'eau augmente alors que pour $x > 25$, le canal diverge linéairement et donc, l'amplitude du niveau de l'eau diminue. De plus, dans toutes les simulations numériques, la masse est conservée. En effet,

pour chaque valeur de ε, nous avons affiché dans la Fig. 1.2(b), le rapport de $\frac{m^n}{m^0}$ où $m^n := \frac{1}{N+2}\sum_{i=0}^{N+1} A_i^n$ est la masse d'eau au moment t_n. Le rapport $\frac{m^n}{m^0}$ est quasiment égal à 1.

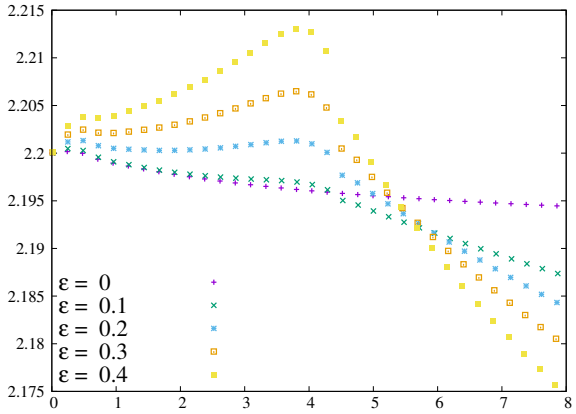

(a) $M^n := \max_{x\in[0,L_c]}(h_i^n)$

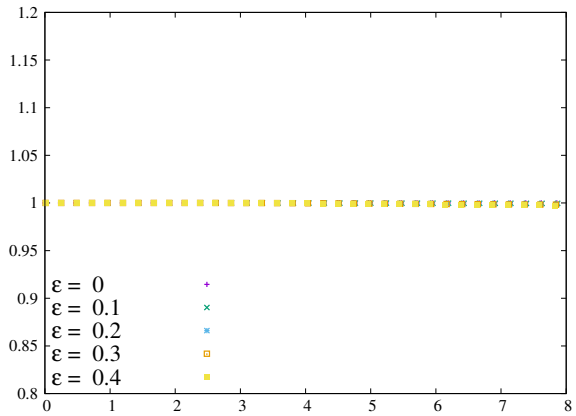

(b) $\frac{m^n}{m^0}$ avec $m^n = \frac{1}{N+2}\sum_{i=0}^{N+1} A_i^n$

Figure 1.2: influence of σ

Le quatrième chapitre est le fruit d'une collaboration lors de la session de recherche du CEMRACS 2019. L'objet est l'étude du système de Serre-Green-Naghdi afin de modéliser des écoulements incompressibles à surface libre en peu profondeur, tout en tenant compte les effets de la pression non-hydrostatique et les phénomènes dispersifs qui jouent un rôle important en particulier en océanographie côtière. Plusieurs schémas numériques sont présentés, basés sur une méthode de splitting, en séparant la partie hyperbolique (prédiction) et la partie non-hydrostatique (correction). Les algorithmes sont comparés en temps de calcul à travers des simulations avec des ondes solitaires. Le modèle est également validé avec des données expérimentales concernant les ondes de Favre [23].

Le système de Serre–Green-Naghdi (apparu initialement dans [86], [50]), également connu sous le nom de système de Boussinesq entièrement non linéaire se lit comme suit :

$$\begin{cases} \partial_t h + \partial_x(hu) = 0, \\ \partial_t(hu) + \partial_x(hu^2) + \partial_x(hq) + q_b \partial_x z_b = -gh\partial_x(h + z_b) - h\partial_x p_{atm}, \\ \partial_t(hw) + \partial_x(huw) - q_b = 0, \\ \partial_t(h\sigma) + \partial_x(hu\sigma) - 2\sqrt{3}\left(q - \dfrac{q_b}{2}\right) = 0, \\ w - u\partial_x z_b - \sqrt{3}\sigma = 0, \\ 2\sqrt{3}\sigma + h\partial_x u = 0 \end{cases} \tag{1.11}$$

où $h(t,x) : \mathbb{R}^+ \times \mathbb{R} \to \mathbb{R}^+$ est la hauteur du fluide à une position x donnée, au temps t ; $u(t,x) : \mathbb{R}^+ \times \mathbb{R} \to \mathbb{R}$ est la vitesse horizontale moyennée en profondeur du fluide, $w(t,x) : \mathbb{R}^+ \times \mathbb{R} \to \mathbb{R}$ est la vitesse verticale moyennée en profondeur, $\sigma(t,x) : \mathbb{R}^+ \times \mathbb{R} \to \mathbb{R}$ est la correction verticale associée à w. Enfin, $q(t,x) : \mathbb{R}^+ \times \mathbb{R} \to \mathbb{R}$ est la pression hydrodynamique moyenne verticale et $q_b(t,x) : \mathbb{R}^+ \times \mathbb{R} \to \mathbb{R}$ est la pression hydrodynamique au fond.
$z_b(x) : \mathbb{R} \to \mathbb{R}$ est la topographie du fond indépendante du temps, et $g = 9,81$ est l'accélération standard due à la gravité. Le système est complété par de multiples conditions aux limites possibles, en fonction du cadre physique modélisé.

Dans ce travail, nous élaborons le schéma de *splitting* de type volume fini - différence finie. Il consiste à résoudre d'abord la partie hyperbolique, puis la partie dispersive. L'étape de prédiction hyperbolique implique la résolution numérique des équations classiques des eaux peu profondes avec une topographie de fond non plat. Quant à la résolution du système résultant de l'étape de correction non hydrostatique - qui est le cœur de ce travail - nous présentons deux algorithmes itératifs : l'algorithme d'Uzawa appliqué au problème mixte vitesse-pression et la méthode de Gauss-Seidel pour l'étape de projection elliptique. Les différents choix de conditions aux limites en fonction de la situation physique en question, ainsi que leurs conséquences sur les procédures de discrétisation, sont également étudiés.

Pour comparer les stratégies numériques, trois cas tests sont considérés :

- Une solution exacte (onde solitaire) où les trois méthodes numériques sont comparées

- Une onde de choc dispersive provenant d'une rupture de barrage simulée avec l'algorithme d'Uzawa dans la Fig. 1.3

- Des comparaisons avec des données expérimentales (ondes de Favre) et les résultats numériques obtenus avec l'algorithme d'Uzawa

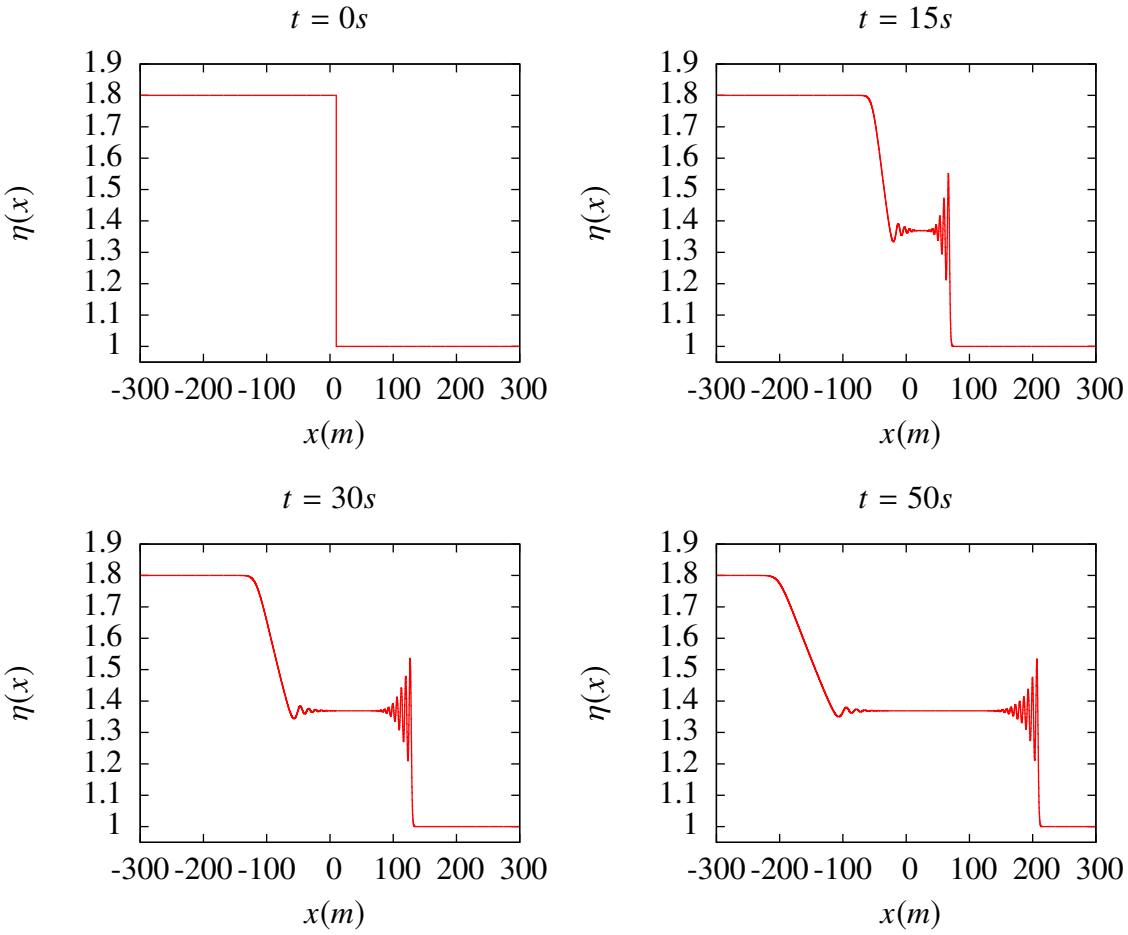

Figure 1.3: Dam-break: La surface de l'eau à différentes reprises.

1.3 Perspectives de recherche

Actuellement et dans les années à venir, je compte développer deux axes de recherche qui s'inscrivent dans le cadre de mes travaux de recherche actuels. Le premier thème porte sur **l'analyse mathématique (l'existence et l'unicité de solution) des modèles Serre-Green-Naghdi** dérivés dans ma thèse, tandis que le deuxième thème s'intéresse à **l'optimisation du code de calcul** $1d$ pour prendre en compte les variations de bathymétrie et de section non limité au cas rectangulaire. L'objectif de mon dernier axe de recherche est de modéliser les risques d'inondation et la propagation des vagues de tsunami en utilisant un couplage d'équations du type Green-Naghdi/Saint-Venant à section variable.

Analyse mathématique des équations de type Serre-Green-Naghdi

Le mouvement d'un fluide parfait, incompressible et irrotationnel sous l'effet de la gravité est décrit par les équations d'Euler ou les équations d'ondes de surfaces "water-waves" à surface libre. L'existence et l'unicité de solutions pour ces équations est maintenant bien comprises suite aux travaux de Wu [95, 96] (voir aussi Yasihara [98] et Lannes [58]). Mais en raison de la complexité de ces équations, ils sont souvent remplacées

par des équations réduites. Ces équations réduites sont obtenues en tant que limite asymptotique formelle des équations d'Euler à surface libre ou les équations d'ondes de surface. La dérivation formelle de ces équations remonte au $XIXe$ siècle tandis que leur justification mathématique a commencé il y a seulement trois décennies avec les travaux de d'Ovsjannikov [73, 72], Craig [28], Kano et Nishada [54] qui ont abordé pour la première fois le problème de la justification des asymptotiques formelles. Récemment en 2008 B. Alvarez Samaniego et D. Lannes [3] ont donné une justification rigoureuse de tout les asymptotiques présentés dans la section précédente.
Les équations de Kortweg-de Vries (KDV) sont mathématiquement justifiées dans [28], les équations de Saint-Venant ou également "Non Linear Shallow Water" sont justifiées dans [73, 3]. Les équations faiblement non linéaires et faiblement dispersives de Boussinsq sont étudiées dans [28, 53, 13], voir également [77, 76, 91, 29] en présence de la topographie. Finalement, les équations fortement non linéaires, faiblement dispersif de Green-Naghdi, également les équations de Serre, sont justifiées dans [65, 3].

En suivant ces travaux, mon objectif est d'apporter une justification rigoureuse du modèle développé dans ma thèse (1.6), plus particulièrement l'étude du caractère bien posé de ce modèle et l'étude de la convergence des solutions vers celle du problème d'Euler à surface libre.

Optimisation du code de calcul

L'ajout d'effets dispersifs dans un modèle ajoute des difficultés importantes pour obtenir un algorithme robuste. En effet, ces termes supplémentaires changent la classe d'équation et de nouvelles approches numériques doivent être développées. Les modèles dispersifs du type Serre-Green-Naghdi (1.6) peuvent être écrits sous la forme suivante :

$$\frac{\partial X}{\partial t} + \operatorname{div} F(X) + \mathcal{D} = S(X) \tag{1.12}$$

où X est définis par

$$X = \begin{pmatrix} h \\ h\bar{u} \end{pmatrix}$$

F est le flux associé et S est le terme source de la topographie. Nous notons $\mathcal{D}$ les termes dispersifs supplémentaires pouvant contenir des opérateurs différentiels en fonction du modèle. Ainsi, pour $\mathcal{D} = 0$, on trouve les équations de Saint-Venant, qui peuvent être résolues avec la méthode des volumes finis. Pour $\mathcal{D} \neq 0$, les difficultés surviennent. De nombreuses stratégies ont été étudiées dans une ou deux dimensions et nous résumons ici brièvement quelques techniques. La détermination de $\mathcal{D}$ dépend de la formulation du modèle et $\mathcal{D}$ contient généralement des termes dérivés d'ordre 3. Il est alors nécessaire d'appliquer un schéma d'ordre supérieur pour discrétiser $\mathcal{D}$. Plusieurs techniques ont été proposées pour résoudre ce problème. Dans [24] un schéma de volumes finis d'ordre supérieur (WENO [97]) et un schéma de différence finie pour le modèle unidimensionnel de Green-Naghdi a été développé en se basant sur la méthode de splitting en séparant la partie hyperbolique et la partie dispersive. De même, dans [63] les auteurs utilisent un schéma HLL pour la partie hyperbolique sur un fond plat et discrétisent les termes dérivés d'ordre supérieur présents dans $\mathcal{D}$ par approximation de différence finie.

Dans le troisième chapitre de ce manuscrit, nous avons construit un schéma numérique d'ordre 1 pour résoudre numériquement le modèle (1.6). Un cas test pour étudier l'influence de la topographie et de la section sur la propagation d'un soliton a été réalisé. D'après la Fig 1.1, on peut remarquer que la discrétisation du premier ordre n'est pas précise pour une simulation de longue durée à cause de la dissipation numérique.

Aussi, pendant la session de recherche CEMRACS, nous avons étudié le modèle de Serre-Green-Naghdi en utilisant un schéma d'ordre 1. La figure 1.3 montre les effets dispersifs générés par le système (5.1) lors de l'utilisation de données initiales discontinues. Ici, nous avons choisi 8000 cellules parce que les effets dispersifs ne peuvent pas être capturés si nous utilisons un schéma numérique du premier ordre 1, et pour capturer correctement les ondes de choc dispersives, nous avons dû utiliser des schémas numériques d'ordre élevé.

L'objectif est alors, de construire un schéma numérique d'ordre supérieur pour la simulation à long terme qui tient en compte la variation de la topographie et de la section transversale.

Part II

Depth averaged models

Chapter 2

Derivation of shallow water equations

Contents

2.1 Introduction

The origin of the water wave problem in fluid mechanics dates back to the 1980s [30]. The classical mathematical formulation of surface gravity waves consists of five equations: fluid incompressibility, surface isobarity, bottom and surface impermeability and flow irrotationality [66] (Mei 1989). This system of equations does not admit an exact analytical solution since the domain of definition of these equations is unknown (the domain is determined by the elevation $\eta(t, \boldsymbol{x})$), therefore, various approximations have been constructed.

For shallow water flows, we have the nonlinear shallow water equations that were derived by Jean Adhémar Saint Venant in 1876[31], Korteweg and Vries (1895) [55], Boussinesq (1871) [17, 18], Serre (1953) [86], Green and Naghdi (1976)[50], Camassa and Holm (1993) [22] and several other variations that were developed after that [60]. Models of type Saint-Venant, for example with finite volume methods, can accurately reproduce the dissipation of breaking waves. On the other hand, the absence of dispersive effects restricts their range of validity to areas where non-linearities predominate. Outside these areas, the absence of dispersive terms in these equations generally leads to an incorrect prediction of the location of the breaking wave.

On the other hand, the Boussinesq type equations take into account the non-linear and dispersive aspects of wave propagation. By introducing the characteristic amplitude of the free surface A, H the characteristic depth, and finally L the characteristic wavelength, we define the dimensionless numbers

$$\mu = \frac{H^2}{L^2}, \qquad \varepsilon = \frac{A}{H}$$

aspect ratio respectively of non-linearity. The Boussinesq type models are in principle derived from a shallow depth assumption $\mu \ll 1$ by imposing an equilibrium between non-linearity and dispersion, i.e. $\varepsilon = O(\mu)$ thus limiting their use to weakly non-linear and weakly dispersive simulations. In fact, these models are not very efficient in surf and swash areas where the amplitude ε can reach $O(1)$. In particular, it is shown that taking into account the strongly non-linear effects for asymptotics in shallow depths $\mu \ll 1$ and $\varepsilon = 0(1)$, allows to capture not only the propagation speed but also the wave heights before surfing (see [91]). The highly non-linear model constructions were built by Serre [86] and then generalized by Green-Naghdi [50]. These equations, also called Serre-Green-Naghdi (SGN) equations, are currently described as the most relevant system for dealing with highly nonlinear and weakly dispersive waves.

These asymptotic models are obtained from a first and second-order approximation of the general equations of fluid mechanics, in particular, the water wave equations, [60], the incompressible Navier Stokes equations [47, 82] and the incompressible Euler equations [39, 61]. These asymptotic models can also be derived via a variational principle such as the relaxation method [37, 26] or augmented Lagrangian [43]. In this chapter, we consider the classical variational principle to derive some asymptotic models in shallow water, namely non-dispersive Saint-Venant equations and Boussinesq and Serre-Green Naghdi dispersive equations.

The chapter is organised as follows: in §2.2, we present the physical and geometric settings of the governing equations. §2.3 is devoted to the modeling of waves in shallow water, based on the underlying variational principle (least action principle). We then study

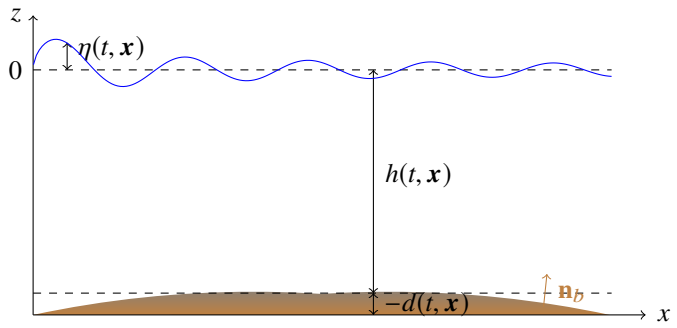

Figure 2.1: Sketch of the Domain

the asymptotic behavior of the Lagrangian in §2.5 and derive the nonlinear equations of shallow waters in §2.6.4. The first-order approximation in asymptotic shallow waters gives the Saint-Venant model. We will then obtain in §2.6.2 the (SGN) model, which provides a second-order approximation to the shallowness parameter. By adding other smallness parameters under the wave amplitude hypothesis, we obtain the Boussinesq-type models derived in §2.6.3. Finally, in §2.7, we derive asymptotic models from the three dimensional Euler equations.

2.2 Physical and geometrical set-up

Let us consider an incompressible, homogeneous, and ideal fluid, of constant density ρ, in a domain $\Omega(t)$. At the time $t \in [0, T)$, the domain occupied by the fluid is, therefore,

$$\Omega(t) = \{(\boldsymbol{x}, z) \in \mathbb{R}^2 \times \mathbb{R}, -d(t, \boldsymbol{x}) \leq z \leq \eta(t, \boldsymbol{x})\}, \tag{2.1}$$

We note that $\boldsymbol{x} = (x, y)$ is the horizontal cartesian coordinate, z is the upward vertical coordinate, t is the time, $\boldsymbol{\nabla} = (\partial_x, \partial_y)^T$ is the horizontal gradient and $\boldsymbol{\nabla}_{\boldsymbol{x},z} = (\partial_x, \partial_y, \partial_z)^T$ is the classical gradient.
There are also two functions, $\eta : [0, T) \times \mathbb{R}^2 \longrightarrow \mathbb{R}$ and $d : [0, T) \times \mathbb{R}^2 \longrightarrow \mathbb{R}$, such that $z = \eta(t, \boldsymbol{x})$ and $z = -d(t, \boldsymbol{x})$ represent the free surface equation and the bottom equation respectively. The local height of the water is

$$h(t, \boldsymbol{x}) = \eta(t, \boldsymbol{x}) + d(t, \boldsymbol{x}).$$

We denote by $\boldsymbol{U}(t, \boldsymbol{x}, z) \in \mathbb{R}^3$, the velocity of the fluid particle located at $(\boldsymbol{x}, z)$ at time t, $\boldsymbol{u}(t, \boldsymbol{x}, z) \in \mathbb{R}^2$ and $w(t, \boldsymbol{x}, z)$ are its horizontal and vertical components respectively. Incompressibilty of the fluid then takes the following form

$$\operatorname{div}[\boldsymbol{U}] = 0. \tag{2.2}$$

Irrotationality of the fluid is useful but not necessary [59], given as follows,

$$\operatorname{curl}[\boldsymbol{U}] = 0. \tag{2.3}$$

In addition to the equations (2.2) and (2.3), we need boundary conditions. One of them is the so-called kinematic boundary condition at the free surface and expressed the fact that the fluid particle do not across the free surface, it read

$$\boldsymbol{U} \cdot \boldsymbol{n}_{fs} = \frac{\partial \boldsymbol{m}}{\partial t} \cdot \boldsymbol{n}_{fs}, \tag{2.4}$$

where $\boldsymbol{m}(\boldsymbol{x}, z = \eta(t, \boldsymbol{x}))$ is a point at the free surface and $\boldsymbol{n}_{fs}$ is the unit outward normal vector to the free surface given by:

$$\boldsymbol{n}_{fs} := \frac{1}{\sqrt{1 + (\boldsymbol{\nabla}\eta)^2}} (-\boldsymbol{\nabla}\eta,\ 1)^T.$$

This leads to the following explicit form:

$$\frac{\partial \eta}{\partial t} + \boldsymbol{u} \cdot \boldsymbol{\nabla}\eta = w. \tag{2.5}$$

The next boundary condition is needed at the bottom, assumed to be impermeable,

$$\boldsymbol{U} \cdot \boldsymbol{n}_b = \frac{\partial \boldsymbol{m}}{\partial t} \cdot \boldsymbol{n}_b. \tag{2.6}$$

Here $\boldsymbol{m} = \boldsymbol{m}(\boldsymbol{x}, z = -d(t, \boldsymbol{x}))$ represents a point at the bottom, and $\boldsymbol{n}_b$ is the unit outward normal at the bottom

$$\boldsymbol{n}_b := \frac{1}{\sqrt{1 + (\boldsymbol{\nabla} d)^2}} (-\boldsymbol{\nabla} d,\ 1)^T,$$

this leads to the following explicit form:

$$-\frac{\partial d}{\partial t} - \boldsymbol{u} \cdot \boldsymbol{\nabla} d = w. \tag{2.7}$$

2.3 Variational principle and Euler-Lagrange equations

Let the fluid be ideal, incompressible, homogeneous and have a free unknown surface, while the other part of the boundary is given. Then, the following variational principle holds [11]:

Variational principle: The motion of the fluid must provide a stationary value to the following functional action:

$$S(\boldsymbol{U}) = \int_{t_0}^{t_1} \rho \mathcal{L}\, dt,$$

on the set of all velocity fields that satisfy the constraint (2.2) and the condition (2.4). Here, ρ is the density of the fluid (taken to be constant) and $\mathcal{L}$ is the classical Lagrangian density defined as:

$$\mathcal{L} := \mathcal{K} + \mathcal{P}$$

where $\mathcal{K}$ and $\mathcal{P}$ are respectively the kinetic and the potential energies of a shallow fluid moving under the force of gravity g:

$$\mathcal{K} := \frac{1}{2} \int_{\Omega(t)} |\boldsymbol{U}|^2(t, \boldsymbol{x}, z) dz d\boldsymbol{x}, \quad \text{and} \quad \mathcal{P} = \int_{\Omega(t)} -gz\, dz d\boldsymbol{x}.$$

We next incorporate the condition of incompressibility (2.2) into the functional $S(\boldsymbol{U})$ using a Lagrange multiplier ϕ, as follows:

$$S(\boldsymbol{U}) = \int_{t_0}^{t_1} \int_{\Omega(t)} \rho \frac{1}{2}|\boldsymbol{u}|^2 + \frac{1}{2}w^2 - gz + \phi(\boldsymbol{\nabla} \cdot \boldsymbol{u} + \frac{\partial w}{\partial z}) dz\, d\boldsymbol{x}\, dt. \tag{2.8}$$

Integrating by parts, it turns out that,

$$S(\boldsymbol{U}) = \int_{t_0}^{t_1} \int_{\Omega(t)} \rho \left(\frac{1}{2}|\boldsymbol{u}|^2 + \frac{1}{2}w^2 - gz - \boldsymbol{u} \cdot \boldsymbol{\nabla}\phi - w\frac{\partial \phi}{\partial z} \right) \; dz\, d\boldsymbol{x}\, dt + \int_{t_0}^{t_1} \int_{\partial\Omega} \rho\phi\, (\boldsymbol{U} \cdot \boldsymbol{n}) dt, \tag{2.9}$$

where $\boldsymbol{n}$ is the outward normal at the boundary.
Using the following Reynolds transport theorem [51, 9], we have:

$$\frac{\partial}{\partial t} \int_{\Omega(t)} \phi \, d\Omega = \int_{\Omega(t)} \frac{\partial \phi}{\partial t} \, d\Omega + \int_{\partial\Omega} \phi(\boldsymbol{U} \cdot \boldsymbol{n}) \, d\partial\Omega, \tag{2.10}$$

then, the functional (2.9) can be written in the following way:

$$S(\boldsymbol{U}) = \int_{t_0}^{t_1} \int_{\Omega(t)} \rho \left(-\frac{\partial \phi}{\partial t} + \frac{1}{2}\boldsymbol{u}^2 + \frac{1}{2}w^2 - gz - \boldsymbol{u} \cdot \boldsymbol{\nabla}\phi - w\frac{\partial \phi}{\partial z} \right) \; dz\, d\boldsymbol{x}\, dt + \left[\int_{\partial\Omega} \phi \quad dz\, d\boldsymbol{x} \right]_{t_0}^{t_1}. \tag{2.11}$$

We can delete the last term of (2.11) by adding the following additional constraint on the admissible values of the potential ϕ:

$$\left[\int_{\partial\Omega} \phi \quad dz\, d\boldsymbol{x} \right]_{t_0}^{t_1} = 0. \tag{2.12}$$

It is clear that adding this constraint does not affect the equations and boundary conditions for ϕ, since it does not contribute to the variations [11], then we obtain:

$$S(\boldsymbol{U}) = \int_{t_0}^{t_1} \int_{\Omega(t)} \rho \left(-\frac{\partial \phi}{\partial t} + \frac{1}{2}\boldsymbol{u}^2 + \frac{1}{2}w^2 - gz - \boldsymbol{u} \cdot \boldsymbol{\nabla}\phi - w\frac{\partial \phi}{\partial z} \right) dz\, d\boldsymbol{x}\, dt. \tag{2.13}$$

The variation δS of the functional $S(\boldsymbol{U})$ with respect to the variation of the velocities $\boldsymbol{u}(\boldsymbol{x}, z, t)$ and $w(\boldsymbol{x}, z, t)$, the potential $\phi(\boldsymbol{x}, z, t)$ as well as with respect to the surface elevation $\eta(\boldsymbol{x}, t)$ have to be zero.
Let us start by the variation with respect to $\boldsymbol{u}(\boldsymbol{x}, z, t)$, let us consider a small variation $\delta\boldsymbol{u}$ in the velocity $\boldsymbol{u}(\boldsymbol{x}, z, t)$. Then the variation of (2.13) with respect to $\boldsymbol{u}$ gives,

$$\begin{aligned} 0 = \delta_{\boldsymbol{u}} S &= S(\boldsymbol{u} + \delta\boldsymbol{u}, \cdot) - S(\boldsymbol{u}, \cdot) \\ &= \int_{t_0}^{t_1} \int_{\Omega} \left\{ \int_{-d(t,\boldsymbol{x})}^{\eta(t,\boldsymbol{x})} \rho\delta\boldsymbol{u}\, (\boldsymbol{u} - \boldsymbol{\nabla}\phi)\, dz \right\} d\boldsymbol{x}\, dt. \end{aligned}$$

Since δu is arbitrary, we deduce

$$\boldsymbol{u}(t, \boldsymbol{x}, z) = \boldsymbol{\nabla} \cdot \phi(t, \boldsymbol{x}, z) \, . \tag{2.14}$$

Similarly, the variation of the Lagrangian (2.13) with respect to $w(\boldsymbol{x}, z, t)$, gives,

$$\begin{aligned} 0 = \delta_w S &= S(w + \delta w, \cdot) - S(w, \cdot) \\ &= \int_{t_0}^{t_1} \int_\Omega \left\{ \int_{-d(t,\boldsymbol{x})}^{\eta(t,\boldsymbol{x})} \rho \delta w \left(w - \frac{\partial \phi}{\partial z} \right) dz \right\} d\boldsymbol{x} dt, \end{aligned}$$

then, since δw can be given also arbitrary, we obtain

$$w(t, \boldsymbol{x}, z) = \frac{\partial}{\partial z} \phi(t, \boldsymbol{x}, z) \, . \tag{2.15}$$

Next, the variation of (2.13) with respect to ϕ leads to,

$$\begin{aligned} \delta_\phi S &= S(\phi + \delta\phi, \cdot) - S(\phi, \cdot) \\ &= \int_{t_0}^{t_1} \int_\Omega \left\{ \int_{-d(t,\boldsymbol{x})}^{\eta(t,\boldsymbol{x})} -\rho \left(\frac{\partial \delta\phi}{\partial t} + \boldsymbol{u} \cdot \boldsymbol{\nabla}(\delta\phi) + w \frac{\partial \delta\phi}{\partial z} \right) dz \right\} d\boldsymbol{x} dt \, . \end{aligned}$$

Using the following Leibniz integral rule,

$$\begin{aligned} \int_{a(x)}^{b(x)} \frac{\partial f}{\partial x}(x, s) \, ds = \frac{\partial}{\partial x} \int_{a(x)}^{b(x)} f(x, s) \, ds \\ - \frac{\partial b}{\partial x}(x) f(x, s)|_{s=b(x)} + \frac{\partial a}{\partial x}(x) f(x, s)|_{s=a(x)} \end{aligned} \tag{2.16}$$

then, for a constant density ρ, we obtain:

$$\begin{aligned} \delta_\phi S = &- \int_{t_0}^{t_1} \int_\Omega \left\{ \frac{\partial}{\partial t} \int_{-d(t,\boldsymbol{x})}^{\eta(t,\boldsymbol{x})} \rho \delta\phi \, dz + \boldsymbol{\nabla} \cdot \int_{-d(t,\boldsymbol{x})}^{\eta(t,\boldsymbol{x})} \rho(\boldsymbol{u} \delta\phi) \, dz \right\} d\boldsymbol{x} dt, \\ &+ \rho \int_{t_0}^{t_1} \int_\Omega \left\{ \int_{-d(t,\boldsymbol{x})}^{\eta(t,\boldsymbol{x})} \delta\phi \left(\boldsymbol{\nabla} \cdot \boldsymbol{u} + \frac{\partial w}{\partial z} \right) dz \right\} d\boldsymbol{x} dt, \\ &+ \rho \int_{t_0}^{t_1} \int_\Omega \left\{ \delta\phi \left(\frac{\partial \eta}{\partial t} + \boldsymbol{u} \cdot \boldsymbol{\nabla}\eta - w \right) |_{z=\eta(t,\boldsymbol{x})} \right\} d\boldsymbol{x} dt, \\ &+ \rho \int_{t_0}^{t_1} \int_\Omega \left\{ \delta\phi \left(\frac{\partial d}{\partial t} + \boldsymbol{u} \cdot \boldsymbol{\nabla} d + w \right) |_{z=-d(t,\boldsymbol{x})} \right\} d\boldsymbol{x} dt, \\ =&0 \end{aligned}$$

which gives for an arbitrary $\delta\phi$, the following equations

$$\begin{cases} \boldsymbol{\nabla} \cdot \boldsymbol{u} + \dfrac{\partial w}{\partial z} = 0, & -d < z < \eta, \\ \dfrac{\partial \eta}{\partial t} + \boldsymbol{u} \cdot \boldsymbol{\nabla}\eta - w = 0, & z = \eta, \\ \dfrac{\partial d}{\partial t} + \boldsymbol{u} \cdot \boldsymbol{\nabla} d + w = 0, & z = -d \, . \end{cases} \tag{2.17}$$

Finally, the variation with respect to $\eta(t, \boldsymbol{x})$, gives,

$$\begin{aligned}\delta_\eta S &= S(\eta + \delta\eta, \cdot) - S(\eta, \cdot) \\ &= \int_{t_0}^{t_1} \int_\Omega \rho\delta\eta \left(-\frac{\partial\phi}{\partial t} + \frac{1}{2}\boldsymbol{u}^2 + \frac{1}{2}w^2 - g\eta - \boldsymbol{u}\cdot\boldsymbol{\nabla}\phi - w\frac{\partial\phi}{\partial z} \right) |_{z=\eta(t,\boldsymbol{x})} d\boldsymbol{x}\, dt \ .\end{aligned}$$

One deduce from the above integral that

$$-\frac{\partial\phi}{\partial t} + \frac{1}{2}\boldsymbol{u}^2 + +\frac{1}{2}w^2 - g\eta - u\cdot\boldsymbol{\nabla}\phi - w\frac{\partial\phi}{\partial z} = 0, \quad z = \eta, \tag{2.18}$$

for an arbitrary $\delta\eta$.
Gathering equations (2.14)–(2.18), we obtain the following so-called **Euler-Lagrange equations**:

$$\boldsymbol{u} = \boldsymbol{\nabla}\phi, \qquad -d < z < \eta, \tag{2.19}$$

$$w = \frac{\partial\phi}{\partial z}, \qquad -d < z < \eta, \tag{2.20}$$

$$\boldsymbol{\nabla}\cdot\boldsymbol{u} + \frac{\partial w}{\partial z} = 0, \qquad -d < z < \eta, \tag{2.21}$$

$$\frac{\partial\eta}{\partial t} + \boldsymbol{u}\cdot\boldsymbol{\nabla}\eta - w = 0, \qquad z = \eta, \tag{2.22}$$

$$\frac{\partial d}{\partial t} + \boldsymbol{u}\cdot\boldsymbol{\nabla}d + w = 0, \qquad z = -d, \tag{2.23}$$

$$-\frac{\partial\phi}{\partial t} + \frac{1}{2}\boldsymbol{u}^2 + +\frac{1}{2}w^2 - g\eta - u\cdot\boldsymbol{\nabla}\phi - w\frac{\partial\phi}{\partial z} = 0, \quad z = \eta, \tag{2.24}$$

where equations (2.19) and (2.20) correspond to the irrotationality condition of the flow. Equation (2.21) is the continuity equation, and the two following equations (2.22), (2.23) are, respectively, the kinematic conditions at the free surface and the bottom. The last equation (2.24) corresponds to the dynamic boundary condition at the free surface.

Remark 1. Injecting the irrotationality relations (2.19)–(2.20) into the Lagrangian (2.13) yields to the following functional:

$$S(U) = \int_{t_0}^{t_1} \int_\Omega \int_{-d}^{\eta} \left[\frac{\partial\phi}{\partial t} + \frac{1}{2}|\boldsymbol{\nabla}\phi|^2 + \frac{1}{2}\left(\frac{\partial\phi}{\partial z}\right)^2 + gz \right] dz d\boldsymbol{x}\, dt, \tag{2.25}$$

which is the functional proposed by Luke in 1967 [67]. It is used to derive approximate wave models in shallow water.

Remark 2. The water wave equations can be recovered by applying the standard procedure of calcul of variations given above to the functional (2.25) with respect to ϕ and η. It read

$$\delta_\phi S : \begin{cases} \boldsymbol{\nabla}^2\phi + \partial_z^2\phi = 0, & -d < z < \eta, \\ \dfrac{\partial\eta}{\partial t} + \boldsymbol{\nabla}\phi\cdot\boldsymbol{\nabla}\eta - \dfrac{\partial\phi}{\partial z} = 0, & z = \eta, \\ \dfrac{\partial d}{\partial t} + \boldsymbol{\nabla}\phi\cdot\boldsymbol{\nabla}d + \dfrac{\partial\phi}{\partial z} = 0, & z = -d, \end{cases} \tag{2.26}$$

$$\delta_\eta S : \frac{\partial\phi}{\partial t} + \frac{1}{2}|\boldsymbol{\nabla}\phi|^2 + \frac{1}{2}\left(\frac{\partial\phi}{\partial z}\right)^2 + g\eta = 0, \qquad z = \eta\ . \tag{2.27}$$

These are the equations commonly used to derive asymptotic models in shallow water regimes (see [60, 59] for a clear and modern derivation of shallow water equations from water wave equations). These equations can also be considered as benchmarks to correct frequency dispersion errors due to the presence of non-hydrostatic pressure in dispersive models [84, 14].

In the sequel, we consider the Euler-Lagrange equation (2.19)–(2.24) to derive asymptotic models in shallow water.

2.4 The nondimensionalized equations

In order to study the asymptotic behavior of the solutions to the Euler-Lagrange equations (2.19)-(2.24), it is convenient to introduce nondimensionalized quantities based on the typical scales of the problem. Five main lengths are involved, namely, a typical water depth H, a typical wavelength L_x, a typical horizontal scale L_y, the order of free surface amplitude A, and the order of the bottom variations B. We define, therefore, the three small parameters

$$\mu = \frac{H^2}{L_x^2}, \quad \varepsilon = \frac{A}{H} \quad \text{and} \quad \beta = \frac{B}{H}.$$

The significations of these three parameters are the following

- μ is the so-called *shallowness* parameter (also called *dispersive* parameter).
- ε is the amplitude parameter (also called *nonlinearity* parameter).
- β represents the *topography* parameter

The shallow-water regime corresponds to the configuration where the wave length L_x of the flow is large compared to the typical depth H:

$$\mu = \frac{H^2}{L_x^2} \ll 1 \ .$$

For the sake of simplicity, we suppose in the rest of this section that $L_x = L_y = L$, then, dimensionless parameters are defined as follows:

$$x = \frac{\tilde{x}}{L}, \quad y = \frac{\tilde{y}}{L}, \quad z = \frac{\tilde{z}}{H}, \quad d = \frac{\tilde{d}}{B}, \quad \eta = \frac{\tilde{\eta}}{A} \ .$$

It is obvious that we nondimensionalize $\boldsymbol{x}$ and z by a unit lengths in a horizontal and vertical direction respectively, and the surface elevation and the bottom by two amplitude variations A and B. But the nondimensionalization of the time T and the potential ϕ differ, they are obtained by the linear wave theory (see [59] for more details). They read

$$t = \frac{\tilde{t}}{T}, \quad \phi = \frac{\tilde{\phi}}{\Phi}$$

where T and Φ are a typical time and potential velocity scales given by:

$$T = \frac{L}{U}, \qquad \Phi = \varepsilon L\, U \ .$$

From the irrotationality relations (2.19),(2.20), one can dimensionalize the velocities as follows,

$$\boldsymbol{u} = \frac{\tilde{\boldsymbol{u}}}{\varepsilon U}, \quad w = \frac{\tilde{w}}{\varepsilon W}$$

where U and W are the scales of fluid velocity. The nondimensionalized water height is then,

$$\tilde{h}(t, \boldsymbol{x}) = \varepsilon\tilde{\eta}(t, \boldsymbol{x}) + \beta\tilde{d}(t, \boldsymbol{x}) \, .$$

Injecting these quantities into equations (2.19)-(2.24), then yields the dimensionless form of the equations. Omitting the "tildes" for the sake of clarity, they read

$$\boldsymbol{u} = \boldsymbol{\nabla}\phi, \qquad -\beta d < z < \varepsilon\eta, \tag{2.28}$$

$$\mu w = \frac{\partial\phi}{\partial z}, \qquad -\beta d < z < \varepsilon\eta, \tag{2.29}$$

$$\boldsymbol{\nabla}\cdot\boldsymbol{u} + \frac{\partial w}{\partial z} = 0, \qquad -\beta d < z < \varepsilon\eta, \tag{2.30}$$

$$\frac{\partial\eta}{\partial t} + \varepsilon\boldsymbol{u}\cdot\boldsymbol{\nabla}\eta - w = 0, \qquad z = \varepsilon\eta, \tag{2.31}$$

$$\beta(\frac{1}{\varepsilon}\frac{\partial d}{\partial t} + \boldsymbol{u}\cdot\boldsymbol{\nabla}d) + w = 0, \qquad z = -\beta d, \tag{2.32}$$

$$-\frac{\partial\phi}{\partial t} + \frac{1}{2}\varepsilon\boldsymbol{u}^2 + \frac{1}{2}\varepsilon\mu w^2 - G\eta - \varepsilon\boldsymbol{u}\cdot\boldsymbol{\nabla}\phi - \varepsilon w\frac{\partial\phi}{\partial z} = 0, \quad z = \varepsilon\eta. \tag{2.33}$$

where equations (2.28) and (2.29) are the nondimensionalized irrotationality conditions. Equation (2.30) is the nondimensionalized continuity equation, and the two following equations (2.31), (2.32) are, respectively, the kinematic conditions at the free surface and the bottom given in the nondimensionalized form. The last equation (2.33) corresponds to the dynamic boundary condition at the free surface.

2.5 Asymptotic expansion

Asymptotic expansion is an essential passage in the derivation of asymptotic models from Euler equations, water wave equations, or, as in our case, the Euler-Lagrange equations. To understand flow's behavior, it is necessary to introduce the parameters given in the previous section, namely the parameters of shallowness μ, nonlinearity ε, and bottom variation β. Many asymptotic regimes can be distinguished based on these three parameters;

- Shallow water regime which corresponds to the case when $\mu \ll 1$. Adding assumptions with respect to the *nonlinearity* parameter, there are other asymptotic regimes;
  - Small/large amplitude regime corresponds to the case when $\varepsilon = O(\mu)$ and $\varepsilon = O(1)$ respectively.
  - Small/large bottom variations correspond to $\beta = O(\mu)$ and $\beta = O(1)$ respectively.
- Intermediate depth corresponds to the situation $\mu \sim 1$.

- Deep water regime when $\mu > 1$.

We are only interested in this work in the case of shallow water limit (see [59, 60] for more details in the other asymptotic regimes).

2.5.1 Taylor-series-type expansion

Keeping in mind that we are in shallow water regime which means that the shallowness parameter is too small ($\mu \ll 1$). From then on, we can consider the following formal asymptotic expansion with respect to $X(t, \boldsymbol{x}, z)$:

$$X(t, \boldsymbol{x}, z) = X_0(t, \boldsymbol{x}, z) + \mu X_1(t, \boldsymbol{x}, z) + \mu^2 X_2(t, \boldsymbol{x}, z) + \cdots . \tag{2.34}$$

Applying this asymptotic expansion to ϕ, $\boldsymbol{u}$ and v and substituting it in equations (2.28)–(2.32). Formally, letting μ goes to zero,

- first order equations are obtained as follows:

$$\boldsymbol{u}_0 = \boldsymbol{\nabla}\phi_0, \qquad \beta d < z < \varepsilon\eta, \tag{2.35}$$

$$0 = \frac{\partial \phi_0}{\partial z}, \qquad -\beta d < z < \varepsilon\eta, \tag{2.36}$$

$$\begin{cases} \boldsymbol{\nabla}\cdot\boldsymbol{u}_0 + \dfrac{\partial w_0}{\partial z} = 0, & -\beta d < z < \varepsilon\eta, \\ \dfrac{\partial \eta}{\partial t} + \varepsilon \boldsymbol{u}_0 \cdot \boldsymbol{\nabla}\eta - w_0 = 0, & z = \varepsilon\eta, \\ \beta(\dfrac{1}{\varepsilon}\dfrac{\partial d}{\partial t} + \boldsymbol{u}_0 \cdot \boldsymbol{\nabla} d) + w_0 = 0, & z = -\beta d\,, \end{cases} \tag{2.37}$$

- and at a second-order, we get the following equations:

$$\boldsymbol{u}_1 = \boldsymbol{\nabla}\phi_1, \qquad \beta d < z < \varepsilon\eta, \tag{2.38}$$

$$w_0 = \frac{\partial \phi_1}{\partial z}, \qquad -\beta d < z < \varepsilon\eta, \tag{2.39}$$

$$\begin{cases} \boldsymbol{\nabla}\cdot\boldsymbol{u}_1 + \dfrac{\partial w_1}{\partial z} = 0, & -\beta d < z < \varepsilon\eta, \\ \dfrac{\partial \eta}{\partial t} + \varepsilon \boldsymbol{u}_1 \cdot \boldsymbol{\nabla}\eta - w_1 = 0, & z = \varepsilon\eta, \\ \beta(\dfrac{1}{\varepsilon}\dfrac{\partial d}{\partial t} + \boldsymbol{u}_1 \cdot \boldsymbol{\nabla} d) + w_1 = 0, & z = -\beta d\,. \end{cases} \tag{2.40}$$

Moreover, from the irrotationality relations (2.36), we get the following important information, the so-called *motion by slices*,

$$\frac{\partial \phi_0}{\partial z} = 0$$

which implies that :

$$\phi_0 = \phi_0(t, \boldsymbol{x})\,.$$

Thus, we deduce from (2.35) that:

$$\boldsymbol{u}_0 = \boldsymbol{\nabla}\phi_0 = \boldsymbol{u}_0(t, \boldsymbol{x}) \ .$$

Therefore, applying the asymptotic expansion to the free surface kinematic boundary condition (2.31) and the dynamic boundary condition (2.33) respectively, by neglecting all terms at order $O(\mu^2)$ and taking into account that $\boldsymbol{u}_0 = \boldsymbol{u}_0(t, \boldsymbol{x})$, one obtain the following equations:

$$\begin{cases} \dfrac{\partial \eta}{\partial t} + \varepsilon \boldsymbol{u}_0 \cdot \boldsymbol{\nabla}\eta + \varepsilon\mu \boldsymbol{u}_1 \cdot \boldsymbol{\nabla}\eta = w_0 + \mu w_1 + O(\mu^2), & z = \varepsilon\eta, \\ \dfrac{\partial \phi_0}{\partial t} + \dfrac{1}{2}\varepsilon \boldsymbol{u}_0^2 + g\eta + \mu P_{NH} = 0 + O(\mu^2), & z = \varepsilon\eta \end{cases} \tag{2.41}$$

where

$$P_{NH}(t, \boldsymbol{x}, z) = \frac{\partial \phi_1}{\partial t} + \varepsilon \boldsymbol{u}_0 \cdot \boldsymbol{u}_1 + \frac{1}{2}\varepsilon w_0^2. \tag{2.42}$$

The unknowns of the last system (2.41) are w_0, ϕ_1, $\boldsymbol{u}_1$ and w_1. In order to obtain the asymptotic equations, it is necessary to calculate their explicit expressions.

Computation of the term w_0

The first order approximation of the continuity equation (2.30) reads,

$$\boldsymbol{\nabla} \cdot \boldsymbol{u}_0 + \frac{\partial w_0}{\partial z} = 0.$$

Integrating it with respect to z for $s \in [-\beta d, z]$ and taking into account the boundary condition at the bottom (2.32), gives

$$w_0(t, \boldsymbol{x}, z) = -(z + \beta d)\boldsymbol{\nabla} \cdot \boldsymbol{u}_0 + \beta w_c, \tag{2.43}$$

with w_c is the vertical acceleration at the bottom given by

$$w_c(t, \boldsymbol{x}) = -\frac{1}{\varepsilon}\frac{\partial d}{\partial t} - \boldsymbol{u}_0 \cdot \boldsymbol{\nabla} d, \tag{2.44}$$

therefore, one can compute the term $w_0^2(t, \boldsymbol{x}, z)$,

$$w_0^2(t, \boldsymbol{x}, z) = (z + \beta d)^2(\boldsymbol{\nabla} \cdot \boldsymbol{u}_0)^2 + \beta^2 w_c^2 - \beta(z + \beta d) w_c \boldsymbol{\nabla} \cdot \boldsymbol{u}_0. \tag{2.45}$$

Computation of the terms ϕ_1

In order to compute the second term of the non-hydrostatic pressure P_{NH}, we have to go back to (2.36), which gives;

$$w_0(t, \boldsymbol{x}, z) = \frac{\partial \phi_1}{\partial z}(t, \boldsymbol{x}, z).$$

Integrating it with respect to z and taking into account (2.43), we get,

$$\phi_1(t, \boldsymbol{x}, z) = -\frac{1}{2}(z + \beta d)^2 \boldsymbol{\nabla} \cdot \boldsymbol{u}_0 + \beta z w_c, \tag{2.46}$$

therefore,

$$\frac{\partial \phi_1}{\partial t}(t, \boldsymbol{x}, z) = -\beta(z + \beta d)(\boldsymbol{\nabla} \cdot \boldsymbol{u}_0)\frac{\partial d}{\partial t} - \frac{1}{2}(z + \beta d)^2 \partial_t(\boldsymbol{\nabla} \cdot \boldsymbol{u}_0) + \beta z \partial_t w_c. \tag{2.47}$$

Computation of the terms $\boldsymbol{u}_1$

According to the irrotationality condition (2.38) we have the following equation,

$$\boldsymbol{u}_1(t, \boldsymbol{x}, z) = \boldsymbol{\nabla}\phi_1,$$

applying the gradient $\boldsymbol{\nabla}$ to (2.46), then it reads as follows:

$$\boldsymbol{u}_1(t, \boldsymbol{x}, z) = -\beta((z + \beta d)\boldsymbol{\nabla} \cdot \boldsymbol{u}_0)\boldsymbol{\nabla} d - \frac{1}{2}(z + \beta d)^2 \boldsymbol{\nabla}[\boldsymbol{\nabla} \cdot \boldsymbol{u}_0] + \beta z \boldsymbol{\nabla} w_c. \tag{2.48}$$

Computation of the terms P_{NH}

Injecting (2.45),(2.46) and (2.48) into (2.49), we get the expression of the term P_{NH} as follows,

$$\begin{aligned} P_{NH}(t, \boldsymbol{x}, z) = \frac{1}{2}\varepsilon\beta^2 w_c^2 + \beta z(\partial_t w_c + \varepsilon \boldsymbol{u}_0 \cdot \boldsymbol{\nabla} w_c) \\ - \frac{1}{2}(z + \beta d)^2 \left(\partial_t(\boldsymbol{\nabla} \cdot \boldsymbol{u}_0) + \varepsilon \boldsymbol{u}_0 \cdot \boldsymbol{\nabla}[\boldsymbol{\nabla} \cdot \boldsymbol{u}_0] - \varepsilon(\boldsymbol{\nabla} \cdot \boldsymbol{u}_0)^2\right) . \end{aligned} \tag{2.49}$$

Computation of the terms w_1

One can compute the explicit expression of the second term of the vertical velocity w_1 from the second-order approximation of the continuity equation. We have

$$\boldsymbol{\nabla} \cdot \boldsymbol{u}_1 + \frac{\partial w_1}{\partial z} = 0. \tag{2.50}$$

Integrating this equation for $s \in [-\beta d, z]$, we get:

$$w_1(t, \boldsymbol{x}, z) - w_1(\boldsymbol{x}, z = -\beta d, t) = -\int_{-\beta d}^{y} \boldsymbol{\nabla} \cdot \boldsymbol{u}_1(\boldsymbol{x}, s, t) ds. \tag{2.51}$$

At the bottom, we have the following kinematic condition:

$$w_1(\boldsymbol{x}, z = -\beta d, t) = -\beta \left(\frac{1}{\varepsilon}\frac{\partial d}{\partial t} + \boldsymbol{u}_1(\boldsymbol{x}, z = -\beta d, t) \cdot \boldsymbol{\nabla} d\right) .$$

Now from the expression of $\boldsymbol{u}_1$ done in (2.48) and after straightforward computations, one can obtain:

$$w_1(\boldsymbol{x}, z = -\beta d, t) = -\beta \left(\frac{1}{\varepsilon}\frac{\partial d}{\partial t} - \beta^2 d \boldsymbol{\nabla} w_c \cdot \boldsymbol{\nabla} d\right) . \tag{2.52}$$

Substituting equation (2.48) and equation (2.52) into equation (2.51) gives:

$$\begin{aligned} w_1(t, \boldsymbol{x}, z) = \frac{\beta(z + \beta d)^2}{2} \boldsymbol{\nabla} \cdot [(\boldsymbol{\nabla} \cdot \boldsymbol{u}_0)\boldsymbol{\nabla} d] + \frac{\beta(z + \beta d)^2}{2} [\boldsymbol{\nabla} d \cdot \boldsymbol{\nabla}(\boldsymbol{\nabla} \cdot \boldsymbol{u}_0)] \\ + \frac{(z + \beta d)^3}{6} \left[\boldsymbol{\nabla}^2(\boldsymbol{\nabla} \cdot \boldsymbol{u}_0)\right] + \beta^2(z + \beta d) \left[(\boldsymbol{\nabla} \cdot \boldsymbol{u}_0)(\boldsymbol{\nabla} d)^2\right] \\ - \beta \left(\frac{z^2 - \beta^2 d^2}{2}\right) \boldsymbol{\nabla}^2 w_c - \beta \left(\frac{1}{\varepsilon}\frac{\partial d}{\partial t} - \beta^2 d \boldsymbol{\nabla} w_c \cdot \boldsymbol{\nabla} d\right). \end{aligned} \tag{2.53}$$

The next step consists of collecting the above calculations and inject them into the system (2.41). We kept all terms in the order of μ, and we neglect all terms that have the order of μ^2. We do not make any assumptions for ε and β. We assume that both have the order $O(1)$. Then, mass and momentum conservation equations can be achieved as follows.

2.5.2 Mass conservation equation

The first equation of system (2.41) gives,

$$\partial_t \eta + \varepsilon \boldsymbol{u}_0 \cdot \boldsymbol{\nabla}\eta + \varepsilon\mu \boldsymbol{u}_1 \cdot \boldsymbol{\nabla}\eta = w_0 + \mu w_1 + O(\mu^2), \qquad z = \varepsilon\eta. \tag{2.54}$$

From (2.43), one have,

$$w_0(t, \boldsymbol{x}, z = \varepsilon\eta) = -h\boldsymbol{\nabla} \cdot \boldsymbol{u}_0 - \frac{\beta}{\varepsilon}\partial_t d - \beta \boldsymbol{u}_0 \cdot \boldsymbol{\nabla} d.$$

Plugging it into (2.54), one obtain,

$$\partial_t h + \varepsilon \boldsymbol{\nabla} \cdot [h\boldsymbol{u}_0] = \mu\varepsilon \mathcal{F}(\boldsymbol{x}, \boldsymbol{u}_0) + O(\mu^2) = 0, \tag{2.55}$$

with $\mathcal{F}$ is the function given by the following formula,

$$\mathcal{F}(\boldsymbol{x}, \boldsymbol{u}_0) = -\varepsilon \boldsymbol{u}_1(t, \boldsymbol{x}, z = \varepsilon\eta) \cdot \boldsymbol{\nabla}\eta + w_1(t, \boldsymbol{x}, z = \varepsilon\eta), \tag{2.56}$$

and hence, we can get its explicit expression from (2.48) and (2.53).

2.5.3 Momentum conservation equation

The momentum conservation equation is obtained from the dynamic boundary condition at the free surface, which corresponds to the second equation of the system (2.41). It is written,

$$\frac{\partial \phi_0}{\partial t} + \frac{1}{2}\varepsilon \boldsymbol{u}_0^2 + g\eta + \mu P_{NH}(t, \boldsymbol{x}, z = \varepsilon\eta) + O(\mu^2) = 0.$$

Applying the gradient $\boldsymbol{\nabla}$ to the previous equation and replacing the non-hydrostatic pressure by its expression given in (2.49), it yields to the following equation:

$$\begin{aligned} \partial_t \boldsymbol{u}_0 + \boldsymbol{\nabla}\left[\frac{1}{2}\varepsilon \boldsymbol{u}_0^2 + g\eta\right] + \mu\boldsymbol{\nabla}\left[\frac{1}{2}\beta^2\varepsilon w_c^2 + \beta(h - \beta d)(\partial_t w_c + \varepsilon \boldsymbol{u}_0 \cdot \boldsymbol{\nabla} w_c)\right] \\ + \mu\boldsymbol{\nabla}\left[\frac{1}{2}h^2\left[\varepsilon(\boldsymbol{\nabla} \cdot \boldsymbol{u}_0)^2 - \varepsilon \boldsymbol{u}_0 \cdot \boldsymbol{\nabla}[\boldsymbol{\nabla} \cdot \boldsymbol{u}_0] - \partial_t(\boldsymbol{\nabla} \cdot \boldsymbol{u}_0)\right]\right] + O(\mu^2) = 0. \end{aligned} \tag{2.57}$$

2.5.4 Asymptotic model

Gathering (2.55) and (2.57), we present the following free surface model

$$\begin{cases} \partial_t h & +\varepsilon \boldsymbol{\nabla} \cdot [h\boldsymbol{u}_0] = \mu\varepsilon \mathcal{F}(\boldsymbol{x}, \boldsymbol{u}_0) + O(\mu^2) = 0, \\ \partial_t \boldsymbol{u}_0 & +\boldsymbol{\nabla}\left[\frac{1}{2}\varepsilon \boldsymbol{u}_0^2 + g\eta\right] + \mu\boldsymbol{\nabla}\left[\frac{1}{2}\beta^2\varepsilon w_c^2 + \beta(h - \beta d)(\partial_t w_c + \varepsilon \boldsymbol{u}_0 \cdot \boldsymbol{\nabla} w_c)\right] \\ & +\mu\boldsymbol{\nabla}\left[\frac{1}{2}h^2\left[\varepsilon(\boldsymbol{\nabla} \cdot \boldsymbol{u}_0)^2 - \varepsilon \boldsymbol{u}_0 \cdot \boldsymbol{\nabla}[\boldsymbol{\nabla} \cdot \boldsymbol{u}_0] - \partial_t(\boldsymbol{\nabla} \cdot \boldsymbol{u}_0)\right]\right] + O(\mu^2) = 0, \end{cases} \tag{2.58}$$

where $h = \varepsilon\eta + \beta d$ is the nondimensionalized local water height, $\boldsymbol{u}_0$ is the first term of the asymptotic expansion (2.34) applied to the horizontal velocity $\boldsymbol{u}(t, \boldsymbol{x}, z)$, w_c is the vertical acceleration at the bottom given in (2.44) and $\mathcal{F}(\boldsymbol{x}, \boldsymbol{u}_0)$ is given in (2.56)
The system of equation (2.58) shows a weakly-dispersive and fully nonlinear ($\varepsilon = O(1)$) free surface model with large variation on the bathymetry ($\beta = O(1)$) for moving bottom (varies in time and in space $d = d(t, x)$).

Remark 3. Note that many other asymptotic models can be obtained from (2.58) according to the specific regime in the first part of this section. For example, in addition to the assumption on the shallowness parameter, we suppose a small amplitude regime $\varepsilon = O(\mu)$, one can recover the Boussinesq type models (see [71] and reference therein for more details). Besides, if we suppose a small variation of the topography, we recover the Peregrin model given in [76].

2.6 Depth-averaged equations

This section is devoted to the derivation of depth-averaged shallow water models (when the shallowness parameter μ is small). The most general model is addressed in §2.6.1 when no assumptions are taken for ε and β, then we obtain in §2.6.2 the Serre-Green-Naghdi model (also called fully nonlinear Boussinesq model). Adding the assumption *small variation of the amplitude* ($\varepsilon = O(\mu)$), Boussinesq type models are obtained in §2.6.3. We finish this section by giving the nonlinear shallow water equations (NSWE) in §2.6.4, which are obtained by neglecting all terms at order μ.
This section's key point is the link between the first-order term of the horizontal velocity $\boldsymbol{u}_0$ and the average one. Let us start by looking for the average velocity $\bar{\boldsymbol{u}}(t, \boldsymbol{x})$ as a function of $\boldsymbol{u}_0(t, \boldsymbol{x})$,

$$\bar{\boldsymbol{u}}(t, \boldsymbol{x}) = \frac{1}{h(t, \boldsymbol{x})} \int_{-\beta d}^{\varepsilon\eta} \boldsymbol{u}(t, \boldsymbol{x}, z)\, dz\ . \tag{2.59}$$

Applying the asymptotic expansion (2.34) to $\boldsymbol{u}(t, \boldsymbol{x}, z)$ and substituting it into the previous equation, we get:

$$\bar{\boldsymbol{u}}(t, \boldsymbol{x}) = \frac{1}{h(t, \boldsymbol{x})} \int_{-\beta d}^{\varepsilon\eta} \Big(\boldsymbol{u}_0(t, \boldsymbol{x}) + \mu \boldsymbol{u}_1(t, \boldsymbol{x}, z) + O(\mu^2)\Big)\ dz.$$

Replace $\boldsymbol{u}_1$ by its explicit expression given in (2.48), we end up with:

$$\bar{\boldsymbol{u}} = \boldsymbol{u}_0 + \frac{\mu}{h}\left(-\frac{1}{2}\beta(h^2\boldsymbol{\nabla}\cdot\boldsymbol{u}_0)\boldsymbol{\nabla}d - \frac{1}{6}h^3\boldsymbol{\nabla}[\boldsymbol{\nabla}\cdot\boldsymbol{u}_0] + \beta\frac{(\varepsilon\eta)^2 - (\beta d^2)}{2}\boldsymbol{\nabla}w_c\right) + O(\mu^2).$$

After some straightforward calculation, we get:

$$\bar{\boldsymbol{u}}(t, \boldsymbol{x}) = \boldsymbol{u}_0 + \mu\left(-\frac{1}{2}\beta(h\boldsymbol{\nabla}\cdot\boldsymbol{u}_0)\boldsymbol{\nabla}d - \frac{1}{6}h^2\boldsymbol{\nabla}\left[\boldsymbol{\nabla}\cdot\boldsymbol{u}_0\right] + \beta\frac{\varepsilon\eta - \beta d}{2}\boldsymbol{\nabla}w_c\right) + O(\mu^2). \tag{2.60}$$

We can then easily obtain the expression of $\boldsymbol{u}_0(t, \boldsymbol{x})$ in terms of $\bar{\boldsymbol{u}}(t, \boldsymbol{x})$, as follows:

$$\boldsymbol{u}_0(t, \boldsymbol{x}) = \bar{\boldsymbol{u}} - \mu\left(-\frac{1}{2}\beta(h\boldsymbol{\nabla}\cdot\bar{\boldsymbol{u}})\boldsymbol{\nabla}d - \frac{1}{6}h^2\boldsymbol{\nabla}[\boldsymbol{\nabla}\cdot\bar{\boldsymbol{u}}] + \beta\frac{\varepsilon\eta - \beta d}{2}\boldsymbol{\nabla}w_c\right) + O(\mu^2). \tag{2.61}$$

Then we can calculate its quadrature as follows:

$$\boldsymbol{u}_0^2 = \bar{\boldsymbol{u}}^2 - 2\mu\bar{\boldsymbol{u}}\cdot\left(-\frac{1}{2}\beta(h\boldsymbol{\nabla}\cdot\bar{\boldsymbol{u}})\boldsymbol{\nabla}d - \frac{1}{6}h^2\boldsymbol{\nabla}[\boldsymbol{\nabla}\cdot\bar{\boldsymbol{u}}] + \beta\frac{\varepsilon\eta - \beta d}{2}\boldsymbol{\nabla}w_c\right) + O(\mu^2).$$

2.6.1 Serre-Green-Naghdi equations for a moving bottom

The Serre-Green-Naghdi (SGN) equations are a second-order approximation of the Euler-Lagrange equations, i.e., the terms of the order $O(\mu)$ are kept in the equations. This model's range is wider than the weakly dispersive weakly nonlinear Boussinesq type models since it retains the terms $O(\varepsilon\mu)$ and $O(\varepsilon\beta)$ which are neglected in Boussinesq equations, which makes it more complex. The model is obtained by replacing $\boldsymbol{u}_0(t,\boldsymbol{x})$ by $\bar{\boldsymbol{u}}(t,\boldsymbol{x})$ in (2.58) using (2.61). After straightforward algebraic, one gets:

$$\begin{cases} \partial_t h + & \varepsilon\boldsymbol{\nabla}\cdot[h\bar{\boldsymbol{u}}] = 0, \\ \partial_t \bar{\boldsymbol{u}} & +\boldsymbol{\nabla}[\frac{1}{2}\varepsilon\bar{\boldsymbol{u}}^2 + G\eta] + \frac{1}{3h}\mu\boldsymbol{\nabla}\left[h^3\left((\boldsymbol{\nabla}\cdot\bar{\boldsymbol{u}})^2 - \boldsymbol{\nabla}\cdot(\partial_t\bar{\boldsymbol{u}}) - \bar{\boldsymbol{u}}\cdot\boldsymbol{\nabla}(\boldsymbol{\nabla}\cdot\bar{\boldsymbol{u}})\right)\right] \\ & +\mu\beta\frac{1}{2h}\boldsymbol{\nabla}\left[h^2\gamma\right] - \mu\beta^2\gamma\boldsymbol{\nabla}d + \mu\beta Q(\bar{\boldsymbol{u}}) = 0, \end{cases} \tag{2.62}$$

where:

$$Q(\bar{\boldsymbol{u}}) = -\varepsilon\frac{h}{2}[(\boldsymbol{\nabla}\cdot\bar{\boldsymbol{u}})^2 - (\bar{\boldsymbol{u}}\cdot\boldsymbol{\nabla}[\boldsymbol{\nabla}\cdot\bar{\boldsymbol{u}}])]\boldsymbol{\nabla}d + \frac{h}{2}\partial_t(\boldsymbol{\nabla}\cdot\bar{\boldsymbol{u}})\boldsymbol{\nabla}d,$$

$$\gamma = \partial_t w_c + \bar{\boldsymbol{u}}\cdot\boldsymbol{\nabla}w_c,$$

$$\text{and} \quad w_c = -\frac{\partial d}{\partial t} - \bar{\boldsymbol{u}}\cdot\boldsymbol{\nabla}d.$$

Another reformulation of the previous system can be obtained by introducing operator $\mathcal{T}$:

$$\begin{cases} \partial_t h + \varepsilon\boldsymbol{\nabla}\cdot[h\bar{\boldsymbol{u}}] = 0, \\ (I+\mu\mathcal{T})\partial_t\bar{\boldsymbol{u}} + \boldsymbol{\nabla}[\frac{1}{2}\varepsilon\bar{\boldsymbol{u}}^2 + G\eta] + \frac{1}{3h}\mu\boldsymbol{\nabla}\left[h^3\left((\boldsymbol{\nabla}\cdot\bar{\boldsymbol{u}})^2 - \bar{\boldsymbol{u}}\cdot\boldsymbol{\nabla}(\boldsymbol{\nabla}\cdot\bar{\boldsymbol{u}})\right)\right] \\ +\mu\left(\frac{1}{2h}\boldsymbol{\nabla}\left[h^2\gamma\right] - \beta\gamma\boldsymbol{\nabla}d - \varepsilon\beta Q_1(\bar{\boldsymbol{u}})\right) = 0. \end{cases} \tag{2.63}$$

with,

$$\mathcal{T}\cdot w = -\frac{1}{3h}\boldsymbol{\nabla}(h^3\boldsymbol{\nabla}\cdot w) + \frac{h}{2}\boldsymbol{\nabla}d\,\boldsymbol{\nabla}\cdot w \tag{2.64}$$

$$\text{and} \quad Q_1(\bar{\boldsymbol{u}}) = \varepsilon\frac{h}{2}[(\boldsymbol{\nabla}\cdot\bar{\boldsymbol{u}})^2 - (\bar{\boldsymbol{u}}\cdot\boldsymbol{\nabla}[\boldsymbol{\nabla}\cdot\bar{\boldsymbol{u}}])]\boldsymbol{\nabla}d. \tag{2.65}$$

The advantage of this form is that by inverting operator $(I+\mu\mathcal{T})$, we add regularity, since, the latter acts as an averaging term and should, therefore, facilitate the numerical computations.
There are other particular reformulations of the Serre-Green-Naghdi system, namely, the hyperbolic system given in [43] and the non-hydrostatic formulation.

2.6.2 Serre-Green-Naghdi equations for fixed bottom

Replacing $d(t,\boldsymbol{x})$ by $d(x)$ in (2.63), the vertical acceleration at the bottom becomes: $w_c = -\beta\bar{\boldsymbol{u}}\cdot\boldsymbol{\nabla}d$, consequently

$$\gamma = \beta(\partial_t w_c + \varepsilon\bar{\boldsymbol{u}}\cdot\boldsymbol{\nabla}w_c) = -\beta\partial_t\bar{\boldsymbol{u}}\cdot\boldsymbol{\nabla}d - \varepsilon\beta\,\bar{\boldsymbol{u}}\cdot\boldsymbol{\nabla}[\bar{\boldsymbol{u}}\cdot\boldsymbol{\nabla}d].$$

Plugging into system (2.63), we get the following famous Serre-Green-Naghdi equation for non-flat bottom

$$\begin{cases} \partial_t h + \varepsilon \boldsymbol{\nabla} \cdot [h\bar{\boldsymbol{u}}] = 0, \\ (I + \mu \mathcal{T}[\beta d, h])\partial_t \bar{\boldsymbol{u}} + \boldsymbol{\nabla}[\frac{1}{2}\varepsilon \bar{\boldsymbol{u}}^2 + G\eta] + \mu\varepsilon \frac{1}{3h}\mu \boldsymbol{\nabla}\left[h^3\left((\boldsymbol{\nabla}\cdot\bar{\boldsymbol{u}})^2 - \bar{\boldsymbol{u}}\cdot\boldsymbol{\nabla}(\boldsymbol{\nabla}\cdot\bar{\boldsymbol{u}})\right)\right] \\ \qquad +\mu\varepsilon\beta Q_1[\beta d, h](\bar{\boldsymbol{u}}) = 0, \end{cases} \tag{2.66}$$

where

$$\mathcal{T}[\beta d, h]\cdot w = -\frac{1}{3h}\boldsymbol{\nabla}(h^3\boldsymbol{\nabla}\cdot w) + \beta\frac{1}{2h}[h^2\boldsymbol{\nabla}d\,\boldsymbol{\nabla}\cdot w - \boldsymbol{\nabla}(h^2\boldsymbol{\nabla}d\cdot w)] + \beta^2\boldsymbol{\nabla}d\boldsymbol{\nabla}d\cdot w \tag{2.67}$$

and the topography term $Q[\beta d, h]$ is defined as:

$$Q_1[\beta d, h] = \frac{1}{2h}\left[h^2(\bar{\boldsymbol{u}}\cdot\boldsymbol{\nabla}[\boldsymbol{\nabla}\cdot\bar{\boldsymbol{u}}] - (\boldsymbol{\nabla}\cdot\bar{\boldsymbol{u}})^2)\boldsymbol{\nabla}d - \boldsymbol{\nabla}(h^2\bar{\boldsymbol{u}}\cdot\boldsymbol{\nabla}[\bar{\boldsymbol{u}}\cdot\boldsymbol{\nabla}d])\right] + \beta\left(\bar{\boldsymbol{u}}\cdot\boldsymbol{\nabla}[\bar{\boldsymbol{u}}\cdot\boldsymbol{\nabla}d]\right)\boldsymbol{\nabla}d. \tag{2.68}$$

Remark 4. The Serre-Green-equations (2.66) can be simplified under the assumption $\varepsilon = O(\sqrt{\mu})$. We distinguish three different regimes by varying the parameter of topography β (the class of this equation is called in [60] moderately nonlinear). For example, if we impose the assumption $\beta = O(\varepsilon)$, the model that we can obtain for a flat bottom ($d = 0$) corresponds to the Camassa-Holm equation [22] (see [60] for more details).

2.6.3 Boussinesq equations

The Boussinesq equations are a second-order approximation of the Euler-Lagrange equations (2.19)–(2.24) with respect to the shallowness parameter μ, which have a better approximation compared to the nonlinear shallow water equations (2.71) ($O(\mu^2)$ instead of $O(\mu)$). In addition to the parameter μ, these equations are obtained under the assumption *weakly nonlinearity* i.e $\varepsilon = O(\mu)$. We consider here two variants in different topography regimes :

1. *Fully nonlinear topography* ($\beta = O(1)$)
   Neglecting in (2.66) the terms at the order $O(\mu^2)$ and $O(\varepsilon\mu)$ under the assumption $\varepsilon = O(\mu)$, we get the following equations:

$$\begin{cases} \partial_t h + \varepsilon \boldsymbol{\nabla} \cdot [h\bar{\boldsymbol{u}}] = 0, \\ \partial_t \bar{\boldsymbol{u}} + \boldsymbol{\nabla}[\frac{1}{2}\varepsilon \bar{\boldsymbol{u}}^2 + G\eta] + \mu Q_1(\boldsymbol{u}) = 0, \end{cases} \tag{2.69}$$

   with

$$Q_1(\boldsymbol{u}) = -\frac{1}{2h}\beta\boldsymbol{\nabla}[h^2\partial_t\boldsymbol{u}\cdot\boldsymbol{\nabla}d] + \beta\boldsymbol{\nabla}d\boldsymbol{\nabla}d\cdot\partial_t\boldsymbol{u},$$

   which corresponds to the Boussinesq model with topography derived by Peregrine in [77].

2. *Weakly non linear topography*
   In addition to the assumption *weakly nonlinearity*, the supplementary assumption *weak variation of the topography* ($(\beta = O(\mu))$ is considered here to obtain the following model

$$\begin{cases} \partial_t h + \varepsilon \boldsymbol{\nabla} \cdot [h\bar{\boldsymbol{u}}] = 0, \\ (1 - \frac{\mu}{3}\Delta)\partial_t \bar{\boldsymbol{u}} + \boldsymbol{\nabla}[\frac{1}{2}\varepsilon \bar{\boldsymbol{u}}^2 + G\eta] = 0. \end{cases} \tag{2.70}$$

The Boussinesq type model (2.69) was first derived in 1967 by D. Peregrine [77]. This model described the propagation of weakly non-linear long waves over a general non-flat bottom. It was from this landmark study that the modern era of long-wave modeling began. Over the past decade, these equations have captured the attention of the mathematics and coastal engineering community. This is due to their ability to correctly describe dispersive and non-linear effects (which is not the case with the Saint Venant equations). The applicability of this model touches several areas such as coastal engineering (harbor design, coastal defense structure, etc.) and offshore engineering (design of offshore platforms, underwater cables, etc.) (see [21] for a reasoned review in this field). This can be justified by the fact that the Boussinesq-type model contains more physics than the Saint-Venant equations. Based on this model, researchers have focused on the development of new models, and there are many variants [71, 69, 14].

2.6.4 Nonlinear shallow water equations

The nonlinear shallow water equations are an approximation of the order $O(\mu)$ of the Euler-Lagrange equations (2.19)–(2.24) in the sense that the terms of the order $O(\mu)$ are dropped :

$$\begin{cases} \partial_t h + \varepsilon \boldsymbol{\nabla} \cdot [h\bar{\boldsymbol{u}}] = 0, \\ \partial_t \bar{\boldsymbol{u}} + \boldsymbol{\nabla}[\frac{1}{2}\varepsilon \bar{\boldsymbol{u}}^2 + G\eta] = 0, \end{cases} \tag{2.71}$$

This model was developed for the first time by Adhémar Jean Claude Barré de Saint-Venant in the 19th Century as a reduction of the Navier-Stokes equations under certain assumptions on the horizontal and vertical scales [31, 47]. Thanks to the hyperbolic structure of these equations, sharp transitions between two different flow states result in a discontinuous solution, both in the water surface and the velocity. These equations are widely used in fluid mechanics because they can be solved analytically by the characteristic method [88]. Also, they can be easily resolved numerically, namely, many efficient finite volume schemes have been proposed [100].

2.7 Derivation via Euler equations

In this section, we present the strategy to derive the depth-averaged asymptotic models via incompressible Euler equations. To this end, we first introduce the Euler equations and the dimensionless problem by introducing the classical dispersive parameter μ.

We assume that the flow is governed, on the space-time domain Ω, by the three-dimensional irrotational and incompressible Euler equations :

$$\begin{aligned} \operatorname{div}[\rho_0 \boldsymbol{U}] &= 0, \\ \frac{\partial}{\partial t}(\rho_0 \boldsymbol{U}) + \operatorname{div}[\rho_0 \boldsymbol{U} \otimes \boldsymbol{U}] + \nabla p - \rho_0 \boldsymbol{F} &= 0 \end{aligned} \tag{2.72}$$

where $\boldsymbol{U} = (\boldsymbol{u}, w)$ is the velocity field, $\boldsymbol{u} = (u, v)$ is the horizontal velocity field, ρ_0 is the density of the fluid (taken to be constant), $\boldsymbol{F} = (0, 0, -g)$ is the external force of gravity with constant g and p is the pressure.

These equations are completed by the irrotational equation

$$\operatorname{curl}[\boldsymbol{U}] = 0 \tag{2.73}$$

and the kinematic boundary condition at the free surface

$$\frac{\partial}{\partial t}\eta + \boldsymbol{u} \cdot \boldsymbol{\nabla}\eta = w \text{ on } z = \eta \,. \tag{2.74}$$

We also assume that the pressure at the free surface level is equal to the atmospheric pressure p_0

$$p = p_0 \text{ on } z = \eta \,. \tag{2.75}$$

In the sequel, without loss of generality, we set $p_0 = 0$.
The impermeability condition at the free surface is given as follows,

$$\boldsymbol{u} \cdot \boldsymbol{\nabla} d = w \text{ on } z = d \,. \tag{2.76}$$

2.7.1 Asymptotic expansions

Let us consider the following scales involved in the wave motion: L a characteristic wave-length in the longitudinal and transversal directions and H a characteristic water depth. We then define the classical dispersive parameter μ (see *e.g.* [59])

$$\mu = \frac{H^2}{L^2}$$

We also introduce $\boldsymbol{U} = (U, W = \sqrt{\mu}U)$ the scale of fluid velocity. The time scale is $T = \dfrac{L}{U}$. We set $P = \dfrac{p}{\rho_0}$ and we define $\mathcal{P} = U^2$. For the sake of clarity, and because the calculations are given in the previous section, we consider here $\varepsilon = \beta = 1$.

This allows us to introduce the dimensionless quantities of time $\widetilde{t}$, space $(\widetilde{\boldsymbol{x}}, \widetilde{z})$, pressure $\widetilde{P}$, depth $\widetilde{d}$, water elevation $\widetilde{\eta}$ and velocity field $(\widetilde{U}, \widetilde{W})$, via the following scaling relation

$$\begin{aligned} \widetilde{\boldsymbol{x}} &= \frac{\boldsymbol{x}}{L}, \quad \widetilde{P} = \frac{P}{\mathcal{P}}, \\ \widetilde{\boldsymbol{u}} &= \frac{\boldsymbol{u}}{U}, \quad \widetilde{d} = \frac{d}{H}, \\ \widetilde{z} &= \frac{z}{H}, \quad \widetilde{\eta} = \frac{\eta}{H}, \\ \widetilde{t} &= \frac{t}{T}, \quad \widetilde{w} = \frac{w}{W} \,. \end{aligned} \tag{2.77}$$

Finally, we define the non-dimensional Froude's number

$$F_r = \frac{U}{\sqrt{gH}} .$$

For the sake of clarity and simplicity, dropping $\widetilde{\cdot}$, dividing the Euler equations (2.72) by ρ_0, using the dimensionless variables (2.77), and reordering the terms with respect to the powers of μ, the dimensionless incompressible Euler system (2.72) reads as follows:

$$\boldsymbol{\nabla} \cdot \boldsymbol{u} + \frac{\partial}{\partial z} w = 0 \tag{2.78}$$

$$\frac{\partial}{\partial t}\boldsymbol{u} + \boldsymbol{u}(\boldsymbol{\nabla} \cdot \boldsymbol{u}) + w\frac{\partial}{\partial z}\boldsymbol{u} + \boldsymbol{\nabla} P = 0 \tag{2.79}$$

$$\mu\left(\frac{\partial}{\partial t} w + \boldsymbol{u} \cdot \boldsymbol{\nabla} w + w\frac{\partial}{\partial z} w\right) + \frac{\partial}{\partial z} P = -\frac{1}{{F_r}^2} \tag{2.80}$$

The boundary conditions (2.74), (2.75) and (2.76) read

$$\frac{\partial}{\partial t}\eta + \boldsymbol{u} \cdot \boldsymbol{\nabla}\eta = w \text{ and } P = 0 \text{ on } z = \eta \tag{2.81}$$

$$\boldsymbol{u} \cdot \boldsymbol{\nabla} d = w \text{ on } z = d \tag{2.82}$$

and the irrotational equation (2.73) becomes

$$\frac{\partial}{\partial z}\boldsymbol{u} = \mu \boldsymbol{\nabla} w . \tag{2.83}$$

In what follows, we note $f_b(t, \boldsymbol{x}) = f(t, \boldsymbol{x}, z = d(\boldsymbol{x}))$ for a given function f and $\bar{f}$

$$\bar{f}(t, \boldsymbol{x}) = \frac{1}{\eta - d}\int_{d(\boldsymbol{x})}^{z} f(t, \boldsymbol{x}, z)\, dz \tag{2.84}$$

2.7.1.1 Asymptotic expansion of the fluid velocity

Let us first integrate Eq. (2.83) for $s \in [d(x), z]$, to get

$$\boldsymbol{u}(t, \boldsymbol{x}, z) = u_b(t, \boldsymbol{x}) + \mu\int_{d(\boldsymbol{x})}^{z} \boldsymbol{\nabla} w\, ds + O(\mu^2) . \tag{2.85}$$

Then, from the continuity equation (4.17), we have

$$\frac{\partial}{\partial z} w = -\boldsymbol{\nabla} \cdot \boldsymbol{u}$$

and integrating the above equation for $s \in [d(x), z]$, keeping in mind the boundary condition (2.82), we obtain

$$w(t, \boldsymbol{x}, z) = -\boldsymbol{\nabla} \cdot \left(\int_{d(x)}^{z} \boldsymbol{u}\, ds\right) .$$

By means of Eq. (2.85), the previous equation becomes:

$$w(t, \boldsymbol{x}, z) = -\boldsymbol{\nabla} \cdot [(z - d(\boldsymbol{x}))\boldsymbol{u}_b(t, \boldsymbol{x})] + O(\mu) . \tag{2.86}$$

By injecting Eq. (2.86) in (2.85), we get

$$\boldsymbol{u}(t,\boldsymbol{x},z) = \boldsymbol{u}_b(t,\boldsymbol{x}) - \mu \int_{d(\boldsymbol{x})}^{z} \boldsymbol{\nabla}\left[\boldsymbol{\nabla}\cdot((s-d(\boldsymbol{x}))\boldsymbol{u}_b(t,\boldsymbol{x}))\right]\, ds + O(\mu^2)\,.$$

Finally, we have

$$\boldsymbol{u}(t,\boldsymbol{x},z) = \boldsymbol{u}_b(t,\boldsymbol{x}) - \mu\boldsymbol{\nabla}\left[\boldsymbol{\nabla}\cdot\left(\frac{(z-d(\boldsymbol{x}))^2}{2}\boldsymbol{u}_b(t,\boldsymbol{x})\right)\right] + O(\mu^2) \tag{2.87}$$

As a consequence and through Eq. (2.87), we obtain

$$\begin{aligned}
\bar{\boldsymbol{u}}(t,\boldsymbol{x}) &= \frac{1}{\eta-d}\int_{d(\boldsymbol{x})}^{\eta(t,\boldsymbol{x})} u(t,\boldsymbol{x},z)\,dz \\
&= \frac{1}{\eta-d}\int_{d(\boldsymbol{x})}^{\eta(t,\boldsymbol{x})} \boldsymbol{u}_b(t,\boldsymbol{x}) - \mu\boldsymbol{\nabla}\left[\boldsymbol{\nabla}\cdot\left(\frac{(z-d(\boldsymbol{x}))^2}{2}\boldsymbol{u}_b(t,\boldsymbol{x})\right)\right]\, dz + O(\mu^2) \\
&= \boldsymbol{u}_b(t,\boldsymbol{x}) - \frac{\mu}{\eta-d}\int_{d(\boldsymbol{x})}^{\eta(t,\boldsymbol{x})} \boldsymbol{\nabla}\left[\boldsymbol{\nabla}\cdot\left(\frac{(z-d(\boldsymbol{x}))^2}{2}\boldsymbol{u}_b(t,\boldsymbol{x})\right)\right]\, dz + O(\mu^2)\,,
\end{aligned}$$

i.e.

$$\boldsymbol{u}_b(t,\boldsymbol{x}) = \bar{\boldsymbol{u}}(t,\boldsymbol{x}) + \frac{\mu}{\eta-d}\int_{d(\boldsymbol{x})}^{\eta(t,\boldsymbol{x})} \boldsymbol{\nabla}\left[\boldsymbol{\nabla}\cdot\left(\frac{(z-d(\boldsymbol{x}))^2}{2}\boldsymbol{u}_b(t,\boldsymbol{x})\right)\right]\, dz + O(\mu^2)\,. \tag{2.88}$$

Using the fact that

$$\boldsymbol{u}_b(t,\boldsymbol{x}) = \bar{\boldsymbol{u}}(t,\boldsymbol{x}) + O(\mu)$$

in Eq. (2.88) allows to write $\boldsymbol{u}_b(t,\boldsymbol{x})$ as a function of $\bar{\boldsymbol{u}}(t,\boldsymbol{x})$:

$$\boldsymbol{u}_b(t,x) = \bar{\boldsymbol{u}}(t,\boldsymbol{x}) + \frac{\mu}{\eta-d}\int_{d(\boldsymbol{x})}^{\eta(t,\boldsymbol{x})} \boldsymbol{\nabla}\left[\boldsymbol{\nabla}\cdot\left(\frac{(z-d(\boldsymbol{x}))^2}{2}\bar{\boldsymbol{u}}(t,\boldsymbol{x})\right)\right]\, dz + O(\mu^2)\,. \tag{2.89}$$

Finally, thanks to (2.85), (2.87), (2.89), we obtain

$$\begin{aligned}
\boldsymbol{u}(t,\boldsymbol{x},z) &= \boldsymbol{u}_b(t,\boldsymbol{x}) - \mu\boldsymbol{\nabla}\left[\boldsymbol{\nabla}\cdot\left(\frac{(z-d(\boldsymbol{x}))^2}{2}\boldsymbol{u}_b(t,\boldsymbol{x})\right)\right] + O(\mu^2)\,, \\
&= \bar{\boldsymbol{u}}(t,\boldsymbol{x}) + \frac{\mu}{\eta-d}\int_{d(\boldsymbol{x})}^{\eta(t,\boldsymbol{x})} \boldsymbol{\nabla}\left[\boldsymbol{\nabla}\cdot\left(\frac{(z-d(\boldsymbol{x}))^2}{2}\bar{\boldsymbol{u}}(t,\boldsymbol{x})\right)\right]\, dz \\
&\quad -\mu\boldsymbol{\nabla}\left[\boldsymbol{\nabla}\cdot\left(\frac{(z-d(\boldsymbol{x}))^2}{2}\bar{\boldsymbol{u}}(t,\boldsymbol{x})\right)\right] + O(\mu^2)\,.
\end{aligned} \tag{2.90}$$

Repeating the computations with Eqs. (2.86) and (2.90), we find

$$w(t,\boldsymbol{x},z) = -\boldsymbol{\nabla}\cdot[(z-d(\boldsymbol{x}))\bar{\boldsymbol{u}}(t,\boldsymbol{x})] + O(\mu)\,. \tag{2.91}$$

2.7.1.2 Pressure decomposition

Integrating for $s \in [z,\eta_{\text{eq}}]$, the equation (2.80), we get

$$P(t,\boldsymbol{x},z) = \frac{(\eta(t,\boldsymbol{x})-z)}{{F_r}^2} + \int_z^{\eta(t,x)} \mu\left(\frac{D}{Dt}w(t,\boldsymbol{x},s)\right)\, ds + O(\mu^2)\,,$$

where $\dfrac{D(\cdot)}{Dt} = \partial_t(\cdot) + \boldsymbol{u} \cdot \boldsymbol{\nabla}(\cdot) + w\partial_z(\cdot)$ is the material derivative.
Thanks to the free surface boundary condition (2.81), Eq. (2.90) and Eq. (4.66), we obtain the asymptotic expansion of the pressure P at order $O(\mu^2)$

$$P(t, x, y, z) = P_{\mathrm{h}}(t, x, z) + \mu P_{\mathrm{nh}}(t, x, z) + O(\mu^2)$$

where

$$P_{\mathrm{h}}(t, \boldsymbol{x}, z) = \frac{(\eta(t, \boldsymbol{x}) - z)}{{F_r}^2} \tag{2.92}$$

is the usual hydrostatic pressure and

$$\begin{aligned} P_{\mathrm{nh}}(t, \boldsymbol{x}, z) \quad = \quad & -\int_z^{\eta(t,\boldsymbol{x})} \frac{\partial}{\partial t}\boldsymbol{\nabla} \cdot ((s-d)\bar{\boldsymbol{u}}) + \bar{\boldsymbol{u}} \cdot \boldsymbol{\nabla}[\boldsymbol{\nabla} \cdot ((s-d)\bar{\boldsymbol{u}})]\, ds \\ & + \int_z^{\eta(t,\boldsymbol{x})} (\boldsymbol{\nabla} \cdot \bar{\boldsymbol{u}})(\bar{\boldsymbol{u}} \cdot \boldsymbol{\nabla} d) + (s-d)(\boldsymbol{\nabla} \cdot \bar{\boldsymbol{u}})^2\, ds \end{aligned}$$

is a non-hydrostatic pressure.

Handling the terms in the non-hydrostatic pressure differently, one can write

$$P_{\mathrm{nh}}(t, \boldsymbol{x}, z) = \mathcal{D}(\bar{\boldsymbol{u}}) \left(\frac{h^2}{2} - \frac{(z-d)^2}{2} \right) + (\eta - z)\mathcal{Q}(\bar{\boldsymbol{u}}) \tag{2.93}$$

where

$$\mathcal{D}(\boldsymbol{u}) = (\boldsymbol{\nabla} \cdot \boldsymbol{u})^2 - \frac{\partial}{\partial t}[\boldsymbol{\nabla} \cdot \boldsymbol{u}] - \boldsymbol{u} \cdot \boldsymbol{\nabla}[\boldsymbol{\nabla} \cdot \boldsymbol{u}]\,, \tag{2.94}$$

and

$$\mathcal{Q}(\boldsymbol{u}) = -\boldsymbol{u}^2 \boldsymbol{\nabla}^2 d + \left(\frac{\partial}{\partial t}\boldsymbol{u} + (\boldsymbol{\nabla} \cdot \boldsymbol{u})\boldsymbol{u} \right) \boldsymbol{\nabla} d\,. \tag{2.95}$$

2.7.2 Depth-averaged models

2.7.2.1 Mass conservation equation

Let us start from the continuity equation

$$\boldsymbol{\nabla} \cdot \boldsymbol{u} + \frac{\partial}{\partial z} w = 0\,.$$

Integration from d to η gives

$$\int_d^\eta \boldsymbol{\nabla} \cdot \boldsymbol{u}\, dz + w(t, \boldsymbol{x}, \eta) - w(t, \boldsymbol{x}, d) = 0\,.$$

Using the integral Leibniz rule (2.16), one gets

$$\boldsymbol{\nabla} \cdot \left(\int_d^\eta \boldsymbol{u}\, dz \right) + w(t, \boldsymbol{x}, \eta) - \boldsymbol{u} \cdot \boldsymbol{\nabla}\eta - w(t, \boldsymbol{x}, d) + \boldsymbol{u} \cdot \boldsymbol{\nabla}\eta = 0\,.$$

Finally, from boundary conditions (2.74) and (2.82), we obtain

$$\frac{\partial}{\partial t}\eta + \boldsymbol{\nabla} \cdot (h\bar{\boldsymbol{u}}) = 0\,. \tag{2.96}$$

2.7.2.2 Momentum conservation equation

Let us start from the momentum equation (2.79),

$$\frac{\partial}{\partial t}\boldsymbol{u} + \boldsymbol{u}(\boldsymbol{\nabla}\cdot\boldsymbol{u}) + w\frac{\partial}{\partial z}\boldsymbol{u} + \boldsymbol{\nabla}P = 0\,.$$

Integrating from d to η, as follows

$$\left(\int_d^\eta \frac{\partial}{\partial t}\boldsymbol{u}\,dz\right) + \int_d^\eta \boldsymbol{\nabla}\boldsymbol{u}^2\,dz + \int_d^\eta \frac{\partial}{\partial z}(\boldsymbol{u}w)\,dz + \int_d^\eta \boldsymbol{\nabla}P\,dz = 0 \tag{2.97}$$

and using the integral Leibniz rule (2.16) and boundary conditions (2.74) and (2.82), we get

$$\frac{\partial}{\partial t}\left(\int_d^\eta \boldsymbol{u}\,dz\right) + \boldsymbol{\nabla}\left(\int_d^\eta \boldsymbol{u}^2\,dz\right) + \boldsymbol{\nabla}\left(\int_d^\eta P\,dz\right) = P(t,\boldsymbol{x},d)\boldsymbol{\nabla}d\,.$$

It gives, using the asymptotic expansions (2.90)

$$\frac{\partial}{\partial t}(h\bar{\boldsymbol{u}}) + \boldsymbol{\nabla}(h\bar{\boldsymbol{u}}^2 + Gh) + \mu\frac{1}{3h}\boldsymbol{\nabla}(h^3(\mathcal{D}(\bar{\boldsymbol{u}}))) + \mu Q_1(\bar{\boldsymbol{u}}) = 0 \tag{2.98}$$

where

$$Q_1(\bar{\boldsymbol{u}}) = \boldsymbol{\nabla}\left(\int_d^\eta (\eta - z)Q(\bar{\boldsymbol{u}})\,dz\right) - hQ(\bar{\boldsymbol{u}})\boldsymbol{\nabla}d \tag{2.99}$$

where $\mathcal{D}$ and Q are given respectively in (2.94) and (2.95).

2.7.2.3 Depth averaged models

Gathering equations (2.96) and (2.98), we present the SGN equation given in §2.6.2 for $\varepsilon = \beta = 1$

$$\begin{cases} \dfrac{\partial}{\partial t}\eta + \boldsymbol{\nabla}\cdot(h\bar{\boldsymbol{u}}) &= 0\,, \\ \dfrac{\partial}{\partial t}(h\bar{\boldsymbol{u}}) + \boldsymbol{\nabla}(h\bar{\boldsymbol{u}}^2 + Gh) + \mu\dfrac{1}{3h}\boldsymbol{\nabla}(h^3(\mathcal{D}(\bar{\boldsymbol{u}}))) + \mu Q_1(\bar{\boldsymbol{u}}) &= 0 \end{cases} \tag{2.100}$$

where $\mathcal{D}$ and Q_1 are given in (2.94) and (2.99).
Note that the weakly nonlinear, weakly dispersive Boussinesq equations (2.69) and the Nonlinear shallow water equations (2.71) can be also recovered from (2.100).

2.8 Conclusion

In this chapter, we have presented two methods, the first based on a variational principle and the second based on Euler's approximation to derive asymptotic models. Next, we derived some shallow water flow models by choosing specific regimes; the non-linear shallow water equations represent a robust system of hyperbolic equations that is not difficult to implement numerically but fails to describe the physical phenomena where the dispersion is present. Dispersive equations such as the Boussinesq or Serre-Green-Naghdi system are more physical than non-linear equations in shallow water because they contain more terms in the momentum conservation equation. These terms have third order derivatives that can lead to errors, including frequency dispersion errors. In the next chapter, we will discuss some techniques to correct these errors due to the presence of dispersion in dispersive models.

Chapter 3

Linear wave theory: dispersion and shoaling

Contents

3.1 Introduction

Due to the difficulty of solving general fluid mechanics equations (Navier-Stokes, Euler, Water-Waves) from an analytical and numerical point of view, many asymptotic models in shallow waters have been derived and developed. The Saint-Venant equations (introduced by Adhémar Jean Claude Barré de Saint-Venant in the 19th century [31, 47]) describe wave propagation. This model fails face to dispersive phenomena. Then, non-linear and dispersive models, namely the SGN and Boussinesq equations, are developed (see chapter 2 for the formal derivation of these equations). These equations have a hyperbolic structure (the same as the Saint Venant equations) combined with higher order derivatives (wave dispersion models) :

$$\begin{cases} \partial_t \eta + \boldsymbol{\nabla} \cdot [(\eta + d)\bar{\boldsymbol{u}}] = 0 \\ \partial_t \bar{\boldsymbol{u}} + \boldsymbol{\nabla}[\frac{1}{2}\bar{\boldsymbol{u}}^2 + g\eta] + \mathcal{D}(\boldsymbol{u}, \eta) = 0 \end{cases} \tag{3.1}$$

where η is free surface elevation, d is bathymetry, $\boldsymbol{u}$ is the mean velocity at depth, g is the gravity constant, and $\mathcal{D}$ is dispersive terms. The term $\mathcal{D}(\boldsymbol{u}, \eta)$ involved in these equations contains third-order derivatives, which may create high frequencies instabilities. Thus, different techniques have been developed to correct these errors, for example, linear wave theory. Since the linearized Boussinesq equation is the same as the SGN equation, we will focus in this chapter only on the weakly nonlinear and weakly dispersive Boussinesq-type equation (3.1).

The linear properties commonly used are phase velocity, group velocity, shoaling gradient, and wave kinematics [69, 68]. Non-linear performance is evaluated by analyzing the energy transfer between the components [71]. In [35], Dingemans proposes a sequence of steps in which Boussinesq-type models can be analyzed and improved:

- linear frequency behavior,
- linear shoaling behavior.

Significant improvements can be obtained both for linear properties such as linear frequency dispersion, linear shoaling, velocity profile, and for non-linear properties such as [21] amplitude dispersion. For example, following the BBM method [12], we can add artificial terms in the equation of the moment to improve the linear behavior in the equations

$$\begin{cases} \partial_t \eta + \boldsymbol{\nabla} \cdot [(\eta + d)\bar{\boldsymbol{u}}] = 0 \\ \partial_t \bar{\boldsymbol{u}} + \boldsymbol{\nabla}[\frac{1}{2}\bar{\boldsymbol{u}}^2 + g\eta] + \mathcal{D}(\boldsymbol{u}, \eta, \alpha) = 0 \end{cases} \tag{3.2}$$

where α is a free coefficient, to improve linear dispersive properties. This model was developed as in [71, 69, 68, 70] (see [45] for an analysis of the slight difference between these methods).

The analysis presented in this chapter is limited to linear dispersion and shoaling properties of Boussinesq type models over a wide range of relative water depths using standard procedures [71, 69, 68, 70]. Our goal is to compare some methods and choose

the most efficient method for the rest of this work. We do not intend to optimize these properties.

The chapter is organised as follows; in §3.2 we recall the linear wave theory, and we also calculate the dispersion relation and the shoaling gradient associated with the water wave equations. In §3.3, we recall some improved models and compare their linear behavior, in particular, the dispersion and the shoaling.

3.2 Linear first order stokes theory

The dispersion relation can be investigated by many methods, such as, the Fourier analysis on a horizontal bottom or the PDE linearization. The method that will be considered in this section is the Stokes linear theory. Let us start with the dispersion relation associated with the equations of water waves.

3.2.1 Linear dispersion properties

To simplify the calculations and the notations, we will place ourselves in a configuration in 2 dimensions of space (the calculations adapt perfectly to the problems in 3 dimensions). We consider the following $2D$ non-dimensional Water-Waves equations :

$$(WW)\begin{cases} \mu\partial_{xx}\phi + \partial_{zz}\phi = 0 & -d_0 + \beta d < z < \varepsilon\eta\,, \\ \partial_t\eta + \varepsilon\partial_x\phi\partial_x\eta - \partial_z\phi = 0 & z = \varepsilon\eta\,, \\ \dfrac{\beta}{\varepsilon}\partial_t d + \beta\partial_x\phi\partial_x d - \partial_z\phi = 0 & z = -d_0 + \beta d\,, \\ -\partial_t\phi + \dfrac{1}{2}\varepsilon(\partial_x\phi)^2 + \dfrac{1}{2}\varepsilon(\partial_z\phi)^2 - G\eta = 0 & z = \varepsilon\eta\,. \end{cases}$$

Here ϕ is the potential velocity, η is the elevation, and d represents the variation of the bottom. We also recall that β is a characteristic parameter of the bottom, and ε is the nonlinearity parameter.

To obtain the dispersion relation, we will first need to linearize the previous system around $\eta = 0$ and $u = 0$, or simply tend ε and β to 0. The layer of water must be of uniform depth, i.e $d = d_0 = cte$

$$(LWW)\begin{cases} \mu\partial_{xx}\phi + \partial_{zz}\phi = 0 & -d_0 < z < 0\,, \\ \partial_t\eta - \partial_z\phi = 0 & z = 0\,, \\ \partial_z\phi = 0 & z = -d_0\,, \\ \partial_t\phi + G\eta = 0 & z = 0\,. \end{cases} \tag{3.3}$$

In order to solve these equations and boundary conditions, we have to plug in a particular solution, in this case, plug in a propagating plane wave.

Here we assume a solution for the surface of a plane wave of amplitude A with wavenumber k and frequency dispersion ω. This solution for $\eta(x,t)$ looks like

$$\eta(x,t) = A\cos(kx - \omega t)\,. \tag{3.4}$$

The next step is to choose a particular form of the solution of ϕ, the same as (3.4) but separable on z as follows:

$$\phi(x, z, t) = \sin(kx - \omega t)\varphi(z) \,. \tag{3.5}$$

Now, by injecting the expression of ϕ into the first equation of the system (3.3), we obtain the following ordinary differential equation of second order:

$$\varphi''(z) - k^2\varphi(z) = 0, \qquad -d_0 < z < 0 \tag{3.6}$$

where the solution to the problem is in the following form:

$$\varphi(z) = \varphi_1 \exp(kz) + \varphi_2 \exp(-kz) \,. \tag{3.7}$$

The boundary condition at the bottom is

$$\varphi'(-d_0) = 0 \tag{3.8}$$

which leads to

$$\varphi_2 = \varphi_1 \exp(-kd_0) \,.$$

Using now the surface kinematic boundary condition

$$\frac{\partial \eta}{\partial t} - \frac{\partial \phi}{\partial z} = 0, \qquad z = 0 \tag{3.9}$$

which result in, join to (3.4), (3.5) and (3.6),

$$A\omega \sin(kx - \omega t) - k(\varphi_1 - \varphi_2)\sin(kx - \omega t) = 0 \,. \tag{3.10}$$

Gathering all the above expression, this leads to an expression for ϕ

$$\phi(x, z, t) = \frac{A\omega}{k} \frac{\cosh(k(z + d_0))}{\sinh(kd_0)} \sin(kx - \omega t) \,. \tag{3.11}$$

Using the following surface dynamic boundary condition,

$$\frac{\partial \phi}{\partial t} + G\eta = 0 \qquad z = 0 \,. \tag{3.12}$$

The dispersion relation is obtained by plugging (3.11) and (3.4) into (3.12), which leads to:

$$\omega^2 = gk \tanh(kd_0) \,. \tag{3.13}$$

Accordingly, the expression of the phase velocity and the phase group of the linear wave theory are respectively obtained:

$$C_S^p = \frac{\omega}{k} = \sqrt{g d_0 \frac{\tanh(kd_0)}{kd_0}} \,, \tag{3.14}$$

$$C_S^g = \frac{\partial \omega}{\partial k} = \left(\frac{1}{2} + \frac{kd_0}{\sinh(kd_0)}\right) C_S^p \,. \tag{3.15}$$

3.2.2 Linear shoaling properties

The shoaling coefficient is obtained in several ways. We prefer to follow the calculations presented by Madsen and Sørensen [69] in order to find the expression of the shoaling coefficient of the Water Waves equations. We use the energy flux conservation principle taking into account a varying bottom d.
It is well-known that wave energy E can be thought of as a sum of kinetic $\mathcal{K}$ and potential $\mathcal{P}$ energy,

$$E = \mathcal{K} + \mathcal{P} \ . \tag{3.16}$$

Depth-integrating the kinetic energy, it leads to,

$$\frac{1}{2}\rho \int_{-d_0}^{\eta} \boldsymbol{U}^2 dz = \frac{1}{2}\rho \int_{-d_0}^{\eta} (u^2 + w^2)\, dz \tag{3.17}$$

where $\boldsymbol{U} = (u, w)^T$ is the field velocity. Thus, for linear waves, by linearizing the last equation with respect to η, we obtain,

$$\frac{1}{2}\rho \int_{-d_0}^{\eta} (u^2 + w^2)\, dz \sim \frac{1}{2}\rho \int_{-d_0}^{0} (u^2 + w^2)\, dz \ .$$

As the flow is supposed to be irrotational, that means that $u = \partial_x \phi$ and $w = \partial_z \phi$, where ϕ is done in (3.11). Thus, from (3.11) one gets,

$$u(x, z, t) = A\omega \frac{\cosh(k(z + d_0))}{\sinh(kd_0)} \cos(kx - \omega t), \tag{3.18}$$

$$w(x, z, t) = A\omega \frac{\cosh(k(z + d_0))}{\sinh(kd_0)} \sin(kx - \omega t). \tag{3.19}$$

Then,

$$\begin{aligned}\frac{1}{2}\rho \int_{-d_0}^{0} (u^2 + w^2)\, dz =& \frac{1}{2}\rho \frac{A^2\omega^2}{\sinh^2(kd_0)} \left(\frac{\sinh(2kd_0) + 2kd_0}{4k} \right) \cos^2(\zeta) \\ &+ \frac{1}{2}\rho \frac{A^2\omega^2}{\sinh^2(kd_0)} \left(\frac{\sinh(2kd_0) - 2kd_0}{4k} \right) \sin^2(\zeta)\end{aligned}$$

with $\zeta = kx - \omega t$.
Now time average the last equation over a wave period, using the following identity

$$\frac{1}{T} \int_0^T cos^2(kx - \omega t)\, dt = \frac{1}{T} \int_0^T sin^2(kx - \omega t)\, dt = \frac{1}{2} \ . \tag{3.20}$$

Replacing ω by its expression given in (3.13), one gets,

$$\mathcal{K} = \frac{1}{4}\rho g A^2 \ . \tag{3.21}$$

The instantaneous potential energy $\mathcal{P}$ is obtained similarly,

$$\rho g \left[\int_{-d_0}^{\eta} z\, dz - \int_{-d_0}^{0} z\, dz \right] = \rho g \int_0^{\eta} z\, dz = \frac{1}{2}\rho g \eta^2 = \frac{1}{4}\rho g A^2 cos^2(\zeta) \ . \tag{3.22}$$

Time average (3.22), using the identity (3.20), one gets

$$\mathcal{P} = \frac{1}{4}\rho g A^2 \,. \tag{3.23}$$

Now consider the total mean energy, one gets from (3.21) and (3.23),

$$E = \mathcal{K} + \mathcal{P} = \frac{1}{2}\rho g A^2 \,. \tag{3.24}$$

From the linear wave theory, the energy flux F is given as follows (see [87] for more details),

$$F = E C_S^g \,, \tag{3.25}$$

where E (3.24) is the total energy and C_S^g is the group velocity associated to the Stokes linear theory.
From the energy flux conservation principle, one gets

$$\frac{\partial}{\partial x}(A^2 C_S^g) = 0 \,, \tag{3.26}$$

where A is the amplitude of the wave and C_S^g previously defined in (3.15)

$$C_S^g = \frac{1}{2}(1 + \mathcal{G}) C_S^p \,,$$

with $\mathcal{G} = \dfrac{2kd_0}{\sinh(kd_0)}$ and C_S^p is the phase velocity given by equation (3.14) for a constant bottom. Equation 3.26 gives

$$\frac{A_x}{A} = -\frac{1}{2}\left(\frac{\mathcal{G}_x}{1+\mathcal{G}} + \frac{(C_S^p)_x}{C_S^p}\right) \,. \tag{3.27}$$

Now, using the following definition of the phase velocity:

$$C^p = \frac{\omega}{k} \,.$$

Differentiating this equation with respect to x and considering a constant frequency ω, we get

$$\frac{(C_S^p)_x}{C_S^p} = -\frac{k_x}{k} \,. \tag{3.28}$$

Furthermore, assuming ω and g are constants and using (3.13) we can express k_x/k as a function of d_x/d as follows

$$\frac{k_x}{k} = -\left(\frac{kd_0}{kd_0 + \sinh(kd_0)\cosh(kd_0)}\right)\frac{d_x}{d} \,. \tag{3.29}$$

Substituting equation (3.28) and (3.29) into the equation (3.27), after straightforward computation, we get the following shoaling relation,

$$\frac{A_x}{A} = \upsilon^s_{Stokes}\frac{d_x}{d} \,, \tag{3.30}$$

where

$$\upsilon^s_{Stokes} = \frac{\left(1 + \frac{1}{2}(1 - \cosh(2kd_0))\mathcal{G}\right)\mathcal{G}}{(1+\mathcal{G})^2}$$

is the so-called coefficient of shoaling of Stokes.

3.3 Linear theory for dispersive models

In this section, we study the linear properties of dispersive models, including linear dispersion and shoaling characteristics. For the sake of simplicity, we consider here a Boussinesq model that is weakly non-linear and weakly dispersive (the linear analysis fits perfectly with the SGN model). We recall that these equations can be obtained as depth-averaged asymptotic approximations of incompressible Euler equations or Euler's Lagrange equations. If a denotes a reference wave amplitude, H a reference water depth and L a typical wavelength, the non-linearity parameter ε and the dispersion parameter μ are defined by:

$$\varepsilon = \frac{a}{H}\,, \qquad \mu = \frac{H^2}{L^2}\,.$$

The Boussinesq equations are obtained under the assumption of the low amplitude $\varepsilon = O(\mu)$, in the form of asymptotic approximations of order $O(\mu^2, \varepsilon\mu)$ (we refer the reader to chapter 2 for more details on the derivation of this model). Since the linear dispersion analysis is the same in one or two dimensions, we recall the models in unidimensional form.

In the remainder of this section, d denotes the bathymetry term, η is the elevation of the wave relative to a reference zero level, and $h = \eta + d$ represents the water depth.

Peregrine Model

The most common model of Boussinesq is the following model, derived by Peregrine in 1976:

$$\left\{\begin{array}{l} \eta_t + [hu]_x = 0\,, \\ u_t + uu_x + g\eta_x - \left(\dfrac{d}{2}[du]_{xxt} - \dfrac{d^2}{6}u_{xxt}\right) = 0\,. \end{array}\right. \tag{3.31}$$

Here u denotes the depth-averaged velocity. This model is presented in a non-dimensional form as follows:

$$\left\{\begin{array}{l} \eta_t + [hu]_x = 0\,, \\ u_t + \varepsilon uu_x + g\eta_x - \mu\left(\dfrac{d}{2}[du]_{xxt} - \dfrac{d^2}{6}u_{xxt}\right) = 0\,. \end{array}\right. \tag{3.32}$$

The previous system can be reformulated by introducing the elliptic operator $\mathcal{T}$, so we get:

$$\left\{\begin{array}{l} \eta_t + [hu]_x = 0 \\ (1 - \mu\mathcal{T})u_t + \varepsilon uu_x + g\eta_x = 0 \end{array}\right. \tag{3.33}$$

with

$$\mathcal{T}(W) = \frac{d}{2}[dW]_{xx} - \frac{d^2}{6}W_{xx}\,. \tag{3.34}$$

Starting from this model, several other variations can be constructed.

3.3.1 Improved models

In this section, we recall various tricks to improve linear frequency dispersion and linear shoaling characteristics. The first one is the so-called BBM *trick* [12] which is based on the observation that

$$\begin{aligned}\partial_t u =& -g\partial_x\eta + O(\varepsilon,\mu)\\ =&\alpha\partial_t u - (1-\alpha)g\partial_x\eta + O(\varepsilon,\mu)\end{aligned}$$

with α is a real number. Then in §3.3.1.2 we recall Beji-Nadaoka method [8] which consists to adding artificial terms in the momentum equation. We finish this section by giving the Nwogu method [71], which consists of a change of unknown for the velocity. More precisely, we introduce the velocity u_θ by $u_\theta = u(t, x, \theta d)$.

3.3.1.1 BBM *trick*

This method was introduced to derive the BBM equations from the KDV equation [8]. This method has subsequently been used by various researchers to improve linear dispersion and shoaling characteristics [14, 25, 61, 16]. Following these works, we can improve the Peregrine model by adding a parameter that will allow the improvement of the frequency dispersion. We perturb the system through a simple process while remaining consistent with the original model (Peregrine). We begin by recalling the Peregrine's system with a flat bottom:

$$\begin{cases}\partial_t\eta + \partial_x(hu) = 0\,,\\ \partial_t u + \partial_x(g\eta + \varepsilon\dfrac{1}{2}u^2) - \mu\dfrac{1}{3}\partial_t\partial_x^2 u = 0\,.\end{cases} \tag{3.35}$$

We can rewrite problem (3.35) in the following form:

$$\begin{cases}\partial_t\eta + \partial_x(hu) = 0\,,\\ (1-\mu\mathcal{T})\partial_t u + \partial_x(g\eta + \varepsilon\dfrac{1}{2}u^2) = 0\,.\end{cases} \tag{3.36}$$

We come back to the problem (3.35), we notice that:

$$\partial_t u = -g\partial_x\eta - O(\mu)\,. \tag{3.37}$$

Let $\alpha \in \mathbb{R}$, multiplying the previous equation by $(1-\alpha)$, we get

$$\partial_t u = \alpha\partial_t u - (1-\alpha)g\partial_x\eta - (1-\alpha)\,O(\mu)\,. \tag{3.38}$$

We replace $\partial_t u$ by its expression given in (3.38) in the second equation of the system (3.36), we obtain the following equation:

$$(1-\mu\mathcal{T})(\alpha\partial_t u - (1-\alpha)g\partial_x\eta - (1-\alpha)\,O(\mu)) + \partial_x(g\eta + \varepsilon u^2) + O(\mu^2) = 0\,.$$

After simplification, we get:

$$\begin{aligned}(I-\mu\alpha\mathcal{T})\partial_t u + (1-\mu(\alpha-1)\mathcal{T})g\partial_x\eta - (1-\alpha)(\partial_t u + g\partial_x\eta) - (1-\alpha)\,O(\mu))\\ + \varepsilon u\partial_x u) + O(\mu^2) = 0\end{aligned}$$

and

$$(I - \mu\alpha\mathcal{T})\partial_t u + 1 - \mu(\alpha - 1)\mathcal{T})g\partial_x\eta + \varepsilon u\partial_x u) + O(\mu^2) = 0 \,.$$

Now, we have

$$(1 - \mu(\alpha - 1)\mathcal{T})g\partial_x\eta = \frac{1}{\alpha}g\partial_x\eta + \frac{\alpha - 1}{\alpha}(I - \mu\alpha\mathcal{T})g\partial_x\eta \,.$$

As a result, the system (3.35) becomes:

$$\begin{cases} \partial_t\eta + \partial_x(hu) = 0 \,, \\ (1 - \mu\alpha\mathcal{T})(\partial_t u + \dfrac{\alpha - 1}{\alpha}g\partial_x\eta) + \varepsilon u\partial_x u + \dfrac{1}{\alpha}g\partial_x\eta = 0 \,. \end{cases} \tag{3.39}$$

After the inversion of the elliptic operator $\mathcal{T}$ we get the following enhancement Boussinesq equations:

$$\begin{cases} \partial_t\eta + \partial_x(hu) = 0 \,, \\ \partial_t u + \dfrac{\alpha - 1}{\alpha}g\partial_x\eta + (1 - \mu\alpha\mathcal{T})^{-1}(\varepsilon u\partial_x u + \dfrac{1}{\alpha}g\partial_x\eta) = 0 \,. \end{cases} \tag{3.40}$$

3.3.1.2 Beji-Nadaoka model

Beji and Nadaoka derived their enhancement model as follows: adding and subtracting term $\mu\beta\mathcal{T}(u_t)$ into the momentum equation of the non-dimensional Peregrine system (3.33). The following fact is used

$$u_t = -g\eta_x + O(\varepsilon, \mu) \,.$$

Subsequently term $\mu\beta\mathcal{T}(u_t)$ is replaced by $\mu\beta\mathcal{T}(\eta_x)$ to get the following system:

$$\begin{cases} \eta_t + [hu]_x = 0 \,, \\ (1 - \mu\mathcal{T})u_t + \varepsilon u u_x + g\eta_x - \mu\beta\mathcal{T}(u_t) - \mu\beta g\mathcal{T}(\eta_x) = 0 \,. \end{cases} \tag{3.41}$$

Another reformulation of the the Beji-Nadaoka model can be obtained as follows:

$$\begin{cases} \eta_t + [hu]_x = 0 \,, \\ (1 - \mu\beta\mathcal{T})(u_t + g\eta_x) + \varepsilon u u_x - \mu\mathcal{T}(u_t) = 0 \,, \end{cases} \tag{3.42}$$

where $\mathcal{T}$ is the elliptic operator (3.34). It's noted that adding parameter β improves the dispersion relation.

3.3.1.3 Nwogu Model

The extended model of Nwogu [71] is obtained by enhancing the Peregrine model by replacing the depth-averaged velocity by the velocity at an arbitrary elevation of z_θ. We denote $u_\theta = u(x, z = -\theta d, t)$. The Nwogu model in the non-dimensional form can be written as:

$$\begin{cases} \eta_t + [hu]_x - \mu[d\mathcal{T}^a(u_\theta)]_x = 0 \,, \\ (1 - \mu\mathcal{T}^b)u_t + \varepsilon u u_x + g\eta_x = 0 \,, \end{cases} \tag{3.43}$$

with

$$\mathcal{T}^a(W) = a_1 \frac{d}{2}[dW]_{xx} - a_2 \frac{d^2}{6} W_{xx} \,, \tag{3.44}$$

$$\mathcal{T}^b(W) = b_1 \frac{d}{2}[dW]_{xx} - b_2 \frac{d^2}{6} W_{xx} \,. \tag{3.45}$$

For $\theta \in (0, 1)$, the values of such expression are given as follows:

$$a_1 = -2\theta - 1; \quad a_2 = 3\theta^2 - 1; \quad b_1 = -2\theta; \quad b_2 = 3\theta^2 \tag{3.46}$$

Remark 5. The addition of operators $\mathcal{T}^a$ and $\mathcal{T}^b$ to the Nwogu model (3.43) makes the structure of the equations more complicated compared to the Peregrine model.

3.3.2 Dispersion properties

By following the section §3.2.1, the linear dispersion relation can be obtained from the linear wave theory for the three extended Boussinesq models presented in §3.3.1. We then compare the three methods at the same time.

3.3.2.1 Dispersion properties for Boussinesq models

BBM *trick*

The dispersion relation is obtained by looking for plane wave solutions in the form $u = u_0 e^{i(kx-\omega t)}$ and $\eta = \eta_0 e^{i(kx-\omega t)}$, where k is the wavenumber and ω is the time pulse of the next linearized system:

$$\begin{cases} \partial_t \eta + \partial_x (hu) = 0 \,, \\ \partial_t u + \dfrac{\alpha - 1}{\alpha} g \partial_x \eta + (1 - \dfrac{1}{3}\mu\alpha\partial_x^2)^{-1}(\dfrac{1}{\alpha} g \partial_x \eta) = 0 \,. \end{cases} \tag{3.47}$$

We replace the solutions in the first equation of the system, then we obtain:

$$\eta_0 = \frac{d_0 k}{\omega} u_0 \,. \tag{3.48}$$

Therefore, from the second equation we obtain the following relation:

$$-u_0\omega + g\eta_0 k - \frac{1}{3}\alpha\omega k^2 + \frac{1}{3}(\alpha - 1) g\eta_0 k^3 = 0 \,. \tag{3.49}$$

Replacing the expression of η_0 given in (3.48), in equation (3.49), we obtain the dispersion relation of the improved Boussinesq equations:

$$\omega_\alpha^2 = g d_0 k^2 \frac{1 + \dfrac{1}{3}(\alpha - 1)(d_0 k)^2}{1 + \dfrac{1}{3}\alpha (d_0 k)^2} \,. \tag{3.50}$$

Hence

$$\omega_\alpha = \pm \sqrt{g d_0 k^2 \frac{1 + (\alpha - 1)(d_0 k)^2/3}{1 + \alpha (d_0 k)^2/3}} \,. \tag{3.51}$$

We can now calculate the phase velocity associated with the improved Boussinesq equations:

$$C_{p,\alpha} = \frac{\omega_\alpha(k)}{k} = \pm\sqrt{g d_0 \frac{1+(\alpha-1)(d_0k)^2/3}{1+\alpha(d_0k)^2/3}}\,. \tag{3.52}$$

Similarly, the group velocity,

$$C_{g,\alpha} = \frac{\partial}{\partial k}\omega_\alpha(k) = \frac{\left(\alpha(\alpha-1)d_0^2(d_0k)^4 + 6(\alpha-1)d_0^2(d_0k)^2 + 9\right)k}{(\alpha(d_0k)^2+3)^{3/2}\sqrt{((\alpha-1)d_0^2(d_0k)^2+3)k^2}}\,. \tag{3.53}$$

Choice of parameter α

The parameter α can be determined in two ways, the first being to equalize the phase velocity associated with the Water Waves equations (3.14) and that of the reduced model, and then perform a Taylor series expansion in the neighborhood of $(kd_0) = 0$, as follows:

$$\frac{C_{p,\alpha}^2}{gd_0} = 1 - \frac{1}{3}k^2 + \frac{1}{9}\alpha k^4 + O(k^6) \tag{3.54}$$

$$\frac{(C_S^p)^2}{gd_0} = \frac{\tanh(kd_0)}{kd_0} = 1 - \frac{1}{3}k^2 + \frac{2}{15}k^4 + O(k^6) \tag{3.55}$$

then

$$\frac{(C_S^p)^2}{gd_0} = \frac{C_{p,\alpha}^2}{gd_0} \qquad \text{yields to} \qquad \alpha = 1.2\,.$$

Following [25], we can also find an optimal value for alpha by minimizing the joint Root Mean Square (RMS) error of the phase and group velocity estimates on the dispersion range $kd_0 \in [0, 3]$. This can be done by introducing the following quadratic form for the common error:

$$Err = \sqrt{\frac{\int_0^3 (C_{p,\alpha} - C_S^p)^2 d(kd_0)}{\int_0^3 C_{p,\alpha} - (C_S^p)^2 d(kd_0)} + \frac{\int_0^3 (C_{g,\alpha} - C_S^g)^2 d(kd_0)}{\int_0^3 C_{g,\alpha} - (C_S^p)^2 d(kd_0)}}\,, \tag{3.56}$$

where $C_{p,\alpha}$ and C_S^p respectively, represent linear phase velocities associated to the improved model (3.47) and the Stokes theory, while $C_{g,\alpha}$ and C_S^g correspond to group velocities.

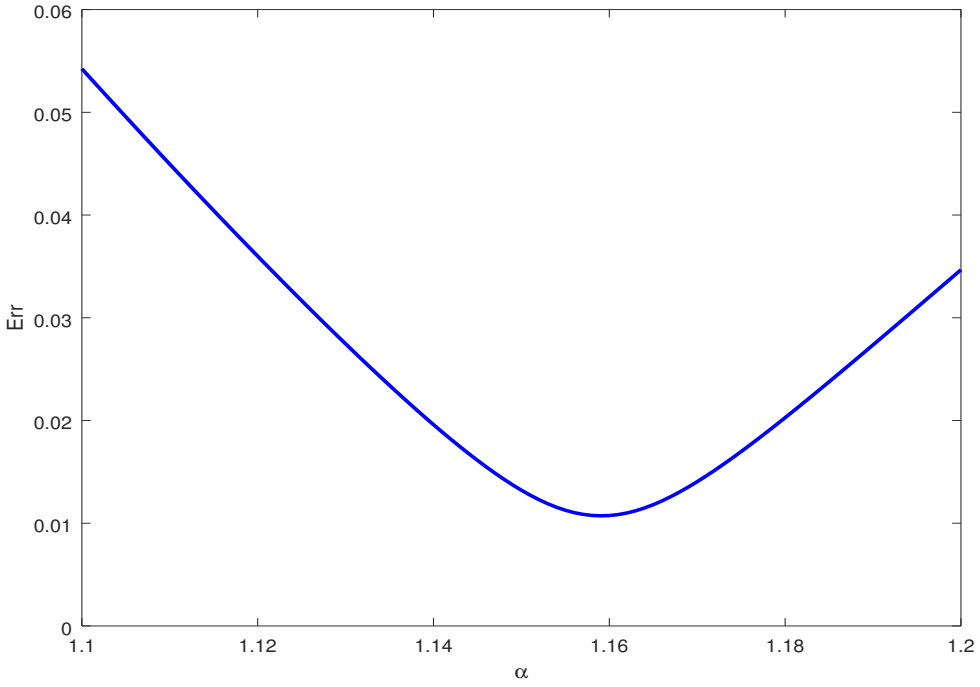

Figure 3.1: Optimum adjustment of dispersion correction parameter α: Joint RMS error for phase and group velocities as a function of α.

The optimization process, therefore, consists in minimizing the error function (3.56) for $(kd_0) \in [0, 3]$. The associated error is plotted in Fig 3.1. It is clear that the functional (3.56) has an absolute minimum in this dispersive range. The optimal value for α is 1.159, which corresponds to the result given in [14].

In Fig 3.3, the phase and group velocities obtained with the two different values of α_{opt} are plotted and compared to the corresponding Stokes relations. The match between the modeled dispersion relations and the theoretical relations is quite suitable for $\alpha = 1.159$.

We can also compute $\alpha_{opt}(k)$ from the equality $\omega_{WW} = \omega_\alpha$ for a large value of k. Such that

$$\alpha_{opt}(k) = 3\frac{\tanh(k) - k + k^3/3}{k^2(k - \tanh(k))} \,. \tag{3.57}$$

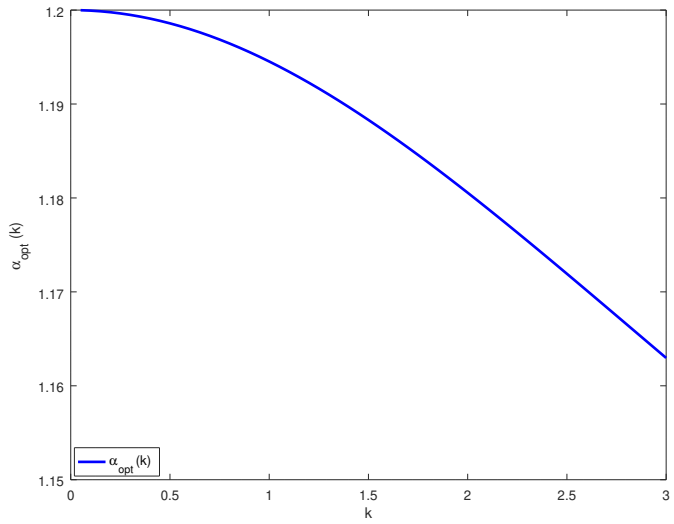

Figure 3.2: $\alpha_{opt}(k)$

Fig 3.2 shows the different values function α_{min} can take.

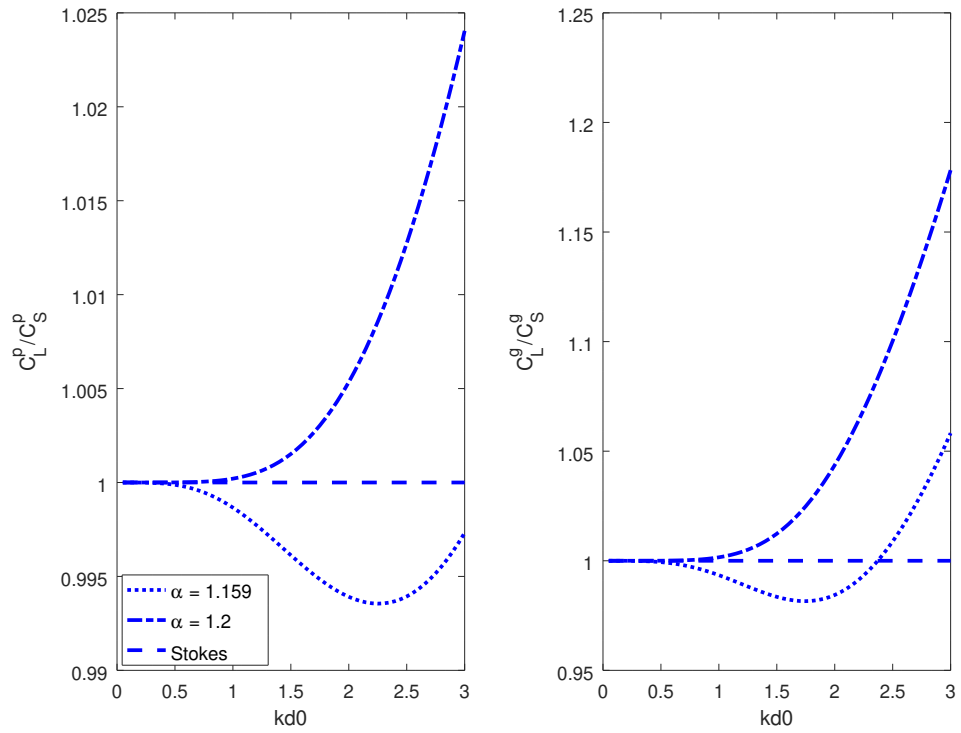

Figure 3.3: Comparison between model phase and group velocities and theoretical Stokes relations for optimum value $\alpha = 1.159$ and $\alpha = 1.2$.

Let us do the same calculations done previously to improve the model and calculate the associated dispersion relationship. We also get these relations for the other models.

Peregrine model

The dispersion relation associated with the Peregrine system can be obtained by making $\alpha = 1$ in the relation associated with the improved model (3.47).

$$\omega = \pm\sqrt{gd_0k^2\frac{1}{1+k^2/3}}\,, \tag{3.58}$$

and the phase velocity associated,

$$C_p = \frac{\omega(k)}{k} = \pm\sqrt{gd_0\frac{1}{1+(d_0k)^2/3}}\,, \tag{3.59}$$

and the group velocity associated,

$$C_g = \frac{\partial\omega(k)}{\partial k} = \pm\frac{3\sqrt{3gd_0}(d_0k)}{((d_0k)^2+3)^2\sqrt{\frac{(d_0k)^2}{(d_0k)^2+3}}}\,. \tag{3.60}$$

Beji and Nadaoka model

The dispersion relation can be obtained as in the case of the BBM trick. So, we repeat the same rules, we get the following dispersion relation associated to Beji and Nadaoka model:

$$\omega_\beta = \pm\sqrt{gd_0k^2\frac{1+\mu\beta(d_0k)^2/3}{1+\mu(1+\beta)(d_0k)^2/3}}\,, \tag{3.61}$$

and the following associated phase velocity:

$$C_{p,\beta} = \frac{\omega_\beta(k)}{k} = \pm\sqrt{gd_0\frac{1+\mu\beta(d_0k)^2/3}{1+\mu(1+\beta)(d_0k)^2/3}}\,, \tag{3.62}$$

and the group velocity,

$$C_{g,\beta} = \frac{\partial\omega_\beta(k)}{\partial k}\,.$$

Nwogu model

We carry out the same analyzes as we did for the first model, we obtain the following dispersion relation

$$\omega_\gamma = \pm\sqrt{gd_0k^2\frac{1-(\gamma+\frac{1}{3})k^2}{1-\gamma k^2}}\,, \tag{3.63}$$

with $\gamma = \dfrac{\theta^2}{2} + \theta$.
and the associated phase velocity is given by

$$C_{p,\gamma} = \frac{\omega(k)}{k} = \pm\sqrt{g d_0 \frac{1 + \mu\beta(d_0 k)^2/3}{1 + \mu(1+\beta)(d_0 k)^2/3}}\,, \tag{3.64}$$

and the group velocity,

$$C_{p,\gamma} = \frac{\partial\omega(k)}{\partial k}\,.$$

3.3.2.2 Comparison of linear dispersion between Boussinesq equations

Here we compare the phase speed ratio and group speed for all models. The comparison is made using the optimal value of (α, β, γ), which corresponds to 1.159 for the BBM and $1/15$ for the Beji and Nadaoka and -0.39 for the Nwogu model. Figure 3.4 the following results; the BBM gives the best approximation among the models considered here. The Peregrine model already provides a large error for a small number of waves Beji and Nadaoka model overestimates the wave amplitudes, with errors almost similar to those of the Nwogu model.

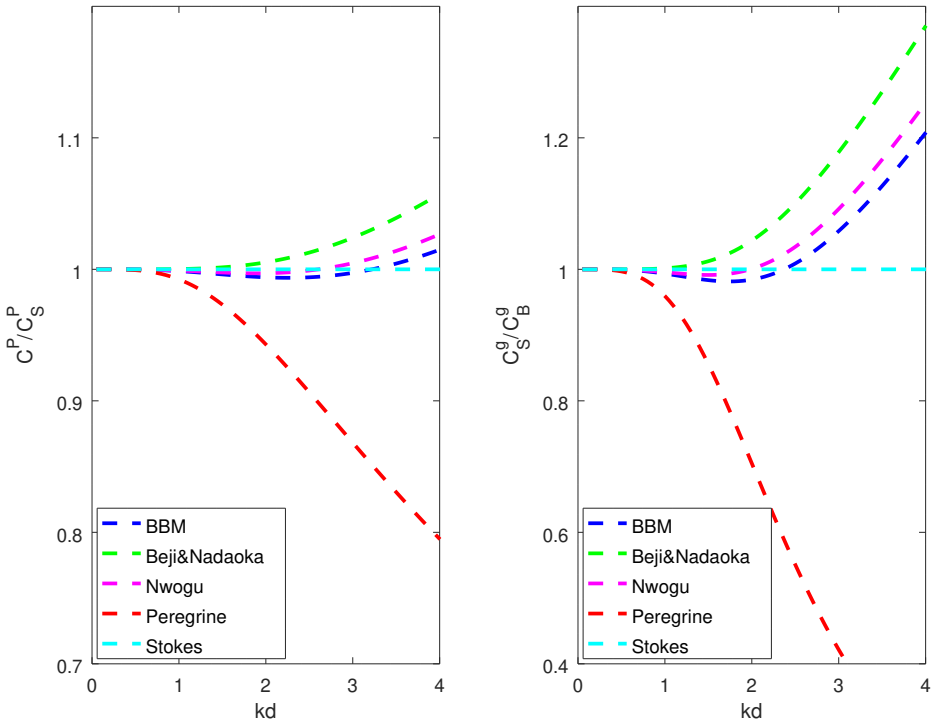

Figure 3.4: Comparisons between linear dispersion characteristics (phase velocity ratio and group velocity ratio) of Boussinesq type models and exact Stokes relations.

3.3.3 Shoaling properties

In the previous section, we have shown the linear dispersion characteristics for different flat-bottom Boussinesq models, the BBM trick gives the best approximation of the frequency dispersion. We follow the study of linear shoaling characteristics for various bottom presented by Madsen and Sørensen [69], to study the linear shoaling characteristics of the different models presented in the first section of this chapter.

3.3.3.1 Shoaling properties for Boussinesq models

We assume that the bathymetry varies slowly, which implies that $d = d(\delta x)$ with $\delta \ll 1$. Furthermore, for this study, we consider solutions u and η of the form

$$u(x,t) = U(\delta x)\exp\left(i(\frac{1}{\delta}S(\delta x) - \omega t)\right), \tag{3.65}$$

$$\eta(x,t) = A(\delta x)\exp\left(i(\frac{1}{\delta}S(\delta x) - \omega t)\right), \tag{3.66}$$

where $S(x) = \int k(x)dx$.

By definition, the linear shoaling coefficient relates the rate of change of the wave amplitude to the rate of change of depth. So we are looking for a function $\upsilon_s = s(d,k)$, such as:

$$\frac{A_x}{A} = -\upsilon_s\frac{d_x}{d}\,. \tag{3.67}$$

Plugging (3.66) into different models leads to particular ODEs. When we keep all the terms in the order of δ^0, we get the phase velocity expression. Those of order δ^1 provide an analytical expression for the shoaling gradient coefficient υ_s.

BBM trick

In this section, we recall the expression of the phase velocity associated with the improved model (3.47), and we calculate the linear shoaling coefficient of this system. Let us start by recalling the linear part of the system

$$\partial_t\eta + \partial_x(du) = 0\,, \tag{3.68}$$

$$(1-\mu\alpha\mathcal{T})(\partial_t u + \frac{\alpha-1}{\alpha}g\partial_x\eta) + \frac{1}{\alpha}g\partial_x\eta = 0\,, \tag{3.69}$$

with $\mathcal{T}$ is designed in (3.34). The terms in η can be eliminated easily applying operator ∂_x to equation ((3.68) and ∂_t to equation (3.69). That gives

$$(1-\mu\alpha\mathcal{T})(\partial_{tt}u - \frac{\alpha-1}{\alpha}g(du)_{xx}) + \frac{1}{\alpha}g(du)_{xx} = 0\,. \tag{3.70}$$

The last equation can be written in the following form:

$$u_{tt}+g(du)_{xx}-\mu\alpha\left[\frac{d}{2}\left((du)_{xx}\right)_{tt} - \frac{d^2}{6}u_{ttxx}\right]+\mu(\alpha-1)g\left[\frac{d}{2}\left(d(du)_{xx}\right)_{xx} - \frac{d^2}{6}(du)_{xxxx}\right] = 0\,.$$

Then, we substitute the expression of u, given by equation (3.65) to obtain a relation between ω, kd and U. Keeping terms of order $O(1)$, we find the phase velocity

$$(C_{p,\alpha})^2 = gd\frac{1+(\alpha-1)(dk)^2/3}{1+\alpha(dk)^2/3}\,. \tag{3.71}$$

When we keep all terms of order δ, we obtain a relation in the following form

$$\upsilon_1\frac{U_x}{U}+\upsilon_2\frac{d_x}{d}+\upsilon\frac{k_x}{k}=0\,. \tag{3.72}$$

Using Mathematica, the coefficients υ_i, $i=1,2,3$ are obtained,

$$\begin{aligned}
\upsilon_1 &= 2+4(\alpha-1)\frac{d^2k^2}{4}+2\alpha(\alpha-1)\frac{d^4k^4}{9}\,,\\
\upsilon_2 &= 2-(1-6(\alpha-1))\frac{d^2k^2}{3}+4\alpha(\alpha-1)\frac{d^4k^4}{9}\,,\\
\upsilon_3 &= 1+2(\alpha-1)d^2k^2+5\alpha(\alpha-1)\frac{d^4k^4}{9}\,.
\end{aligned}$$

In order to express k_x/k in terms of d_x/d, we differentiate (3.71) considering ω as a constant. It leads to the following relation

$$\frac{k_x}{k}=-\upsilon_4\frac{d_x}{d}\,, \tag{3.73}$$

where

$$\upsilon_4=\frac{1}{2}\frac{1+(2\alpha-3)\frac{d^2k^2}{3}+\alpha(\alpha-1)\frac{d^4k^4}{9}}{1+2(\alpha-1)\frac{d^2k^2}{3}+\alpha(\alpha-1)\frac{d^4k^4}{9}}\,.$$

Substituting this relation in equation (3.72), we express U_x/U as a function of d_x/d,

$$\frac{U_x}{U}=-\upsilon_5\frac{d_x}{d}\,, \tag{3.74}$$

where

$$\upsilon_5=\frac{\upsilon_2-\upsilon_3\upsilon_4}{\upsilon_1}\,.$$

To conclude, substituting (3.66) in Equation (3.68), we get at the first order:

$$-i\omega A+ikdU=0\,, \tag{3.75}$$

it leads to

$$A=\frac{kd}{\omega}U\,. \tag{3.76}$$

Applying ∂_x to Equation (3.76), we get after some calculation:

$$\frac{A_x}{A}=\frac{U_x}{U}+\frac{k_x}{k}+\frac{d_x}{d}\,. \tag{3.77}$$

Substituting (3.73) and (3.74) in Equation (3.77), we obtain the linear shoaling coefficient,

$$\frac{A_x}{A}=-\upsilon_s\frac{d_x}{d}\,, \tag{3.78}$$

with

$$\upsilon_s=1-\upsilon_5-\upsilon_4\,.$$

Beji and Nadaoka model

Using the same computations presented above, one gets the following expression

$$\frac{A_x}{A} = -\upsilon_s \frac{d_x}{d} \,. \tag{3.79}$$

The shoaling coefficient associated to the Beji and Nadaoka model (3.3.1.2) is obtained similarly,

$$\upsilon_s = 1 - \upsilon_5 - \upsilon_4 \,,$$

where

$$\begin{aligned}
\upsilon_1 &= 2 + 4\beta\frac{d^2k^2}{4} + 2\beta(\beta+1)\frac{d^4k^4}{9} \,, \\
\upsilon_2 &= 2 - (1-6\beta)\frac{d^2k^2}{3} + 4\beta(\beta+1)\frac{d^4k^4}{9} \,, \\
\upsilon_3 &= 1 + \beta\frac{d^2k^2}{3} \,.
\end{aligned}$$

and

$$\upsilon_4 = \frac{1}{2}\frac{1 + (2\beta-1)\frac{d^2k^2}{3} + \beta(\beta+1)\frac{d^4k^4}{9}}{1 + 2\beta\frac{d^2k^2}{3} + \beta(\beta+1)\frac{d^4k^4}{9}} \,.$$

Nwogu model

Following the computation given for the BBM trick, one gets

$$\frac{A_x}{A} = -\upsilon_s \frac{d_x}{d} \,, \tag{3.80}$$

with υ_s is the shoaling gradient associated to the Nwogu model (3.43),

$$\upsilon_s = -3\gamma - (\frac{2}{3} - \gamma)\upsilon_5 + 3\gamma\upsilon_4 \,.$$

where,

$$\begin{aligned}
\upsilon_1 &= 2 - 4(\gamma + 1/3)d^2k^2 + 2\gamma(\gamma + \frac{1}{3})d^4k^4 \,. \\
\upsilon_2 &= 2 + 2(\frac{b_1}{2} - \frac{a_2}{2} + 2a_1)d^2k^2 + \left[\frac{b_2}{3}\left(\frac{a_2}{2} - 2a_1\right) - b_1\left(\frac{a_2}{3} - \frac{3a_1}{2}\right)\right]d^4k^4 \,. \\
\upsilon_3 &= 1 - 6(\gamma + \frac{1}{3})d^2k^2 + 5\gamma(\gamma + \frac{1}{3})d^4k^4 \,.
\end{aligned}$$

and,

$$\upsilon_4 = \frac{1}{2}\frac{1 + \left[\gamma - 3(\gamma + \frac{1}{3})\right]d^2k^2 + \gamma(\gamma + \frac{1}{3})d^4k^4}{1 - 2\gamma d^2k^2 + \gamma(\gamma + \frac{1}{3})d^4k^4} \,.$$

3.3.3.2 Comparisons between Boussinesq models

Here we compare the behavior of the shoaling characteristics of all models presented in this chapter. The comparison is made using the optimal value of (α, β, γ), which corresponds to 1.159 for the BBM and $1/15$ for the Beji and Nadaoka and -0.39 for the Nwogu model. Figure 3.5 the following results; the BBM gives the best approximation among the models considered here, the Peregrine model already provides a large error for a small number of waves, the Beji and Nadaoka model overestimates the wave amplitudes, and the Nwogu model underestimates them.

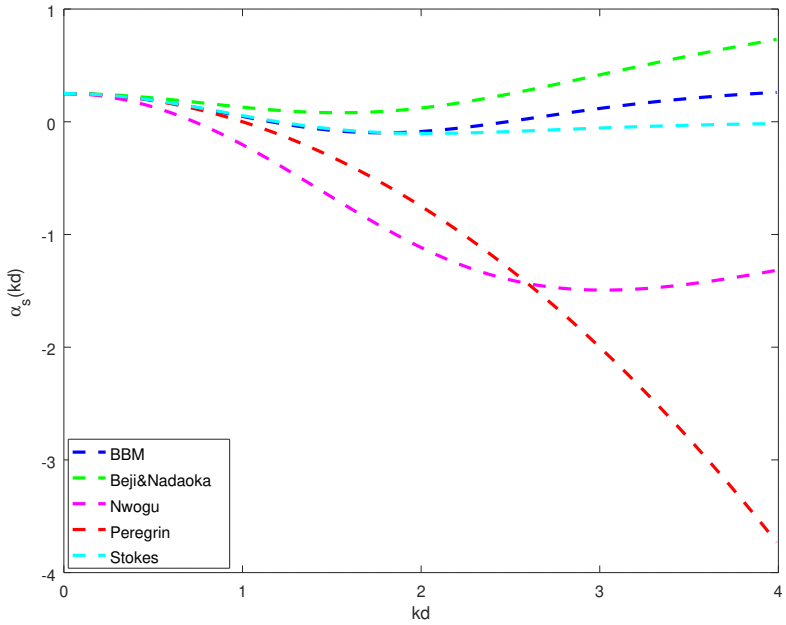

Figure 3.5: Linear shoaling: comparison between Boussinesq type models using the shoaling gradient

3.4 Conclusion

This chapter has studied the linear properties of Boussinesq type models and expects similar results for Green-Naghdi models on a flat bottom. The BBM method has shown an excellent correction at the level of dispersion error, so we will adopt this method to study a model of the Green-Naghdi type in the next chapter.

Part III

Section averaged models

Chapter 4

Generalized SGN equations for open channels and river flows

Contents

This chapter is a development of the following papers:

- *M-A. Debyaoui and M. Ersoy. Generalised Serre-Green-Naghdi equations for open channel and for natural river hydraulics. To appear in Asymptotic Analysis.*
- *M-A. Debyaoui and M. Ersoy. A Generalised Serre-Green-Naghdi equations for variable rectangular open channel hydraulics and its finite volume approximation. To appear in SEMA-SIMAI.*
- *M-A. Debyaoui and M. Ersoy. A new form of the Generalised Serre-Green-Naghdi equations with improved linear dispersion characteristics. In preparation.*

4.1 Introduction

The modeling of the hydrology of catchment basins and rivers holds a central place in environmental sciences, particularly in connection with water availability, urban sewer systems, flood risks, and in particular, for tsunamis. Indeed, rivers are known to be tsunami highways. Waves penetrate through rivers much faster inland than the coastal inundation reaches over the ground, and may lead flooding in low-lying areas located several km away from the coastline [90]. This is important today in understanding and forecasting the impact of climate variability on the human and natural environment. Modeling these processes and predicting the motion of water is a difficult task for which substantial effort has been devoted [49, 94, 90, 99, 42, 92, 81].

One of the most widely used models to describe the channel and river motion of watercourses is the *section-averaged free surface model* [34, 15, 39] which is a generalisation of the well-known *Saint-Venant system* (introduced by Adhémar Jean Claude Barré de Saint-Venant in the 19th Century [31, 47]):

$$\left\{\begin{array}{rcl} \dfrac{\partial}{\partial t}A + \dfrac{\partial}{\partial x}Q & = & 0\,, \\ \dfrac{\partial}{\partial t}Q + \dfrac{\partial}{\partial x}\left(\dfrac{Q^2}{A} + I_1(x,A)\right) & = & I_2(x,A)\,. \end{array}\right. \tag{4.1}$$

In these equations, A is the wet area of fluid cross-section, Q is the water discharge, I_1 is the hydrostatic pressure and I_2 is the hydrostatic pressure source term which takes into account of the variation of the section. The Model (4.1) reduces to the well-known one-dimensional Saint-Venant equations for uniform rectangular section. The free surface model is the first order shallow water approximation of the section-averaged Navier-Stokes or Euler equations under suitable assumptions on the horizontal and the vertical scales (see, *e.g.*, [48, 34, 47, 15, 39] and the reference therein).

Thanks to these equations' hyperbolic structure, sharp transitions between two different flow states result in a discontinuous solution, both in the water surface and in the velocity. These discontinuous solutions (called shocks and referred to as bores) are well-suited to approximate breaking waves with turbulent rollers for large transitions of the Froude's number. However, for small or moderate transitions, the advancing wavefront can be followed by a train of free-surface undulations, sometimes called "whelps". This phenomenon, called undular bore (also called dispersive shock waves), is induced by a non-hydrostatic pressure distribution [75]. Consequently, wave solutions spread out in space as they evolve in time, *i.e.* waves of different wavelengths travel at different speeds. This is the so-called dispersive effect. Consequently, undular bores are not reproducible with the non-dispersive free surface system, and non-hydrostatic pressure is required.

Dispersive equations were first introduced by Boussinesq [17] in 1872 to mathematically justify the existence of solitary waves observed by Russell's experiments in 1834. These equations enter in the framework of shallow water equations. They can be obtained as the second-order asymptotic approximation in μ^2, with $\mu = \left(\dfrac{H}{L}\right)^2$, of the depth-averaged Euler equations where H represents a characteristic water depth and L is a characteristic horizontal scale. The Boussinesq type equations, which are weakly nonlinear and weakly dispersive, are defined by an additional small non-linearity parameter

$\varepsilon = \dfrac{a}{H} = O(\mu) \ll 1$ where a is the order of the free surface amplitude. These equations for a flat bottom, for instance in 1D, are given by

$$\left\{ \begin{array}{lcl} \dfrac{\partial}{\partial t}\xi + \dfrac{\partial}{\partial x}(h\overline{u}) & = & O(\mu^2) \\ \dfrac{\partial}{\partial t}\overline{u} + \varepsilon\overline{u}\dfrac{\partial}{\partial x}\overline{u} + \nabla\xi + \mu\mathbb{D} & = & O(\mu^2) \end{array} \right. \tag{4.2}$$

where h is the water depth, ξ is the free surface elevation and $\overline{u}$ is the depth-averaged velocity. The term $\mathbb{D}$ represents the dispersive term. In 1877, the KdV equation was discovered by Boussinesq [17] and was later derived by Korteweg and Gustav de Vries (KdV) [55]. This equation approximately describes the evolution of long, one-dimensional waves in many physical settings, including shallow-water waves with weakly non-linear behaviour. This equation can also be obtained in the case of unidirectional waves for which the theoretical framework allows to compute an analytical solution such as 1D solitary wave propagation on flat bottom (see e.g. Boussinesq [17, 55, 7]). We have also the Benjamin, Bona, and Mahony (BBM) equation which is an improvement of the KdV equation [10]. However, in practice and especially in coastal engineering applications, the nearshore wave dynamics being often varying-bottom dependent, dispersive and non-linear, the Boussinesq type equations are not appropriate. In 1967, Peregrine [77] introduced the first weakly non-linear two dimensional Boussinesq type equations for the non-flat bottom. Witting [93] proposed a method based on Padé expansion to improve the frequency dispersion of the Boussinesq-type equations. From this method, several equations of order $O(\mu^2)$ with improved dispersion characteristics have been proposed; see, for instance, [69, 71, 84]. In 1953, a one-dimensional, fully non-linear ($\varepsilon = O(1)$) and weakly dispersive equations for flat bottom were derived by Serre [86], independently of Su and Gardner [89] with

$$\mathbb{D}(v) = \frac{1}{h}\frac{\partial}{\partial x}\left(\frac{h^3}{3}\mathcal{D}(v)\right) \tag{4.3}$$

where

$$\mathcal{D}(v) = \left(\frac{\partial}{\partial x}v\right)^2 - \frac{\partial}{\partial x}\frac{\partial}{\partial t}v - v\partial_x^2 v\ . \tag{4.4}$$

This model was then extended to non flat bottom by Seabra-Santos [85], see also [25]. Finally, Green and Naghdi [50] derived the two dimensional fully non-linear dispersive equations for the uneven bottom, which are the extension of Serre equations. In the literature, this system is often called SGN equations. Further interesting extensions are also presented in [91, 60, 61, 80, 27, 78] based on either Euler equations, water waves equations or variational principles.

All of the previous dispersive models are obtained either from 3D-2D or 2D-1D reduction, but, up to our knowledge, the 3D-1D reduction has never been done before. Thus, our main goal is to derive from the three-dimensional incompressible and irrotational Euler equations with suitable boundary conditions, a model akin to (4.2)–(4.4) via section averaging under the shallow water assumption. The section averaged model that we obtain extends the section-averaged free surface model (4.1) and the SGN equations

(4.2)–(4.4):

$$\begin{cases} \dfrac{\partial}{\partial t}A + \dfrac{\partial}{\partial x}Q = 0 \\ \dfrac{\partial}{\partial t}Q + \dfrac{\partial}{\partial x}\left(\dfrac{Q^2}{A} + I_1(x,A)\right) + \mu_2 \dfrac{\partial}{\partial x}(G(x,A)\mathcal{D}(u)) = I_2(x,A) + \mathcal{G}(x,A,Q) \\ +O(\mu_2^2) \end{cases}$$

where A is the wet area, $Q = Au$ is the water discharge, u is the section-averaged velocity, I_1 (resp. I_2) is the hydrostatic pressure (resp. source) term, $G(x,A)$ generalises $\dfrac{h^3}{3}$ in (4.3), the term $\mathcal{G}(x,A,Q)$ extends the uneven bottom source term, $\mathcal{D}$ is the term given by (4.4) and therefore $\mathbb{D} = \dfrac{\partial}{\partial x}(G(x,A)\mathcal{D}(u))$ represents the dispersive term.

The chapter is organised as follows: in §4.2 we present the geometrical settings of the physical domain and the governing equations. In §4.3, we obtain the key asymptotic approximation of the horizontal velocity u and the pressure P is decomposed into a hydrostatic P_{h} and a non-hydrostatic part P_{nh}. Finally, we present in §4.4 the derivation of the new section-averaged non-linear dispersive model for arbitrary varying non rectangular open channel/river flows in §4.4.3 and for varying rectangular channel in §4.4.4. We show in §4.5 that the section-averaged model is fully consistent with the Euler system. Finally, in Sect. 4.7, we construct a first-order well-balanced finite volume approximation, and we present some numerical test cases.

4.2 The three-dimensional Incompressible Euler equations

We start in §4.2.1 by reviewing the irrotational and incompressible Euler equations in the special geometric setting, describing the physics with a wet boundary on the bottom of the watercourse and a free surface on the top. Boundary conditions are presented in §4.2.2.

4.2.1 Geometric set-up and the Euler equations

Let $T > 0$ be an arbitrary time. We consider an incompressible and irrotational fluid moving in the time-space box $[0,T] \times C$ with typical point $(t,(x,y,z))$ where C is the geometrical definition of a convex (non-rectangular) channel/river

$$C = \left\{(x,y,z) \in \mathbb{R}^3;\ x \in [0,L_c],\ \alpha(x,z) \le y \le \beta(x,z) \text{ and } d(x,y) \le z\right\}.$$

$L_c > 0$ is the horizontal length of the domain and for $z \ge d(x,y)$, $\alpha(x,z)$ (respectively $\beta(x,z)$) is the left (respectively right) boundary point at the elevation z as displayed in Fig. 4.1. The height of the surface of the water level and the boundary of the section are modeled, respectively, by the functions $\eta(t,x,y)$ and $d(x,y)$ with respect to a reference horizontal height $z = 0$. For all $x \in [0,L_c]$, we assume that the function $y \mapsto d(x,y)$, has a global minimum at

$$y^*(x) \textit{ i.e. } d^*(x) = d(x,y^*(x)) = \min_y d(x,y)$$

where y^* describes the transversal variation of the channel with respect to the main channel/river direction.

We define the local height of the water by

$$h(t,x,y) := \eta(t,x,y) - d(x,y).$$

The boundary of the section can be also described as a function of y by

$$\forall x \in [0, L_c],\ \varphi(x,z) = \begin{cases} \alpha(x,z) \text{ if } & \varphi(x,z) < y^*(x) \\ \beta(x,z) \text{ otherwise.} \end{cases} \tag{4.5}$$

The width of the section at the elevation z is given by an increasing function

$$z \mapsto \sigma(x,z) = \beta(x,z) - \alpha(x,z)\ .$$

The wet region is defined as the region in which the fluid resides at each time $t \in [0,T]$

$$\Omega(t) = \bigcup_{0\le x\le L} \Omega(t,x)$$

with its global counterpart

$$\Omega := \bigcup_{0\le t\le T} \Omega(t). \tag{4.6}$$

$\Omega(t,x)$ is the cross-section of fluid at the position x of the channel C:

$$\Omega(t,x) = \left\{(y,z) \in \mathbb{R}^2;\ \alpha(x,z) \le y \le \beta(x,z) \text{ and } d(x,y) \le z \le \eta(t,x,y)\right\} \tag{4.7}$$

and $A(t,x) = |\Omega(t,x)|$ is the wet area of the cross-section of fluid:

$$\begin{aligned} A(t,x) = \int_{\Omega(t,x)} d\omega &= \int_{y^-(t,x)}^{y^+(t,x)} \eta(t,x,y) - d(x,y)\, dy \\ &= \int_{d^*(x)}^{\max_y \eta(t,x,y)} \int_{\alpha(x,z)}^{\beta(x,z)} \mathbb{1}_{\{d(x,y)\le z\le \eta(t,x,y)\}}\, dydz \end{aligned} \tag{4.8}$$

where

$$y^-(t,x) := \min\{y \in \mathbb{R};\ \eta(t,x,y) = d(x,y)\} \text{ and}$$
$$y^+(t,x) := \max\{y \in \mathbb{R};\ \eta(t,x,y) = d(x,y)\}$$

stands for the left and the right transversal limit at $z = \eta$ as shown in Fig. 4.1.

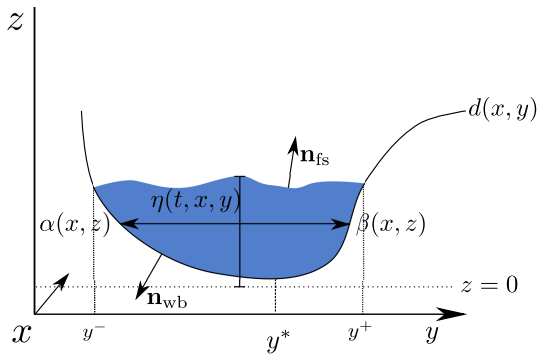

Figure 4.1: Geometric set-up

We assume that the flow is governed, on the space-time domain Ω, by the three-dimensional irrotational and incompressible Euler equations

$$\begin{aligned} \operatorname{div}[\rho_0 \bar{\boldsymbol{u}}] &= 0, \\ \frac{\partial}{\partial t}(\rho_0 \bar{\boldsymbol{u}}) + \operatorname{div}[\rho_0 \bar{\boldsymbol{u}} \otimes \bar{\boldsymbol{u}}] + \nabla p - \rho_0 \boldsymbol{F} &= 0 \end{aligned} \tag{4.9}$$

where $\bar{\boldsymbol{u}} = (u, v, w)$ is the velocity field, ρ_0 is the density of the fluid (taken to be constant), $\boldsymbol{F} = (0, 0, -g)$ is the external force of gravity with constant g and p is the pressure.

These equations are completed by the irrotational equation:

$$\operatorname{curl}[\bar{\boldsymbol{u}}] = 0 \,. \tag{4.10}$$

4.2.2 Boundary conditions

For a given time $t \in [0, T]$ and $x \in [0, L_c]$, the boundary of the fluid cross-section $\Omega(t, x)$ is composed of a free surface $\Gamma_{\mathrm{fs}}(t, x) = \{(y, z) \in \mathbb{R}^2;\ z = \eta(t, x, y)\}$ and a wet boundary (part of the boundary in contact with water) $\Gamma_{\mathrm{wb}}(x) = \{(y, z) \in \mathbb{R}^2;\ z = d(x, y)\}$ such that

$$\partial\Omega(t, x) = \Gamma_{\mathrm{fs}}(t, x) \cup \Gamma_{\mathrm{wb}}(x) \,. \tag{4.11}$$

We prescribe a kinematic boundary condition at the free surface boundary and a no-penetration condition at the wet boundary as described below.

4.2.2.1 Free surface boundary conditions

Assuming a kinematic boundary condition, we set for all points $\boldsymbol{m}(t, x, y) = (x, y, \eta(t, x, y)) \in \Gamma_{\mathrm{fs}}(t, x)$,

$$\bar{\boldsymbol{u}} \cdot \boldsymbol{n}_{\mathrm{fs}} = \frac{\partial}{\partial t}\boldsymbol{m} \cdot \boldsymbol{n}_{\mathrm{fs}}$$

where

$$\boldsymbol{n}_{\mathrm{fs}}(t, x, y) = \frac{1}{\sqrt{1 + \left(\frac{\partial}{\partial x}\eta(t, x, y)\right)^2 + \left(\frac{\partial}{\partial y}\eta(t, x, y)\right)^2}} \begin{pmatrix} -\frac{\partial}{\partial x}\eta(t, x, y) \\ -\frac{\partial}{\partial y}\eta(t, x, y) \\ 1 \end{pmatrix}$$

is the unit outward normal vector to the free surface. This leads to the following explicit form of the kinematic boundary condition

$$\frac{\partial}{\partial t}\eta + u\frac{\partial}{\partial x}\eta + v\frac{\partial}{\partial y}\eta = w \text{ on } \ z = \eta \,. \tag{4.12}$$

We also assume that the pressure at the free surface level is equal to the atmospheric pressure p_0

$$p = p_0 \text{ on } \ z = \eta \,. \tag{4.13}$$

In the sequel, without loss of generality, we set $p_0 = 0$.

4.2.2.2 Wet boundary conditions

On the wet boundary, *i.e.*, the part of the boundary in contact with water, prescribing a no-penetration condition, we set for all points $\boldsymbol{m}(x, y) = (x, y, d(x, y)) \in \Gamma_{\mathrm{wb}}(x)$,

$$\bar{\boldsymbol{u}} \cdot \boldsymbol{n}_{\mathrm{wb}} = 0$$

which leads to the following explicit form:

$$u\frac{\partial}{\partial x}d + v\frac{\partial}{\partial y}d = w \text{ on } z = d \tag{4.14}$$

where

$$\boldsymbol{n}_{\mathrm{wb}}(x, y) = \frac{1}{\sqrt{1 + \left(\frac{\partial}{\partial x}d(x, y)\right)^2 + \left(\frac{\partial}{\partial y}d(x, y)\right)^2}} \begin{pmatrix} \frac{\partial}{\partial x}d(x, y) \\ \frac{\partial}{\partial y}d(x, y) \\ -1 \end{pmatrix}$$

is the unit outward normal vector to the wet boundary. In view of the definition of the function φ, see Eq. (4.5), the no-penetration condition can be also expressed as a function of (x, z) by

$$u\frac{\partial}{\partial x}\varphi + w\frac{\partial}{\partial z}\varphi = v \text{ on } y = \varphi \tag{4.15}$$

where the unit outward normal vector to the wet boundary is

$$\boldsymbol{n}_{\mathrm{wb}}(x, z) = \frac{1}{\sqrt{1 + \left(\frac{\partial}{\partial x}\varphi(x, z)\right)^2 + \left(\frac{\partial}{\partial z}\varphi(x, z)\right)^2}} \begin{pmatrix} \frac{\partial}{\partial x}\varphi(x, z) \\ -1 \\ \frac{\partial}{\partial z}\varphi(x, z) \end{pmatrix}.$$

In this work, we neglect some physical processes arising in river flows: sedimentation, exchange between groundwater flows and subsurface flows, porosities, *etc*. However, these phenomena can be easily integrated to this work, see for instance [38, 40], by considering the following boundary condition $\bar{\boldsymbol{u}} \cdot \boldsymbol{n}_{\mathrm{wb}} = (\frac{\partial}{\partial t}\boldsymbol{m} + I) \cdot \boldsymbol{n}_{\mathrm{wb}}$ where $\frac{\partial}{\partial t}\boldsymbol{m}$ models the evolution in time of the bed and I is the infiltration function. I models the amount of water that leaves ($I > 0$) or enters ($I < 0$) the flow per elementary boundary element.

4.3 Width-averaged and depth-averaged asymptotic expansions

In this section, we present the strategy to derive the section-averaged non-linear dispersive model (see §4.4). To this end, we first introduce in §4.3.1 the dimensionless problem by introducing the classical dispersive parameter μ_2. We also introduce a dispersive parameter μ_1 but in the transversal direction. In this work, we assume that $\mu_1 < \mu_2$ to obtain the section-averaged dispersive model with respect to μ_2 as usually done. Due to

the structure of the equations, we cannot obtain the model by a direct section-averaging. We need to develop first suitable asymptotic expansions in two steps, briefly summarized below:

- in §4.3.3, the Euler equations (4.9)-(4.10) are width-averaged to get the following asymptotic expansion of the horizontal fluid velocity

$$u(t, x, y, z) = \langle u \rangle(t, x, z) + O(\mu_1)$$

  where $\langle u \rangle$ is the width-averaged velocity.

- in §4.3.4, the width-averaged Euler equations allows to obtain the asymptotic expansion of the horizontal width-averaged fluid velocity

$$\langle u \rangle(t, x, z) = \overline{u}(t, x) + \mu_2 f(\overline{u}(t, x), \Omega(t, x)) + O(\mu_2^2)$$

  where $\bar{u}$ is the section-averaged velocity for some function f given later on.

  Thus, the asymptotic expansion of u up to order $O(\mu_2^2)$, the so-called "motion by slices" (see [47]), can be written as follows:

$$u(t, x, y, z) = \overline{u}(t, x) + \mu_2 f(\overline{u}(t, x), \Omega(t, x)) + O(\mu_2^2) \, .$$

Finally, using these asymptotic expansions, we are able in §4.4 to section-average the Euler equations (4.9)-(4.10) to obtain the new one-dimensional non-linear dispersive equations.

4.3.1 Dimensionless Euler equations

Let us consider the following scales involved in the wave motion: L a characteristic wave-length in the longitudinal direction, H_2 a characteristic water depth, H_1 a characteristic scale of the channel width and h_1 a characteristic wave-length in the transversal direction. We then define the classical dispersive parameter μ_2 (see *e.g.* [59])

$$\mu_2 = \frac{H_2^2}{L^2}$$

and $\mu_1 = \dfrac{h_1^2}{L^2}$ where μ_1 is also a dispersive parameter but in the transversal direction.

In the following, we consider the asymptotic regime:

$$h_1 < H_1 = H_2 \ll L$$

such that the following inequality holds

$$\mu_1 < \mu_2^2 \, .$$

Under these assumptions, we get the following ordering:

$$\mu_1^2 < \frac{\mu_1^2}{\mu_2} < \min\left(\frac{\mu_1^2}{\mu_2^2}, \mu_1\mu_2\right) < \max\left(\frac{\mu_1^2}{\mu_2^2}, \mu_1\mu_2\right) < \mu_1$$
$$< \min\left(\frac{\mu_1}{\mu_2}, \mu_2^2\right) < \max\left(\frac{\mu_1}{\mu_2}, \mu_2^2\right) < \mu_2 .$$

We also introduce $\boldsymbol{U} = (U, V = \sqrt{\mu_1}U, W = \sqrt{\mu_2}U)$ the scale of fluid velocity so that $V < W < U$. The time scale is $T = \dfrac{L}{U}$. We set $P = \dfrac{p}{\rho_0}$ and we define $\mathcal{P} = U^2$.

This allows us to introduce the dimensionless quantities of time $\widetilde{t}$, space $(\widetilde{x}, \widetilde{y}, \widetilde{z})$, pressure $\widetilde{P}$, depth $\widetilde{d}$, water elevation $\widetilde{\eta}$ and velocity field $(\widetilde{U}, \widetilde{V}, \widetilde{W})$, via the following scaling relation

$$\begin{aligned}
&\widetilde{x} = \frac{x}{L}, \quad \widetilde{P} = \frac{P}{\mathcal{P}}, \quad \widetilde{\varphi} = \frac{\varphi}{h_1}, \\
&\widetilde{y} = \frac{y}{h_1}, \quad \widetilde{u} = \frac{u}{U}, \quad \widetilde{d} = \frac{d}{H_2}, \\
&\widetilde{z} = \frac{z}{H_2}, \quad \widetilde{v} = \frac{v}{V}, \quad \widetilde{\eta} = \frac{\eta}{H_2}, \\
&\widetilde{t} = \frac{t}{T}, \quad \widetilde{w} = \frac{w}{W} .
\end{aligned} \tag{4.16}$$

Finally, we define the non-dimensional Froude's number

$$F_r = \frac{U}{\sqrt{gH_2}} .$$

For the sake of clarity and simplicity dropping $\widetilde{\cdot}$, dividing the Euler equations (4.9) by ρ_0, using the dimensionless variables (4.16), and reordering the terms with respect to the powers of μ_1 and μ_2, the dimensionless incompressible Euler system (4.9) reads as follows:

$$\frac{\partial}{\partial x}u + \frac{\partial}{\partial y}v + \frac{\partial}{\partial z}w = 0 \tag{4.17}$$

$$\frac{\partial}{\partial t}u + u\frac{\partial}{\partial x}u + v\frac{\partial}{\partial y}u + w\frac{\partial}{\partial z}u + \frac{\partial}{\partial x}P = 0 \tag{4.18}$$

$$\mu_1\left(\frac{\partial}{\partial t}v + u\frac{\partial}{\partial x}v + v\frac{\partial}{\partial y}v + w\frac{\partial}{\partial z}v\right) + \frac{\partial}{\partial y}P = 0 \tag{4.19}$$

$$\mu_2\left(\frac{\partial}{\partial t}w + u\frac{\partial}{\partial x}w + v\frac{\partial}{\partial y}w + w\frac{\partial}{\partial z}w\right) + \frac{\partial}{\partial z}P = -\frac{1}{{F_r}^2} \tag{4.20}$$

The boundary conditions (4.12), (4.13), (4.14) and (4.15) read

$$\frac{\partial}{\partial t}\eta + u\frac{\partial}{\partial x}\eta + v\frac{\partial}{\partial y}\eta = w \text{ and } P = 0 \text{ on } z = \eta \tag{4.21}$$

$$u\frac{\partial}{\partial x}d + v\frac{\partial}{\partial y}d = w \text{ on } z = d \tag{4.22}$$

$$\text{or } u\frac{\partial}{\partial x}\varphi + w\frac{\partial}{\partial z}\varphi = v \text{ on } y = \varphi \tag{4.23}$$

and the irrotational equation (4.10) becomes

$$\frac{\partial}{\partial y}u = \mu_1 \frac{\partial}{\partial x}v,\ \mu_1 \frac{\partial}{\partial z}v = \mu_2 \frac{\partial}{\partial y}w,\ \frac{\partial}{\partial z}u = \mu_2 \frac{\partial}{\partial x}w\ . \tag{4.24}$$

4.3.2 Validity of the asymptotic and the section-averaging process

In this section, we want to argue about the justification of the asymptotic presented in this chapter. The choice of the parameter h_1 and $H_1 = H_2$ are crucial in this work. Indeed, as we will see below, these parameters allows us to preserve the structure of the equations.

To simplify our justification, we assume that the fluid motion is contained in a box $\mathcal{B}$ such as

$$\mathcal{B} = \{(x, y, z) \in \mathbb{R}^3\ , 0 \leq x \leq L\ , 0 \leq y \leq H_1 \text{ and } 0 \leq z \leq H_2\}$$

As a consequence, there exists a potential function ϕ such that $\bar{\boldsymbol{u}} = (u, v, w)^T = \nabla\phi$ where ϕ solves the Laplace problem

$$\partial_z\phi_{|z=0} = 0, \qquad \partial_z\phi_{|z=H_2} = \psi\ , \tag{4.25}$$

$$\phi_{|z=0} = \psi, \qquad \phi_{|z=0} = 0\ , \tag{4.26}$$

$$\partial_y\phi_{|y=0} = 0, \qquad \partial_y\phi_{|y=H_1} = 0\ , \tag{4.27}$$

$$\partial_x\phi_{|x=0} = 0, \qquad \partial_x\phi_{|x=L_c} = 0\ . \tag{4.28}$$

Proposition 4.3.1. *Using the separation of variables method, one can show that the velocity potential can be solved explicitly as a sum of terms of the form, for all* $(p, q) \in \mathbb{N}^2$,

$$\phi_{p,q}(x, y, z) = \psi \cos\left(p\pi\frac{x}{L_c}\right)\cos\left(q\pi\frac{y}{H_1}\right)\frac{\cosh\left(\pi z\sqrt{p^2\frac{H_2^2}{L^2} + q^2\frac{H_2^2}{H_1^2}}\right)}{\cosh\left(\pi\sqrt{p^2\frac{H_2^2}{L^2} + q^2\frac{H_2^2}{H_1^2}}\right)}\ .$$

Proof 1. Let us start by introducing three functions $X_i,\ i = 1, 2, 3$ such as $X : \mathbb{R} \longrightarrow \mathbb{R}$, then one can write the velocity potential ϕ as follows:

$$\phi(x, y, z) = X_1(x)X_2(y)X_3(z)\ , \tag{4.29}$$

Plugging (4.29) into (4.25), one gets the following ordinary equation

$$\frac{\partial^2_{xx}X_1}{X_1} + \frac{\partial^2_{yy}X_2}{X_2} + \frac{\partial^2_{zz}X_3}{X_3} = 0$$

The next step consists to separate the variables, then the previous system can be written as follows

$$-\frac{\partial^2_{xx}X_1}{X_1} = \frac{\partial^2_{yy}X_2}{X_2} + \frac{\partial^2_{zz}X_3}{X_3} = \lambda_1^2\ ,$$

where λ is a separation constant. Then, one has to resolve the following second order ordinary equation:

$$-\partial^2_{xx}X_1 + \lambda_1^2 X_1 = 0\ ,$$

which admits a solution in the following form:

$$X_1(x) = C_1 \cos(\lambda_1 x) + C_2 \sin(\lambda_1 x), \tag{4.30}$$

where C_1 and C_2 are two constants to be determined. Using the boundary condition (4.28), the first one gives that $C_2 = 0$ and the second gives $C_1 \sin(\lambda_1 L_c) = 0$, which would allow us to deduce that $\lambda_1 = \dfrac{p}{L_c}\pi$ for $p \in \mathbb{N}$. Then

$$X_1(x) = C_1 \cos(\frac{p}{L_c}\pi x) \tag{4.31}$$

Similarly, using the same technique, one deduce an analytical expressions for $X_2(y)$ and $X_3(z)$,

$$X_2(y) = C_2 \cos(\frac{q}{H_1}\pi y), \qquad q \in \mathbb{N} \tag{4.32}$$

$$X_3(z) = C_3 \cosh\left(\pi z \sqrt{\frac{p^2}{L_c^2} + \frac{q^2}{H_2^2}}\right). \tag{4.33}$$

Finally, the expression of ϕ is given as follows,

$$\phi(x, y, z) = C_4 \cos(\frac{p}{L}\pi x) \cos(\frac{q}{H_1}\pi y) \cosh\left(\sqrt{\frac{p^2}{L^2} + \frac{q^2}{H_2^2}}\pi(z + H_2)\right)$$

with $C_4 = C_1 C_2 C_3$. The value of the constant C_4 is determined using the boundary condition (4.26) for $z = H_2$. That gives $C_4 = \psi$.
Hence the result.

The function $\phi_{p,q}$ is of order $O(1)$ but its k-th derivatives with respect to z are of order $O\left(\left(\dfrac{H_2}{H_1}\right)^k\right)$. More precisely, for $z = 1$, $\partial_z \phi_{p,q} \to +\infty$ if $H_1 < H_2 \ll L$ whenever $H_2 \to 0$. To ensure that derivatives are small or of order O(1), we have to assume that $H_1 \geq H_2$.

If we assume that $H_2 < H_1 \ll L$ and if we set $\mu_i = \dfrac{H_i}{L}$, $i = 1, 2$ then the preponderant dispersive parameter is μ_1 but not μ_2. As a consequence, the resulting dispersive model will be defined through the transversal dispersive parameter and it is somehow unusual (see Eqs. (4.19) and (4.20)).

If we set $\mu_i = \dfrac{H_i}{L}$, $i = 1, 2$ and if we assume that $H_1 = H_2$ then $\mu_1 = \mu_2$. In this case, we are unable to write the asymptotic term of u with respect to v and w simultaneously up to the order $O(\mu_2)$. Indeed, in this case, the irrotational equations (4.24) become

$$\nabla_{y,z}(u) = \mu_2 \frac{\partial}{\partial x}\begin{pmatrix} v \\ w \end{pmatrix}, \ \frac{\partial}{\partial z} v = \frac{\partial}{\partial y} w \ .$$

For all these reasons, we have introduced a parameter $h_1 < H_1 = H_2$ such that the velocity scales $V < W < U$ in order to obtain a dispersive model defined by the

classical dispersive parameter μ_2 and not μ_1. Our asymptotic preserves the structure of the equations. Once this parameter is introduced, we have to first average in the transversal direction and second following the depth. This choice is naturally imposed by the irrotational equations (4.24) and more precisely by the equation $\frac{\partial}{\partial y} w = \frac{\mu_1}{\mu_2} \frac{\partial}{\partial z} v$ since $\frac{\mu_1}{\mu_2} < 1$.

4.3.3 3D-2D model reduction and asymptotic expansions

In this first step, we focus on the width-averaging of System (4.17)–(4.20). In particular, we compute the asymptotic expansions of the velocity (u, v) and the pressure P of System (4.17)–(4.20) as a function of their width-averages. We obtain what we call "flat free surface approximation" property which means that the variations of the free surface following y can be neglected in the three-dimensional Euler system (4.17)–(4.20). Finally, the asymptotic approximation of the width-averaged Euler system is obtained. This averaged model is the starting point for the second step (see §4.3.4).

4.3.3.1 Asymptotic expansions of the fluid velocity

Given a function $(t, x, y, z) \mapsto X(t, x, y, z)$ and $(x, z) \mapsto q(x, z)$, we define X_q as follows

$$X_q(t, x, z) := X\left(t, x, q(x, z), z\right)$$

and we use the notations

$$\boldsymbol{w} = \begin{pmatrix} u \\ w \end{pmatrix}, \ \mathrm{div}_{x,z}\left[\boldsymbol{w}\right] = \frac{\partial}{\partial x} u + \frac{\partial}{\partial z} w \text{ and } \nabla_{x,z}(u) = \begin{pmatrix} \frac{\partial}{\partial x} u \\ \frac{\partial}{\partial z} u \end{pmatrix}$$

to represent the vector $\boldsymbol{w}$, the two dimensional divergence operator and the gradient operator with respect to the variable x and z.

Integrating the two first equations of the irrotational equations (4.24) for $s \in [\alpha(x, z), y]$, we get

$$u(t, x, y, z) = u_\alpha\left(t, x, z\right) + \mu_1 \int_{\alpha(x,z)}^{y} \frac{\partial}{\partial x} v \, ds \tag{4.34}$$

and

$$w(t, x, y, z) = w_\alpha\left(t, x, z\right) + \frac{\mu_1}{\mu_2} \int_{\alpha(x,z)}^{y} \frac{\partial}{\partial z} v \, ds \, . \tag{4.35}$$

Then, integrating the divergence equation (4.17) for $s \in [\alpha(x, z), y]$, we obtain

$$\int_{\alpha(x,z)}^{y} \frac{\partial}{\partial y} v \, dy = - \int_{\alpha(x,z)}^{y} \mathrm{div}_{x,z}\left[\boldsymbol{w}\right] \, dy \, . \tag{4.36}$$

Thanks to Eqs. (4.34), (4.35) and (4.36) and the wet boundary condition (4.23) for $\varphi = \alpha$ the fluid velocity v is approximated by

$$v(t, x, y, z) = -\mathrm{div}_{x,z}\left[\boldsymbol{w}_\alpha(t, x, z)(y - \alpha(x, z))\right] + O\left(\frac{\mu_1}{\mu_2}\right) \, . \tag{4.37}$$

Coming back to Eqs. (4.34) and (4.35) together with Eq. (4.37), the fluid velocity (u, w) can be written as

$$u(t,x,y,z) = u_\alpha(t,x,z) - \frac{\mu_1}{2}\frac{\partial}{\partial x}\mathrm{div}_{x,z}\left[\boldsymbol{w}_\alpha(t,x,z)(y-\alpha(x,z))^2\right] + O\left(\frac{\mu_1^2}{\mu_2}\right) \quad (4.38)$$

and

$$w(t,x,y,z) = w_\alpha(t,x,z) - \frac{\mu_1}{2\mu_2}\frac{\partial}{\partial z}\mathrm{div}_{x,z}\left[\boldsymbol{w}_\alpha(t,x,z)(y-\alpha(x,z))^2\right] + O\left(\frac{\mu_1^2}{\mu_2^2}\right). \quad (4.39)$$

4.3.3.2 Width-averaged Euler equations

Given a function $(t,x,y,z) \mapsto X(t,x,y,z)$, we define the width-average of X by the quantity

$$\langle X\rangle(t,x,z) := \frac{1}{\sigma(x,z)}\int_{\alpha(x,z)}^{\beta(x,z)} X(t,x,y,z)\,dy$$

where $\sigma(x,z) = \beta(x,z) - \alpha(x,z)$ is the width of the section at the elevation z.

We average the equations (4.17)–(4.20) for $y \in [\alpha(x,z), \beta(x,z)]$ using Leibniz integral rule, to get the width-averaged Euler system:

$$\begin{cases} \dfrac{\partial}{\partial x}(\sigma\langle u\rangle) + \dfrac{\partial}{\partial z}(\sigma\langle w\rangle) = 0 \\ \dfrac{\partial}{\partial t}(\sigma\langle u\rangle) + \dfrac{\partial}{\partial x}(\sigma\langle u^2\rangle) + \dfrac{\partial}{\partial z}(\sigma\langle uw\rangle) + \dfrac{\partial}{\partial x}(\sigma\langle P\rangle) = P_\beta\dfrac{\partial\beta}{\partial x} - P_\alpha\dfrac{\partial\alpha}{\partial x} \\ \mu_2\left(\dfrac{\partial}{\partial t}(\sigma\langle w\rangle) + \dfrac{\partial}{\partial x}(\sigma\langle uw\rangle) + \dfrac{\partial}{\partial z}(\sigma\langle w^2\rangle)\right) + \dfrac{\partial}{\partial z}(\sigma\langle P\rangle) = -\dfrac{\sigma}{{F_r}^2} + P_\beta\dfrac{\partial\beta}{\partial z} \\ \qquad\qquad -P_\alpha\dfrac{\partial\alpha}{\partial z} \\ P_\beta = P_\alpha - \mu_1\left\langle\dfrac{Dv}{Dt}\right\rangle \end{cases} \quad (4.40)$$

where $\dfrac{Dv}{Dt}$ stands for the material derivative

$$\frac{Dv}{Dt} := \frac{\partial}{\partial t}v + u\frac{\partial}{\partial x}v + v\frac{\partial}{\partial y}v + w\frac{\partial}{\partial z}v\,.$$

Asymptotic expansions of the width-averaged terms in System (4.40)**.**

Thanks to the expressions (4.38) and (4.39), the average of the terms in System (4.40)

can be written

$$\begin{aligned}
\sigma(x,z)\langle u\rangle(t,x,z) &= \sigma(x,z)u_\alpha(t,x,z) \\
&\quad -\frac{\mu_1}{6}\frac{\partial}{\partial x}\mathrm{div}_{x,z}\left[\boldsymbol{w}_\alpha(t,x,z)\sigma(x,z)^3\right] + O\left(\frac{\mu_1^2}{\mu_2}\right), \qquad (4.41)\\
\sigma(x,z)\langle w\rangle(t,x,z) &= \sigma(x,z)w_\alpha(t,x,z) \\
&\quad -\frac{\mu_1}{6\mu_2}\frac{\partial}{\partial z}\mathrm{div}_{x,z}\left[\boldsymbol{w}_\alpha(t,x,z)\sigma(x,z)^3\right] + O\left(\frac{\mu_1^2}{\mu_2^2}\right), \qquad (4.42)\\
\sigma(x,z)\langle u^2\rangle(t,x,z) &= \sigma(x,z)u_\alpha^2(t,x,z) + O\left(\frac{\mu_1^2}{\mu_2}\right), \qquad (4.43)\\
\sigma(x,z)\langle w^2\rangle(t,x,z) &= \sigma(x,z)w_\alpha^2(t,x,z) + O\left(\frac{\mu_1^2}{\mu_2^2}\right), \qquad (4.44)\\
\sigma(x,z)\langle uw\rangle(t,x,z) &= \sigma(x,z)u_\alpha(t,x,z)w_\alpha(t,x,z) \\
&\quad -u_\alpha(t,x,z)\frac{\mu_1}{6\mu_2}\frac{\partial}{\partial z}\mathrm{div}_{x,z}\left[\boldsymbol{w}_\alpha(t,x,z)\sigma(x,z)^3\right] \\
&\quad +O\left(\frac{\mu_1^2}{\mu_2^2}\right). \qquad (4.45)
\end{aligned}$$

Irrotationality.

We lose the irrotational condition (4.24) by width-averaging since we get

$$\frac{\partial}{\partial z}\left(\sigma\langle u\rangle\right) = \mu_2\frac{\partial}{\partial x}\left(\sigma\langle w\rangle\right) + \left(u_\beta\frac{\partial}{\partial z}\beta - w_\beta\frac{\partial}{\partial x}\beta - u_\alpha\frac{\partial}{\partial z}\alpha + w_\alpha\frac{\partial}{\partial x}\alpha\right).$$

However, using the last equation in (4.24) together with Eqs. (4.38) and (4.39), we obtain

$$\frac{\partial u_\alpha}{\partial z} = \mu_2\frac{\partial w_\alpha}{\partial x} + O(\mu_1). \qquad (4.46)$$

The approximated irrotational condition can be also written as a function of $(\langle u\rangle, \langle w\rangle)$ by means of Eqs. (4.41) and (4.42).

Asymptotic expansion of the pressure.

The last equation in System (4.40) allows to write

$$P_\beta = P_\alpha + O(\mu_1). \qquad (4.47)$$

Thanks to (4.47), on one hand, the terms in the right hand side of the second and third equations of System (4.40) can be simplified in

$$P_\beta\nabla_{x,z}(\beta) - P_\alpha\nabla_{x,z}(\alpha) = P_\alpha\nabla_{x,z}(\sigma) + O(\mu_1).$$

On the other hand, coming back to System (4.17)–(4.20) together with Eq. (4.47), integrating Eq. (4.19) for $s \in [\alpha(x,z), y]$, we show that

$$P(t,x,y,z) = P_\alpha(t,x,z) - \mu_1\int_{\alpha(x,z)}^{y}\frac{Dv}{Dt}\,ds = P_\alpha(t,x,z) + O(\mu_1). \qquad (4.48)$$

As a consequence, the width-averaged pressure $\langle P \rangle$ can be approximated by P_α at order $O(\mu_1)$, *i.e.*

$$\langle P \rangle(t,x,z) = P_\alpha(t,x,z) + O(\mu_1) \; .$$

Asymptotic expansion of the free surface.

Using Eqs. (4.39) and (4.48) in Eq. (4.20), we can write the z-gradient of the pressure as

$$\frac{\partial}{\partial z} P_\alpha(t,x,z) = -\frac{1}{{F_r}^2} - \mu_2 \frac{D}{Dt} w_\alpha(t,x,z) + O(\mu_1) \; .$$

Next, integrating this equation for $s \in [z, \eta(t,x,y)]$ using the boundary condition (4.21) with Eq. (4.48) lead to

$$P_\alpha(t,x,z) \;=\; \frac{\eta(t,x,y) - z}{{F_r}^2} + \mu_2 \int_z^{\eta(t,x,y)} \frac{D}{Dt} w_\alpha(t,x,s)\, ds + O(\mu_1) \; .$$

Thus, taking the y-derivative of this expression yields to

$$0 = \partial_y \eta \left(\frac{1}{F_r^2} + \mu_2 \frac{D}{Dt} w_{\alpha\,|z=\eta} \right) + O(\mu_1) = -\partial_y \eta \, \partial_z P_{|z=\eta} + O(\mu_1) \; .$$

Consequently, since $\partial_z P_{|z=\eta} \neq 0$, we get $\partial_y \eta = O(\mu_1)$, *i.e.*, we obtain the flat surface approximation

$$\eta(t,x,y) = \eta_{\rm eq}(t,x) + O(\mu_1) \tag{4.49}$$

for some function $\eta_{\rm eq}$ defined hereafter. It means that one can neglect the y-variations of the free surface of the three-dimensional model (4.17)–(4.20) (see Fig. 4.2). In other words, the fluid cross-section $\Omega(t,x)$ (4.7) and the wet area $A(t,x)$ (4.8) can be simplified in

$$\Omega_{\rm eq}(t,x) = \left\{ (y,z) \in \mathbb{R}^2;\; \alpha(x,z) \leq y \leq \beta(x,z) \;\text{ and } d^*(x) \leq z \leq \eta_{\rm eq}(t,x) \right\} \tag{4.50}$$

with

$$A_{\rm eq} = \left| \Omega_{\rm eq}(t,x) \right| \tag{4.51}$$

thanks to

$$\begin{aligned}
A(t,x) &= \int_{\Omega(t,x)} dy\; dz \\
&= \int_{y^-(t,x)}^{y^+(t,x)} \eta(t,x,y) - d(x,y)\; dy \\
&= \int_{y^-(t,x)}^{y^+(t,x)} \eta_{\rm eq}(t,x) - d(x,y)\; dy + O(\mu_1) \\
&= \int_{d^*(x)}^{\eta_{\rm eq}(t,x)} \sigma(x,z)\; dz + O(\mu_1) \\
&= \int_{\Omega_{\rm eq}(t,x)} dy\; dz + O(\mu_1) \\
&= A_{\rm eq}(t,x) + O(\mu_1)
\end{aligned} \tag{4.52}$$

Therefore, in the following, we consider the fluid cross-section $\Omega_{\rm eq}$ instead of Ω for which computations are easier. In the following, we set $\eta_{\rm eq}$ as

$$\eta_{\rm eq}(t,x) = \eta(t,x,y^*(x)) \; .$$

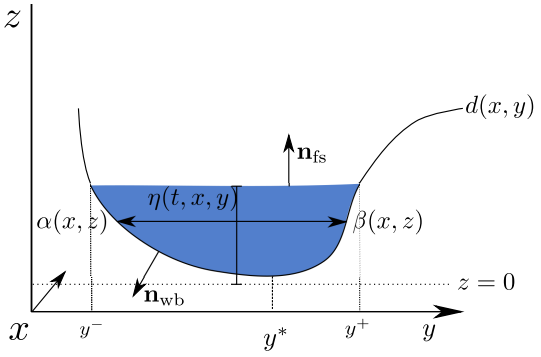

Figure 4.2: Equivalent geometric set-up

Width-averaged equations.

Using all the previous equations (4.41)–(4.45) and (4.48)–(4.49) in System (4.40), we obtain the width-averaged Euler equations expressed as the couple of unknown $(\boldsymbol{w}_\alpha, P_\alpha)$:

$$\begin{aligned}
&\mathrm{div}_{x,z}\left[\sigma \boldsymbol{w}_\alpha\right] + O\left(\frac{\mu_1^2}{\mu_2^2}\right) \quad = \quad \frac{\mu_1}{6\mu_2}\frac{\partial}{\partial z}\left(\sigma\frac{\partial}{\partial z}\left(\mathrm{div}_{x,z}\left[\boldsymbol{w}_\alpha\sigma^3\right]\right)\right)\\
&\frac{\partial}{\partial t}(\sigma u_\alpha) + \mathrm{div}_{x,z}\left[\sigma u_\alpha \boldsymbol{w}_\alpha\right] + \frac{\partial}{\partial x}(\sigma P_\alpha) + O\left(\frac{\mu_1^2}{\mu_2^2}\right) \quad = \quad P_\alpha\frac{\partial \sigma}{\partial x}\\
&\qquad\qquad + \frac{\mu_1}{6\mu_2}\frac{\partial}{\partial x}\left(u_\alpha\frac{\partial}{\partial z}\mathrm{div}_{x,z}\left[\boldsymbol{w}_\alpha\sigma^3\right]\right)\\
&\mu_2\left(\frac{\partial}{\partial t}(\sigma w_\alpha) + \mathrm{div}_{x,z}\left[\sigma w_\alpha \boldsymbol{w}_\alpha\right]\right) + \frac{\partial}{\partial z}(\sigma P_\alpha) \quad = \quad -\frac{\sigma}{{F_r}^2} + P_\alpha\frac{\partial \sigma}{\partial z} + O(\mu_1)
\end{aligned} \tag{4.53}$$

where the fluid domain is now defined (see Eqs. (4.49)-(4.50) and Fig. 4.3) by

$$\langle\Omega\rangle(t,x) = \left\{z\in\mathbb{R};\ d^*(x)\le z\le \eta_{\mathrm{eq}}(t,x)\right\}\ .$$

For a given time $t\in[0,T]$ and $x\in[0,L_c]$, the boundary of the fluid cross-section $\partial\langle\Omega\rangle(t,x)$ is composed of a free surface $\langle\Gamma_{\mathrm{fs}}\rangle(t,x) = \{z\in\mathbb{R};\ z=\eta_{\mathrm{eq}}(t,x)\}$ and a wet boundary $\langle\Gamma_{\mathrm{wb}}\rangle(x) = \{z\in\mathbb{R};\ z=d^*(x)\}$ such that

$$\partial\langle\Omega\rangle(t,x) = \langle\Gamma_{\mathrm{fs}}\rangle(t,x)\cup\langle\Gamma_{\mathrm{wb}}\rangle(x)$$

The unit outward normal vector to the free surface is

$$\langle\boldsymbol{n}_{\mathrm{fs}}\rangle(t,x) = \frac{1}{\sqrt{1+\left(\dfrac{\partial}{\partial x}\eta_{\mathrm{eq}}(t,x)\right)^2}}\begin{pmatrix}-\dfrac{\partial}{\partial x}\eta_{\mathrm{eq}}(t,x)\\ 1\end{pmatrix}$$

and the unit outward normal vector to the wet boundary is

$$\langle\boldsymbol{n}_{\mathrm{wb}}\rangle(x) = \frac{1}{\sqrt{1+\left(\dfrac{\partial}{\partial x}d^*(x)\right)^2}}\begin{pmatrix}\dfrac{\partial}{\partial x}d^*(x)\\ -1\end{pmatrix}\ .$$

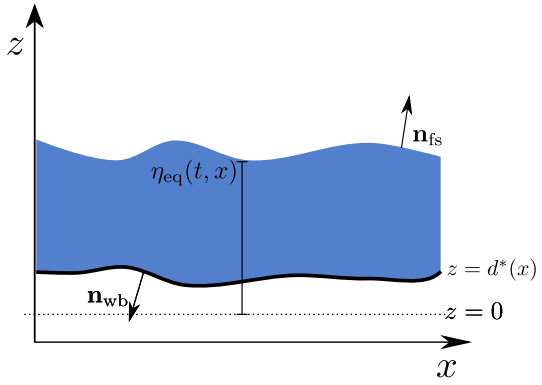

Figure 4.3: Width-averaged geometric set-up

These equations are completed with the irrotational condition (4.46) and the following boundary conditions

$$\frac{\partial \eta_{\text{eq}}}{\partial t} + u_\alpha \frac{\partial \eta_{\text{eq}}}{\partial x} = w_\alpha + O\left(\frac{\mu_1}{\mu_2}\right) \text{ and } P_\alpha = O(\mu_1) \text{ on } z = \eta_{\text{eq}} \tag{4.54}$$

$$u_\alpha \frac{\partial}{\partial x} d = w_\alpha + O\left(\frac{\mu_1}{\mu_2}\right) \text{ on } z = d \tag{4.55}$$

which are obtained through Eqs. (4.21) and (4.22) using Eqs. (4.37), (4.38), (4.39).

These end the first step.

4.3.4 2D-1D like model reduction and asymptotic expansions

In what follows, we note $f_b(t,x) = f_\alpha(t,x,d^*(x))$ for a given function f and S

$$S(x,z) = \int_{d^*(x)}^{z} \sigma(x,s)\, ds \tag{4.56}$$

the wet area of water between $d^*(x)$ and z.

In the sequel, we consider the fluid cross-section (4.50) $\Omega_{\text{eq}}(t,x)$ instead of $\Omega(t,x)$ thanks to (4.52) (see also (4.7)). Thus, we define the local height of the water in $\Omega_{\text{eq}}(t,x)$ by

$$h_{\text{eq}}(t,x,y) = \eta_{\text{eq}}(t,x) - d(x,y)\ . \tag{4.57}$$

In this new setting, the section-average $\bar{f}_{\text{eq}}$ of a function f can be defined by

$$\bar{f}_{\text{eq}} = \frac{1}{A_{\text{eq}}(t,x)} \int_{d^*(x)}^{\eta_{\text{eq}}(t,x)} \int_{\alpha(x,z)}^{\beta(x,z)} f(t,x,y,z)\, dydz\ .$$

4.3.4.1 Asymptotic expansion of the fluid velocity

Let us first integrate Eq. (4.46) for $s \in [d^*(x), z]$, to get

$$u_\alpha(t,x,z) = u_b(t,x) + \mu_2 \int_{d^*(x)}^{z} \frac{\partial w_\alpha}{\partial x} ds + O(\mu_1)\ . \tag{4.58}$$

Then, dropping all the lower terms in $O\left(\frac{\mu_1}{\mu_2}\right)$ in the first equation of System (4.53):

$$\frac{\partial}{\partial z}(\sigma w_\alpha) = -\frac{\partial}{\partial x}(\sigma u_\alpha) + O\left(\frac{\mu_1}{\mu_2}\right)$$

and integrating the above equation for $s \in [d^*(x), z]$, keeping in mind the boundary condition (4.55), we obtain

$$\sigma(x,z) w_\alpha(t,x,z) \;=\; -\frac{\partial}{\partial x}\left(\int_{d^*(x)}^{z} \sigma u_\alpha \, ds\right) + O\left(\frac{\mu_1}{\mu_2}\right) .$$

By means of Eq. (4.58), the previous equation becomes:

$$w_\alpha(t,x,z) \;= -\frac{1}{\sigma(x,z)}\frac{\partial}{\partial x}\left(u_b(t,x) S(x,z)\right) + O(\mu_2) . \tag{4.59}$$

By injecting Eq. (4.59) in (4.58), we get

$$u_\alpha(t,x,z) = u_b(t,x) - \mu_2 \int_{d^*(x)}^{z} \frac{\partial}{\partial x}\mathcal{S}(u_b,x,s)\, ds + O(\mu_2^2) \tag{4.60}$$

where

$$\mathcal{S}(u,x,z) = \frac{1}{\sigma(x,z)}\frac{\partial}{\partial x}\left(uS(x,z)\right) . \tag{4.61}$$

As a consequence, we have

$$\begin{aligned}
\bar{u}_{\text{eq}} &= \frac{1}{A_{\text{eq}}(t,x)} \int_{d^*(x)}^{\eta_{\text{eq}}(t,x)} \int_{\alpha(x,z)}^{\beta(x,z)} u(t,x,y,z)\, dy\, dz \\
&= \frac{1}{A_{\text{eq}}(t,x)} \int_{d^*(x)}^{\eta_{\text{eq}}(t,x)} \sigma(x,z)\langle u\rangle(t,x,z) dz \\
&= \frac{1}{A_{\text{eq}}(t,x)} \int_{d^*(x)}^{\eta_{\text{eq}}(t,x)} \sigma(x,z) u_\alpha(t,x,z)\, dz + O(\mu_1)
\end{aligned}$$

and through Eq. (4.60), we obtain

$$\begin{aligned}
\bar{u}_{\text{eq}}(t,x) &= \frac{1}{A_{\text{eq}}(t,x)} \int_{d^*(x)}^{\eta_{\text{eq}}(t,x)} \sigma(x,z)\left(u_b(t,x) - \mu_2 \int_{d^*(x)}^{z} \frac{\partial}{\partial x}\mathcal{S}(u_b,x,s)\, ds\right) dz \\
&\quad + O(\mu_2^2) \\
&= u_b(t,x) - \frac{\mu_2}{A_{\text{eq}}(t,x)} \int_{d^*(x)}^{\eta_{\text{eq}}(t,x)} \sigma(x,z)\left(\int_{d^*(x)}^{z} \frac{\partial}{\partial x}\mathcal{S}(u_b,x,s)\, ds\right) dz \\
&\quad + O(\mu_2^2)
\end{aligned}$$

i.e.

$$u_b(t,x) = \bar{u}_{\text{eq}}(t,x) + \frac{\mu_2}{A_{\text{eq}}(t,x)} \int_{d^*(x)}^{\eta_{\text{eq}}(t,x)} \sigma(x,z)\left(\int_{d^*(x)}^{z} \frac{\partial}{\partial x}\mathcal{S}(u_b,x,s)\, ds\right) dz + O(\mu_2^2) . \tag{4.62}$$

Using the fact that

$$u_b(t,x) = \bar{u}_{\text{eq}}(t,x) + O(\mu_2)$$

in Eq. (4.62) allows to write $u_b(t,x)$ as a function of $\bar{u}_{\rm eq}$:

$$u_b(t,x) = \bar{u}_{\rm eq}(t,x) + \frac{\mu_2}{A_{\rm eq}(t,x)} \int_{d^*(x)}^{\eta_{\rm eq}(t,x)} \sigma(x,z) \left(\int_{d^*(x)}^{z} \frac{\partial}{\partial x} \mathcal{S}(\bar{u}_{\rm eq},x,s)\, ds \right) dz + O(\mu_2^2)\,. \tag{4.63}$$

Finally, thanks to (4.34), (4.60), (4.63), by linearity of $\mathcal{S}$ (4.61), we obtain

$$\begin{aligned} u(t,x,y,z) &= u_\alpha(t,x,z) + O(\mu_1) \\ &= u_b(t,x) - \mu_2 \int_{d^*(x)}^{z} \frac{\partial}{\partial x} \mathcal{S}(u_b,x,s)\, ds + O(\mu_2^2) \\ &= \bar{u}_{\rm eq}(t,x) + \mu_2 B_0(\bar{u}_{\rm eq},x,z) + O(\mu_2^2) \end{aligned} \tag{4.64}$$

where

$$B_0(\bar{u}_{\rm eq},x,z) = \frac{1}{A_{\rm eq}(t,x)} \int_{d^*(x)}^{\eta_{\rm eq}(t,x)} \left(\sigma(x,z) \int_{d^*(x)}^{z} \frac{\partial}{\partial x} \mathcal{S}(\bar{u}_{\rm eq},x,s)\, ds \right) dz - \int_{d^*(x)}^{z} \frac{\partial}{\partial x} \mathcal{S}(\bar{u}_{\rm eq},x,s)\, ds\,. \tag{4.65}$$

Repeating the computations with Eqs. (4.39), (4.59) and (4.64), we find

$$w(t,x,y,z) = -\mathcal{S}(\bar{u}_{\rm eq},x,z) + O\left(\frac{\mu_1}{\mu_2}\right)\,. \tag{4.66}$$

4.3.4.2 Pressure decomposition

Integrating for $s \in [z, \eta_{\rm eq}]$, the third equation of System (4.53), we get

$$\begin{aligned} P_\alpha(t,x,z) &= \frac{(\eta_{\rm eq}(t,x)-z)}{{F_r}^2} + \int_z^{\eta_{\rm eq}(t,x)} \frac{\mu_2}{\sigma} \left(\frac{\partial}{\partial t}(\sigma w_\alpha) + {\rm div}_{x,z}\left[\sigma w_\alpha \boldsymbol{w}_\alpha\right] \right) ds \\ &\quad + O(\mu_1)\,. \end{aligned}$$

Thanks to the free surface boundary condition (4.54), Eq. (4.64) and Eq. (4.66), we obtain the asymptotic expansion of the pressure P at order $O(\mu_2^2)$

$$P(t,x,y,z) = P_{\rm h}(t,x,z) + \mu_2 P_{\rm nh}(t,x,z) + O(\mu_2^2)$$

where

$$P_{\rm h}(t,x,z) = \frac{(\eta_{\rm eq}(t,x)-z)}{{F_r}^2} \tag{4.67}$$

is the usual hydrostatic pressure and

$$\begin{aligned} P_{\rm nh}(t,x,z) &= \int_z^{\eta_{\rm eq}(t,x)} \frac{1}{2\sigma(x,s)^2} \frac{\partial}{\partial z} \left(\left(\sigma(x,s)\mathcal{S}(\bar{u}_{\rm eq},x,s)\right)^2 \right) ds \\ &\quad - \int_z^{\eta_{\rm eq}(t,x)} \frac{\partial}{\partial t} \mathcal{S}(\bar{u}_{\rm eq},x,s) + \frac{\bar{u}_{\rm eq}(t,x)}{\sigma(x,s)} \frac{\partial}{\partial x} \left(\sigma(x,s)\mathcal{S}(\bar{u}_{\rm eq},x,s)\right) ds \end{aligned}$$

is a non-hydrostatic pressure.

Handling the terms in the non-hydrostatic pressure differently, one can write

$$P_{\text{nh}}(t,x,z) = \mathcal{D}(\bar{u}_{\text{eq}}) \int_z^{\eta_{\text{eq}}} \frac{S(x,s)}{\sigma(x,s)}\, ds + \int_z^{\eta_{\text{eq}}} \mathcal{Q}(\bar{u}_{\text{eq}}, S, \sigma)\, ds \tag{4.68}$$

where

$$\mathcal{D}(u) = \left(\frac{\partial}{\partial x} u\right)^2 - \frac{\partial}{\partial t}\frac{\partial}{\partial x} u - u\partial_x^2 u\,, \tag{4.69}$$

and

$$\begin{aligned} \mathcal{Q}(u,S,\sigma) \;=\; & \frac{u^2}{\sigma(x,s)}\left(\frac{\frac{\partial}{\partial x}S(x,s)\frac{\partial}{\partial x}\sigma(x,s)}{\sigma(x,s)} - \partial_x^2 S(x,s)\right) \\ & + \frac{\partial}{\partial x}\left(\frac{u^2}{2}\right)\frac{S(x,s)\frac{\partial}{\partial x}\sigma(x,s)}{\sigma(x,s)^2} - \left(\frac{\partial}{\partial t}u + u\frac{\partial}{\partial x}u\right)\frac{\frac{\partial}{\partial x}S(x,s)}{\sigma(x,s)} \end{aligned} \,. \tag{4.70}$$

The non-hydrostatic pressure (4.68) is more suitable to have a formulation akin to the SGN equations (4.2)-(4.4).

4.4 A new non-linear dispersive model

In this section, we assume that the flow is governed, on the space-time domain $\Omega_{\text{eq}} = \bigcup_{0\le t\le 1} \Omega_{\text{eq}}(t)$, instead of Ω (see Def. (4.6)), by the three-dimensional incompressible and irrotational Euler equations (4.17)–(4.20), (4.24) where the wet region is defined as the region in which the fluid resides at each time $t \in [0,1]$, $\Omega_{\text{eq}}(t) = \bigcup_{0\le x\le 1} \Omega_{\text{eq}}(t,x)$ with $\Omega_{\text{eq}}(t,x)$ the fluid cross-section defined by (4.50).

These equations (4.17)–(4.20) are completed with the kinematic boundary condition at the free surface (4.21) $\Gamma_{\text{fs}}(t,x) = \{z \in \mathbb{R};\ z = \eta_{\text{eq}}(t,x)\}$, and a no-penetration condition on the wet boundary (4.22) $\Gamma_{\text{wb}}(x) = \{(y,z) \in \mathbb{R}^2;\ z = d(x,y)\}$ where

$$\partial\Omega_{\text{eq}}(t,x) = \Gamma_{\text{fs}}(t,x) \cup \Gamma_{\text{wb}}(x)\,.$$

These boundary conditions can be written under the following form:

$$\int_{\partial\Omega_{\text{eq}}(t,x)} \left(\frac{\partial}{\partial t}\boldsymbol{m} + u\frac{\partial}{\partial x}\boldsymbol{m} - \boldsymbol{v}\right)\cdot \boldsymbol{n}\; ds = 0 \text{ on } \partial\Omega_{\text{eq}}(t,x) \tag{4.71}$$

where $\boldsymbol{m}(t,x,y,z) = \begin{cases} (y, \eta_{\text{eq}}(t,x)) & \text{if} \quad \boldsymbol{m} \in \Gamma_{\text{fs}}(t,x) \\ (y, d(x,y)) & \text{if} \quad \boldsymbol{m} \in \Gamma_{\text{wb}}(t,x) \end{cases}$ is a boundary point,

$\boldsymbol{n} = \begin{cases} \boldsymbol{n}_{\text{fs}} & \text{if} \quad \boldsymbol{m} \in \Gamma_{\text{fs}}(t,x) \\ \boldsymbol{n}_{\text{wb}} & \text{if} \quad \boldsymbol{m} \in \Gamma_{\text{wb}}(t,x) \end{cases}$ stands for the outward unit normal vector in the $\Omega_{\text{eq}}(t,x)$-plane (see Fig. 4.2) and $\boldsymbol{v} = \begin{pmatrix} v \\ w \end{pmatrix}$.

To work with the wet region, we introduce its indicator function

$$\Phi(t, x, y, z) := \mathbb{1}_{\Omega_{\text{eq}}(t,x)} \text{ for all } t, x, y, z \in \mathbb{R}$$

where

$$\mathbb{1}_P := \begin{cases} 1 & \text{if } P \text{ is true,} \\ 0 & \text{if } P \text{ is false.} \end{cases}$$

The function Φ is advected by the flow so its material derivative, with respect to the flow $\bar{\boldsymbol{u}}$, must, therefore, be zero. Moreover, thanks to the incompressibility condition, Φ satisfies the following indicator transport equation

$$\frac{\partial}{\partial t}\Phi + \frac{\partial}{\partial x}(\Phi u) + \text{div}_{y,z}\left[\Phi \boldsymbol{v}\right] = 0 \text{ on } \Omega_{\text{eq}}(t) \tag{4.72}$$

where $\text{div}_{y,z}\left[\boldsymbol{v}\right] = \dfrac{\partial}{\partial y}v + \dfrac{\partial}{\partial z}w$ with $\boldsymbol{v} = (v, w)$.

4.4.1 Eq. of the conservation of the mass

Integrating Eq. (4.72) over the section $\Omega_{\text{eq}}(t, x)$ and using Leibniz integral rule, we get the following conservation of the mass equation

$$\int_{\Omega_{\text{eq}}(t,x)} \frac{\partial}{\partial t}\Phi + \frac{\partial}{\partial x}(\Phi u) + \text{div}_{y,z}\left[\Phi \boldsymbol{v}\right]\ dy\ dz = \frac{\partial}{\partial t}A_{\text{eq}} + \frac{\partial}{\partial x}Q_{\text{eq}} = 0 \tag{4.73}$$

where Q_{eq} is the water discharge

$$Q_{\text{eq}} = A_{\text{eq}}\bar{u}_{\text{eq}} \tag{4.74}$$

and $\bar{u}_{\text{eq}}$ is $\Omega_{\text{eq}}(t, x)$ section-averaged velocity given by

$$\bar{u}_{\text{eq}} = \frac{1}{A_{\text{eq}}(t, x)} \int_{\Omega_{\text{eq}}(t,x)} u(t, x, y, z)\ dydz\ .$$

4.4.2 Eq. of the conservation of the momentum

In order to get the momentum equation of the section-averaged free surface model, we integrate each term of (4.18) along the section $\Omega_{\text{eq}}(t, x)$ as follows:

$$\int_{\Omega_{\text{eq}}(t,x)} \underbrace{\frac{\partial}{\partial t}(u)}_{a_1} + \underbrace{\frac{\partial}{\partial x}(u^2)}_{a_2} + \underbrace{\text{div}_{y,z}\left[u\boldsymbol{v}\right]}_{a_3} + \underbrace{\frac{\partial}{\partial x}P}_{a_4}\ dy\ dz = 0\ .$$

Computation of the term $\displaystyle\int_{\Omega_{\text{eq}}(t,x)} a_1\ dy\ dz$

We have

$$\int_{\Omega_{\text{eq}}(t,x)} \frac{\partial}{\partial t}(u)dy\ dz = \frac{\partial}{\partial t}\int_{\Omega_{\text{eq}}(t,x)} u\ dy\ dz - \int_{\partial\Omega_{\text{eq}}(t,x)} u\frac{\partial}{\partial t}\boldsymbol{m}\cdot\boldsymbol{n}\ ds\ . \tag{4.75}$$

Computation of the term $\displaystyle\int_{\Omega_{\text{eq}}(t,x)} a_2 \, dy \, dz$

Thanks to the asymptotic approximation of the term u (4.64) up to order $O(\mu_2^2)$, the non-linear term u^2 can be written as:

$$u^2(t,x,y,z) = \bar{u}_{\text{eq}}(t,x)^2 + 2\mu_2 \bar{u}_{\text{eq}} B_0(\bar{u}_{\text{eq}}, x, z) + O\left(\mu_2^2\right) \ .$$

Therefore, we have

$$\int_{\Omega_{\text{eq}}(t,x)} \frac{\partial}{\partial x}(u^2) \, dy \, dz \ = \ \frac{\partial}{\partial x}\int_{\Omega_{\text{eq}}(t,x)} u^2 \, dy \, dz - \int_{\partial\Omega_{\text{eq}}(t,x)} u^2 \frac{\partial}{\partial x}\boldsymbol{m}\cdot\boldsymbol{n} \, ds$$

i.e.

$$\begin{aligned}\int_{\Omega_{\text{eq}}(t,x)} \frac{\partial}{\partial x}(u^2) \, dy \, dz \ &= \ \frac{\partial}{\partial x}({Q_{\text{eq}}}^2/A_{\text{eq}}) + \mu_2 \frac{\partial}{\partial x}\left(\frac{Q_{\text{eq}} B(x, Q_{\text{eq}}/A_{\text{eq}})}{A_{\text{eq}}}\right) \\ &\quad - \int_{\partial\Omega_{\text{eq}}(t,x)} u^2 \frac{\partial}{\partial x}\boldsymbol{m}\cdot\boldsymbol{n} \, ds + O\left(\mu_2^2\right)\end{aligned} \tag{4.76}$$

where B stands for the quadratic part of the fluid velocity, defined via B_0 (4.65), and

$$\begin{aligned}B(x, Q_{\text{eq}}/A_{\text{eq}}) \ &= \ \int_{\Omega_{\text{eq}}(t,x)} 2B_0(Q_{\text{eq}}/A_{\text{eq}}, x, z) \, dy \, dz \\ &= \ 2\int_{d^*(x)}^{\eta_{\text{eq}}(t,x)} \sigma(x,z) B_0(Q_{\text{eq}}/A_{\text{eq}}, x, z) \, dz = 0 \ .\end{aligned}$$

Computation of the term $\displaystyle\int_{\Omega_{\text{eq}}(t,x)} a_3 \, dy \, dz$

We have

$$\int_{\Omega_{\text{eq}}(t,x)} \text{div}_{y,z}\left[u\boldsymbol{v}\right] \, dy \, dz = \int_{\partial\Omega_{\text{eq}}(t,x)} u\boldsymbol{v}\cdot\boldsymbol{n} \, ds \ . \tag{4.77}$$

Computation of the term $\displaystyle\int_{\Omega_{\text{eq}}(t,x)} a_1 + a_2 + a_3 \, dy \, dz$

Gathering the results of the computations (4.75), (4.76) and (4.77), using the boundary conditions (4.71), we get

$$\begin{aligned}\int_{\Omega_{\text{eq}}(t,x)} a_1 + a_2 + a_3 dy \, dz \ &= \ \frac{\partial}{\partial t}Q_{\text{eq}} + \frac{\partial}{\partial x}({Q_{\text{eq}}}^2/A_{\text{eq}}) + \mu_2 \frac{\partial}{\partial x}\left(\frac{Q_{\text{eq}} B(x, Q_{\text{eq}}/A_{\text{eq}})}{A_{\text{eq}}}\right) \\ &\quad - \int_{\partial\Omega_{\text{eq}}(t,x)} u\left(\frac{\partial}{\partial t}\boldsymbol{m} + u\frac{\partial}{\partial x}\boldsymbol{m} - \boldsymbol{v}\right)\cdot\boldsymbol{n} \, ds + O\left(\mu_2^2\right) \\ &= \ \frac{\partial}{\partial t}Q_{\text{eq}} + \frac{\partial}{\partial x}({Q_{\text{eq}}}^2/A_{\text{eq}}) + O\left(\mu_2^2\right) \ .\end{aligned} \tag{4.78}$$

Computation of the term $\displaystyle\int_{\Omega_{\text{eq}}(t,x)} a_4 dy\ dz$

We apply the Leibniz rule to the gradient of the pressure and we obtain

$$\int_{\Omega_{\text{eq}}(t,x)} \frac{\partial}{\partial x} P\, dy\ dz = \frac{\partial}{\partial x}\int_{\Omega_{\text{eq}}(t,x)} P\, dy\ dz - \int_{\partial\Omega_{\text{eq}}(t,x)} P \frac{\partial}{\partial x}\boldsymbol{m}\cdot\boldsymbol{n}\, ds \tag{4.79}$$

where

$$\int_{\partial\Omega_{\text{eq}}(t,x)} P \frac{\partial}{\partial x}\boldsymbol{m}\cdot\boldsymbol{n}\, ds = \int_{\Gamma_{\text{wb}}(x)} P \frac{\partial}{\partial x}\boldsymbol{m}\cdot\boldsymbol{n}\, ds$$

thanks to the free surface boundary condition (4.13).

To compute the above boundary integral, we consider the parametrisation

$$z \in [d^*(x), \eta_{\text{eq}}(t,x)] \mapsto \boldsymbol{m}(x,z) = \begin{pmatrix} \varphi(x,z) \\ z \end{pmatrix}$$

where φ is given by (4.5). The unit speed curve parameterisation is

$$\left\| \frac{\partial}{\partial y}\boldsymbol{m}(x,z) \right\| = \sqrt{1 + \left(\frac{\partial}{\partial y}\varphi(x,z)\right)^2}\ .$$

The outward unit normal is given by

$$\boldsymbol{n} = \begin{cases} \dfrac{1}{\|\boldsymbol{n}\|}\begin{pmatrix} -1 \\ \dfrac{\partial}{\partial z}\alpha \end{pmatrix} & \text{if} \qquad \varphi(x,z) < y^*(x) \\ \dfrac{1}{\|\boldsymbol{n}\|}\begin{pmatrix} 1 \\ \dfrac{\partial}{\partial z}\beta \end{pmatrix} & \text{otherwise} \end{cases}$$

where

$$\|\boldsymbol{n}(x,z)\| = \left\| \frac{\partial}{\partial y}\boldsymbol{m}(x,z) \right\|\ .$$

Thus, we obtain

$$\int_{\Gamma_{\text{wb}}(x)} P \frac{\partial}{\partial x}\boldsymbol{m}\cdot\boldsymbol{n}\, ds = \int_{d^*(x)}^{\eta_{\text{eq}}(t,x)} P(t,x,z)\frac{\partial}{\partial x}\sigma(x,z)\, dz\ . \tag{4.80}$$

which is the formulation of the pressure source term as done in, for instance [33, 32]

Hydrostatic part: (see Eq. (4.67)) Using $P = P_{\text{h}}$ in Eq. (4.79), we get:

$$\int_{\Omega_{\text{eq}}(t,x)} \partial_x P_{\text{h}}(t,x,z)\, dy\ dz \quad = \quad \partial_x(I_1(t,x)) - I_2(t,x) \tag{4.81}$$

where

$$I_1(t,x) = \int_{\Omega_{\text{eq}}(t,x)} P_{\text{h}}(t,x,z)\, dy\ dz = \int_{d^*(x)}^{\eta_{\text{eq}}(t,x)} \frac{(\eta_{\text{eq}}(t,x) - z)}{{F_r}^2}\sigma(x,z)\, dz \tag{4.82}$$

and

$$I_2(t,x) = \int_{d^*(x)}^{\eta_{\text{eq}}(t,x)} \frac{(\eta_{\text{eq}}(t,x) - z)}{{F_r}^2} \frac{\partial}{\partial x}\sigma(x,z)\, dz \tag{4.83}$$

are respectively the hydrostatic pressure term and the hydrostatic pressure source term.

Non-hydrostatic part: (see Eq. (4.68)) Using $P = P_{\text{nh}}$ in Eq. (4.79), we get

$$\int_{\Omega_{\text{eq}}(t,x)} \partial_x P_{\text{nh}}(t,x,z)\, dy\, dz \;=\; \partial_x(DI_1(t,x)) - DI_2(t,x) \tag{4.84}$$

where

$$\begin{aligned} DI_1(t,x) &= \int_{d^*(x)}^{\eta_{\text{eq}}(t,x)} P_{\text{nh}}(t,x,z)\sigma(x,z)\, dz \\ &= G(x, A_{\text{eq}}(t,x))\mathcal{D}(\bar{u}_{\text{eq}}(t,x)) \\ &\quad + \int_{d^*(x)}^{\eta_{\text{eq}}} \sigma(x,z) \int_z^{\eta_{\text{eq}}} \mathcal{Q}(\bar{u}_{\text{eq}}(t,x), S(x,s), \sigma)\, ds\, dz \end{aligned} \tag{4.85}$$

where

$$G(x, A_{\text{eq}}) = \int_{d^*(x)}^{\eta_{\text{eq}}} \sigma(x,z) \int_z^{\eta_{\text{eq}}} \frac{S(x,s)}{\sigma(x,s)}\, ds\, dz\,. \tag{4.86}$$

The quantities $\mathcal{D}$ and $\mathcal{Q}$ are given by (4.69), (4.70), and

$$DI_2(t,x) = \int_{d^*(x)}^{\eta_{\text{eq}}(t,x)} P_{\text{nh}}(t,x,z) \frac{\partial}{\partial x}\sigma(x,z)\, dz\,. \tag{4.87}$$

Each term DI_j for $j = 1, 2$ is the non-hydrostatic counterpart of the term I_j for $j = 1, 2$.

Remark 6. The terms $I_j(t,x)$ and $DI_j(t,x)$, respectively, can be written $I_j(x, A_{\text{eq}}(t,x))$ and $DI_j(x, A_{\text{eq}}(t,x), Q_{\text{eq}}(t,x)$ for $j = 1$ and $j = 2$. In what follows, we make use of these notations.

Finally, gathering Eq. (4.81) and Eq. (4.84), noting

$$\mathcal{G}(x, A_{\text{eq}}, Q_{\text{eq}}) = -\frac{\partial}{\partial x}\left(\int_{d^*(x)}^{\eta_{\text{eq}}} \sigma(x,z) \int_z^{\eta_{\text{eq}}} \mathcal{Q}\left(\frac{Q_{\text{eq}}}{A_{\text{eq}}}, S, \sigma\right)\, ds\, dz\right) + DI_2\,, \tag{4.88}$$

we obtain

$$\begin{aligned} \int_{\Omega_{\text{eq}}(t,x)} \partial_x P\, dy\, dz &= \partial_x(I_1(x, A_{\text{eq}})) - I_2(x, A_{\text{eq}}) \\ &\quad + \mu_2\Big(\partial_x(G(x, A_{\text{eq}})\mathcal{D}(\bar{u}_{\text{eq}})) - \mathcal{G}(x, A_{\text{eq}}, Q_{\text{eq}})\Big) \end{aligned} \tag{4.89}$$

Gathering results (4.78) and (4.89), we get the equation of the conservation of the momentum.

4.4.3 The dispersive model for arbitrary non rectangular channel/river

From now on, we omit the notations X_{eq} and $\overline{X}$ for the sake of readability.

Gathering Eqs. (4.73),(4.78) and (4.89), we present the new one-dimensional dispersive model for open channel/river flows

$$\begin{cases} \dfrac{\partial}{\partial t}A + \dfrac{\partial}{\partial x}Q = 0 \\ \dfrac{\partial}{\partial t}Q + \dfrac{\partial}{\partial x}\left(\dfrac{Q^2}{A} + I_1(x,A)\right) + \mu_2\dfrac{\partial}{\partial x}(G(x,A)\mathcal{D}(u)) = I_2(x,A) + \mu_2\mathcal{G}(x,A,Q) \\ +O(\mu_2^2) \end{cases} \tag{4.90}$$

where A is the wet area (4.51), Q is the water discharge (4.74), I_1 (resp. I_2) is the hydrostatic pressure (resp. source) terms (4.82) (resp. (4.83)), $G(x,A)$ (4.86) generalises $\dfrac{h^3}{3}$ in the classical SGN equations (see (4.3)), $\mathcal{G}(x,A,Q)$ (4.88) extends the uneven bottom source term in the classical SGN equations and $\dfrac{\partial}{\partial x}(G(x,A)\mathcal{D}(u))$ is the dispersive term where $\mathcal{D}$ is given by (4.69).

The new section-averaged model extends the section-averaged free surface model for open channel flows [38, 15] by taking $\mu_2 = 0$ and extends the SGN equations for uneven bottom [86, 6, 85, 50] to arbitrary channel/river section.

4.4.4 The dispersive model for a rectangular section

For the specific case of the rectangular section (see [33] for instance), almost all the previous computations are the same. The changes are mainly in the geometrical definition and the boundaries of the channel.

We consider the motion of an incompressible and irrotational fluid with constant density $\rho_0 > 0$ in a three dimensional domain (see Fig. 4.4)

$$\Omega(t) = \left\{(x,y,z) \in \mathbb{R}^3;\ x \in [0, L_c],\ \alpha(x) \le y - y^*(x) \le \beta(x),\ d(x) \le z \le \eta(t,x)\right\}$$

where $y^*(x)$ describes the transversal variation of the channel with respect to the main channel direction, defined by

$$y^*(x) = \frac{\alpha(x) + \beta(x)}{2}$$

where α and β are the transversal limit of the channel. Here the bottom d is now a function of x only and $d^*(x) = d(x)$ by definition. Thus, in view of the definition of the fluid domain, since $\sigma = \sigma(x) = \beta(x) - \alpha(x)$ and $y^-(x) = \alpha(x)$ and $y^+(x) = \beta(x)$, the wet-area can be simply defined by

$$A(t,x) = \sigma(x)\langle h(t,x)\rangle$$

where $\langle h(t,x)\rangle$ is width-averaged of the local height of the water $h(t,x,y) := \eta(t,x,y) - d(x)$, *i.e.*, $\langle h(t,x)\rangle = \langle \eta(t,x)\rangle - d(x)$.

The boundary of the domain $\Omega(t)$ is defined by $\partial\Omega(t)$ and is decomposed into four parts: the free surface $\Gamma_{\text{fs}}(t)$, the wet boundary $\Gamma_{\text{wb}}(t)$, the inflow boundary $\Gamma_{\text{i}}(t)$ and the ouflow boundary $\Gamma_{\text{o}}(t)$. The wet boundary can be decomposed itself in three parts: the bottom $\Gamma_{\text{b}}(t)$, the left lateral boundary $\Gamma_{\text{lb}}(t)$ and the right one $\Gamma_{\text{rb}}(t)$.

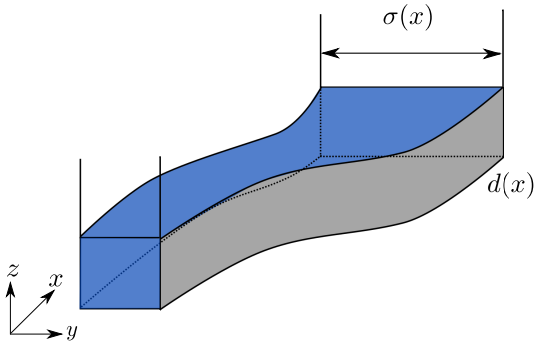

Figure 4.4: Geometric set-up

The kinematic free surface condition and the wet boundary condition are the same, except the definition of the outward unit normal vector, which is now

$$\boldsymbol{n}_{\text{wb}} = \begin{cases} \dfrac{1}{\sqrt{1+\left(\dfrac{\partial}{\partial x}d\right)^2}}\left(\dfrac{\partial}{\partial x}d,\ 0,\ -1\right)^T & \text{if} \quad \boldsymbol{n}_{\text{wb}} = \boldsymbol{n}_{\text{b}} \\ \dfrac{1}{\sqrt{1+\left(\dfrac{\partial}{\partial x}\alpha\right)^2}}\left(\dfrac{\partial}{\partial x}\alpha,\ -1,\ 0\right)^T & \text{if} \quad \boldsymbol{n}_{\text{wb}} = \boldsymbol{n}_{\text{lb}} \\ \dfrac{1}{\sqrt{1+\left(\dfrac{\partial}{\partial x}\beta\right)^2}}\left(\dfrac{\partial}{\partial x}\beta,\ 1,\ 0\right)^T & \text{if} \quad \boldsymbol{n}_{\text{wb}} = \boldsymbol{n}_{\text{rb}} \end{cases}$$

Thus, we have now

$$\begin{aligned} u\frac{\partial}{\partial x}d - w &= 0 \quad \text{on } \Gamma_{\text{b}}(t)\,, \\ u\frac{\partial}{\partial x}\alpha - v &= 0 \quad \text{on } \Gamma_{\text{lb}}(t)\,, \\ u\frac{\partial}{\partial x}\beta + v &= 0 \quad \text{on } \Gamma_{\text{rb}}(t)\,. \end{aligned}$$

In this section, we present the model in the case of a rectangular channel. We assume that $\sigma(x,z) = \sigma(x)$, $d(x,y) = d(x) = d^*(x)$ as displayed in Figure 4.4. Thus, thanks to (4.51), (4.57) and (4.56), we have

$$A_{\text{eq}}(t,x) = \int_{\Omega_{\text{eq}}(t,x)} dy\ dz = \int_{d(x)}^{\eta_{\text{eq}}(t,x)} \int_{\alpha(x)}^{\beta(x)} dy\ dz = \sigma(x)h(t,x)$$

and

$$S(x,z) = \int_{d(x)}^{z} \sigma(x)\ ds = \sigma(x)(z-d(x))\,.$$

As a consequence, we have

- Hydrostatic pressure (4.82) :

$$I_1(t,x) = \sigma(x)\frac{h(t,x)^2}{2F_r^2} \ .$$

- Hydrostatic pressure source term (4.83):

$$I_2(t,x) = \sigma'(x)\frac{h_{\rm eq}(t,x)^2}{2{F_r}^2} - \sigma(x)\frac{h_{\rm eq}(t,x)}{{F_r}^2}d'(x) \ .$$

- Dispersive pressure counterpart (4.68): we have

$$\mathcal{S}(u,x,s) = (s-d(x))\kappa(u,x) - ud'(x)$$

where

$$\kappa(u,x) = \frac{1}{\sigma(x)}\frac{\partial}{\partial x}(\sigma(x)u) \ .$$

Therefore, the dispersive pressure writes:

$$\begin{array}{rcl} P_{\rm nh}(t,x,z) & = & \displaystyle\int_z^{\eta_{\rm eq}(t,x)} \frac{1}{2}\frac{\partial}{\partial z}\mathcal{S}(\bar{u}_{\rm eq}(t,x),x,s)^2\ ds \\ & & \displaystyle -\int_z^{\eta_{\rm eq}(t,x)} \frac{\partial}{\partial t}\mathcal{S}(\bar{u}_{\rm eq}(t,x),x,s) \\ & & \displaystyle +\frac{\bar{u}_{\rm eq}(t,x)}{\sigma(x)}\frac{\partial}{\partial x}\big(\sigma(x)\mathcal{S}(\bar{u}_{\rm eq}(t,x),x,s)\big)\ ds \\ & = & \displaystyle\left(\frac{{h_{\rm eq}}^2-(z-d(x))^2}{2}\right)P^{\rm i}_{\rm nh}(\bar{u}_{\rm eq}(t,x),x) \\ & & -(h_{\rm eq}-(z-d(x)))P^{\rm g_1}_{\rm nh}(\bar{u}_{\rm eq}(t,x),x) \\ & & +(\eta_{\rm eq}(t,x)-z)P^{\rm g2}_{\rm nh}(\bar{u}_{\rm eq}(t,x),x) \end{array} \tag{4.91}$$

where $P^{\rm i}_{\rm nh}$, $P^{\rm g_1}_{\rm nh}$ and $P^{\rm g_2}_{\rm nh}$ stands for the inertial term and the geometric terms

$$\begin{array}{rcl} P^{\rm i}_{\rm nh}(\bar{u}_{\rm eq}(t,x),x) & = & \kappa(\bar{u}_{\rm eq}(t,x),x)^2 - \displaystyle\frac{\partial}{\partial t}\kappa(\bar{u}_{\rm eq}(t,x),x) \\ & & \displaystyle -\frac{\bar{u}_{\rm eq}(t,x)}{\sigma(x)}\frac{\partial}{\partial x}(\sigma(x)\kappa(\bar{u}_{\rm eq}(t,x),x))\ , \end{array} \tag{4.92}$$

$$P^{\rm g_1}_{\rm nh}(\bar{u}_{\rm eq}(t,x),x) = \kappa(\bar{u}_{\rm eq}(t,x),x)\bar{u}_{\rm eq}(t,x)d'(x)$$

and

$$\begin{array}{rcl} P^{\rm g_2}_{\rm nh}(\bar{u}_{\rm eq}(t,x),x) & = & \big(\bar{u}_{\rm eq}(t,x)d'(x)\big)^2 + \displaystyle\frac{\partial}{\partial t}\big(\bar{u}_{\rm eq}(t,x)d'(x)\big) \\ & & +\kappa(\bar{u}_{\rm eq}(t,x),x)\bar{u}_{\rm eq}(t,x)d'(x) \\ & & \displaystyle +\frac{\bar{u}_{\rm eq}(t,x)}{\sigma(x)}\frac{\partial}{\partial x}\big(\sigma(x)\bar{u}_{\rm eq}(t,x)d'(x)\big) \end{array}$$

Finally, the dispersive counterparts of the pressure read:

$$DI_1(t,x) = \sigma(x)\int_{d(x)}^{\eta_{\rm eq}(t,x)} P_{\rm nh}(t,x,z)\,dz \tag{4.93}$$

and

$$DI_2(t,x) = \sigma'(x)\int_{d(x)}^{\eta_{\rm eq}(t,x)} P_{\rm nh}(t,x,z)\,dz - \sigma(x)d'(x)P_{\rm nh}(t,x,d(x)) \tag{4.94}$$

where

$$\int_{d(x)}^{\eta_{\rm eq}(t,x)} P_{\rm nh}(t,x,z)\,dz = \frac{{h_{\rm eq}}^3}{3}P^{\rm i}_{\rm nh}(\bar u_{\rm eq}(t,x),x) + \frac{{h_{\rm eq}}^2}{2}P^{\rm g}_{\rm nh}(\bar u_{\rm eq}(t,x),x)$$

with

$$\begin{aligned} P^{\rm g}_{\rm nh}(\bar u_{\rm eq}(t,x),x) &= \big(\bar u_{\rm eq}(t,x)d'(x)\big)^2 + \frac{\partial}{\partial t}\big(\bar u_{\rm eq}(t,x)d'(x)\big) \\ &\quad + + \frac{\bar u_{\rm eq}(t,x)}{\sigma(x)}\frac{\partial}{\partial x}\big(\sigma(x)\bar u_{\rm eq}(t,x)d'(x)\big) \end{aligned} \tag{4.95}$$

Finally, the system for rectangular channel is given by the following set of equations

$$\begin{cases} \dfrac{\partial}{\partial t}A_{\rm eq} + \dfrac{\partial}{\partial x}Q_{\rm eq} = 0 \\ \dfrac{\partial}{\partial t}Q_{\rm eq} + \dfrac{\partial}{\partial x}\left(\dfrac{{Q_{\rm eq}}^2}{A_{\rm eq}} + \dfrac{{A_{\rm eq}}^2}{2\sigma(x)F_r^2}\right) + \mu_2\dfrac{\partial}{\partial x}\left(\dfrac{{A_{\rm eq}}^3}{\sigma(x)^2}P^{\rm i}_{\rm nh}\left(\dfrac{Q_{\rm eq}}{A_{\rm eq}},x\right) + \dfrac{{A_{\rm eq}}^2}{\sigma(x)}P^{\rm g}_{\rm nh}\left(\dfrac{Q_{\rm eq}}{A_{\rm eq}},x\right)\right) \\ = S_\sigma(A_{\rm eq},Q_{\rm eq},x)\sigma'(x) - S_d(A_{\rm eq},Q_{\rm eq},x)d'(x) + O(\mu_2^2) \end{cases} \tag{4.96}$$

where the term S_σ and S_d take into account, respectively, of the section and the bathymetry variation

$$S_\sigma(A_{\rm eq},Q_{\rm eq},x) = \left(\frac{{A_{\rm eq}}^2}{2\sigma(x){F_r}^2} + \mu_2\frac{{A_{\rm eq}}^3}{\sigma(x)^3}P^{\rm i}_{\rm nh}\left(\frac{Q_{\rm eq}}{A_{\rm eq}},x\right) + \mu_2\frac{{A_{\rm eq}}^2}{\sigma(x)^2}P^{\rm g}_{\rm nh}\left(\frac{Q_{\rm eq}}{A_{\rm eq}},x\right)\right)$$

and

$$S_d(A_{\rm eq},Q_{\rm eq},x) = \left(\frac{A_{\rm eq}}{{F_r}^2} + \mu_2\frac{{A_{\rm eq}}^2}{\sigma(x)}P^{\rm i}_{\rm nh}\left(\frac{Q_{\rm eq}}{A_{\rm eq}},x\right) + \mu_2 A_{\rm eq}P^{\rm g}_{\rm nh}\left(\frac{Q_{\rm eq}}{A_{\rm eq}},x\right)\right).$$

Therefore, in the case of a uniform rectangular channel on a flat bottom, we recover the classical Serre-Green-Naghdi equations:

$$\begin{cases} \dfrac{\partial}{\partial t}h_{\rm eq} + \dfrac{\partial}{\partial x}(h_{\rm eq}u_{\rm eq}) = 0 \\ \dfrac{\partial}{\partial t}(h_{\rm eq}u_{\rm eq}) + \dfrac{\partial}{\partial x}\left(h_{\rm eq}{u_{\rm eq}}^2 + \dfrac{{h_{\rm eq}}^2}{2F_r^2}\right) + \\ \mu_2\dfrac{\partial}{\partial x}\left(\dfrac{{h_{\rm eq}}^3}{3}\left(\left(\dfrac{\partial}{\partial x}\bar u_{\rm eq}\right)^2 - \dfrac{\partial}{\partial t}\dfrac{\partial}{\partial x}\bar u_{\rm eq} - \bar u_{\rm eq}(t,x)\dfrac{\partial}{\partial x}\dfrac{\partial}{\partial x}\bar u_{\rm eq}\right)\right) = 0 + O(\mu_2^2) \end{cases} \tag{4.97}$$

4.5 Energy

The generalised Serre-Green-Naghdi equations (4.90) are by construction asymptotically consistent with the Euler system (4.17)–(4.20). We have the following result:

Theorem 1. *System* (4.90) *admits a total energy*

$$E = A\frac{\bar{u}_{\text{eq}}^2}{2} + A\frac{\eta}{F_r^2} - I_1 + \frac{\mu_2}{2}\int_\Omega \mathcal{S}^2(u_\beta, x, z)\, dydz \tag{4.98}$$

which satisfies the following energy equation

$$\frac{\partial}{\partial t}E + \frac{\partial}{\partial x}((E + I_1 + \mu_2 DI_1)u_\beta) = 0\ . \tag{4.99}$$

Moreover, the quantity E is consistent with the total energy $\mathcal{E} = \dfrac{u^2 + \mu_1 v^2 + \mu_2 w^2}{2} + \dfrac{z}{F_r^2}$ *of the Euler equation* (4.17)–(4.20)*, in the sense that*

$$\frac{\partial}{\partial t}\int_\Omega \mathcal{E}\, dydz + \frac{\partial}{\partial x}\int_\Omega (\mathcal{E} + P)u\, dydz = \frac{\partial}{\partial t}E + \frac{\partial}{\partial x}((E + I_1 + \mu_2 DI_1)\bar{u}_{\text{eq}}) + O(\mu_2^2)\ .$$

Remark 7. This is a positive feature of the approximate model (4.90), which provides the richness of content for this model and can be used to estimate the accuracy of numerical algorithms. Moreover, it is well-known that the energy conservation law plays a fundamental role in justifying the theory of shallow water equations.

Remark 8. As a direct consequence of (4.98) and (4.99), we are able to recover the energy conservation law of the usual models in the case of $\sigma \equiv 1$, *i.e.* $A = h$:

- if $\mu_2 = 0$, we recover the classical total energy of the Saint-Venant system, namely

$$E = \frac{hu^2}{2} + \frac{h(h + 2d)}{2F_r^2}\ .$$

- if $\mu_2 \neq 0$, we recover the classical total energy of the Serre-Green-Naghdi system (see for instance [44]), namely

$$E = \frac{hu^2}{2} + \frac{h(h + 2d)}{2F_r^2} + \mu_2\left(\frac{h^3}{6}\left(\frac{\partial}{\partial x}u\right)^2 - d'\frac{h^2}{2}\frac{\partial}{\partial x}u + \frac{(d')^2}{2}\right)\ .$$

Proof 2. Let us start by looking for the energy equation corresponding to the nondimensionalized form of Euler system (4.17)–(4.20). Multiplying (4.18) by u, (4.19) by v and (4.20) by w and summing, we find the following equation for the kinetic energy

$$\frac{\partial \mathcal{K}}{\partial t} + u\frac{\partial}{\partial x}(\mathcal{K} + P) + v\frac{\partial}{\partial y}(\mathcal{K} + P) + w\frac{\partial}{\partial z}(\mathcal{K} + P) + \frac{1}{Fr^2}w = 0 \tag{4.100}$$

with $\mathcal{K} = \dfrac{u^2 + \mu_1 v^2 + \mu_2 w^2}{2}$.
The equation for the potential energy $\mathcal{P} = gz$ can be given as follows:

$$\frac{\partial \mathcal{P}}{\partial t} + u\frac{\partial \mathcal{P}}{\partial x} + v\frac{\partial \mathcal{P}}{\partial y} + w\frac{\partial \mathcal{P}}{\partial z} - \frac{1}{Fr^2}w = 0 \tag{4.101}$$

The equation for the total Energy $\mathcal{E} = \mathcal{K}+\mathcal{P}$ is obtained by summing (4.100) and (4.101),

$$\frac{\partial \mathcal{E}}{\partial t} + u\frac{\partial}{\partial x}(\mathcal{E}+P) + v\frac{\partial}{\partial y}(\mathcal{E}+P) + w\frac{\partial}{\partial z}(\mathcal{E}+P) = 0 \tag{4.102}$$

Integration equation (4.102) over the domain Ω taking into account boundary conditions (4.21)–(4.23), one obtains the following equation:

$$\frac{\partial}{\partial t}\int_\Omega \mathcal{E}\, dydz + \frac{\partial}{\partial x}\int_\Omega (\mathcal{E}+P)u\, dydz = 0 \tag{4.103}$$

In the other hand, applying the asymptotic analysis, thus, from (4.64) and (4.66), the total energy equation (4.102) becomes

$$\mathcal{E} = \frac{\bar{u}_{\text{eq}}^2 + \mu_2\mathcal{S}^2}{2} + \mu_2\bar{u}_{\text{eq}}B_0 + \frac{z}{Fr^2} + O(\mu_1,\mu_2^2)$$

Then

$$E = \int_\Omega \mathcal{E}\, dydz = A\frac{\bar{u}_{\text{eq}}^2}{2} + A\frac{\eta}{F_r^2} - I_1 + \frac{\mu_2}{2}\int_\Omega \mathcal{S}^2(\bar{u}_{\text{eq}},x,z)\, dydz + O(\mu_1,\mu_2^2)$$

Similarly, from (4.48), it's easy to get that:

$$\int_\Omega (\mathcal{E}+P)u = (E + I_1 + \mu_2 DI_1)\bar{u}_{\text{eq}}) + O(\mu_1,\mu_2^2).$$

Hence the result.

4.6 Improved cSGN equations

This section is devoted to the reformulation of Problem (4.90) by introducing a linear and a quadratic operator to avoid the direct computation of the partial derivatives of order 3 (see, for instance, Equation (4.85)). The reformulated problem is, in general, more adapted to construct a robust Finite Volume numerical scheme for its resolution. Moreover, this reformulated problem allows us to construct an equivalent model to (4.90) for which we can improve the frequency dispersion by adding some terms of order $O(\mu_2^2)$ to the momentum equation without affecting the accuracy of the model.

4.6.1 Reformulation of the cSGN equations

Let us first remark that, by defining the linear operator

$$\mathcal{T}[A_{\text{eq}},d,\sigma,z](u) = \frac{\partial}{\partial x}(u)\int_z^{\eta_{\text{eq}}}\frac{S(x,s)}{\sigma(x,s)}\,ds + u\int_z^{\eta_{\text{eq}}}\frac{1}{\sigma(x,s)}\frac{\partial}{\partial x}S(x,s)\,ds\,, \tag{4.104}$$

and the quadratic operator

$$\begin{aligned}\mathcal{G}[A_{\rm eq},d,\sigma,z](u) &= \int_z^{\eta_{\rm eq}} 2\left(\frac{\partial}{\partial x}u\right)^2\frac{S(x,s)}{\sigma(x,s)}\\ &\quad+\frac{u^2}{\sigma(x,s)}\left(\frac{\frac{\partial}{\partial x}S(x,s)\frac{\partial}{\partial x}\sigma(x,s)}{\sigma(x,s)}-\frac{\partial}{\partial x}\frac{\partial}{\partial x}S(x,s)\right)\\ &\quad+\frac{\partial}{\partial x}\left(\frac{u^2}{2}\right)\frac{S(x,s)\frac{\partial}{\partial x}\sigma(x,s)}{\sigma(x,s)^2}\,ds\end{aligned}$$

we can write the pressure $P_{\rm nh}$ as

$$P_{\rm nh}(t,x,z)=-\mathcal{T}[A_{\rm eq},d,\sigma,z]\left(\frac{\partial}{\partial t}u_{\rm eq}+u_{\rm eq}\frac{\partial}{\partial x}u_{\rm eq}\right)+\mathcal{G}[A_{\rm eq},d,\sigma,z](u_{\rm eq}) \tag{4.105}$$

Remark 9. In view of the definition of S (4.56), we can also write $S = S(d,\sigma,z)$, therefore, we have written $[A_{\rm eq},d,\sigma,z]$ instead of $[\eta_{\rm eq},S,\sigma,z]$ for the definition of the operators.

Then, defining the averaged operators

$$\overline{\mathcal{T}}[A_{\rm eq},d,\sigma](u,\psi) = \int_{d^*(x)}^{\eta_{\rm eq}}\psi\mathcal{T}[A_{\rm eq},d,\sigma,z](u)\,dz \tag{4.106}$$

and

$$\overline{\mathcal{G}}[A_{\rm eq},d,\sigma](u,\psi) = \int_{d^*(x)}^{\eta_{\rm eq}}\psi\mathcal{G}[A_{\rm eq},d,\sigma,z](u)\,dz \tag{4.107}$$

we can write

$$\begin{aligned}\int_{d^*(x)}^{\eta_{\rm eq}}P_{\rm nh}(t,x,z)\psi(x,z)\,dz &= -\overline{\mathcal{T}}[A_{\rm eq},d,\sigma]\left(\left(\frac{\partial}{\partial t}u_{\rm eq}+u_{\rm eq}\frac{\partial}{\partial x}u_{\rm eq}\right),\psi\right)\\ &\quad+\overline{\mathcal{G}}[A_{\rm eq},d,\sigma](u_{\rm eq},\psi)\,.\end{aligned}$$

In what follows, it is more convenient to use the second definition of the pressure source term (4.80) with $P = P_{\rm nh}$. Thus, if we set

$$\mathcal{L}[A_{\rm eq},d,\sigma](u)=\frac{1}{A_{\rm eq}}\left[\frac{\partial}{\partial x}\left(\overline{\mathcal{T}}[A_{\rm eq},d,\sigma](u,\sigma)\right)-\overline{\mathcal{T}}[A_{\rm eq},d,\sigma]\left(u,\frac{\partial}{\partial x}\sigma\right)\right] \tag{4.108}$$

and

$$Q[A_{\rm eq},d,\sigma](u)=\frac{1}{A_{\rm eq}}\left[\frac{\partial}{\partial x}\left(\overline{\mathcal{G}}[A_{\rm eq},d,\sigma](u,\sigma)\right)-\overline{\mathcal{G}}[A_{\rm eq},d,\sigma]\left(u,\frac{\partial}{\partial x}\sigma\right)\right] \tag{4.109}$$

we get

$$\frac{\partial}{\partial x}DI_1-DI_2=-A_{\rm eq}\mathcal{L}[A_{\rm eq},d,\sigma]\left(\frac{\partial}{\partial t}u_{\rm eq}+u_{\rm eq}\frac{\partial}{\partial x}u_{\rm eq}\right)+A_{\rm eq}Q[A_{\rm eq},d,\sigma](u_{\rm eq})\,.$$

Finally, defining the operator

$$\mathbb{L}[A_{\text{eq}}, d, \sigma](u) \quad = \quad A_{\text{eq}}\mathcal{L}[A_{\text{eq}}, d, \sigma]\left(\frac{u}{A_{\text{eq}}}\right) \tag{4.110}$$

we can reformulate System (4.90) as follows:

$$\begin{cases} \dfrac{\partial}{\partial t}A_{\text{eq}} + \dfrac{\partial}{\partial x}(A_{\text{eq}}u_{\text{eq}}) = 0 \\ \left(I_d - \mu_2\mathbb{L}[A_{\text{eq}}, d, \sigma]\right)\left(\dfrac{\partial}{\partial t}(A_{\text{eq}}u_{\text{eq}}) + \dfrac{\partial}{\partial x}\left(A_{\text{eq}}{u_{\text{eq}}}^2\right)\right) + \dfrac{\partial}{\partial x}I_1(x, A_{\text{eq}}) \\ +\mu_2 A_{\text{eq}}\mathcal{Q}[A_{\text{eq}}, d, \sigma](u_{\text{eq}}) = I_2(x, A_{\text{eq}}) + O(\mu_2^2) \end{cases} \tag{4.111}$$

where I_d stands for the Identity operator. This reformulated model is valid for non rectangular channel section since we have used the definition (4.80). For rectangular section, the definition of the linear $\mathcal{L}$ and the averaged quadratic operators $\mathcal{Q}$ (4.108)-(4.109) (according to the definition of the term DI_2 (4.94)) are given by

$$\begin{aligned} \mathcal{L}[A_{\text{eq}}, d, \sigma](u) \quad = \quad & \frac{1}{A_{\text{eq}}}\left[\frac{\partial}{\partial x}\left(\overline{\mathcal{T}}[A_{\text{eq}}, d, \sigma]\,(u, \sigma)\right) - \overline{\mathcal{T}}[A_{\text{eq}}, d, \sigma]\left(u, \frac{\partial}{\partial x}\sigma\right)\right] \\ & + \frac{1}{A_{\text{eq}}}\sigma(x)d'(x)\,\mathcal{T}[A_{\text{eq}}, d, \sigma, z = d(x)]\,(u) \end{aligned} \tag{4.112}$$

and

$$\begin{aligned} \mathcal{Q}[A_{\text{eq}}, d, \sigma](u) \quad = \quad & \frac{1}{A_{\text{eq}}}\left[\frac{\partial}{\partial x}\left(\overline{\mathcal{G}}[A_{\text{eq}}, d, \sigma]\,(u, \sigma)\right) - \overline{\mathcal{G}}[A_{\text{eq}}, d, \sigma]\left(u, \frac{\partial}{\partial x}\sigma\right)\right] \\ & + \frac{1}{A_{\text{eq}}}\sigma(x)d'(x)\,\mathcal{G}[A_{\text{eq}}, d, \sigma, z = d(x)]\,(u) \end{aligned} \tag{4.113}$$

Let us remark that System (4.134) does not require the computation of any third-order derivative as in System (4.90) (due to the term DI_1). This is a crucial remark since it is well-known that third-order derivatives involved in the a model such as (4.90) may create high frequencies instabilities. The operator $I_d - \mathbb{L}$ in the second equation reinforces the stability of the numerical scheme. It also plays a crucial role in the well-posedness problem (see the reference therein and [52]). However, due to the time-dependency of $\mathbb{L}$, the operator $I_d - \mathbb{L}$ has to be inverted at each iterations and increases the cost of the numerical method.

4.6.2 Improved dispersion frequency

It is observed that for the dispersion frequency for the SGN equations, see also (4.134), converge towards the Stokes first-order theory for waves on arbitrary depth for small wavenumbers. As the wavenumber increases, the celerity expressions become more and more inaccurate relative to the Stokes theory. However, the frequency dispersion of System (4.134) can be improved (see for instance [93, 70, 68, 69, 71, 91, 25, 14, 24]). It can be achieved by adding suitable terms of order $O(\mu_2)$ and/or by parameterising the velocity at a certain depth $z = \theta$ instead of $z = d$ ([71]), and/or by considering a modified velocity (see [24]). All of these models introduce parameters for which the more n large

is the more is the improvements of the dispersive properties. For the sake of simplicity, we consider in the sequel the one-parameter family of SGN systems (4.134) by adding some terms of order $O(\mu_2)$ to the momentum equation. Since the added terms are of order $O(\mu_2)$, the model's accuracy is not affected.

Going back to the non conservative form of the momentum equation in (4.134), *i.e.* using (4.108) and $\frac{\partial}{\partial x} I_1(x, A) = \frac{\partial}{\partial A_{\text{eq}}} I_1(x, A) \frac{\partial}{\partial x} A + I_2(x, A)$, and dividing the equation by A_{eq}, we can write

$$\left(I_d - \mu_2 \mathcal{L}[A_{\text{eq}}, d, \sigma]\right) \left(\frac{\partial}{\partial t} u_{\text{eq}} + u_{\text{eq}} \frac{\partial}{\partial x} u_{\text{eq}}\right) + \frac{\frac{\partial}{\partial A_{\text{eq}}} I_1}{A} \frac{\partial}{\partial x} A + \mu_2 \mathcal{Q}[A_{\text{eq}}, d, \sigma](u_{\text{eq}}) = O(\mu_2^2) \quad (4.114)$$

and in particular, we have

$$\frac{\partial}{\partial t} u_{\text{eq}} = -u_{\text{eq}} \frac{\partial}{\partial x} u_{\text{eq}} - \frac{\frac{\partial}{\partial A_{\text{eq}}} I_1}{A_{\text{eq}}} \frac{\partial}{\partial x} A_{\text{eq}} + O(\mu_2) \, . \quad (4.115)$$

Let us fix $\kappa \in \mathbb{R}$. Writing $\frac{\partial}{\partial t} u_{\text{eq}} = \kappa \frac{\partial}{\partial t} u_{\text{eq}} + (1 - \kappa) \frac{\partial}{\partial t} u_{\text{eq}}$ and using (4.115) leads to

$$\frac{\partial}{\partial t} u_{\text{eq}} = \kappa \frac{\partial}{\partial t} u_{\text{eq}} - (1 - \kappa) \left(u_{\text{eq}} \frac{\partial}{\partial x} u_{\text{eq}} + \frac{\frac{\partial}{\partial A_{\text{eq}}} I_1}{A_{\text{eq}}} \frac{\partial}{\partial x} A_{\text{eq}} \right) + O(\mu_2) \, .$$

or equivalently

$$\frac{\partial}{\partial t} u_{\text{eq}} + u_{\text{eq}} \frac{\partial}{\partial x} u_{\text{eq}} = \kappa \left(\frac{\partial}{\partial t} u_{\text{eq}} + u_{\text{eq}} \frac{\partial}{\partial x} u_{\text{eq}} + (\kappa - 1) \frac{\frac{\partial}{\partial A_{\text{eq}}} I_1}{A_{\text{eq}}} \frac{\partial}{\partial x} A_{\text{eq}} \right) + O(\mu_2) \, . \quad (4.116)$$

As a consequence of (4.116), in Equation (4.114), the term $\mu_2 \mathcal{L}[A_{\text{eq}}, d, \sigma]$ can be approximated as

$$\mu_2 \mathcal{L}[A_{\text{eq}}, d, \sigma] \left(\frac{\partial}{\partial t} u_{\text{eq}} + u_{\text{eq}} \frac{\partial}{\partial x} u_{\text{eq}} \right) = \mu_2 \kappa \mathcal{L}[A_{\text{eq}}, d, \sigma] \left(\frac{\partial}{\partial t} u_{\text{eq}} + u_{\text{eq}} \frac{\partial}{\partial x} u_{\text{eq}} + \frac{(\kappa - 1)}{\kappa} \frac{\frac{\partial}{\partial A_{\text{eq}}} I_1}{A_{\text{eq}}} \frac{\partial}{\partial x} A_{\text{eq}} \right) + O(\mu_2^2) \quad (4.117)$$

Finally, writing the term $\dfrac{\dfrac{\partial}{\partial A_{\text{eq}}} I_1}{A_{\text{eq}}} \dfrac{\partial}{\partial x} A_{\text{eq}}$ as

$$\frac{\dfrac{\partial}{\partial A_{\text{eq}}} I_1}{A_{\text{eq}}} \frac{\partial}{\partial x} A_{\text{eq}} = \frac{(\kappa - 1)}{\kappa} \frac{\dfrac{\partial}{\partial A_{\text{eq}}} I_1}{A_{\text{eq}}} \frac{\partial}{\partial x} A_{\text{eq}} + \frac{1}{\kappa} \frac{\dfrac{\partial}{\partial A_{\text{eq}}} I_1}{A_{\text{eq}}} \frac{\partial}{\partial x} A_{\text{eq}}$$

and using Equation (4.117) into (4.114), we get the one-parameter family of SGN equations with improved dispersion under the non conservative form:

$$\begin{cases} \dfrac{\partial}{\partial t} A_{\text{eq}} + u_{\text{eq}} \dfrac{\partial}{\partial x} A_{\text{eq}} + A_{\text{eq}} \dfrac{\partial}{\partial x} u_{\text{eq}} = 0 \\ \left(I_d - \mu_2 \kappa \mathcal{L}[A_{\text{eq}}, d, \sigma]\right) \left(\dfrac{\partial}{\partial t} u_{\text{eq}} + u_{\text{eq}} \dfrac{\partial}{\partial x} u_{\text{eq}} + \dfrac{(\kappa - 1)}{\kappa} \dfrac{\dfrac{\partial}{\partial A_{\text{eq}}} I_1}{A_{\text{eq}}} \dfrac{\partial}{\partial x} A_{\text{eq}} \right) \\ + \dfrac{1}{\kappa} \dfrac{\dfrac{\partial}{\partial A_{\text{eq}}} I_1}{A_{\text{eq}}} \dfrac{\partial}{\partial x} A_{\text{eq}} + \mu_2 Q[A_{\text{eq}}, d, \sigma](u_{\text{eq}}) = O(\mu_2^2) \end{cases} \tag{4.118}$$

Multiplying the second equation in System (4.118) by A_{eq} and using

$$\frac{\partial}{\partial A_{\text{eq}}} I_1(x, A) \frac{\partial}{\partial x} A = \frac{\partial}{\partial x} I_1(x, A) - I_2(x, A)\,,$$

we get the one-parameter family of SGN equations with improved dispersion under the conservative form:

$$\begin{cases} \dfrac{\partial}{\partial t} A_{\text{eq}} + \dfrac{\partial}{\partial x} (A_{\text{eq}} u_{\text{eq}}) = 0 \\ \left(I_d - \mu_2 \kappa \mathbb{L}[A_{\text{eq}}, d, \sigma]\right) \left(\dfrac{\partial}{\partial t} (A_{\text{eq}} u_{\text{eq}}) + \dfrac{\partial}{\partial x} (A_{\text{eq}} {u_{\text{eq}}}^2) + \dfrac{(\kappa - 1)}{\kappa} \left(\dfrac{\partial}{\partial x} I_1 - I_2 \right) \right) \\ + \dfrac{1}{\kappa} \left(\dfrac{\partial}{\partial x} I_1 - I_2 \right) + \mu_2 A_{\text{eq}} Q[A_{\text{eq}}, d, \sigma](u_{\text{eq}}) = O(\mu_2^2) \end{cases} \tag{4.119}$$

These new formulations (4.118) and (4.119) do not contain any third-order derivative, thus we can expect more stable and robust numerical computations.

4.6.3 Stokes first-order theory and the choice of the parameter κ

In this section, we present a qualitative discussion about the stability of our new model (4.119) an how to choose the parameter κ in order to improve the frequency dispersion, compared to the Stokes first-order theory. Here, we consider the case of a rectangular section ${A_{\text{eq}}}^0 = \sigma({\eta_{\text{eq}}}^0 - d_0)$ and we focus on the linear behaviour of small perturbation $(\eta^1, {u_{\text{eq}}}^1)$ to a constant state solution $({\eta_{\text{eq}}}^0, {u_{\text{eq}}}^0) = (0, 0)$. For a given quantity X, we note $X^1(\cdot; \varepsilon) := \dfrac{d}{d\varepsilon} X(\cdot; \varepsilon)$ and to simplify the notations we omit the ε-dependency unless some confusion is possible. The perturbations are defined by the following relations

$$\eta_{\text{eq}}(t, x) = {\eta_{\text{eq}}}^0 + \varepsilon {\eta_{\text{eq}}}^1(t, x) + O(\varepsilon^2) \text{ and } u_{\text{eq}}(t, x) = {u_{\text{eq}}}^0 + \varepsilon {u_{\text{eq}}}^1(t, x) + O(\varepsilon^2) \tag{4.120}$$

for some $\varepsilon > 0$.

Since the calculations are almost similar to the one-dimensional SGN equations (see for instance [14, 61] or [36]), we briefly present how to obtain the linearized equations. Let us first remark since we are looking for perturbed solutions around the state solution $({A_{\text{eq}}}^0, {u_{\text{eq}}}^0)$, we assume that $\sigma(x, z) = \sigma_0$ and $d(x, y) = d_0$. Therefore, System (4.118), we get:

Mass equation:

Dividing by ε, and taking the limit $\varepsilon \to 0$, we obtain the linearised mass equation

$$\frac{\partial}{\partial t}{\eta_{\text{eq}}}^1 - \frac{\partial}{\partial x} d_0 {u_{\text{eq}}}^1 = 0 \,. \tag{4.121}$$

Momentum equation:

From the second equation of System (4.118), dividing by ε and taking the limit $\varepsilon \to 0$, we get the linearised momentum equation

$$\left(I_d - \mu_2 \kappa \mathcal{L}[{A_{\text{eq}}}^0, d_0, \sigma_0]\right) \left(\frac{\partial}{\partial t}{u_{\text{eq}}}^1 + \frac{(\kappa - 1)}{F_r^2 \kappa}\frac{\partial}{\partial x}{\eta_{\text{eq}}}^1\right) + \frac{1}{F_r^2 \kappa}\frac{\partial}{\partial x}{\eta_{\text{eq}}}^1 = O(\mu_2^2) \tag{4.122}$$

with

$$\begin{aligned} \mathcal{L}[{A_{\text{eq}}}^0, d, \sigma](u) &= \frac{1}{{A_{\text{eq}}}^0}\frac{\partial}{\partial x}\left(\frac{\partial}{\partial x} u \left(\int_d^{{\eta_{\text{eq}}}^0} \int_z^{{\eta_{\text{eq}}}^0} S(s)\, ds\, dz\right)\right) \\ &= d_0^2 \frac{\partial}{\partial x}\left(\frac{\partial}{\partial x} u\right) \end{aligned} \tag{4.123}$$

Dispersion relation.

Noting k the spatial wavenumber and ω the time pulsation, we look for plane wave solution of the form

$$(A_{\text{eq}}, u_{\text{eq}}) = (A_{\text{eq}_0}, u_{\text{eq}_0}) \exp\left(i(kx - \omega t)\right)$$

with $\eta_{\text{eq}} = \eta_{\text{eq}_0} \exp\left(i(kx - \omega t)\right) = \dfrac{\eta_{\text{eq}_0}}{A_{\text{eq}_0}} A_{\text{eq}}$ to this system (4.121)-(4.122). Without loss of generality, one can consider the linearisation around the still water steady state solution $({\eta_{\text{eq}}}^0, {u_{\text{eq}}}^0 = 0)$. We find the following dispersion relation

$$\omega_{\text{SGN}}(k; \kappa) = \pm \frac{k}{F_r} \sqrt{\frac{1 + \mu_2 (d_0 k)^2 (\kappa - 1)}{1 + \mu_2 (d_0 k)^2 \kappa}} \tag{4.124}$$

for which the perturbations are always stable if and only if $\kappa \geq 1$, *i.e.* $\omega_{\text{SGN}}(\cdot; \kappa) \in \mathbb{R}$, for all $\kappa \geq 1$. The dispersion relation (4.124) is the classical one associated to the SGN equations (see for instance [68, 69] and chapter 2 for more details). As mentioned before, the parameter κ can be helpful in minimising the dispersive error of linear phase and group velocities denoted, respectively by

$$C^p_{\text{SGN}}(k; \kappa) = \frac{\omega_{\text{SGN}}(k; \kappa)}{k}$$

and

$$C^g_{\mathrm{SGN}}(k;\kappa) = \frac{\partial}{\partial k}\omega_{\mathrm{SGN}}(k;\kappa)$$

to the reference phase and group velocities C^p_{s} and C^g_{s} of Stokes first-order theory (that we recall hereafter for the sake of completeness).

Stokes first-order dispersion relation.

To obtain the Stokes first-order dispersion relation, we first come back to the Euler equations (4.9)-(4.10) with the boundary conditions (4.12)–(4.14) (see also (4.7) and (4.11)) under the Bernouilli's formulation in terms of a velocity potential ψ (*i.e.* the velocity field is given by $\bar{\boldsymbol{u}} = \nabla\psi$):

$$\left\{\begin{array}{lcll} \Delta\psi & = & 0 & \text{in } \Omega \\ \dfrac{\partial}{\partial \boldsymbol{n}}\psi & = & 0 & \text{in } \Gamma_{\mathrm{wb}} \\ \dfrac{\partial}{\partial t}\eta + \nabla_{x,y}(\psi)\cdot\nabla_{x,y}(\eta) & = & \dfrac{\partial}{\partial z}\psi & \text{in } \Gamma_{\mathrm{fs}} \\ \dfrac{\partial}{\partial t}\psi + \dfrac{1}{2}\left(\left|\nabla_{x,y}(\psi)\right|^2 + \left|\dfrac{\partial}{\partial z}\psi\right|^2\right) + gz & = & 0 & \text{in } \Gamma_{\mathrm{fs}} \end{array}\right. \tag{4.125}$$

where

$$\frac{\partial}{\partial \boldsymbol{n}}\psi := \nabla\psi\cdot\boldsymbol{n},\ \bar{\boldsymbol{u}} = \begin{pmatrix} u \\ v \\ w \end{pmatrix},\ \nabla_{x,y}(u) = \begin{pmatrix} \dfrac{\partial}{\partial x}u \\ \dfrac{\partial}{\partial y}u \end{pmatrix}$$

represent the outward normal derivative at the boundary of the fluid domain, the vector $\bar{\boldsymbol{u}}$ and the gradient operator with respect to the variable x and y.

To obtain the first order Stokes dispersion relation, we linearise System (4.125) around the rest state ($\eta^0 = 0, \bar{\boldsymbol{u}}^0 = 0$) by considering the following perturbation

$$\begin{array}{rclcll} \bar{\boldsymbol{u}} & = & \bar{\boldsymbol{u}}^0 & + & \varepsilon\bar{\boldsymbol{u}}^1 & + & O(\varepsilon^2) \\ \eta & = & \eta^0 & + & \varepsilon\eta^1 & + & O(\varepsilon^2) \\ \psi & = & \psi^0 & + & \varepsilon\psi^1 & + & O(\varepsilon^2) \\ d & = & d^0 & & & & \\ \alpha & = & \alpha^0 & & & & \\ \beta & = & \beta^0 & & & & \end{array}$$

where $(d^0, \alpha^0, \beta^0, \eta^0, \psi^0) \in \mathbb{R}^5$.

Using these perturbations into System (4.125), collecting with respect to the power of ε, dividing by ε and taking the limit when $\varepsilon \to 0$, we get the linearised equations

$$\left\{\begin{array}{lcll} \Delta\psi^1 & = & 0 & \text{in } \Omega^0 \\ \nabla\psi^1\cdot\boldsymbol{n}^0 & = & 0 & \text{in } \Gamma^0_{\mathrm{wb}} \\ \dfrac{\partial}{\partial t}\eta^1 - \dfrac{\partial}{\partial z}\psi_1 & = & 0 & \text{in } \Gamma^0_{\mathrm{fs}} \\ \dfrac{\partial}{\partial t}\psi^1 + g\eta^1 & = & 0 & \text{in } \Gamma^0_{\mathrm{fs}} \end{array}\right. \tag{4.126}$$

where

$$\Omega^0 = \left\{(x,y,z) \in [0,L]\times\mathbb{R}^2;\ \alpha_0 \le y \le \beta_0 \text{ and } d_0 \le z \le \eta^0\right\}$$

$$\Gamma^0_{\text{fs}} = \{(x,y,z) \in [0,L]\times\mathbb{R}^2;\ z = \eta^0\}$$

$$\Gamma^0_{\text{wb}} = \{(x,y,z) \in [0,L]\times\mathbb{R}^2;\ z = d_0\}$$

and

$$\boldsymbol{n}^0 := \lim_{\varepsilon\to 0}\left(\frac{1}{\sqrt{1+\left(\frac{\partial}{\partial y}d_0\right)^2+\left(\frac{\partial}{\partial z}d_0\right)^2}}\begin{pmatrix}\frac{\partial}{\partial x}d_0\\ \frac{\partial}{\partial y}d_0\\ -1\end{pmatrix}\right) = \begin{pmatrix}0\\0\\-1\end{pmatrix}$$

Let us remark that using the third and the fourth equation, we can write

$$\frac{\partial}{\partial t}\frac{\partial}{\partial t}\psi^1 + g\frac{\partial}{\partial z}\psi^1 = 0 \text{ in } \Gamma^0_{\text{fs}}\ .$$

Let us also note that, first, in view of the boundary conditions of System (4.126), we can reduce to the two-dimensional problem by omitting the y-dependency, and second, if we apply the Fourier transform with respect to x to the first equation of System (4.126), we get the following equation

$$\Delta_{y,z}\widehat{\psi^1} - k^2\widehat{\psi^1} = 0 \text{ in } \Omega^0$$

whose solutions are under the form

$$\widehat{\psi^1} = A(k)\exp(k\sqrt{2}z) + B(k)\exp(-k\sqrt{2}z)\ .$$

Therefore, without loss of generality one can look for solutions under the form

$$\psi^1 = \Psi(z)\exp(i(kx-\omega t)\ .$$

Using this equation into System (4.126), we get for all $k \in \mathbb{R}$

$$\begin{cases}\Psi''(z) - k^2\Psi(z) &= 0 \quad d_0 \leqslant z \leqslant \eta_0\\ \Psi'(z) &= 0 \quad z = d_0\\ -\omega^2\Psi(z) + g\Psi'(z) &= 0 \quad z = \eta_0\end{cases} \tag{4.127}$$

whose solutions are

$$\Psi_k(z) = A(k)\exp(kz) + B(k)\exp(-kz)\ . \tag{4.128}$$

Applying the boundary condition in Γ^0_{wb}, we get

$$A(k) = B(k)\exp(-2kd_0) \tag{4.129}$$

and applying the boundary condition in Γ^0_{fs}, we get

$$\omega^2(k) = gk\frac{A(k)\exp(k\eta^0) - B(k)\exp(-k\eta^0)}{A(k)\exp(k\eta^0) + B(k)\exp(-k\eta^0)}\ . \tag{4.130}$$

Finally, using Equation (4.129) into (4.130), we obtain the dispersion relation

$$\omega_{\rm s}(k) = \omega(k) = \pm\sqrt{gk\tanh(kd_0)} \tag{4.131}$$

with the reference phase and group speed

$$C_{\rm s}^{p}(k) = \frac{\omega_{\rm s}(k)}{k} = \pm\frac{\sqrt{g\tanh(kd_0)}}{\sqrt{k}} \tag{4.132}$$

and

$$C_{\rm s}^{g}(k) = \frac{\partial}{\partial k}\omega_{\rm s}(k) = \pm\frac{\omega_{\rm s}^2(k)/k + kC^2(1-\tanh(kd_0)^2)}{2\omega_{\rm s}(k)} \tag{4.133}$$

where $C = \sqrt{gd^0}$ is the sound speed.

Comparisons of the dispersion relations and the choice of κ.

One can easily check that the Taylor expansions of the dispersion relations (4.124) and (4.131) are equivalent for small wavenumbers. As a consequence for small wavenumbers the choice of κ has no influence. However, since we are interested in large wavenumber (*i.e.* small wavelength) dispersion cases, we are thus motivated to propose an optimal value of κ in order to minimise the dispersive error of linear phase and group velocities to the reference linear phase and group velocities.
For our new model (4.119), the dispersion relation (4.124) is the same as that derived for the standard SGN equations (see [68, 69, 25, 14] for instance), when we consider the linearization around the rest state $(\eta_{\rm eq}, u_{\rm eq}) = (0, 0)$ and a rectangular geometry. The discussion concerning the choice of κ in order to improve the dispersive properties of the model therefore follows the usual procedure is detailed in Chapter 3. We take throughout this chapter $\kappa = 1.159$.

4.7 A well-balanced finite volume approximation in the case of a non-uniform rectangular section

The main drawback of Eqs. (4.90) is that it has third-order terms in space, which may lead to instabilities at the numerical level. Therefore, we first propose a more stable formulation of Eqs. (4.90) before presenting its numerical approximation.

Skipping the technical details (it is presented in the next chapter) shows that System (4.90) can be written:

$$\begin{cases} \dfrac{\partial}{\partial t}A + \dfrac{\partial}{\partial x}(Au_\beta) = 0 \\ \left(I_d - \mu_2\mathbb{L}[A,d,\sigma]\right)\left(\dfrac{\partial}{\partial t}(Au_\beta) + \dfrac{\partial}{\partial x}\left(Au_\beta^2\right)\right) + \dfrac{\partial}{\partial x}I_1(x,A) + \mu_2 AQ[A,d,\sigma](u_\beta) = \\ I_2(x,A) + O(\mu_2^2) \end{cases} \tag{4.134}$$

where I_d stands for the identity operator, $\mathcal{L}$ is a linear operator

$$\begin{aligned} \mathcal{L}[A,d,\sigma](u) &= \frac{1}{A}\left[\frac{\partial}{\partial x}\left(\overline{\mathcal{T}}[A,d,\sigma]\,(u,\sigma)\right) - \overline{\mathcal{T}}[A,d,\sigma]\left(u,\frac{\partial}{\partial x}\sigma\right)\right] \\ &\quad + \frac{1}{A}\sigma(x)d'(x)\,\mathcal{T}[A,d,\sigma,z=d(x)]\,(u) \end{aligned}$$

and Q is a quadratic operator

$$\begin{aligned} Q[A,d,\sigma](u) &= \frac{1}{A}\left[\frac{\partial}{\partial x}\left(\overline{\mathcal{G}}[A,d,\sigma]\,(u,\sigma)\right) - \overline{\mathcal{G}}[A,d,\sigma]\left(u,\frac{\partial}{\partial x}\sigma\right)\right] \\ &\quad + \frac{1}{A}\sigma(x)d'(x)\,\mathcal{G}[A,d,\sigma,z=d(x)]\,(u) \end{aligned}$$

with $\mathcal{T}$, $\mathcal{G}$ are given by

$$\mathcal{T}[A,d,\sigma,z](u) = \frac{\partial}{\partial x}(u)\int_z^\eta \frac{S(x,s)}{\sigma(x)}\,ds + u\int_z^\eta \frac{1}{\sigma(x)}\frac{\partial}{\partial x}S(x,s)\,ds\,,$$

and

$$\begin{aligned} \mathcal{G}[A,d,\sigma,z](u) &= \int_z^\eta 2\left(\frac{\partial}{\partial x}u\right)^2\frac{S(x,s)}{\sigma(x)} + \frac{u^2}{\sigma(x)}\left(\frac{\frac{\partial}{\partial x}S(x,s)\frac{\partial}{\partial x}\sigma(x)}{\sigma(x)} - \frac{\partial}{\partial x}\frac{\partial}{\partial x}S(x,s)\right) \\ &\quad + \frac{\partial}{\partial x}\left(\frac{u^2}{2}\right)\frac{S(x,s)\frac{\partial}{\partial x}\sigma(x)}{\sigma(x)^2}\,ds \end{aligned}$$

with

$$\overline{\mathcal{X}}[A,d,\sigma](u,\psi) = \int_{d(x)}^\eta \psi\mathcal{X}[A,d,\sigma,z](u)\,dz\,.$$

In particular, one can explicitly compute those operators:

- if $\sigma \in \mathbb{R}_*^+$ and $d \in \mathbb{R}$ are constant then we recover the standard one dimensional SGN equations (see for instance [60, 61, 62]) over flat bottom with

$$\mathcal{L}[A,d,\sigma](u) = \mathcal{L}_0[A,\sigma](u) = \frac{1}{\sigma h}\frac{\partial}{\partial x}\left(\frac{\sigma h^3}{3}\frac{\partial}{\partial x}u\right)$$

and

$$Q[A,d,\sigma](u) = Q_0[A,\sigma](u) = \frac{1}{\sigma h}\frac{\partial}{\partial x}\left(\frac{2}{3}\sigma h^3\left(\frac{\partial}{\partial x}u\right)^2\right).$$

- if $\sigma \in \mathbb{R}_*^+$ is constant and $d = d(x)$ then we recover the standard one dimensional SGN equations (see for instance [60, 61, 62]) over uneven bottom with

$$\begin{aligned} \mathcal{L}[A,d,\sigma](u) &= \mathcal{L}_1[A,d,\sigma](u) = \mathcal{L}_0[A,\sigma](u) - \frac{1}{\sigma h}\frac{\partial}{\partial x}\left(\frac{\sigma h^2}{2}ud'(x)\right) \\ &\quad + \frac{h}{2}\frac{\partial}{\partial x}ud'(x) - u\,(d'(x))^2 \end{aligned}$$

and

$$\begin{aligned} Q[A,d,\sigma](u) &= Q_1[A,d](u) = Q_0[A,\sigma](u) + \frac{1}{\sigma h}\frac{\partial}{\partial x}\left(\sigma\frac{h^2}{2}u^2d''(x)\right) \\ &\quad + h\left(\frac{\partial}{\partial x}u\right)^2 d'(x) + u^2d'(x)\,d''(x)\,. \end{aligned}$$

- if $\sigma = \sigma(x)$ and $d = d(x)$ then we get the generalised one dimensional SGN equations for non uniform rectangular channel over uneven bottom with

$$\begin{aligned}\mathcal{L}[A,d,\sigma](u) &= \mathcal{L}_1[A,d,\sigma](u) + \frac{1}{\sigma h}\frac{\partial}{\partial x}\left(\sigma'(x)\frac{h^3}{3}u\right)\\ &\quad -\frac{\sigma'(x)}{\sigma}\left(\frac{\partial}{\partial x}u\frac{h^2}{3} + u\frac{h^2}{3}\frac{\sigma'(x)}{\sigma} - u\frac{h}{2}d'(x)\right)\end{aligned}$$

and

$$\begin{aligned}Q[A,d,\sigma](u) &= Q_1[A,d,\sigma](u) + \frac{1}{\sigma h}\frac{\partial}{\partial x}\left((\sigma'(x))^2\frac{u^2}{\sigma}\frac{h^3}{3}\right)\\ &\quad +\frac{1}{\sigma h}\frac{\partial}{\partial x}\left(d'(x)\sigma'(x)u^2\frac{h^2}{2}\right) - \frac{1}{\sigma h}\frac{\partial}{\partial x}\left(\sigma'(x)u^2\frac{h^3}{3}\right)\\ &\quad +\frac{\partial}{\partial x}\left(\frac{\partial}{\partial x}\left(\frac{u^2}{2}\right)\sigma'(x)\frac{h^3}{3}\right) - \frac{1}{\sigma h}\sigma'(x)\mathcal{R}[A,d,\sigma](u)\end{aligned}$$

with

$$\begin{aligned}\mathcal{R}[A,d,\sigma](u) &= \left(\frac{\partial}{\partial x}u\right)^2\frac{h^3}{3} + u^2\left(\frac{\sigma'(x)}{\sigma}\right)^2\frac{h^3}{3} + u^2\left(\frac{\sigma'(x)}{\sigma}\right)d'(x)\frac{h^2}{2}\\ &\quad -u^2\left(\frac{\sigma''(x)}{\sigma}\right)^2\frac{h^3}{3} + u^2d''(x)\frac{h^2}{2} + \frac{\partial}{\partial x}\left(\frac{u^2}{2}\right)\frac{\sigma'(x)}{\sigma}\frac{h^3}{3}\\ &\quad -u^2d'(x)\frac{\sigma'(x)}{\sigma}\frac{h^2}{2} - u^2\sigma'(x)\left(d'(x)\right)^2h + u^2\sigma''(x)d'(x)\frac{h^2}{2}\\ &\quad -\frac{\partial}{\partial x}\left(\frac{u^2}{2}\right)\sigma'(x)d'(x)\frac{h^2}{2}\,.\end{aligned}$$

It is known that third order derivatives involved in the initial model (4.90) may create high frequencies instabilities, but the presence of the $\left(I_d - \mu_2\mathbb{L}[A,d,\sigma]\right)^{-1}$ in the second equation of (4.134) stabilises the equations with respect to these perturbations. Therefore, in the following, we construct a numerical scheme for Eqs. (4.134) instead of Eqs. (4.90).

4.7.1 Numerical method

This section is devoted to the numerical method to solve the reformulated dispersive model (4.134). It is rather natural to split the hyperbolic part to the dispersive one as done by several authors (see for instance [25, 24, 16]).

Let $N \in \mathbb{N}^*$. Let us consider the following uniform mesh on $[0, L_c]$. Cells are denoted for every $i \in [0, N+1]$, by $m_i = (x_{i-1/2}, x_{i+1/2})$ with $x_i = \dfrac{x_{i-1/2} + x_{i+1/2}}{2}$ the cell center and $\delta x = x_{i+1/2} - x_{i-1/2}$ the space mesh. The interfaces $x_{1/2} = 0$ and $x = x_{N+1/2}$ denote the upstream and the downstream ends. We also consider a time discretisation t_n defined by $t_{n+1} = t_n + \delta t_n$ where the time step δt_n is computed through a CFL condition related to the hyperbolic part.

Let us first highlight that the still water steady state for Eqs. (4.134) is independent of μ_2. Indeed, one has $\forall \mu_2 > 0$, the still water steady state equation reads

$$u = 0, \frac{A}{\sigma} + d = h_0$$

for some positive h_0. As a consequence, the construction of a well-balanced scheme can be easily achieved considering only the hyperbolic part of Eqs. (4.134), for instance, by the use of the hydrostatic reconstruction (see for instance [4]).

Let us define $d_{i+1/2} = \max(d_i, d_{i+1})$ where $d_i = \dfrac{1}{\delta x}\displaystyle\int_{m_i} d(x)dx$, $\sigma_{i+1/2} = \max(\sigma_i, \sigma_{i+1})$ where $\sigma_i = \dfrac{1}{\delta x}\displaystyle\int_{m_i} \sigma(x)dx$ and let us define the reconstructed states

$$A^-_{i+1/2} = \sigma_{i+1/2}\left(\frac{A_i}{\sigma_i} + d_i - d_{i+1/2}\right),\ A^+_{i+1/2} = \sigma_{i+1/2}\left(\frac{A_{i+1}}{\sigma_{i+1}} + d_{i+1} - d_{i+1/2}\right)$$

with

$$U^-_{i+1/2} = (A^-_{i+1/2}, A^-_{i+1/2}u_i),\ U^+_{i+1/2} = (A^+_{i+1/2}, A^+_{i+1/2}u_{i+1})$$

where $U_i = (A_i, A_iu_i)^T \approx \dfrac{1}{\delta x}\displaystyle\int_{m_i} (A, Au)^T dx$.

Let us introduce the flux

$$F_1(U) = Q,\ F_2(U) = Q^2/A \text{ and } F_3(x, U) = I_1(x, A) + \mu_2\overline{\mathcal{G}}[A, d, \sigma]\,(u, \sigma)$$

and

$$\mathfrak{S}(x, U) = I_2 + \mu_2\overline{\mathcal{G}}[A, d, \sigma]\left(u, \frac{\partial}{\partial x}\sigma\right) - \mu_2\sigma(x)d'(x)\,\mathcal{G}[A, d, \sigma, z = d(x)]\,(u)\ .$$

Then, one can write System (4.134) as follows:

$$\begin{aligned}
&\frac{\partial}{\partial t}A + \frac{\partial}{\partial x}F_1(U) &&= 0\\
&\left(I_d - \mu_2\mathbb{L}[A, d, \sigma]\right)\left(\frac{\partial}{\partial t}Q + \frac{\partial}{\partial x}F_2(U)\right) + \frac{\partial}{\partial x}F_3(x, U) - \mathfrak{S}(x, U) &&= 0
\end{aligned}$$

With these settings, we define the following numerical scheme:

$$\begin{aligned}
A_i^{n+1} &= A_i^n - \frac{\delta t_n}{\delta x}\left(\mathcal{F}_1\left(U^{-,n}_{i+1/2}, U^{+,n}_{i+1/2}\right) - \mathcal{F}_1\left(U^{-,n}_{i-1/2}, U^{+,n}_{i-1/2}\right)\right)\\
Q_i^{*} &= Q_i^n - \frac{\delta t_n}{\delta x}\left(\mathcal{F}_2\left(U^{-,n}_{i+1/2}, U^{+,n}_{i+1/2}\right) - \mathcal{F}_2\left(U^{-,n}_{i-1/2}, U^{+,n}_{i-1/2}\right)\right)\\
Q_i^{n+1} &= Q_i^{*} - \frac{\delta t_n}{\delta x}(Y^n)_i
\end{aligned}$$

where

$$\mathcal{A}^nY^n = \left(\mathcal{F}_3\left(x_{i+1/2}, U^{-,n}_{i+1/2}, U^{+,n}_{i+1/2}\right) - \mathcal{F}_3\left(x_{i-1/2}, U^{-,n}_{i-1/2}, U^{+,n}_{i-1/2}\right) + \mu_2\mathcal{N}_i^n\right)_{1\le i\le N}\ .$$

The matrix $\mathcal{A}^n$ is the cell-centered approximation of the linear operator $\left(I_d - \mu_2\mathbb{L}[A, d, \sigma]\right)$ and $\mathcal{N}_i^n$ is the cell-centered approximation of $-\overline{\mathcal{G}}[A, d, \sigma]\left(u, \dfrac{\partial}{\partial x}\sigma\right) + \sigma(x)d'(x)\,\mathcal{G}[A, d, \sigma, z = d(x)]\,(u)$.

The numerical fluxes are defined by

$$\begin{aligned}
\mathcal{F}_1\left(U^{-,n}_{i+1/2}, U^{+,n}_{i+1/2}\right) &= \frac{F_1\left(U^{-,n}_{i+1/2}\right) + F_1\left(U^{+,n}_{i+1/2}\right)}{2} - s^n_{i+1/2}(A^{+,n}_{i+1/2} - A^{-,n}_{i+1/2}) \\
\mathcal{F}_2\left(U^{-,n}_{i+1/2}, U^{+,n}_{i+1/2}\right) &= \frac{F_2\left(U^{-,n}_{i+1/2}\right) + F_2\left(U^{+,n}_{i+1/2}\right)}{2} - s^n_{i+1/2}(Q^{+,n}_{i+1/2} - Q^{-,n}_{i+1/2}) \\
\mathcal{F}_3\left(x_{i+1/2}, U^{-,n}_{i+1/2}, U^{+,n}_{i+1/2}\right) &= \frac{F_3\left(x_{i+1/2}, U^{-,n}_{i+1/2}\right) + F_3\left(x_{i+1/2}, U^{+,n}_{i+1/2}\right)}{2} \\
&+ \left(\frac{A^{n\,2}_i}{2\sigma_i F_r^2} - \frac{{A^{-,n}_{i+1/2}}^2}{2\sigma_{i+1/2}F_r^2}\right) \\
\mathcal{F}_3\left(x_{i+1/2}, U^{-,n}_{i+1/2}, U^{+,n}_{i+1/2}\right) &= \frac{F_3\left(x_{i+1/2}, U^{-,n}_{i+1/2}\right) + F_3\left(x_{i+1/2}, U^{+,n}_{i+1/2}\right)}{2} \\
&+ \left(\frac{{A^n_{i+1}}^2}{2\sigma_{i+1}F_r^2} - \frac{{A^{+,n}_{i+1/2}}^2}{2\sigma_{i+1/2}F_r^2}\right)
\end{aligned}$$

such that whenever $\mu_2 = 0$, we recover the classical numerical scheme[1] for the hyperbolic part

$$U^{n+1}_i = U^n_i - \frac{\delta t_n}{\delta x}\left(\mathcal{F}(x_{i+1/2}, U^{-,n}_{i+1/2}, U^{+,n}_{i+1/2}) - \mathcal{F}(x_{i-1/2}, U^{-,n}_{i-1/2}, U^{+,n}_{i-1/2})\right)$$

with $\mathcal{F}(x, U, V) = (\mathcal{F}_1(U, V), \mathcal{F}_2(U, V) + \mathcal{F}_3(x, U, V))$. In these expressions,

$$s_{i+1/2} = \max_{j=1,2}\left|\lambda_j(x_{i+1/2}, U^{-,n}_{i+1/2})\right|, \left|\lambda_j(x_{i+1/2}, U^{+,n}_{i+1/2})\right|$$

where $\lambda_j(x, U) = Q/A + (-1)^j\sqrt{\dfrac{A}{\sigma(x)F_r^2}}$, $j = 1, 2$ are the eigenvalues of the Jacobian matrix of $(F_1, F_2 + F_3)^T$.

The numerical scheme is consistent and stable under the CFL condition

$$\max_{1\le i\le N}\left(\left|\lambda_1(x_i, U^n_i)\right|, \left|\lambda_2(x_i, U^n_i)\right|\right)\frac{\delta t_n}{\delta x} \le 1\ .$$

4.7.2 Propagation of a solitary wave

In this section, we test the accuracy of the method, and we show the influence of the section variation in the case of the propagation of a solitary wave numerically. For this purpose, we consider the exact solitary wave solutions of the Green-Naghdi equations in the one-dimensional setting over a flat bottom (see [61]), given in variables with dimensions, by

$$\begin{cases} \eta(t, x) = a\,\mathrm{sech}^2(k(x - ct)), \quad u(t, x) = c\left(\dfrac{\eta(t, x)}{\eta(t, x) + z_0}\right) \\ \text{with } k = \dfrac{\sqrt{3a}}{2z_0\sqrt{z_0 + a}} \text{ and } c = \sqrt{g(z_0 + a)} \end{cases} \tag{4.135}$$

[1]For the sake of simplicity and clarity, we have presented the finite volume method using the Rusanov solver but the method is not limited to this one.

where z_0 is the depth of the fluid and a is the relative amplitude.

Accuracy The propagation of the solitary wave (4.135) is initially centered at $x_0 = 10$ m with a relative amplitude $a = 0.2$ m over a constant water depth $z_0 = 2$ m. The computational domain is $L_c = 100$ m and it is discretized with N cells. The single solitary wave propagates from left to right. In this test, since the solitary wave is initially far from boundaries, the boundary conditions do not affect the computation, thus we choose to impose free boundary conditions at the downstream and upstream ends. The exact solution is computed in a channel of width $\sigma = 1$.

In what follows, we quantify the numerical accuracy of our numerical scheme by computing the numerical solution for this particular test case for an increasing number of cells N over a duration $T = 20$ s. Starting with $N = 100$ number of cells, we successively multiply the number of cells by two. For all n, we compare, in Fig. 4.5, $M^n := \max_{0\leq i\leq N+2}(h_i^n)$ of our numerical solution provided by Eqs. (4.134) with the exact one $M(t_n) := \max h(t_n, x)_{x\in[0,L_c]} = 2.2$ given by (4.135). One can easily remark that the first order discretisation is not accurate for long time simulation due to the numerical dissipation. However, to limit the numerical dissipation of the first order numerical scheme, one can either limit the simulation time or consider a very large number of cells. However, it is better to increase the order of the numerical scheme but this is left to future work. Therefore, in what follows, we consider a shorter simulation time and a large number of cells, just to illustrate the influence of the variation of the channel.

Figure 4.5: $M^n := \max_{0\leq i\leq N+2}(h_i^n)$

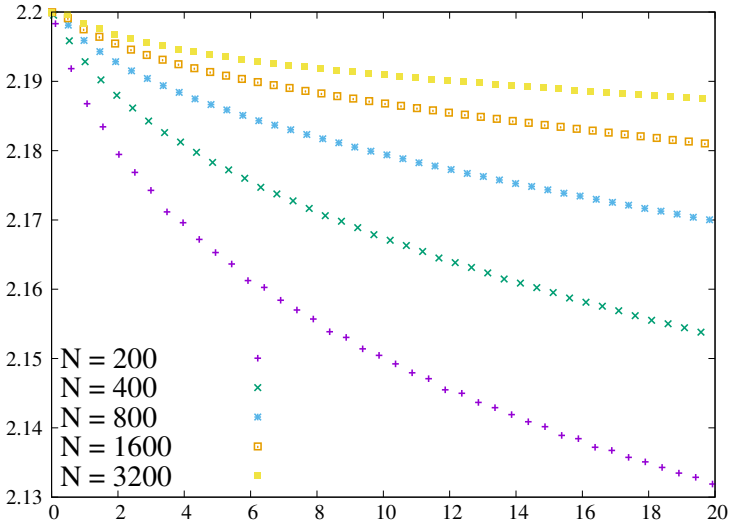

Influence of the section variation: We consider again the propagation of a solitary wave initially centered at $x_0 = 10$ m of relative amplitude $a = 0.2$ m, over a constant water depth $z_0 = 2$ m onto a computational domain of $L_c = 50$ m and discretized with $N = 5000$ cells. The final simulation time is $T = 8$ s.

Initially starting with $(\eta(0, x), u(0, x))$ (see Eqs. (4.135)), we compute the numerical simulation for the channels defined by

$\sigma(x;\varepsilon) = \beta(x;\varepsilon) - \alpha(x;\varepsilon)$ with $\beta = \dfrac{1}{2} - \dfrac{\varepsilon}{2}\exp\left(-\varepsilon^2\left(x - L/2)^2\right)\right)$ and $\alpha = -\beta$ with $\epsilon = 0$, $\epsilon = 0.1$, $\epsilon = 0.2$, $\epsilon = 0.3$ and $\epsilon = 0.4$. The obtained results are presented in Fig. 4.6. In Fig.4.7(a), for each geometry, we show the evolution of the maximum of the water level $M^n := \max\limits_{0\leq i\leq N+2}(h_i^n)$. As expected, since the first part for $x \leq 25$ is linearly converging, the water level increases while for $x > 25$, the channel is linearly diverging and therefore, the amplitude of the water level decreases. Moreover, in all numerical simulations, the mass is conserved. Indeed, for each value of ε, we have displayed in Fig. 4.7(b), the ratio of $\dfrac{m^n}{m^0}$ where $m^n := \dfrac{1}{N+2}\displaystyle\sum_{i=0}^{N+1} A_i^n$ is the mass of water at time t_n. The ratio $\dfrac{m^n}{m^0}$ is almost equal to 1, up to the order of accuracy of the numerical scheme.

Figure 4.6: Influence of σ

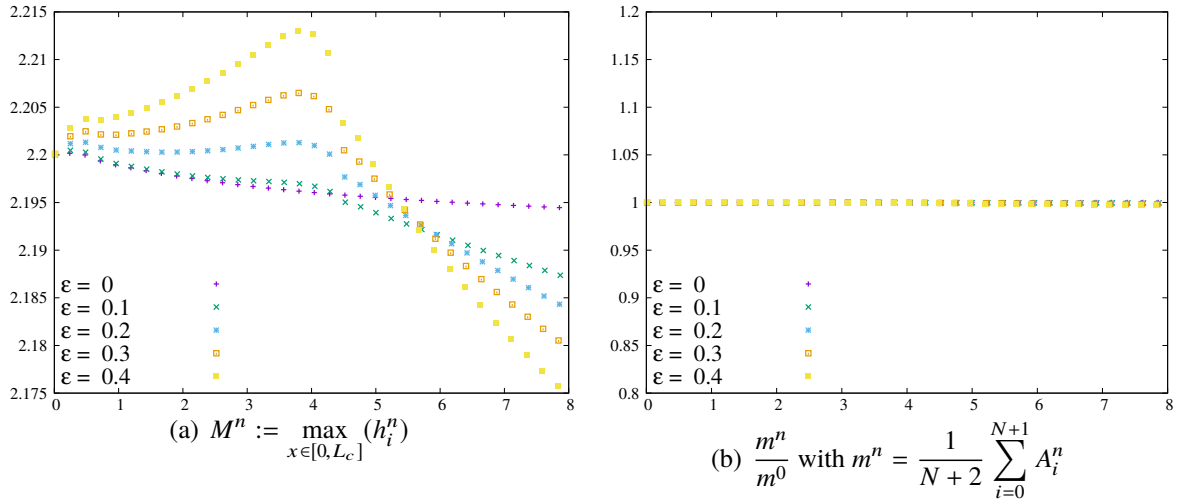

(a) $M^n := \max\limits_{x\in[0,L_c]}(h_i^n)$

(b) $\dfrac{m^n}{m^0}$ with $m^n = \dfrac{1}{N+2}\displaystyle\sum_{i=0}^{N+1} A_i^n$

In what follows, we quantify the numerical accuracy of our numerical scheme. Starting with $N = 100$ number of cells, we successively multiply the number of cells by two. The errors on the water surface deformation are presented in Table 4.1 and in Table 4.2. These errors are computed at $t = 8$ s using the L^2 :

$$\left\|\eta_{\text{num}} - \eta_{\text{ref}}\right\|_2 = \sqrt{\delta x \sum_i \left|\eta_{\text{num}_i}(t=8) - \eta_{\text{ref}}(t=8, x_i)\right|}$$

and the L^∞ norms where η_{ref} is the exact solution in the case $\varepsilon = 0$ and is a reference one computed with 10 000 cells for $\varepsilon = 0.4$. Since the results are almost the same whatever ε is, we have decided to present only the results for $\varepsilon = 0$ and $\varepsilon = 0.4$ in Table 4.1 and in Table 4.2.

As expected, the obtain numerical order is slow because of the numerical dissipation of the solitary wave (as already pointed out in several works, see for instance [16] for which we obtain almost the same order of convergence in the case of a uniform section). Moreover, as expected, cross-sectional variations do not influence the convergence rate.

Let us emphasise that the convergence rates are slightly better in the case of the non-uniform section because we are comparing our results to a reference solution and not to the exact one.

Table 4.1: Convergence rate of the L^2 error for $\varepsilon = 0$. The order is computed through first order interpolation polynomial

N	$\|\eta\text{num} - \eta_{exact}\|_2$	$\|\eta\text{num} - \eta_{exact}\|_\infty$
100	0.0789	0.0449
200	0.0497	0.0288
400	0.0304	0.0180
800	0.0198	0.0116
1600	0.0153	0.0081
3200	0.0138	0.0062
Order	0.53	0.58

Table 4.2: Convergence rate of the L^2 error for $\varepsilon = 0.4$. The reference solution is computed with 10 000 cells. The order is computed through first order interpolation polynomial

N	$\left\|\eta\text{num} - \eta_{\text{ref}}\right\|_2$	$\left\|\eta\text{num} - \eta_{\text{ref}}\right\|_\infty$
100	0.05212	0.02533
200	0.02096	0.01082
400	0.01079	0.00554
800	0.00748	0.00503
1600	0.00635	0.00412
3200	0.00505	0.00300
Order	0.64	0.56

4.8 Conclusion

This chapter has proposed to derive the first section-averaged non-linear dispersive model for open channel and river flows. These equations generalise both the classical section-averaged free surface model and the well-known SGN equations to the arbitrary section. We have presented a numerical finite volume approximation for the uniform-rectangular section, for which we have proposed two simple test cases.
In the next work, we will focus on the arbitrary channel section's case, and we will propose a high order numerical scheme.

Chapter 5

Simulation of complex free surface flows using SGN type models

Contents

This work was carried out in collaboration with Krisztian Benyo, Ayoub Charhabil and Yohan Penel and will be published in the proceedings of CEMRACS 2019.
I only contributed to the first three sections of this work.

5.1 Introduction

The simulation of incompressible, homogeneous, inviscid free surface fluid flows as a means to describe and examine the propagation of surface water waves has been a focal point of research oriented towards oceanographic applications for the past several decades. In general, such a physical system is governed by the free surface Euler equations, which, to this day, remains an analytically and numerically challenging topic.

For coastal, or large scale applications, it is commonly replaced by an adequate approximation based on the shallowness of the fluid domain. Diverse models based on the (nonlinear) shallow water [or Saint Venant] system [31] have been proposed and analysed in the past (see for instance [18, 77, 12, 69, 22, 71, 13]). Although the base model provides a reasonable tool for capturing the nonlinear transformation of waves, it fails to represent dispersive effects due to the underlying hydrostatic assumption.

The object of interest of the present work is the Serre–Green-Naghdi system (originally appeared in [86], [50]), also known as fully nonlinear Boussinesq system, a model derived from the free surface Euler equations. The system reads [74, 41]

$$\begin{cases} \partial_t h + \partial_x(hu) = 0, \\ \partial_t(hu) + \partial_x(hu^2) + \partial_x(hq) + q_b\partial_x z_b = -gh\partial_x(h + z_b) - h\partial_x p_{atm}, \\ \partial_t(hw) + \partial_x(huw) - q_b = 0, \\ \partial_t(h\sigma) + \partial_x(hu\sigma) - 2\sqrt{3}\left(q - \dfrac{q_b}{2}\right) = 0, \\ w - u\partial_x z_b - \sqrt{3}\sigma = 0, \\ 2\sqrt{3}\sigma + h\partial_x u = 0. \end{cases} \tag{5.1}$$

Unknowns. Here $h(t, x) : \mathbb{R}^+ \times \mathbb{R} \to \mathbb{R}^+$ is the fluid height at a given position in space x, at time t; $u(t, x) : \mathbb{R}^+ \times \mathbb{R} \to \mathbb{R}$ is the vertically averaged horizontal velocity of the fluid, $w(t, x) : \mathbb{R}^+ \times \mathbb{R} \to \mathbb{R}$ is the vertically averaged vertical velocity and $\sigma(t, x) : \mathbb{R}^+ \times \mathbb{R} \to \mathbb{R}$ is the vertical correction associated to w. Finally $q(t, x) : \mathbb{R}^+ \times \mathbb{R} \to \mathbb{R}$ is the vertically averaged hydrodynamic pressure and $q_b(t, x) : \mathbb{R}^+ \times \mathbb{R} \to \mathbb{R}$ is the hydrodynamic pressure at the bottom.

Data. $z_b(x) : \mathbb{R} \to \mathbb{R}$ is the time-independent bottom topography, and $g = 9.81$ is the standard acceleration due to gravity. The system is complemented with multiple possible boundary conditions, depending on the physical setting modeled.

The main focus of the chapter is to examine certain numerical algorithms for this system as well as to analyze some of the properties of the system in the more general two-dimensional case. Developing robust and efficient algorithms for the numerical resolution of the Serre–Green-Naghdi system has been of great interest lately, partially due to the amassed knowledge from theoretical analyses and the surge in computational power (see for instance [63, 14, 24, 64, 61, 74]). Our approach relies on a finite volume based splitting scheme that has shown promising results ([2],[1]) when applied to the non-hydrostatic shallow water model introduced in [20].

The basic outline of the document is as follows. In §5.2 we elaborate the finite volume - finite difference type splitting scheme. It consists in separating the hyperbolic part from the dispersive part of the equations. The hyperbolic prediction step involves the numerical

resolution of the classical shallow water equations, we opted for a finite volume scheme with hydrostatic reconstruction ([5]) to better incorporate the effects of a possibly non-flat bottom topography. As for the resolution of the system arising from the non-hydrostatic correction step, we present two iterative algorithms: the Uzawa algorithm for the mixed velocity-pressure problem and the Gauss-Seidel method for the projected elliptic pressure equations. The different choices for the boundary conditions depending on the physical situation at hand, as well as their consequences on the discretized numerical schemes, will be presented at the end.

In §5.3, we describe the various numerical test cases simulated with the aforementioned algorithms. Simulations concerning the propagation of exact solitary wave solutions over a flat bottom topography will be presented in order to compare the two algorithms, mainly in terms of computation time. It is followed by illustrations concerning the dispersive dam-break problem as well as the perturbation of steady state solutions; even though the scheme is not well-balanced, it behaves admissibly under small perturbations. Finally, the numerical validation against the experimental data obtained from the Favre secondary wave experiment [23] is presented and compared with previous results [19].

At last, in §5.4, we present the two dimensional extension of system (5.1). The reformulations and properties detailed in this section are also true for the original, one dimensional counterpart as well. At the end, some pertinent remarks are made on the variational formulation of the problem.

5.2 Numerical algorithms

In what follows we elaborate the two algorithms examined during our study. In order to propose the corresponding discretizations of system (5.1), we present first of all a semi-discretization of it in time, in order to establish some characteristics of the classical splitting scheme adopted.

To compactify the notation, we introduce the following to vectorial variables:

$$X = (u, w, \sigma)^T \quad \text{and} \quad Q = (q, q_b)^T.$$

We shall also make use of the following (dispersive) divergence and gradient type operators:

$$\nabla_{sgn} Q = \begin{pmatrix} \partial_x(hq) + q_b \partial_x z_b \\ -q_b \\ -2\sqrt{3}q + \sqrt{3}q_b \end{pmatrix}, \quad \text{and} \quad \nabla_{sgn} \cdot X = \begin{pmatrix} 2\sqrt{3}\sigma + h\partial_x u \\ w - u\partial_x z_b - \sqrt{3}\sigma \end{pmatrix}. \tag{5.2}$$

A crucial remark concerning these two operators is that

Lemma 5.2.1. *The dispersive divergence and gradient operators defined by (5.2) verify the partial integration type formula:*

$$Q \cdot (\nabla_{SGN} \cdot X) + X \cdot (\nabla_{SGN} Q) = \partial_x(hqu). \tag{5.3}$$

Indeed, this structural observation will be a key element in the correction step of the splitting method, since it will allow us to simplify the spatial discretization due to the "symmetry" of these two operators.

5.2.1 The splitting scheme

With the previous notation, we have that system (5.1) writes as

$$\partial_t h + \partial_x(hu) = 0, \tag{5.4a}$$
$$\partial_t(hX) + \partial_x(huX) + \nabla_{SGN} Q = S(h, z_b), \tag{5.4b}$$
$$\nabla_{SGN} \cdot X = 0, \tag{5.4c}$$

where

$$S(h, z_b) = (-gh\partial_x(h + z_b) - h\partial_x p_{atm}, 0, 0)^T .$$

This condensed formulation highlights the interest in proceeding with a splitting scheme. Indeed, let us take $n \in \mathbb{N}$ and discretize the system in time. Given a series of timesteps Δt^k, $k \in \mathbb{N}$ (defined later by an appropriate CFL-condition) giving rise to the times $t^n = \sum_{k \leq n} \Delta t^k$, one has that for the step $n + 1$, the system can be split into two parts:

1. A prediction step for the hyperbolic part of the system:

$$\frac{h^{n+1/2} - h^n}{\Delta t^{n+1}} + \partial_x(h^n u^n) = 0, \tag{5.5a}$$
$$\frac{(hX)^{n+1/2} - (hX)^n}{\Delta t^{n+1}} + \partial_x(h^n u^n X^n) = S(h^n, z_b), \tag{5.5b}$$

   for variables h and hX, where h^n denotes $h(t^n, \cdot)$, and $h^{n+1/2}$ is the hydrostatic approximated value of $h(t^{n+1}, \cdot)$, and similarly for the other variables. Notice that this system is essentially the Saint-Venant equations with uneven bottom topography, its resolution is classical and well-known. In the numerical simulations to follow (in §5.3) we opted for the implementation of a first order finite volume approach, a Rusanov solver with hydrostatic reconstruction for the well-balancedness for a potentially uneven bottom [5].

2. A projection / correction step involving the non-hydrostatic (dispersive) part of the system:

$$\frac{(hX)^{n+1} - (hX)^{n+1/2}}{\Delta t^{n+1}} + \nabla_{SGN} Q^{n+1} = 0, \tag{5.6a}$$
$$\nabla_{SGN} \cdot X^{n+1} = 0, \tag{5.6b}$$

   for variables X and Q. Herein lies the novelty of the problem, in the efficient resolution of this nonlinear problem. In what follows, we will detail two approaches concerning the discretization and numerical resolution of this step, both of them make use of some particular (structural) properties of the system and both of them are iterative methods for computational efficiency.

5.2.2 Spatial discretization

Let us give some general information on the discretization in space. We consider our domain to be the (finite) interval $I = [a, b]$ with $a, b \in \mathbb{R}$. The mesh is defined as

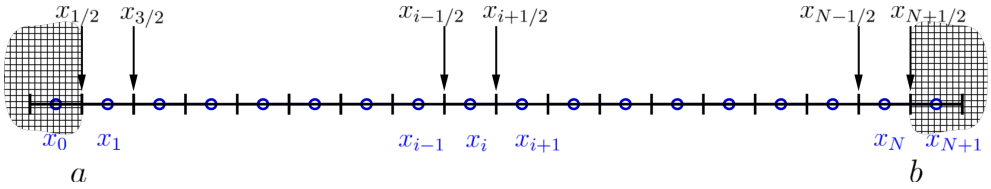

Figure 5.1: Schematic representation of the staggered grid

a homogeneous Cartesian grid on I, with $N \in \mathbb{N}$ cells of size $\Delta x = (b-a)/N$. All variables of the system will be defined at the cell centers x_i ($i \in \{0, \dots, N+1\}$) with x_0 and x_{N+1} corresponding to ghost cells at the boundaries (see Figure 5.1). The use of a colocated scheme (especially for the pressure variables Q) is justified by the presence of the dispersive gradient term $\nabla_{SGN} Q$ for the equation on X.

Hyperbolic step: System (5.5) consists of the classic $1D$ shallow water equations for (h, hu) and two transport equations for $(hw, h\sigma)$. As it was already mentioned before, a first order finite volume scheme was implemented, with a full discretization of:

$$\frac{(hX^*)_i^{n+1/2} - (hX^*)_i^n}{\Delta t^{n+1}} + \frac{\mathcal{F}_{i+1/2}^n - \mathcal{F}_{i-1/2}^n}{\Delta x} = S(h_{i-1}^n, h_i^n, h_{i+1}^n, z_b), \tag{5.7}$$

where $X^* = (1, X^T)^T$. The numerical fluxes $\mathcal{F}_{i+1/2}^n$ ($i \in \{0, \dots, N\}$) approximate the flux at the interfaces; for the simulations, a Rusanov solver was chosen as an approximation.

Such a numerical scheme is stable, provided the following Courant–Friedrichs–Lewy condition holds:

$$\Delta t^{n+1} \leq c_{\mathcal{F}} \frac{\Delta x}{\max\limits_{i \in \{1,\dots,N\}} (|u_i^n| + \sqrt{g h_i^n})}, \tag{5.8}$$

where $c_{\mathcal{F}}$ is a constant dependent on the chosen numerical solver. We define Δt^{n+1} for our scheme such that this CFL-condition is respected. For boundary condition treatment, we refer to §5.2.5.

Velocity-pressure system: System (5.6) is a Stokes-type system in which no correction is made on the variable h. Indeed, the height function has been completely determined during the prediction step, therefore

$$h_i^{n+1} = h_i^{n+1/2}.$$

Let us denote by $\mathcal{H}^{n+1} \in \mathcal{M}_{N,N}(\mathbb{R})$ the diagonal $N \times N$ matrix with the corresponding diagonal elements h_i^{n+1}, and by $\overline{\mathcal{H}}^{n+1} \in \mathcal{M}_{3N,3N}(\mathbb{R})$ the $3N \times 3N$ block-diagonal matrix with block entries $\mathcal{H}^{n+1}$.

The dispersive gradient $\nabla_{SGN} Q^{n+1}$ is discretized as $B\mathbf{Q}^{n+1}$, as part of a finite difference type discretization scheme on the mesh of the interval I. Here, and in what follows throughout this section, boldfaced vectors refer to the discretized values over all cells ($i \in \{1, \dots, N\}$), such as for instance

$$\mathbf{Q}^{n+1} = (q_1^{n+1}, q_2^{n+1}, \dots, q_N^{n+1}, q_{b,1}^{n+1}, q_{b,2}^{n+1}, \dots, q_{b,N}^{n+1})^T.$$

The matrix $B \in \mathcal{M}_{3N,2N}(\mathbb{R})$ has a relatively simple structure:

$$B = \begin{pmatrix} B_{11} & B_{12} \\ 0_{N,N} & -\mathrm{Id}_N \\ -2\sqrt{3}\,\mathrm{Id}_N & \sqrt{3}\,\mathrm{Id}_N \end{pmatrix},$$

where the matrix $B_{12} \in \mathcal{M}_{N,N}(\mathbb{R})$ is diagonal, with elements $(\partial_x z_b)_i$, and $B_{11} \in \mathcal{M}_{N,N}(\mathbb{R})$ is an appropriate discretization for the term $\partial_x(hq)$. We consider two different finite difference schemes for this

1. Second order central scheme on mesh points: for any interior cell ($i \in \{2, \dots, N-1\}$) we have that

$$\begin{aligned} (\partial_x(hq))_i &\simeq \frac{1}{\Delta x}\left(h_{i+1/2}q_{i+1/2} - h_{i-1/2}q_{i-1/2}\right) \\ &= \frac{(h_{i+1}+h_i)(q_{i+1}+q_i) - (h_i+h_{i-1})(q_i+q_{i-1})}{4\Delta x}. \end{aligned} \tag{5.9}$$

   Here, cell boundaries are $x_{i+1/2}$ ($i \in \{0, \dots, N\}$) and the corresponding indexes refer to the averaged values

$$h_{i+1/2} = \frac{h_i + h_{i+1}}{2}.$$

   For this discretization, the corresponding tridiagonal matrix B_{11}^1 has

$$\frac{1}{2\Delta x}\begin{pmatrix} \dots & -h_{i-1/2} & (h_{i+1/2} - h_{i-1/2}) & h_{i+1/2} & \dots \end{pmatrix}$$

   as the i^{th} row.

2. Second order central scheme on adjacent cells: for any interior cell ($i \in \{2, \dots, N-1\}$) we have that

$$(\partial_x(hq))_i \simeq \frac{h_{i+1}q_{i+1} - h_{i-1}q_{i-1}}{2\Delta x}. \tag{5.10}$$

   For this discretization, the corresponding tridiagonal matrix B_{11}^2 has

$$\frac{1}{2\Delta x}\begin{pmatrix} \dots & -h_{i-1} & 0 & h_{i+1} & \dots \end{pmatrix}$$

   as the i^{th} row.

When not specified, matrices B_{11} and B can refer to either of these discretization schemes. Notice that the first and last rows of B_{11} may contain only the truncated discretized formulae; the missing terms in the discretization correspond to information on the two ghost cells. With the establishment of the boundary conditions, the values on the ghost cells call for corrections on the first and last elements of the diagonals, up to an error term $\widehat{0}$. The exact corrections to be made depending on the boundary conditions chosen, they will be precised in §5.2.5.

With this at our disposal, the equation (5.6a) is discretized as

$$\frac{\overline{\mathcal{H}}^{n+1}\mathbf{X}^{n+1} - \overline{\mathcal{H}}^{n+1}\mathbf{X}^{n+1/2}}{\Delta t^{n+1}} + B\mathbf{Q}^{n+1} = \widehat{\mathbf{0}}, \tag{5.11}$$

where $\widehat{\mathbf{0}}$ is the error terms (independent of the variables X and Q) due to the correction associated to the boundary condition.

Owing to Lemma 5.2.1, equation (5.6b) admits a natural discretization of $B^T\mathbf{X}^{n+1} = \tilde{\mathbf{0}}$ since B^T is a suitable discretization of the dispersive divergence, up to a boundary term correction induced error term of $\tilde{0}$ (independent of variables X and Q).

To sum it up, we are left with the resolution of the following discretization of system (5.6):

$$\begin{pmatrix} \frac{1}{\Delta t^{n+1}}\overline{\mathcal{H}}^{n+1} & B \\ B^T & 0_{2N,2N} \end{pmatrix} \cdot \begin{pmatrix} \mathbf{X}^{n+1} \\ \mathbf{Q}^{n+1} \end{pmatrix} = \begin{pmatrix} \frac{1}{\Delta t^{n+1}}\overline{\mathcal{H}}^{n+1}\mathbf{X}^{n+1/2} + \widehat{\mathbf{0}} \\ \tilde{\mathbf{0}} \end{pmatrix}. \tag{5.12}$$

In the next part, we detail two iterative algorithms for the resolution of this system, both of them utilising the symmetric structure of equations (5.12). We chose the iterative approach to circumvent solving directly the $5N$ system of equations.

5.2.3 Iterative methods: the Uzawa algorithm

Given the symmetric nature of system (5.12) a natural alternative to directly solving the mixed velocity-pressure problem is to consider the Uzawa algorithm. This consists in, for an iterative parameter α, the following consecutive iterations:

$$\mathbf{X}^{n+1,p+1} = \mathbf{X}^{n+1/2} - \Delta t^{n+1}\left(\overline{\mathcal{H}}^{n+1}\right)^{-1} B\mathbf{Q}^{n+1,p} + \Delta t^{n+1}\left(\overline{\mathcal{H}}^{n+1}\right)^{-1}\widehat{\mathbf{0}}, \tag{5.13a}$$

$$\mathbf{Q}^{n+1,p+1} = \mathbf{Q}^{n+1,p} + \alpha(B^T\mathbf{X}^{n+1,p+1} - \tilde{\mathbf{0}}), \tag{5.13b}$$

for $p \in \mathbb{N}$ the current iteration index. We remark that the matrix $\overline{\mathcal{H}}$ is diagonal, its inversion has no additional computational cost. As the initialization of the iterative process, $\mathbf{Q}^{n+1,0} = \mathbf{Q}^n$ is taken (since Q is not involved in the prediction step of the algorithm).

One additional concern about the initialization has to be adressed, which is the very first time step. Contrary to the variables X, which are natural, physically easily measurable quantities, obtaining a priori knowledge on the hydrodynamic pressure components Q is rarely available. Throughout the implementation of the algorithm, an (arbitrary) initial quess of 0 was considered for these variables. This can obviously result in a high number of iterations during the first timestep, which can be spread out on multiple timesteps by imposing a maximal number of iterations $p \leq p_{max}$ (with p_{max} being constant).

Apart from the upper bound on the iterations, the Uzawa algorithm is carried out until the error on the correction is reasonably small, namely an error threshold of ϵ. The error itself is measured as the discrete L^∞-norm of the difference between two consecutive iterations, that is:

$$\|\mathbf{Q}^{n+1,p+1} - \mathbf{Q}^{n+1,p}\|_{l^\infty(I)} \leq \epsilon.$$

Notice that the system (5.13) can be simplified into an iterative algorithm on $\mathbf{Q}$ uniquely, since

$$\mathbf{Q}^{n+1,p+1} = \left(\mathrm{Id}_{2N} - \alpha\Delta t^{n+1} B^T (\overline{\mathcal{H}}^{n+1})^{-1} B\right) \mathbf{Q}^{n+1,p} + \alpha(B^T \mathbf{X}^{n+1/2} + \Delta t^{n+1} B^T (\overline{\mathcal{H}}^{n+1})^{-1} \widehat{\mathbf{0}} - \tilde{\mathbf{0}}), \quad (5.14)$$

which gives us direct information on the convergence of the Uzawa algorithm [57] as a function of the eigenvalues of the matrix $\Delta t^{n+1} C := \Delta t^{n+1} B^T (\overline{\mathcal{H}}^{n+1})^{-1} B$.

Lemma 5.2.2. *The algorithm converges iff the parameter α satisfies*

$$0 < \alpha < \frac{2}{\Lambda_{max}},$$

where Λ_{max} is the largest eigenvalue of the aforementioned matrix $\Delta t^{n+1} C$. The optimal iterative parameter is given by

$$\alpha_{opt} = \frac{2}{\Lambda_{min} + \Lambda_{max}},$$

Λ_{min} being the smallest eigenvalue of $\Delta t^{n+1} C$.

However, obtaining information on the eigenvalues of this matrix is highly nontrivial, except for very particular cases (for example a lake at rest situation with flat bottom topography).

5.2.4 Iterative methods: the Gauss-Seidel approach

Multiplying the first equation of (5.12) by $\Delta t^{n+1} B^T (\overline{\mathcal{H}})^{-1}$ and substituting the second equation in it yields

$$\Delta t^{n+1} C \mathbf{Q}^{n+1} \left(= \Delta t^{n+1} B^T (\overline{\mathcal{H}}^{n+1})^{-1} B \mathbf{Q}^{n+1}\right) = B^T \mathbf{X}^{n+1/2} + \Delta t^{n+1} B^T (\overline{\mathcal{H}}^{n+1})^{-1} \widehat{\mathbf{0}} - \tilde{\mathbf{0}} =: \mathbf{f}, \quad (5.15)$$

an equation similar to (5.14), with $\mathbf{f} = (\mathbf{f}_q^T, \mathbf{f}_{q_b}^T)^T$ as the right hand side.

Remark 10. In fact, this corresponds to a direct discretization of the projected system obtained from (5.4) by essentially applying the dispersive gradient operator on the second set of equations. Indeed, one has that system (5.1) can be rewritten as

$$-12\frac{q}{h} + h\partial_x\left(\frac{1}{h}\partial_x(hq)\right) + 6\frac{q_b}{h} + h\partial_x\left(\frac{q_b}{h}\partial_x z_b\right) = -h\partial_{xx}(g(h+z_b) + p_{atm}) - 2h(\partial_x u)^2, \quad (5.16a)$$

$$-6\frac{q}{h} + \frac{1}{h}\partial_x z_b \partial_x(hq) + (4 + (\partial_x z_b)^2)\frac{q_b}{h} = u^2 \partial_{xx} z_b - \partial_x z_b \partial_x(g(h+z_b) + p_{atm}). \quad (5.16b)$$

The symmetric matrix C has a particular block structure of the following form

$$C = \begin{pmatrix} C_{11} & C_{12} \\ C_{12}^T & C_{22} \end{pmatrix} = \begin{pmatrix} B_{11}^T (\mathcal{H}^{n+1})^{-1} B_{11} + 12(\mathcal{H}^{n+1})^{-1} & B_{11}^T (\mathcal{H}^{n+1})^{-1} B_{12} - 6(\mathcal{H}^{n+1})^{-1} \\ B_{12}^T (\mathcal{H}^{n+1})^{-1} B_{11} - 6(\mathcal{H}^{n+1})^{-1} & B_{12}^T (\mathcal{H}^{n+1})^{-1} B_{12} + 4(\mathcal{H}^{n+1})^{-1} \end{pmatrix},$$

with C_{11} and C_{22} being symmetric and positive definite $N \times N$ matrices.

Direct resolution of (5.15), much like the full velocity pressure system (5.12), is ill-advised and rather time consuming, even though the matrix possesses a pleasant "quasi-diagonal"-by-block structure. Since C_{22} is, in fact, a diagonal matrix, one could once again implement an Uzawa type iterative algorithm for the resolution of the discretized elliptic problem.

However, we present instead of a block Gauss-Seidel type method. This basically entails in performing a simple block-LU decomposition to separate C_{12} for the explicit part of the algorithm and keeping the rest as an implicit part. For the iterative step $k \in \mathbb{N}$ we have the following two subsequent iterations to perform:

$$C_{11}\mathbf{q}^{n+1,p+1} = \frac{1}{\Delta t^{n+1}}\mathbf{f} - C_{12}\mathbf{q}_b^{n+1,p}, \tag{5.17a}$$

$$C_{22}\mathbf{q}_b^{n+1,p+1} = \frac{1}{\Delta t^{n+1}}\mathbf{f}_b - C_{12}^T\mathbf{q}^{n+1,p+1}, \tag{5.17b}$$

up to a maximal iteration of $p \leq p_{max}$, or sufficiently small error term, the error being measured by the norm of the relative difference between two subsequent iterations, exactly the same way as in the Uzawa algorithm. Once again, we initialize by taking $\mathbf{q}_b^{n+1,0} = \mathbf{q}_b^n$.

Owing to the positiveness of matrices C_{11} and C_{22} [83], one can show that

Lemma 5.2.3. *The block Gauss-Seidel type algorithm converges (with respect to the norm induced by the matrix C).*

5.2.5 Boundary conditions for the iterative algorithms

As far as boundary conditions are concerned, the three important variables are h, u (or equivalently the flux hu) and q (or its conservative counterpart hq). In what follows, we analyze different boundary conditions: the solid wall boundaries (mixed Dirichlet and Neumann boundary conditions) and a fluvial type inflow-outflow setting. We remark that boundary conditions on the boundary pressure term q_b have no actual influence on the algorithm since boundary terms for q_b do not appear in the scheme at any given moment.

In what follows we will precise not only the appropriate boundary conditions but the calculations concerning the related error terms for both discretization schemes: (1) the central scheme on mesh points and (2) the central scheme on adjacent cells.

5.2.5.1 Solid wall boundaries

We assume that the boundary is a mirror, meaning that the spatial derivative (normal derivative) of quantities vanishes, except for the horizontal velocity, which simply vanishes at the boundary. In particular, on the left hand side boundary, we have that

$$(\partial_x h)_{i=1/2} = 0, \quad u_{i=1/2} = 0, \quad (\partial_x w)_{i=1/2} = 0, \quad \text{and } (\partial_x \sigma)_{i=1/2} = 0,$$

that is, on the ghost cells $i = 0$ these quantities are defined through basic discretization as

$$h_0 = h_1, \quad u_0 = -u_1, \quad w_0 = w_1, \quad \text{and } \sigma_0 = \sigma_1.$$

For the Dirichlet boundary condition on the velocity u, we impose Neumann boundary condition on the pressure q, as well as on q_b, therefore

$$(\partial_x q)_{i=1/2} = 0, \quad (\partial_x q_b)_{i=1/2} = 0 \quad \Longrightarrow \quad q_0 = q_1, \quad q_{b0} = q_{b1}.$$

Similarly, one has on the right hand side boundary:

$$h_{N+1} = h_N, \quad u_{N+1} = -u_N, \quad w_{N+1} = w_N, \quad \sigma_{N+1} = \sigma_N, \quad q_{N+1} = q_N, \quad \text{and } q_{bN+1} = q_{bN}.$$

1. With the boundary conditions at our disposal, we can write the discretization of the momentum equation for the first cell:

$$\frac{h_1 u_1^{n+1} - h_1 u_1^{n+1/2}}{\Delta t} + \frac{1}{2\Delta x}(h_{3/2}(q_1 + q_2) - h_{1/2}(q_0 + q_1)) + q_{b1}(\partial_x z_b)_1 = 0.$$

   Since $q_0 = q_1$, this means that

$$(B^1\mathbf{Q})_1 = \frac{1}{2\Delta x}(h_{3/2} - 2h_{1/2})q_1 + \frac{1}{2\Delta x}h_{3/2}q_2 + q_{b1}(\partial_x z_b)_1,$$

   and that no correction is required, $\widehat{0}_1 = 0$.

   So, given the matrix B^1, we can compute the approximation for the divergence

$$\begin{aligned}((B^1)^T\mathbf{X})_1 &= \frac{1}{2\Delta x}(h_{3/2} - 2h_{1/2})u_1 - \frac{1}{2\Delta x}h_{3/2}u_2 - 2\sqrt{3}\sigma_1 \\ &= -\frac{1}{2\Delta x}(h_{3/2}(u_2 - u_1) + h_{1/2}(u_1 + u_1)) - 2\sqrt{3}\sigma_1.\end{aligned}$$

   Given that $u_1 = -u_0$, we obtain that

$$((B^1)^T\mathbf{X})_1 = -\frac{1}{2}\left(h_{3/2}\frac{u_2 - u_1}{\Delta x} + h_{1/2}\frac{u_1 - u_0}{\Delta x}\right) - 2\sqrt{3}\sigma_1,$$

   which is exactly a first order discretization of $-(h\partial_x u + 2\sqrt{3}\sigma)$. Therefore no corrections are necessary either; $\tilde{0}_1 = 0$.

   With the same reasoning, we have that

$$(B^1\mathbf{Q})_N = -\frac{1}{2\Delta x}h_{N-1/2}q_{N-1} + \frac{1}{2\Delta x}(2h_{N+1/2} - h_{N-1/2})q_N + q_{bN}(\partial_x z_b)_N,$$

   and that corrections are not necessary neither for the gradient nor for the divergence: $\widehat{0}_N = 0$, $\tilde{0}_N = 0$.

2. With the boundary conditions at our disposal, we can write the discretization of the momentum equation for the first cell:

$$\frac{h_1 u_1^{n+1} - h_1 u_1^{n+1/2}}{\Delta t} + \frac{1}{2\Delta x}(h_2 q_2 - h_0 q_0) + q_{b1}(\partial_x z_b)_1 = 0.$$

   Since $q_0 = q_1$, and that $h_0 = h_1$, this means that

$$(B^2\mathbf{Q})_1 = -\frac{1}{2\Delta x}h_1 q_1 + \frac{1}{2\Delta x}h_2 q_2 + q_{b1}(\partial_x z_b)_1,$$

and that no correction is required, $\widehat{0}_1 = 0$.

So, given the matrix B^2, we can compute the approximation for the divergence

$$((B^2)^T\mathbf{X})_1 = -\frac{1}{2\Delta x}h_1u_1 - \frac{1}{2\Delta x}h_1u_2 - 2\sqrt{3}\sigma_1$$

Given that $u_1 = -u_0$ we obtain that

$$((B^2)^T\mathbf{X})_1 = -h_1\frac{u_2 - u_0}{2\Delta x} - 2\sqrt{3}\sigma_1,$$

which is exactly a first order discretization of $-(h\partial_x u + 2\sqrt{3}\sigma)$. Therefore no corrections are necessary either; $\tilde{0}_1 = 0$.

With the same reasoning, we have that

$$(B^2\mathbf{Q})_N = -\frac{1}{2\Delta x}h_{N-1}q_{N-1} + \frac{1}{2\Delta x}h_Nq_N + q_{bN}(\partial_x z_b)_N,$$

and that corrections are not necessary neither for the gradient nor for the divergence: $\widehat{0}_N = 0$, $\tilde{0}_N = 0$

5.2.5.2 Fluvial inflow-outflow

For this case, we suppose that we are in a fluvial regime, meaning that $|u| < \sqrt{gh}$. In this case, it is enough to prescribe either the fluid height or the flow flux at each of the boundaries. In our case we will prescribe a constant inflow flux $Q_{inc} > 0$ on the left hand side boundary and a constant height H_{out} on the right hand side boundary. The missing variables (h or hu respectively) can be recovered due to the underlying hyperbolic problem and the conservation of the associated Riemann-invariant on the outgoing characteristic.

Incoming flux on the left hand side: Let us start with the lower end of the domain. We prescribe a Dirichlet type condition on the flux, that is $(hu)_{i=1/2} = Q_{inc}$. This means that

$$\frac{h_0u_0 + h_1u_1}{2} = Q_{inc} \quad \Longrightarrow \quad h_0u_0 = 2Q_{inc} - h_1u_1. \tag{5.18}$$

Since we are in a fluvial regime, the outgoing characteristic $u + \sqrt{gh}$ is always positive, therefore the corresponding Riemann-invariant is preserved. This yields a second equation on h_0 and u_0:

$$u_0 + 2\sqrt{gh_0} = u_1 + 2\sqrt{gh_1}$$

Expressing u_0 from one equation and substituting it in the other one leads to a third order polynomial in $\sqrt{h_0}$:

$$2\sqrt{g}(\sqrt{h_0})^3 - (u_1 + 2\sqrt{gh_1})h_0 + (2Q_{inc} - h_1u_1) = 0, \tag{5.19}$$

potentially having 3 real roots, depending on the sign of the discriminant

$$\Delta = \left(4(u_1 + 2\sqrt{gh_1})^3 - 108g(2Q_{inc} - h_1u_1)\right)(2Q_{inc} - h_1u_1).$$

Remark 11. Using Mathematica, one can compute the exact solution. With the auxiliary quantities:

$$A_1 = 16gh_1\sqrt{gh_1} - 216gQ_{inc} + 132gh_1u_1 + 12\sqrt{gh_1}u_1^2 + 2u_1^3,$$
$$A_2 = \sqrt[3]{A_1 + \sqrt{-4(u_1 + 2\sqrt{gh_1})^6 + A_1^2}},$$

we have that

$$h_{0,1} = \frac{1}{6\sqrt{g}}\left(u_1 + 2\sqrt{gh_1} + \sqrt[3]{2}(u_1 + 2\sqrt{gh_1})^2\frac{1}{A_2} + \frac{1}{\sqrt[3]{2}}A_2\right),$$
$$h_{0,2} = \frac{1}{6\sqrt{g}}\left(u_1 + 2\sqrt{gh_1} + \frac{1+\sqrt{3}i}{2}\sqrt[3]{2}(u_1 + 2\sqrt{gh_1})^2\frac{1}{A_2} + \frac{1-\sqrt{3}i}{2}\frac{1}{\sqrt[3]{2}}A_2\right),$$
$$h_{0,3} = \frac{1}{6\sqrt{g}}\left(u_1 + 2\sqrt{gh_1} + \frac{1-\sqrt{3}i}{2}\sqrt[3]{2}(u_1 + 2\sqrt{gh_1})^2\frac{1}{A_2} + \frac{1+\sqrt{3}i}{2}\frac{1}{\sqrt[3]{2}}A_2\right).$$

Depending on the Q_{inc} and initial state chosen, we cannot exclude the possibility of having multiple adequate h_0s for the problem. What is worse, h_0 depends nonlinearly on u_1 which makes it impossible to correct the discretization for $\nabla_{sgn}\cdot$. Therefore, one could simply impose continuity of the fluid height on the boundary $h_0 = h_1$, even though this would theoretically make the problem overdetermined.

Once h_0 is determined, one can express u_0 from the inflow flux condition, so we have that

$$u_0 = \frac{2Q_{inc} - h_1u_1}{h_0}.$$

For the vertical components of the velocity, we impose Neumann boundary condition, just as before, hence

$$(\partial_x w)_{i=1/2} = 0, \quad (\partial_x \sigma)_{i=1/2} = 0 \quad \Longrightarrow \quad w_0 = w_1, \quad \sigma_0 = \sigma_1.$$

Since we imposed a Dirichlet type boundary condition on the velocity u, we prescribe a Neumann type boundary condition on the conservative pressure term hq and q_b:

$$(\partial_x(hq))_{i=1/2} = 0, \quad (\partial_x q_b)_{i=1/2} = 0 \quad \Longrightarrow \quad q_0 = \frac{h_1}{h_0}q_1, \quad q_{b0} = q_{b1}.$$

1. With the boundary conditions at our disposal, we can write the discretization of the momentum equation for the first cell:

$$\frac{h_1u_1^{n+1} - h_1u_1^{n+1/2}}{\Delta t} + \frac{1}{2\Delta x}(h_{3/2}(q_1 + q_2) - h_{1/2}(q_0 + q_1)) + q_{b1}(\partial_x z_b)_1 = 0.$$

Since $q_0 = \frac{h_1}{h_0}q_1$, this means that

$$(B^1\mathbf{Q})_1 = \frac{1}{2\Delta x}\left(h_{3/2} - h_{1/2}\left(1 + \frac{h_1}{h_0}\right)\right)q_1 + \frac{1}{2\Delta x}h_{3/2}q_2 + q_{b1}(\partial_x z_b)_1,$$

and that no correction is required, $\widehat{0}_1 = 0$.

So, given the matrix B^1, we can compute the approximation for the divergence

$$\begin{aligned}((B^1)^T\mathbf{X})_1 &= \frac{1}{2\Delta x}\left(h_{3/2} - h_{1/2}\left(1 + \frac{h_1}{h_0}\right)\right)u_1 - \frac{1}{2\Delta x}h_{3/2}u_2 - 2\sqrt{3}\sigma_1 \\ &= -\frac{1}{2\Delta x}\left(h_{3/2}(u_2 - u_1) + h_{1/2}\left(1 + \frac{h_1}{h_0}\right)u_1\right) - 2\sqrt{3}\sigma_1.\end{aligned}$$

Given that $u_1 = \dfrac{2Q_{inc} - h_0u_0}{h_1}$, we obtain that

$$((B^1)^T\mathbf{X})_1 = -\frac{1}{2}\left(h_{3/2}\frac{u_2 - u_1}{\Delta x} + h_{1/2}\frac{u_1 - u_0}{\Delta x}\right) - \frac{1}{\Delta x}\frac{h_{1/2}}{h_0}Q_{inc} - 2\sqrt{3}\sigma_1,$$

which is a first order discretization of $-(h\partial_x u + 2\sqrt{3}\sigma)$ up to a correction term $\tilde{0}_1 = \dfrac{1}{\Delta x}\dfrac{h_{1/2}}{h_0}Q_{inc}$. It is at this point that we need that h_0 is not a function of u_1.

2. Here we only treat the special case when $h_0 = h_1$. With the boundary conditions at our disposal, we can write the discretization of the momentum equation for the first cell:

$$\frac{h_1u_1^{n+1} - h_1u_1^{n+1/2}}{\Delta t} + \frac{1}{2\Delta x}(h_2q_2 - h_0q_0) + q_{b1}(\partial_x z_b)_1 = 0.$$

Since $q_0 = q_1$, and our additional hypothesis on h_0, this means that

$$(B^2\mathbf{Q})_1 = -\frac{1}{2\Delta x}h_1q_1 + \frac{1}{2\Delta x}h_2q_2 + q_{b1}(\partial_x z_b)_1,$$

and that no correction is required, $\widehat{0}_1 = 0$.

So, given the matrix B^2, we can compute the approximation for the divergence

$$((B^2)^T\mathbf{X})_1 = -\frac{1}{2\Delta x}h_1u_1 - \frac{1}{2\Delta x}h_1u_2 - 2\sqrt{3}\sigma_1$$

Given that $u_1 = \dfrac{2Q_{inc} - h_0u_0}{h_1}$ and that $h_0 = h_1$, we obtain that

$$((B^2)^T\mathbf{X})_1 = -h_1\frac{u_2 - u_0}{2\Delta x} - \frac{h_1Q_{inc}}{\Delta x} - 2\sqrt{3}\sigma_1,$$

which is a first order discretization of $-(h\partial_x u + 2\sqrt{3}\sigma)$ up to the error term $\tilde{0}_1 = \dfrac{h_1Q_{inc}}{\Delta x}$.

Remark 12. We note that in case the incoming flux has a vertical component as well Q_{vert} then one has to modify the boundary conditions associated to w and σ in order to take into account the divergence constraint. This means that, while one imposes the verical flux on hw, $h\sigma$ on the boundary has to verify the corresponding equation, yielding:

$$w_0 = \frac{2Q_{vert} - h_1w_1}{h_0}, \qquad \sigma_0 = \frac{2(Q_{vert} - Q_{inc}\cdot(\partial_x z_b)|_{i=1/2}) - \sqrt{3}h_1\sigma_1}{\sqrt{3}h_0}.$$

Outgoing flow with prescribed height: For the outgoing flow, we impose a Dirichlet type boundary condition for the fluid height:

$$h_{i=N+1/2} = H_{out} \quad \Longrightarrow \quad h_{N+1} = 2H_{out} - h_N.$$

Once again, the outgoing characteristic of the hyperbolic problem preserves the corresponding Riemann-invariant, so

$$u_N + 2\sqrt{gh_N} = u_{N+1} + 2\sqrt{gh_{N+1}}.$$

This means that the velocity on the right hand side phantom cell is given by

$$u_{N+1} = u_N + 2\sqrt{g}(\sqrt{2H_{out} - h_N} - \sqrt{h_N}).$$

For the vertical components of the velocity, we impose Neumann boundary condition, just as before, hence

$$(\partial_x w)_{i=N+1/2} = 0, \quad (\partial_x \sigma)_{i=N+1/2} = 0 \quad \Longrightarrow \quad w_{N+1} = w_N, \quad \sigma_{N+1} = \sigma_N.$$

Since we imposed a Neumann type boundary condition on the velocity u, we prescribe a Dirichlet type boundary condition on the pressure terms. However, we have to distinguish between the to discretizations when defining whether we impose Dirichlet type boundary condition on the conservative variable hq or the nonconservative variable q to ensure the compatibility for the transposed quantities.

1. In this case, we impose the Dirichlet type boundary condition on the nonconservative variable q:

   $$q_{i=N+1/2} = 0, \quad q_{b,i=N+1/2} = 0 \quad \Longrightarrow \quad q_{N+1} = -q_N, \quad q_{b,N+1} = -q_{b,N}.$$

   With the boundary conditions at our disposal, we can write the discretization of the momentum equation for the first cell:

   $$\frac{h_N u_N^{n+1} - h_N u_N^{n+1/2}}{\Delta t} + \frac{1}{2\Delta x}(h_{N+1/2}(q_N + q_{N+1}) - h_{N-1/2}(q_{N-1} + q_N)) + q_{b,N}(\partial_x z_b)_N = 0.$$

   Since $q_{N+1} = -q_N$, this means that

   $$(B^1\mathbf{Q})_N = -\frac{1}{2\Delta x} h_{N-1/2} q_{N-1} - \frac{1}{2\Delta x} h_{N-1/2} q_N + q_{b,N}(\partial_x z_b)_N,$$

   and that no correction is required, $\widehat{0}_N = 0$.

   So, given the matrix B^1, we can compute the approximation for the divergence

   $$\begin{aligned}((B^1)^T\mathbf{X})_N &= \frac{1}{2\Delta x} h_{N-1/2} u_{N-1} - \frac{1}{2\Delta x} h_{N-1/2} u_N - 2\sqrt{3}\sigma_N \\ &= \frac{1}{2\Delta x}\left(-h_{N-1/2}(u_N - u_{N-1})\right) - 2\sqrt{3}\sigma_N.\end{aligned}$$

Given that $u_N = u_{N+1} - 2\sqrt{g}(\sqrt{2H_{out} - h_N} - \sqrt{h_N})$, we obtain that

$$((B^1)^T\mathbf{X})_N = -\frac{1}{2}\left(h_{N+1/2}\frac{\frac{h_N}{h_{N+1}}u_{N+1} - u_N}{\Delta x} + h_{N-1/2}\frac{u_N - u_{N-1}}{\Delta x}\right) - 2\sqrt{3}\sigma_1 - \frac{1}{\Delta x}\sqrt{g}(\sqrt{2H_{out} - h_N} - \sqrt{h_N}),$$

which is a first order discretization of $-(h\partial_x u + 2\sqrt{3}\sigma)$. The corresponding correction term is given by $\tilde{0}_N = -\dfrac{\sqrt{g}(\sqrt{2H_{out} - h_N} - \sqrt{h_N})}{\Delta x}$.

2. In this case, we impose the Dirichlet type boundary condition on the conservative variable hq:

$$(hq)_{i=N+1/2} = 0, \quad q_{bi=N+1/2} = 0 \quad \Longrightarrow \quad q_{N+1} = -\frac{h_N}{h_{N+1}}q_N, \quad q_{bN+1} = q_{bN}.$$

With the boundary conditions at our disposal, we can write the discretization of the momentum equation for the first cell:

$$\frac{h_N u_N^{n+1} - h_N u_N^{n+1/2}}{\Delta t} + \frac{1}{2\Delta x}(h_{N+1}q_{N+1} - h_{N-1}q_{N-1}) + q_{bN}(\partial_x z_b)_N = 0.$$

Since $q_{N+1} = -\dfrac{h_N}{h_{N+1}}q_N$ this means that

$$(B^2\mathbf{Q})_N = -\frac{1}{2\Delta x}h_{N-1}q_{N-1} - \frac{1}{2\Delta x}h_N q_N + q_{bN}(\partial_x z_b)_N,$$

and that no correction is required, $\widehat{0}_N = 0$.

So, given the matrix B^2, we can compute the approximation for the divergence

$$((B^2)^T\mathbf{X})_N = \frac{1}{2\Delta x}h_N u_{N-1} - \frac{1}{2\Delta x}h_N u_N - 2\sqrt{3}\sigma_N$$

Given that $u_N = u_{N+1} - 2\sqrt{g}(\sqrt{2H_{out} - h_N} - \sqrt{h_N})$ we obtain that

$$((B^2)^T\mathbf{X})_N = -h_N\frac{u_{N+1} - u_{N-1}}{2\Delta x} + \frac{\sqrt{g}(\sqrt{2H_{out} - h_N} - \sqrt{h_N})}{\Delta x} - 2\sqrt{3}\sigma_1,$$

which is a first order discretization of $-(h\partial_x u + 2\sqrt{3}\sigma)$ up to the error term $\tilde{0}_N = -\dfrac{\sqrt{g}(\sqrt{2H - h_N} - \sqrt{h_N})}{\Delta x}$.

5.3 Numerical validation

The Serre–Green-Naghdi system admits analytic solutions for certain choices of bottom topography and atmospheric pressure. In what follows we present two particular solutions, that will be used for testing and validating the implemented numerical schemes.

5.3.1 Solitary wave solution

It is a well-known fact that the system admits solitary wave solutions in the case of constant atmospheric pressure and flat bottom topography.

Let us fix $p_{atm} \equiv cst$ and $z_b \equiv cst$. For a constant $c \in \mathbb{R}$, let us introduce the variable $\xi = x - ct$. For a solitary wave solution, we are looking for solutions of the form

$$\begin{aligned} h(t,x) = h_c(\xi), \quad u(t,x) = u_c(\xi), \quad w(t,x) = w_c(\xi), \quad \sigma(t,x) = \sigma_c(\xi), \\ q(t,x) = q_c(\xi), \quad q_b(t,x) = q_{bc}(\xi). \end{aligned} \tag{5.20}$$

with lake-at-rest limits

$$\begin{aligned} &\lim_{\xi\to\pm\infty} h_c(\xi) = H_0, \quad \lim_{\xi\to\pm\infty} u_c(\xi) = 0, \quad \lim_{\xi\to\pm\infty} w_c(\xi) = 0, \quad \lim_{\xi\to\pm\infty} \sigma_c(\xi) = 0, \\ &\lim_{\xi\to\pm\infty} q_c(\xi) = 0, \quad \lim_{\xi\to\pm\infty} q_{bc}(\xi) = 0. \end{aligned}$$

Here $H_0 > 0$ is a positive constant (base fluid depth).

Substituting the profiles (5.20) into equations (5.1) and integrating with respect to ξ, one is able to express the other variables with the function h_c, yielding

$$\begin{aligned} u_c = c\left(1 - \frac{H_0}{h_c}\right), \quad w_c = -\frac{cH_0}{2}\frac{(h_c)'}{h_c}, \quad \sigma_c = -\frac{cH_0}{2\sqrt{3}}\frac{(h_c)'}{h_c}, \\ q_c = \frac{c^2H_0^2}{3h_c^2}\left[h_c(h_c)'' - ((h_c)')^2\right], \quad q_{bc} = \frac{c^2H_0^2}{2h_c^2}\left[h_c(h_c)'' - ((h_c)')^2\right]. \end{aligned}$$

Here, the prime $'$ denotes the derivative with respect to ξ.

Furthermore, h_c verifies the following second order ordinary differential equation

$$\frac{1}{3}c^2H_0^2\left[h_c(h_c)'' - ((h_c)')^2\right] + \frac{1}{2}gh_c^3 - \frac{1}{2}H_0\left(gH_0 + 2c^2\right)h_c + c^2H_0^2 = 0. \tag{5.21}$$

This equation can be solved by the sech or the tanh methods. For an amplitude parameter $a > 0$, we have that

$$h_c(\xi) = H_0 + a\,\mathrm{sech}^2\left(\frac{\sqrt{3a}}{2H_0\sqrt{H_0+a}}\xi\right), \tag{5.22}$$

and the propagation speed of the solitary wave is given by $c = \sqrt{g(H_0+a)}$.
Gathering the quantities calculated above, the exact solitary waves for the one-dimensional

Serre-Green-Naghdi equations (5.1) can be written as follows,

$$
\begin{cases}
h_c(t,x) = H_0 + a\,\mathrm{sech}^2\left(\dfrac{\sqrt{3a}}{2H_0\sqrt{H_0+a}}(x-ct)\right),\\
u_c(t,x) = c\,(1 - H_0/h_c(t,x)),\\
w_c(t,x) = -\dfrac{cH_0}{2}\dfrac{(h_c(t,x))'}{h_c(t,x)},\\
\sigma_c(t,x) = -\dfrac{cH_0}{2\sqrt{3}}\dfrac{(h_c(t,x))'}{h_c(t,x)},\\
q_c(t,x) = \dfrac{c^2H_0^2}{3h_c(t,x)^2}\left[h_c(t,x)(h_c(t,x))'' - ((h_c(t,x))')^2\right],\\
q_{bc}(t,x) = \dfrac{c^2H_0^2}{2h_c(t,x)^2}\left[h_c(t,x)(h_c(t,x))'' - ((h_c(t,x))')^2\right],\\
c = \sqrt{g(H_0+a)}.
\end{cases}
\tag{5.23a}
$$

For this test case, we consider the propagation of a solitary wave from left to right, initially centered at $x_0 = 10m$, of relative amplitude $a = 0.2m$, over a constant water depth $H_0 = 1m$. The computational domain is $100m$ on length and discretized with 1280 cells. Since the solitary wave is initially far from boundaries, the boundary conditions do not affect the computation, so we have chosen to impose free boundary conditions at the downstream and upstream ends for the sake of simplicity. We compare the water surface profile of our numerical solutions provided by the model (5.1), with the exact profile given by (5.23) at several times using two iterative methods, namely Uzawa and Gauss-Seidel, and a direct method (see Fig. 5.2).

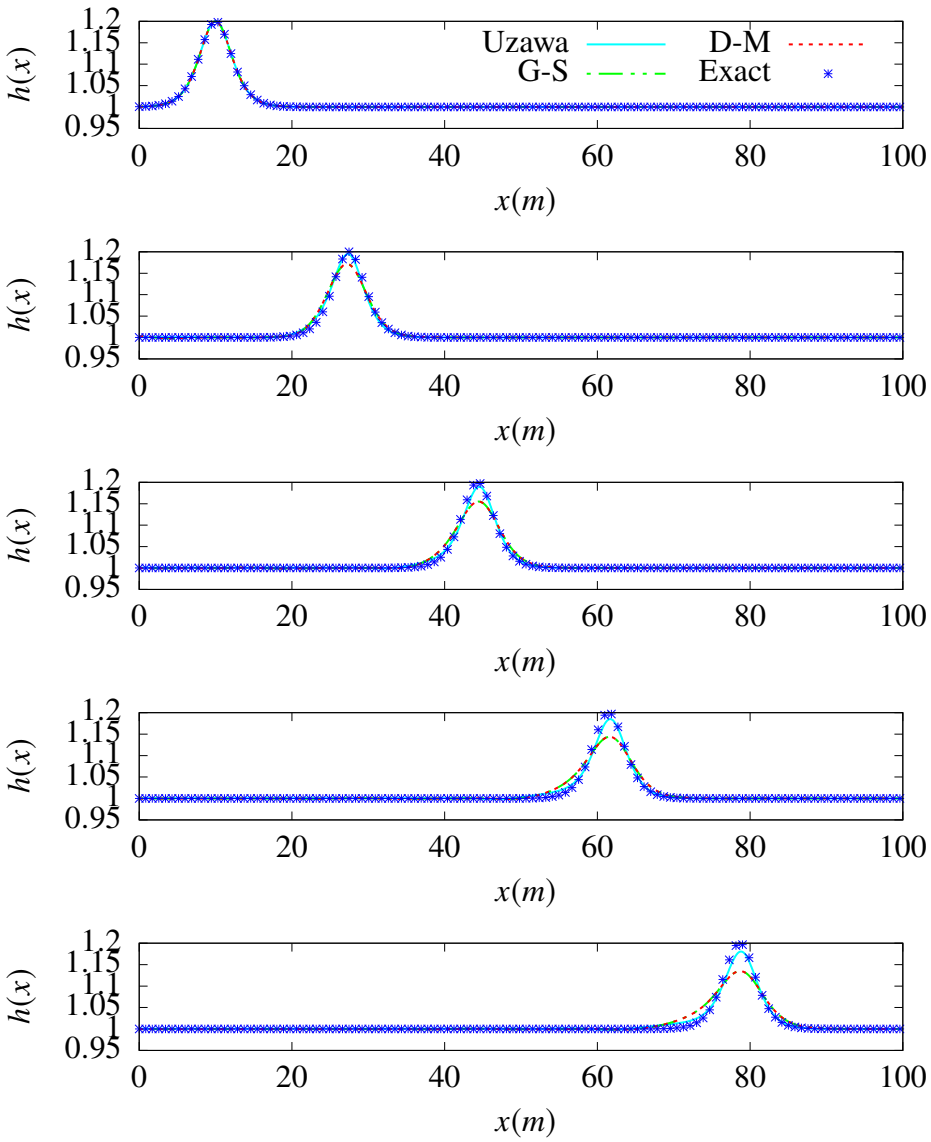

Figure 5.2: Propagation of solitary wave over a flat bottom: water surface profiles at t=5, 10, 15 and 20s. Comparison of the numerical and exact solutions for the Uzawa, Gauss-Seidel and a direct method

	Uzawa algorithm		Gauss-Seidel approach		Direct solver	
N	$E_{L^2}(h)$	$E_{L^2}(u)$	$E_{L^2}(h)$	$E_{L^2}(u)$	$E_{L^2}(h)$	$E_{L^2}(u)$
80	1.2×10^{-2}	4.3×10^{-1}	2.19×10^{-2}	1.34×10^{-1}	2.19×10^{-2}	1.34×10^{-1}
160	8.4×10^{-3}	2.8×10^{-1}	1.7×10^{-2}	1.4×10^{-1}	1.7×10^{-2}	1.4×10^{-1}
320	5.4×10^{-3}	1.8×10^{-1}	1.2×10^{-2}	1.94×10^{-1}	1.2×10^{-2}	1.94×10^{-1}
640	3.4×10^{-3}	1.1×10^{-1}	7.78×10^{-3}	1.54×10^{-1}	7.78×10^{-3}	1.54×10^{-1}
1280	2.1×10^{-3}	6.9×10^{-2}	4.73×10^{-3}	1.58×10^{-1}	4.73×10^{-3}	1.58×10^{-1}

Table 5.1: Relative L^2-error table for the variables h and u and and time execution

The table 5.1 shows the time execution and the relative error between the numerical

solutions of the model (5.1) and the exact one given in (5.23) given by the following relation:

$$E_{L^2}(h) = \frac{\|h_{num} - h_{ex}\|_2}{\|h_{ex}\|_2} \qquad E_{L^2}(u) = \frac{\|u_{num} - u_{ex}\|_2}{\|u_{ex}\|_2}$$

where (h_{num}, u_{num}) are numerical solutions of the $1D$ SGN equations (5.1), (h_{ex}, u_{ex}) are solutions of the system (5.23) and $\|\cdot\|_2$ is the standard discret L_2 norm. To obtain these results, we set a time $T = 5s$ and calculate the numerical solution by increasing the number of cells from $N = 80$ to $N = 1280$.

Remark 13. Note that the Gauss-Seidel method and the direct method were implemented using python, whereas the Uzawa method was implemented using Fortran 95. This may explain the delay in calculation times (CPU) between these 3 methods.

5.3.2 Stationary solution

The Serre–Green-Naghdi system (5.1) admits analytic steady (time independent) solutions as well. A straightforward computation yields that for a constant inflow flux of $Q \in \mathbb{R}^*$, any $h(x)$, $z_b(x)$ and $p_{atm}(x)$ functions satisfying the differential equality:

$$\partial_x p_{atm} = -g\partial_x(h + z_b) + \frac{Q^2}{h}\left[\frac{\partial_x h}{h^2} - \frac{1}{2}\partial_x\left(h\partial_x\left(\frac{1}{h}\partial_x\left(\frac{2h}{3} + z_b\right)\right)\right)\right.$$
$$\left. - \partial_x z_b \partial_x\left(\frac{1}{h}\partial_x\left(\frac{h}{2} + z_b\right)\right)\right)$$

leads to a stationary solutions profile. For such h and z_b, one has

$$u = \frac{Q}{h}, \quad w = \frac{Q}{h}\partial_x\left(\frac{h}{2} + z_b\right), \quad \sigma = \frac{Q}{2\sqrt{3}h}\partial_x h,$$
$$q = \frac{Q^2}{2}\partial_x\left(\frac{1}{h}\partial_x\left(\frac{2h}{3} + z_b\right)\right), \quad q_b = Q^2\partial_x\left(\frac{1}{h}\partial_x\left(\frac{h}{2} + z_b\right)\right).$$

More specifically, let us take an interval $[a, b]$ with $a, b \in \mathbb{R}$. Moreover, let

$$h(x) = H_0 e^{P(x)}, \quad \text{and} \quad z_b(x) = K - h(x)$$

with H_0 and K real constants, and $P(x)$ a polinom to be chosen according to the boundary conditions.

In this case, we have that

$$u = \frac{Q}{H_0}e^{-P(x)}, \quad w = -\frac{Q}{2}P'(x), \quad \sigma = \frac{Q}{2\sqrt{3}}P'(x), \quad q = -\frac{Q^2}{6}P''(x),$$
$$q_b = -\frac{Q^2}{2}P''(x), \quad p_{atm} = -Q^2\left(\frac{1}{2H_0^2}e^{-2P(x)} - \frac{1}{6}(P''(x) - (P'(x))^2)\right).$$

In the case a fluvial flow, if we impose that a debit Q enters the domain at a and the fluid height is given by h_R at b, with the boundary conditions $\partial_x z_b|_{x=a} = \partial_x z_b|_{x=b} = 0$, $\partial_x(hq)|_{x=a} = 0$, $hq(b) = 0$, we can prescribe the polinom $P(x)$ as

$$P(x) = 8\left(\frac{x-a}{b-a}\right)^5 - 15\left(\frac{x-a}{b-a}\right)^4 + 10\left(\frac{x-a}{b-a}\right)^2 + \alpha$$

with an α constant given by the boundary condition on the height at b:

$$\alpha = \ln\left(\frac{h_R}{H_0}\right) - 3.$$

5.3.3 Dam-break

We next consider the dam-break problem in order to study the ability of our numerical scheme to capture dispersive shocks. It is well-known that discontinuous initial data of this type generate dispersive shock waves due to dispersive effects [14]. This dispersive shock waves problem for non-linear and dispersive shallow water equations was also carried out in [14, 24, 63]. We consider the following initial data :

$$\eta(0,x) = \begin{cases} 1.8 & \text{if} \quad x \leq 0 \\ 1 & \text{else} \end{cases} \tag{5.24a}$$

$$u(0,x) = w(0,x) = \sigma(0,x) = 0 \tag{5.24b}$$

The computation domain is the interval $(-300, 300)$ and discretized with 8000 cells.

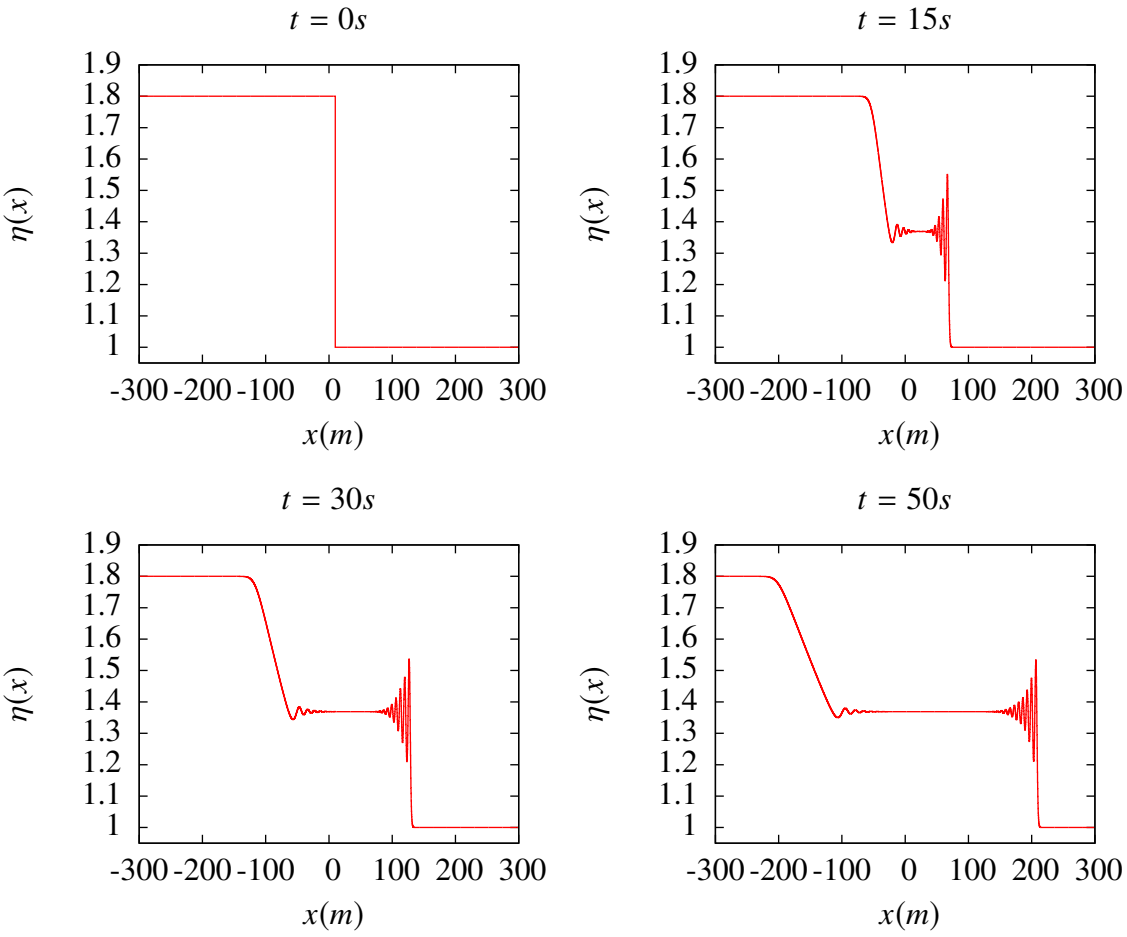

Figure 5.3: Dam-break: water surface at several times

The figure 5.3 shows the dispersive effects generated by the model (5.1) when using discontinuous initial data. Here, we chose 8000 cells because it is shown in [16, 63] that the dispersive effect cannot be captured if we use a first order numerical scheme, and to properly capture the dispersive shock waves, we had to use high-order numerical schemes, and that is out of our objective in this manuscript.

5.3.4 Favre waves

In the following section, we compare our numerical scheme based on the Uzawa algorithm with experimental data. A good example of a physical situation in which the non-hydrostatic pressure terms pay a significant role is the so called Favre wave experiment. Favre waves are secondary free surface waves, undular bores that appear typically in a channel following a sudden change in the flow discharge.

One such situation arises in the case when a sluice gate is suddenly closed, realised during the physical experiments carried out at EDF (Electricité de France) [23]. A long and thin wave tank is considered with a small constant slope and open uphill entry and downhill exit as well as vertical walls (see Figure 5.4). A stationary water flow is generated in the basin up until a time t_0 at which point a gate rapidly descends at the exit level, blocking the flow and generating and upstream moving series of undulating waves.

In the experiments, a wave tank of length $40m$ was taken, of which the lower $30m$ section plays a significant role. The tank is of width $0.4m$, the walls on the side are vertical and the bottom is of a constant slope of

$$\partial_x z_b = -0.0004.$$

At the lower end of the basin, a vertical solid gate is placed perpendicular above the water flow. Additionally, three sensors were also placed over the basin, each one measuring the water height at its horizontal position. The first sensor is situated $2m$ from the exit of the tank, the second sensor is $15m$ from the lower end, and finally the third sensor is at a distance of $30m$ from the gate (see Figure 5.5).

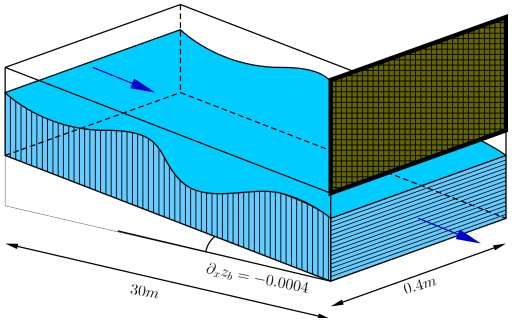

Figure 5.4: The wave tank of the experiment

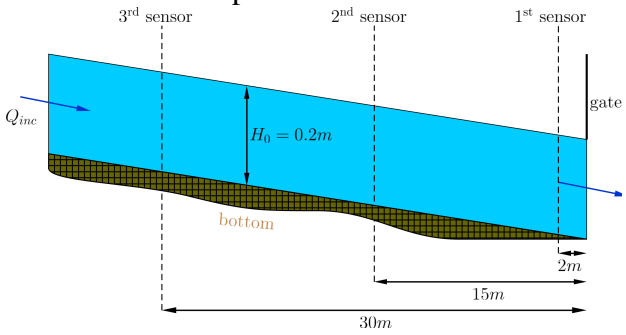

Figure 5.5: A cross section of the wave tank

Figure 5.6: Schematic representation of the Favre wave experiment

In the experiment chosen for validation, a stationary gravity flow is generated in the tank by a constant inflow (and outflow) volumic flux of

$$Q_{in} = 0.0351 \frac{1}{s}.$$

The associated stationary water height is observed to be approximately $0.2m$.

As it was mentioned before, the gate is closed at time t_0 (when the flow has attained a stationary regime with the above give physical parameters). The closure takes place rapidly, in a time frame of $T = 0.07s$, at which point the gate completely blocks the exit, forming a solid wall boundary for the gravity flow. Measurements on the water height are available in the timeframe of $[t_0 + 1.31, t_0 + 5.35]$ for the first sensor, in the timeframe of $[t_0 + 10, t_0 + 16.9]$ for the second sensor, as well as in the timeframe of $[t_0 + 21, t_0 + 28.92]$ for the third sensor.

In the context of an extended Saint-Venant system, in which non-hydrostatic pressure terms complement the classical shallow water equations, first and second order finite volume solvers have already been developed and validated against this particular experimental case [19].

In our case, the simulations were implemented for a one horizontal dimensional problem corresponding to the experiments (see Figure 5.5). The implemented physical parameters were the same, except for the the flux, which had to be recomputed for its one dimensional equivalent:

$$Q_{inc} = \frac{1}{0.4} Q_{in} = 0.08775 \frac{1}{s}.$$

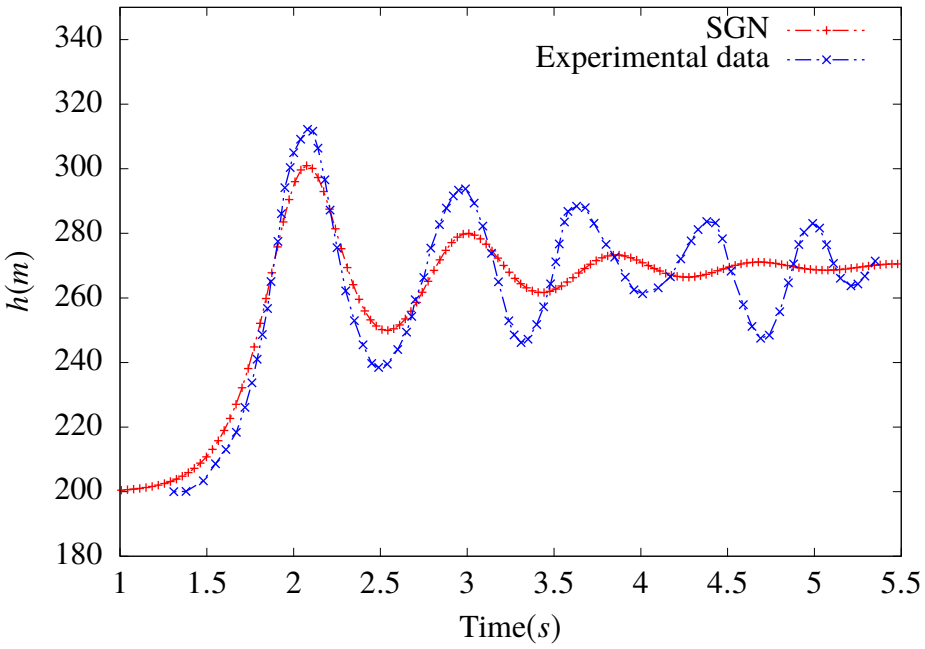

Figure 5.7: Comparison between the numerical solution and the experimental data for sensor1. $N = 3000$

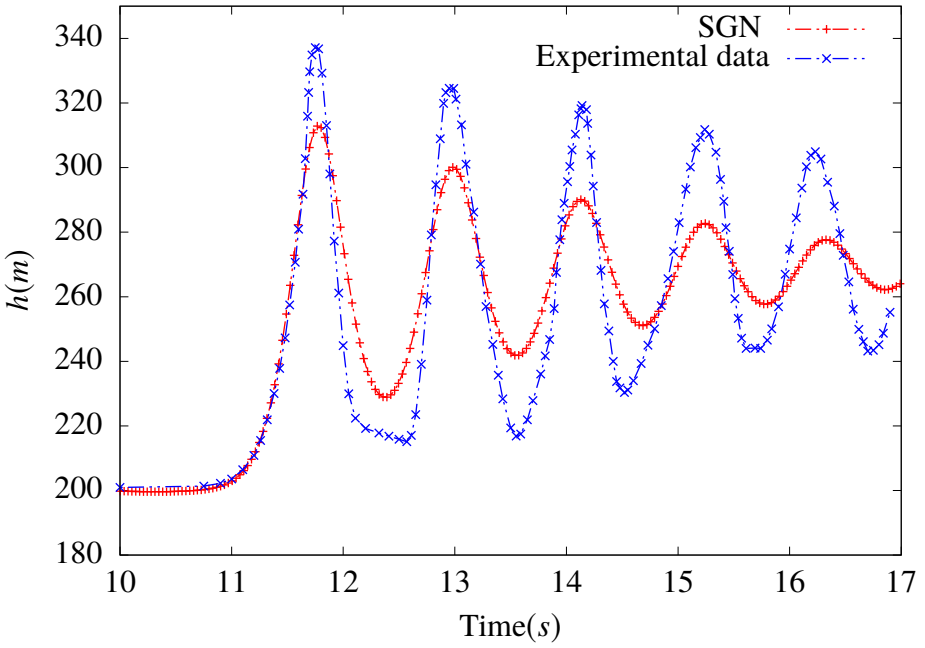

Figure 5.8: Comparison between the numerical solution and the experimental data for sensor2. $N = 3000$

5.4 The two dimensional Serre–Green-Naghdi system

Here we are interested in the two dimensional extension of the aforementioned system (5.1). For this, we are now considering the horizontal plane $(x, y) \in \mathbb{R}^2$ as the domain of our functions. Moreover, in addition to the horizontal velocity u in the x-direction, we have to add a new variable v which describes the (vertically averaged) horizontal velocity in the y-direction.

The system writes as

$$\partial_t h + \partial_x(hu) + \partial_y(hv) = 0, \tag{5.25a}$$
$$\partial_t(hu) + \partial_x(hu^2) + \partial_y(huv) + \partial_x(hq) + q_b\partial_x z_b = -gh\partial_x(h + z_b) - h\partial_x p_{atm}, \tag{5.25b}$$
$$\partial_t(hv) + \partial_x(huv) + \partial_y(hv^2) + \partial_y(hq) + q_b\partial_y z_b = -gh\partial_y(h + z_b) - h\partial_y p_{atm}, \tag{5.25c}$$
$$\partial_t(hw) + \partial_x(huw) + \partial_y(hvw) - q_b = 0, \tag{5.25d}$$
$$\partial_t(h\sigma) + \partial_x(hu\sigma) + \partial_y(hv\sigma) - 2\sqrt{3}\left(q - \frac{q_b}{2}\right) = 0, \tag{5.25e}$$
$$w - u\partial_x z_b - v\partial_y z_b - \sqrt{3}\sigma = 0, \tag{5.25f}$$
$$2\sqrt{3}\sigma + h(\partial_x u + \partial_y v) = 0, \tag{5.25g}$$

or, with the classical two-dimensional gradient $\nabla = \nabla_{x,y}$ and divergence $\nabla\cdot = \nabla_{x,y}\cdot$ operators, as well as the two dimensional horizontal velocity $U = (u, v)^T$, we have that

$$\partial_t h + \nabla \cdot (hU) = 0, \tag{5.26a}$$
$$\partial_t(hU) + \nabla \cdot (hU \otimes U) + \nabla(hq) + q_b\nabla z_b = -gh\nabla(h + z_b) - h\nabla p_{atm}, \tag{5.26b}$$
$$\partial_t(hw) + \nabla \cdot (hwU) - q_b = 0, \tag{5.26c}$$
$$\partial_t(h\sigma) + \nabla \cdot (h\sigma U) - 2\sqrt{3}\left(q - \frac{q_b}{2}\right) = 0, \tag{5.26d}$$
$$w - U \cdot \nabla z_b - \sqrt{3}\sigma = 0, \tag{5.26e}$$
$$2\sqrt{3}\sigma + h\nabla \cdot U = 0. \tag{5.26f}$$

5.4.1 Reformulations of the system

Remark 14. System (5.25) can be rewritten under the Boussinesq formulation, in a more compact form:

$$\partial_t h + \nabla \cdot (hU) = 0, \tag{5.27a}$$
$$(1 + \mathcal{T}[h, z_b])(\partial_t U + (U \cdot \nabla)U) + g\nabla(h + z_b) + \mathcal{Q}[h, z_b]U = 0, \tag{5.27b}$$

where we have that

$$\mathcal{T}[h, z_b]V = \mathcal{R}_1[h, z_b](\nabla \cdot V) + \mathcal{R}_2[h, z_b](\nabla z_b \cdot V),$$
$$\mathcal{Q}[h, z_b]U = -2\mathcal{R}_1[h, z_b]\left(\partial_x U \cdot \partial_y U^\perp + (\nabla \cdot U)^2\right) + \mathcal{R}_2[h, z_b]\left(U \cdot (U \cdot \nabla)\nabla z_b\right),$$
$$\mathcal{R}_1[h, z_b]f = -\frac{1}{3h}\nabla(h^3 f) - \frac{h}{2}f\nabla z_b,$$
$$\mathcal{R}_2[h, z_b]g = \frac{1}{2h}\nabla(h^2 g) + g\nabla z_b.$$

Here we made use of the notation $U^\perp = (-v, u)^T$.

Additionally, with the help of the vectors $\mathbf{X} = (u, v, w, \sigma)^T$ and $\mathbf{Q} = (q, q_b)^T$, one can define the two-dimensional extensions of the dispersive divergence and gradient operators, that is

$$\nabla_{SGN}\mathbf{Q} = \begin{pmatrix} \partial_x(hq) + q_b\partial_x z_b \\ \partial_y(hq) + q_b\partial_y z_b \\ -q_b \\ -2\sqrt{3}q + \sqrt{3}q_b \end{pmatrix}, \quad \text{and} \quad \nabla_{SGN}\cdot\mathbf{X} = \begin{pmatrix} 2\sqrt{3}\sigma + h(\partial_x u + \partial_y v) \\ w - u\partial_x z_b - v\partial_y z_b - \sqrt{3}\sigma \end{pmatrix}. \tag{5.28}$$

With the source term vector

$$S(h, z_b) = \left(-gh\partial_x(h + z_b) - h\partial_x p_{atm}, -gh\partial_y(h + z_b) - h\partial_y p_{atm}, 0, 0\right)^T,$$

we have that the system (5.25) writes as

$$\partial_t h + \nabla\cdot(hU) = 0, \tag{5.29a}$$
$$\partial_t(h\mathbf{X}) + \partial_x(hu\mathbf{X}) + \partial_y(hv\mathbf{X}) + \nabla_{SGN}\mathbf{Q} = S(h, z_b), \tag{5.29b}$$
$$\nabla_{SGN}\cdot\mathbf{X} = 0. \tag{5.29c}$$

Lemma 5.4.1. *The dispersive divergence and gradient operators defined by (5.28) verify the partial integration type formula:*

$$\mathbf{Q}\cdot(\nabla_{SGN}\cdot\mathbf{X}) + \mathbf{X}\cdot(\nabla_{SGN}\mathbf{Q}) = \nabla\cdot(hqU). \tag{5.30}$$

Proof 3. A straightforward computation calculating the scalar products, using the definition (5.28), leads to the desired result.

The system (5.25) also admits a pressure based reformulation.

Proposition 5.4.2. *Equations (5.25) can be rewritten as*

$$-12\frac{q}{h} + h\nabla\cdot\left(\frac{1}{h}\nabla(hq)\right) + 6\frac{q_b}{h} + h\nabla\cdot\left(\frac{q_b}{h}\nabla z_b\right) \tag{5.31a}$$
$$= -h\Delta(g(h + z_b) + p_{atm}) - 2h(\partial_x U\cdot\partial_y U^{\perp} + (\nabla\cdot U)^2),$$
$$-6\frac{q}{h} + \frac{1}{h}\nabla z_b\cdot\nabla(hq) + (4 + |\nabla z_b|^2)\frac{q_b}{h} = (U\cdot\nabla)^2 z_b - \nabla z_b\cdot\nabla(g(h + z_b) + p_{atm}). \tag{5.31b}$$

Proof 4. One differentiates with respect to time the equations (5.25f)-(5.25g) (corresponding to $\nabla_{SGN}\cdot\mathbf{X} = 0$). After that, one substitutes the quantities $\partial_t u$, $\partial_t v$, $\partial_t w$ and $\partial_t\sigma$ with their values given by the non-conservative reformulation of equations (5.25b)-(5.25e). Regrouping the terms containing q and q_b on the left hand side and the terms with u, v, p_{atm}, h and z_b on the right hand side yields the result.

5.4.2 Energy

The two dimensional Serre–Green-Naghdi equations (5.25), much like their one-dimensional counterpart (5.1) admit an energy balance identity.

Proposition 5.4.3. *Smooth solutions of the system (5.25) satisfy the following identity:*

$$\partial_t \left[h \left(\frac{1}{2}|\mathbf{X}|^2 + g\left(\frac{1}{2}h + z_b\right) + p_{atm} \right) \right] + \nabla \cdot \left[h \left(\frac{1}{2}|\mathbf{X}|^2 + g\left(h + z_b\right) + p_{atm} + q \right) U \right] = 0. \tag{5.32}$$

Proof 5. Let us multiply (5.25b) by u, (5.25c) by v, (5.25d) by w and (5.25e) by σ and sum the results. This leads to

$$\partial_t \left(\frac{1}{2}h|\mathbf{X}|^2 \right) + \nabla \cdot \left(\frac{1}{2}h|\mathbf{X}|^2 U \right) + \frac{1}{2}|\mathbf{X}|^2(\partial_t h + \nabla \cdot (hU)) + \nabla_{SGN}\mathbf{Q} \cdot \mathbf{X} + hU \cdot \nabla(g(h + z_b) + p_{atm}) = 0.$$

By making use of equation (5.25a), the third term is 0, and one may add the following to the equality:

$$(\partial_t h + \nabla \cdot (hU))(g(h + z_b) + p_{atm}) = 0.$$

Furthermore, using the identity (5.30), we have that

$$\mathbf{X} \cdot (\nabla_{SGN}\mathbf{Q}) = \nabla \cdot (hqU) - \mathbf{Q} \cdot (\nabla_{SGN} \cdot \mathbf{X}) = \nabla \cdot (hqU)$$

since $\mathbf{X}$ verifies equations (5.25f)-(5.25g). Putting all this together, one obtains the desired energy identity.

5.4.3 Variational formulation

One can associate a variational problem to the pressure formulation of the system (5.31). Let us take a control volume Ω, bounded, open, regular with regular boundaries.

We define the following operators:

$$\begin{aligned}
\mathcal{A}(\varphi, \tilde{\varphi}) &= \int_\Omega \frac{1}{h}\nabla(h\varphi) \cdot \nabla(h\tilde{\varphi}) + \frac{12}{h}\varphi\tilde{\varphi}\, dx\, dy, && \varphi, \tilde{\varphi} \in H^1(\Omega) \\
\mathcal{A}_b(\psi, \tilde{\psi}) &= \int_\Omega \frac{1}{h}\left(4 + |\nabla z_b|^2\right)\psi\tilde{\psi}\, dx\, dy, && \psi, \tilde{\psi} \in L^2(\Omega) \\
\mathcal{B}(\varphi, \psi) &= \int_\Omega \frac{\psi}{h}\nabla(h\varphi) \cdot \nabla z_b - \frac{6}{h}\varphi\psi\, dx\, dy, && \varphi \in H^1(\Omega), \psi \in L^2(\Omega).
\end{aligned}$$

By multiplying the first equation of (5.31) with a test function φ such that $h\varphi \in H^1(\Omega)$ and the second equation with $\psi \in L^2(\Omega)$, we obtain the following system:

$$\begin{aligned}
\mathcal{A}(q, \varphi) + \mathcal{B}(\varphi, q_b) =& \langle \varphi, -h\Delta(g(h + z_b) + p_{atm}) - 2h(\partial_x U \cdot \partial_y U^\perp + (\nabla \cdot U)^2)\rangle_{L^2(\Omega)} \\
&+ C(\varphi, q, q_b), \\
\mathcal{A}_b(q_b, \psi) + \mathcal{B}(hq, \psi) =& \langle \psi, (U \cdot \nabla)^2 z_b - \nabla z_b \cdot \nabla(g(h + z_b) + p_{atm})\rangle_{L^2(\Omega)}.
\end{aligned} \tag{5.33}$$

Here the boundary term C appears due to the integrations by part, it is given by

$$C(\bar{\varphi}, \varphi_1, \psi_1) = \int_{\partial\Omega} \bar{\varphi}\nabla(h\varphi_1) \cdot \mathbf{n}\, ds + \int_{\partial\Omega} \bar{\varphi}\psi_1 \nabla z_b \cdot \mathbf{n}\, ds.$$

We remark that by choosing the test function φ compactly supported in Ω, the boundary terms disappear automatically.

For what follows, let us suppose that the fluid height is bounded from below and from above: that is,

$$\exists H_{min}, H_{max} \in \mathbb{R}^+, \forall (x,t) \in \Omega \times \mathbb{R}^+ H_{min} < h(t,x) < H_{max}. \tag{H}$$

Proposition 5.4.4. *Let us suppose (H) as well as $z_b \in C^1(\Omega)$ and $h \in H^2(\Omega)$. For $s > 1$ real, we have that operators $\mathcal{A}$ over $H^s(\Omega)^2$, $\mathcal{A}_b$ over $L^2(\Omega)^2$ and $\mathcal{B}$ over $H^s(\Omega) \times L^2(\Omega)$ are continuous bilinear forms.*

Proof 6. We check the definition of continuity for each bilinear form.

$$\begin{aligned}
|\mathcal{A}(\varphi_1, \varphi_2)| &\leq \frac{1}{H_{min}} \|\nabla(h\varphi_1)\|_{L^2(\Omega)} \|\nabla(h\varphi_2)\|_{L^2(\Omega)} + \frac{12}{H_{min}} \|\varphi_1\|_{L^2(\Omega)} \|\varphi_2\|_{L^2(\Omega)} \\
&\leq \frac{12}{H_{min}} \max(1, \|h\|_{H^s(\Omega)}) \|\varphi_1\|_{H^s(\Omega)} \|\varphi_2\|_{H^s(\Omega)},
\end{aligned}$$

using the Sobolev embeddings $H^s(\Omega) \hookrightarrow H^1(\Omega)$ and $H^s(\Omega) \hookrightarrow L^\infty(\Omega)$ for $s > 1$ and for $\Omega \subset \mathbb{R}^2$ compact Lipschitz domain, as well as the product estimate:

$$\|h\varphi\|_{H^s(\Omega)} \leq \|h\|_{L^\infty(\Omega)} \|\varphi\|_{H^s(\Omega)} + \|h\|_{L^\infty(\Omega)} \|\varphi\|_{H^s(\Omega)}.$$

Similarly,

$$|\mathcal{A}_b(\psi_1, \psi_2)| \leq \frac{4 + \|z_b\|^2_{C^1(\Omega)}}{H_{min}} \|\psi_1\|_{L^2(\Omega)} \|\psi_2\|_{L^2(\Omega)}.$$

And finally

$$\begin{aligned}
|\mathcal{B}(\varphi_1, \psi_1)| &\leq \frac{\|z_b\|_{C^1(\Omega)}}{H_{min}} \|\nabla(h\varphi_1)\|_{L^2(\Omega)} \|\psi_1\|_{L^2(\Omega)} + \frac{6}{H_{min}} \|\varphi_1\|_{L^2\Omega} \|\psi_1\|_{L^2\Omega} \\
&\leq \frac{1}{H_{min}} \left(\|h\|_{H^s(\Omega)} \|z_b\|_{C^1(\Omega)} + 6 \right) \|\varphi_1\|_{H^s\Omega} \|\psi_1\|_{L^2\Omega}.
\end{aligned}$$

Definition 5.4.5. *For $h \in H^1(\Omega)$, let us define the following function space*

$$\mathcal{H}^1_h(\Omega) := \{ f \in H^1(\Omega), \|f\|_h < \infty \},$$

where the definition of the h-norm is as follows:

$$\|f\|^2_h = \|f\|^2_{L^2(\Omega)} + \|\nabla(hf)\|^2_{L^2(\Omega)}.$$

By the aforementioned Sobolev embeddings and product estimates, as well as elementary properties of the L^2-norm, one can easily ascertain that

Lemma 5.4.6. *The h-norm is indeed a norm, the space $\mathcal{H}^1_h(\Omega)$ is a Hilbert space, equipped with the scalar product*

$$\langle f, g \rangle_h = \langle f, g \rangle_{L^2(\Omega)} + \langle \nabla(hf), \nabla(hg) \rangle_{L^2(\Omega)}.$$

Furthermore, for $s > 1$ $H^s(\Omega) \hookrightarrow \mathcal{H}^1_h(\Omega)$.

Remark 15. One can easily see that operators $\mathcal{A}$ and $\mathcal{B}$ are also continuous over $(\mathcal{H}_h^1(\Omega))^2$ and $\mathcal{H}_h^1(\Omega) \times L^2(\Omega)$ respectively.

Let us define the bilinear form $\mathbf{A}$ on $H^s(\Omega) \times L^2(\Omega)$ as follows:

$$\mathbf{A}((\varphi_1, \psi_1), (\varphi_2, \psi_2)) = \mathcal{A}(\varphi_1, \varphi_2) + \mathcal{B}(\varphi_2, \psi_1) - \mathcal{B}(\varphi_1, \psi_2) + \mathcal{A}_b(\psi_1, \psi_2)$$

Proposition 5.4.7. *Under hypothesis (H) as well as for $z_b \in C^1(\Omega)$, we have that the operator $\mathbf{A}$ is coercive over $\mathcal{H}_h^1(\Omega) \times L^2(\Omega)$.*

Proof 7. We want to verify the definition of coercivity. For $\epsilon > 0$ we have that

$$2\psi \nabla(h\varphi) \cdot \nabla z_b = \left(\epsilon \nabla(h\varphi) + \frac{\psi \nabla z_b}{\epsilon}\right)^2 - \epsilon^2 (\nabla(h\varphi))^2 - \frac{(\nabla z_b)^2 \psi^2}{\epsilon^2}.$$

Therefore, we have that

$$\begin{aligned}
\mathbf{A}((\varphi, \psi), (\varphi, \psi)) &= \int_\Omega \frac{1}{h} \left[(\nabla(h\varphi))^2 + 2\psi \nabla(h\varphi) \cdot \nabla z_b + (\nabla z_b)^2 \psi^2 + 12\varphi^2 - 12\varphi\psi + 4\psi^2\right] dx\, dy \\
&= \int_\Omega \frac{1}{h} \left[(1 - \epsilon^2)(\nabla(h\varphi))^2 + \left(\epsilon \nabla(h\varphi) + \frac{\psi \nabla z_b}{\epsilon}\right)^2\right] dx\, dy \\
&\quad + \int_\Omega \frac{1}{h} \left[12\varphi^2 - 12\varphi\psi + \left(\left(1 - \frac{1}{\epsilon^2}\right)(\nabla z_b)^2 + 4\right)\psi^2\right] dx\, dy.
\end{aligned}$$

Let us denote by β^2 the factor of ψ^2, that is

$$\beta^2 := \left(1 - \frac{1}{\epsilon^2}\right)(\nabla z_b)^2 + 4.$$

To ensure the positivity of all the necessary terms, we impose that ϵ verifies the following inequalities:

$$1 > \epsilon^2 > 1 - \frac{1}{1 + \sup_\Omega \|\nabla z_b\|^2}; \tag{5.34}$$

such ϵ exists due to our hypothesis on the regularity of z_b. These inequalities on ϵ ensure that

$$1 - \epsilon^2 > 0, \qquad \beta^2 > 3.$$

Since

$$-12\varphi\psi = \left(\frac{6}{\beta}\varphi + \beta\psi\right)^2 - \frac{36}{\beta^2}\varphi^2 - \beta^2\psi^2,$$

we obtain that

$$\begin{aligned}
\mathbf{A}((\varphi, \psi), (\varphi, \psi)) &= \int_\Omega \frac{1}{h} \left[(1 - \epsilon^2)(\nabla(h\varphi))^2 + \left(\epsilon \nabla(h\varphi) + \frac{\psi \nabla z_b}{\epsilon}\right)^2\right] dx\, dy \\
&\quad + \int_\Omega \frac{1}{h} \left[\left(12 - \frac{36}{\beta^2}\right)\varphi^2 + \left(\frac{6}{\beta}\varphi - \beta\psi\right)^2\right] dx\, dy.
\end{aligned}$$

Hence we can establish a lower estimate on the bilinear form using the $\mathcal{H}_h^1(\Omega)$ norm of φ. By choosing a slightly smaller β, we can guarantee that a term with ψ^2 stays in the integral as well, therefore we have the desired lower bound.

5.5 Conclusion

The non-hydrostatic formulation of the well-known Serre – Green-Naghdi equations is investigated in this chapter. Unlike the Boussinesq formulation, only first order derivatives are involved. The consequence is a larger number of unknowns. The physical content of this model is richer than the shallow water equations but the computational cost is higher: at each time step, in addition to the resolution of a shallow water system, an elliptic equation must be solved involving non-standard operators.
Before investigating the 2D case, we designed some numerical schemes in 1D. They provide reliable results whether it be for analytical solutions or experimental solutions.

Bibliography

[1] N. Aïssiouene, M.-O. Bristeau, E. Godlewski, and J. Sainte-Marie. A combined finite volume - finite element scheme for a dispersive shallow water system. *Networks and Heterogeneous Media*, 11(1):1–27, 2016.

[2] N. Aïssiouene, M.-O. Bristeau, E. Godlewski, and J. Sainte-Marie. A robust and stable numerical scheme for a depth-averaged Euler system. hal-01162109, submitted.

[3] B. Alvarez-Samaniego and D. Lannes. Large time existence for 3d water-waves and asymptotics. *Inventiones mathematicae*, 171(3):485–541, 2008.

[4] E. Audusse, F. Bouchut, M.-O. Bristeau, R. Klein, and B. Perthame. A fast and stable well-balanced scheme with hydrostatic reconstruction for shallow water flows. *SIAM Journal on Scientific Computing*, 25(6):2050–2065, 2004.

[5] E. Audusse, F. Bouchut, M.-O. Bristeau, R. Klein, and B. Perthame. A fast and stable well-balanced scheme with hydrostatic reconstruction for shallow water flows. *SIAM J. Sci. Comput.*, 25(6):2050–2065, 2004.

[6] E. Barthélemy. Nonlinear shallow water theories for coastal waves. *Surveys in Geophysics*, 25(3-4):315–337, 2004.

[7] D. J. Bayraktar and S. L. Beji. A new numerical scheme for improved businnesque equations with surface pressure. In *Sustainable Maritime Transportation and Exploitation of Sea Resources*, volume 847, pages 847–854. ROUTLEDGE in association with GSE Research, 2011.

[8] S. Beji and K. Nadaoka. A formal derivation and numerical modelling of the improved boussinesq equations for varying depth. *Ocean Engineering*, 23(8):691–704, 1996.

[9] T. Belytschko, W. K. Liu, B. Moran, and K. Elkhodary. *Nonlinear finite elements for continua and structures.* John wiley & sons, 2013.

[10] T. B. Benjamin. The stability of solitary waves. *Proceedings of the Royal Society of London. A. Mathematical and Physical Sciences*, 328(1573):153–183, 1972.

[11] V. Berdichevsky. *Variational principles of continuum mechanics: I. Fundamentals*. Springer Science & Business Media, 2009.

[12] J. L. Bona, T. B. Benjamin, and J. J. Mahony. Model equations for long waves in nonlinear dispersive systems. *Philos. Trans. Royal Soc. London Series A*, 272:47–78, 1972.

[13] J. L. Bona, M. Chen, and J.-C. Saut. Boussinesq equations and other systems for small-amplitude long waves in nonlinear dispersive media. i: Derivation and linear theory. *Journal of Nonlinear Science*, 12(4), 2002.

[14] P. Bonneton, F. Chazel, D. Lannes, F. Marche, and M. Tissier. A splitting approach for the fully nonlinear and weakly dispersive Green–Naghdi model. *Journal of Computational Physics*, 230(4):1479–1498, 2011.

[15] C. Bourdarias, M. Ersoy, and S. Gerbi. A mathematical model for unsteady mixed flows in closed water pipes. *Science China Mathematics*, 55(2):221–244, Feb. 2012.

[16] C. Bourdarias, S. Gerbi, and R. Lteif. A numerical scheme for an improved Green–Naghdi model in the Camassa–Holm regime for the propagation of internal waves. *Computers & Fluids*, 156:283–304, 2017.

[17] J. Boussinesq. Théorie de l'intumescence liquide appelée onde solitaire ou de translation se propageant dans un canal rectangulaire. *Comptes Rendus Acad. Sci (Paris)*, 72:755–759, 1871.

[18] J. V. Boussinesq. Théorie générale des mouvements qui sont propagés dans un canal rectangulaire horizontal. *CR Acad. Sci. Paris*, 73:256–260, 1871.

[19] M.-O. Bristeau, N. Goutal, and J. Sainte-Marie. Numerical simulations of a non-hydrostatic shallow water model. *Computers & fluids*, 47(1):51–64, 2011.

[20] M.-O. Bristeau, A. Mangeney, J. Sainte-Marie, and N. Seguin. An energy-consistent depth-averaged Euler system: derivation and properties. *Discrete and Continuous Dynamical Systems - Series B*, 20(4):961–988, 2015.

[21] M. Brocchini. A reasoned overview on boussinesq-type models: the interplay between physics, mathematics and numerics. *Proceedings of the Royal Society A: Mathematical, Physical and Engineering Sciences*, 469(2160):20130496, 2013.

[22] R. Camassa and D. D. Holm. An integrable shallow water equation with peaked solitons. *Physical Review Letters*, 71(11):1661, 1993.

[23] L. Caudron. Contribution à l'étude des ondes de favre. Technical report, Technical Report HC. 032-E230, Laboratoire National d'Hydraulique . . . , 1968.

[24] F. Chazel, D. Lannes, and F. Marche. Numerical simulation of strongly nonlinear and dispersive waves using a Green–Naghdi model. *Journal of Scientific Computing*, 48(1-3):105–116, 2011.

[25] R. Cienfuegos, E. Barthélemy, and P. Bonneton. A fourth-order compact finite volume scheme for fully nonlinear and weakly dispersive boussinesq-type equations. part ii: boundary conditions and validation. *International Journal for Numerical Methods in Fluids*, 53(9):1423–1455, 2007.

[26] D. Clamond and D. Dutykh. Practical use of variational principles for modeling water waves. *Physica D: Nonlinear Phenomena*, 241(1):25–36, 2012.

[27] D. Clamond, D. Dutykh, and D. Mitsotakis. Conservative modified serre–Green–Naghdi equations with improved dispersion characteristics. *Communications in Nonlinear Science and Numerical Simulation*, 45:245–257, 2017.

[28] W. Craig. An existence theory for water waves and the boussinesq and korteweg-devries scaling limits. *Communications in Partial Differential Equations*, 10(8):787–1003, 1985.

[29] W. Craig, D. Lannes, and C. Sulem. Water waves over a rough bottom in the shallow water regime. *Annales de l'Institut Henri Poincaré (C) Non Linear Analysis*, 29(2):233–259, 2012.

[30] A. D. Craik. The origins of water wave theory. *Annual review of fluid mechanics*, 36, 2004.

[31] A.-J.-C. B. de Saint-Venant. Théorie du mouvement non-permanent des eaux, avec application aux crues des rivières at à l'introduction des marées dans leur lit. *Comptes rendus hebdomadaires des séances de l'Académie des sciences*, 73:147–154, 1871.

[32] M. A. Debyaoui and M. Ersoy. A Generalised Serre-Green-Naghdi equations for variable rectangular open channel hydraulics and its finite volume approximation. May 2020. working paper or preprint.

[33] M. A. Debyaoui and M. Ersoy. Generalised Serre–Green–Naghdi equations for open channel and for natural river hydraulics, issn = 18758576, 09217134. *Asymptotic Analysis*, page 1–27, Oct. 2020.

[34] A. Decoene, L. Bonaventura, E. Miglio, and F. Saleri. Asymptotic derivation of the section-averaged shallow water equations for natural river hydraulics. *Mathematical Models and Methods in Applied Sciences*, 19(03):387–417, 2009.

[35] M. W. Dingemans. *Water wave propagation over uneven bottoms*, volume 13. World Scientific, 1997.

[36] A. Duran and F. Marche. Discontinuous-galerkin discretization of a new class of Green-Naghdi equations. *Communications in Computational Physics*, 17(3):721–760, 2015.

[37] D. Dutykh and D. Clamond. Modified shallow water equations for significantly varying bottoms. *arXiv preprint arXiv:1202.6542*, 2012.

[38] M. Ersoy. *Modeling, mathematical and numerical analysis of various compressible or incompressible flows in thin layer*. Theses, Université de Savoie, Sept. 2010.

[39] M. Ersoy. Dimension reduction for incompressible pipe and open channel flow including friction. In *Conference Applications of Mathematics 2015, in honor of the 90th birthday of Ivo Babuška and 85th birthday of Milan Práger and Emil*

Vitásek , pages 17–33, Prague, France, Nov. 2015. J. Brandts and S. Korotov and M. Krizek and K. Segeth and J. Sistek and T. Vejchodsky.

[40] M. Ersoy, O. Lakkis, and P. Townsend. A Saint-Venant shallow water model for overland flows with precipitation and recharge. working paper or preprint, July 2016.

[41] C. Escalante Sanchez, E. D. Fernandez-Nieto, T. Morales de Luna, Y. Penel, and J. Sainte-Marie. Numerical simulations of Serre – Green-Naghdi type models for dispersive free surface flows. 2019.

[42] M. Esteves, X. Faucher, S. Galle, and M. Vauclin. Overland flow and infiltration modelling for small plots during unsteady rain: numerical results versus observed values. *Journal of hydrology*, 228(3):265–282, 2000.

[43] N. Favrie and S. Gavrilyuk. A rapid numerical method for solving serre–Green–Naghdi equations describing long free surface gravity waves. *Nonlinearity*, 30(7):2718, 2017.

[44] Z. I. Fedotova, G. S. Khakimzyanov, and D. Dutykh. Energy equation for certain approximate models of long-wave hydrodynamics. *Russian Journal of Numerical Analysis and Mathematical Modelling*, 29(3):167–178, 2014.

[45] A. G. Filippini, S. Bellec, M. Colin, and M. Ricchiuto. On the nonlinear behaviour of boussinesq type models: Amplitude-velocity vs amplitude-flux forms. *Coastal Engineering*, 99:109–123, 2015.

[46] J.-F. Gerbeau and B. Perthame. *Derivation of viscous Saint-Venant system for laminar shallow water; numerical validation*. PhD thesis, INRIA, 2000.

[47] J.-F. Gerbeau and B. Perthame. Derivation of viscous Saint-Venant system for laminar shallow water; numerical validation. *Discrete Cont. Dyn. Syst. Ser. B*, 1(1):89–102, 2001.

[48] N. Gouta and F. Maurel. A finite volume solver for 1d shallow-water equations applied to an actual river. *International Journal for Numerical Methods in Fluids*, 38(1):1–19, 2002.

[49] R. Grace and P. S. Eagleson. The modeling of overland flow. *Water Resources Research*, 2(3):393–403, 1966.

[50] A. E. Green and P. M. Naghdi. A derivation of equations for wave propagation in water of variable depth. *Journal of Fluid Mechanics*, 78(02):237–246, 1976.

[51] M. E. Gurtin. *An introduction to continuum mechanics*, volume 158. Academic press, 1982.

[52] S. Israwi. Large time existence for 1d Green-Naghdi equations. *Nonlinear Analysis: Theory, Methods & Applications*, 74(1):81–93, 2011.

[53] T. Kano and T. Nishida. A mathematical justification for korteweg-de vries equation and boussinesq equation of water surface waves. *Osaka Journal of Mathematics*, 23(2):389–413, 1986.

[54] T. Kano, T. Nishida, et al. Sur les ondes de surface de l'eau avec une justification mathématique des équations des ondes en eau peu profonde. *Journal of Mathematics of Kyoto University*, 19(2):335–370, 1979.

[55] D. J. Korteweg and G. De Vries. Xli. on the change of form of long waves advancing in a rectangular canal, and on a new type of long stationary waves. *The London, Edinburgh, and Dublin Philosophical Magazine and Journal of Science*, 39(240):422–443, 1895.

[56] J. L. Lagrange. *Mécanique analytique*, volume 1. Mallet-Bachelier, 1853.

[57] U. Langer and W. Queck. On the convergence factor of uzawa's algorithm. *Journal of Computational and Applied Mathematics*, 15:191–202, 1986.

[58] D. Lannes. Well-posedness of the water-waves equations. *Journal of the American Mathematical Society*, 18(3):605–654, 2005.

[59] D. Lannes. *The water waves problem: mathematical analysis and asymptotics*, volume 188. American Mathematical Soc., 2013.

[60] D. Lannes and P. Bonneton. Derivation of asymptotic two-dimensional time-dependent equations for surface water wave propagation. *Physics of Fluids (1994-present)*, 21(1):016601, 2009.

[61] D. Lannes and F. Marche. A new class of fully nonlinear and weakly dispersive Green–Naghdi models for efficient 2d simulations. *Journal of Computational Physics*, 282:238–268, 2015.

[62] D. Lannes and F. Marche. Nonlinear wave–current interactions in shallow water. *Studies in applied mathematics*, 136(4):382–423, 2016.

[63] O. Le Métayer, S. Gavrilyuk, and S. Hank. A numerical scheme for the Green–Naghdi model. *Journal of Computational Physics*, 229(6):2034–2045, 2010.

[64] M. Li, P. Guyenne, F. Li, and L. Xu. High order well-balanced CDG-FE methods for shallow water waves by a Green-Naghdi model. *Journal of Comutational Physics*, 257:169–192, 2014.

[65] Y. A. Li. A shallow-water approximation to the full water wave problem. *Communications on Pure and Applied Mathematics: A Journal Issued by the Courant Institute of Mathematical Sciences*, 59(9):1225–1285, 2006.

[66] K. Liu and C. C. Mei. Effects of wave-induced friction on a muddy seabed modelled as a bingham-plastic fluid. *Journal of coastal research*, pages 777–789, 1989.

[67] J. Luke. A variational principle for a fluid with a free surface. *Journal of Fluid Mechanics*, 27(02):395–397, 1967.

[68] P. A. Madsen, R. Murray, and O. R. Sørensen. A new form of the boussinesq equations with improved linear dispersion characteristics. *Coastal engineering*, 15(4):371–388, 1991.

[69] P. A. Madsen and O. R. Sørensen. A new form of the boussinesq equations with improved linear dispersion characteristics. part 2. a slowly-varying bathymetry. *Coastal engineering*, 18(3-4):183–204, 1992.

[70] R. Murray et al. Short wave modelling using new equations of boussinesq type. In *Ninth Australasian Conference on Coastal and Ocean Engineering, 1989: Preprints of Papers*, page 332. Institution of Engineers, Australia, 1989.

[71] O. Nwogu. Alternative form of boussinesq equations for nearshore wave propagation. *Journal of waterway, port, coastal, and ocean engineering*, 119(6):618–638, 1993.

[72] L. Ovsjannikov. Cauchy problem in a scale of banach spaces and its application to the shallow water theory justification. In *Applications of methods of functional analysis to problems in mechanics*, pages 426–437. Springer, 1976.

[73] L. V. Ovsjannikov. Shallow-water theory foundation. *Archives of Mechanics*, 26(3):407–422, 1974.

[74] M. Parisot. Entropy-satisfying scheme for a hierarchy of dispersive reduced models of free surface flow. *International Journal for Numerical Methods in Fluids*, 91(10):509–531, 2019.

[75] D. Peregrine. Calculations of the development of an undular bore. *Journal of Fluid Mechanics*, 25(2):321–330, 1966.

[76] D. Peregrine. Breaking waves on beaches. *Annu. Rev. Fluid Mech.*, 15:149–178, 1983.

[77] D. H. Peregrine. Long waves on a beach. *Journal of fluid mechanics*, 27(4):815–827, 1967.

[78] K. Pons. *Modélisation des tsunamis : Propagation et impact*. PhD thesis, Université de Toulon, 2018.

[79] D. Riabouchinsky. Sur un probleme de variation. *CR Acad. Sci. Paris*, 185:840–841, 1927.

[80] G. Richard and S. Gavrilyuk. Modelling turbulence generation in solitary waves on shear shallow water flows. *Journal of Fluid Mechanics*, 773:49–74, 2015.

[81] M. Rousseau, O. Cerdan, A. Ern, O. Le Maitre, and P. Sochala. Study of overland flow with uncertain infiltration using stochastic tools. *Advances in Water Resources*, 38:1–12, 2012.

[82] J. Sainte-Marie and M.-O. Bristeau. Derivation of a non-hydrostatic shallow water model; comparison with saint-venant and boussinesq systems. *arXiv preprint arXiv:0802.0250*, 2008.

[83] A. A. Samarskii and E. S. Nikolaev. *Numerical methods for grid equations II: Iterative methods*. Birkhäuser, 1989. Translated from Russian by Stephen G. Nash.

[84] H. A. Schäffer and P. A. Madsen. Further enhancements of boussinesq-type equations. *Coastal Engineering*, 26(1-2):1–14, 1995.

[85] F. J. Seabra-Santos, D. P. Renouard, and A. M. Temperville. Numerical and experimental study of the transformation of a solitary wave over a shelf or isolated obstacle. *Journal of Fluid Mechanics*, 176:117–134, 1987.

[86] F. Serre. Contribution à l'étude des écoulements permanents et variables dans les canaux. *La Houille Blanche*, (6):830–872, 1953.

[87] F. F. SIO. Notes on nearshore physical oceanography. 2015.

[88] J. J. Stoker. *Water waves: The mathematical theory with applications*, volume 36. John Wiley & Sons, 2011.

[89] C. H. Su and C. S. Gardner. Korteweg-de vries equation and generalizations. iii. derivation of the korteweg-de vries equation and burgers equation. *Journal of Mathematical Physics*, 10(3):536–539, 1969.

[90] Y. Tsuji, T. Yanuma, I. Murata, and C. Fujiwara. Tsunami ascending in rivers as an undular bore. *Natural Hazards*, 4(2-3):257–266, 1991.

[91] G. Wei, J. T. Kirby, S. T. Grilli, and R. Subramanya. A fully nonlinear boussinesq model for surface waves. part 1. highly nonlinear unsteady waves. *Journal of Fluid Mechanics*, 294:71–92, 1995.

[92] S. Weill, E. Mouche, and J. Patin. A generalized Richards equation for surface/subsurface flow modelling. *Journal of Hydrology*, 366(1):9–20, 2009.

[93] J. M. Witting. A unified model for the evolution nonlinear water waves. *Journal of Computational Physics*, 56(2):203–236, 1984.

[94] D. A. Woolhiser and J. A. Liggett. Unsteady, one-dimensional flow over a plane – the rising hydrograph. *Water Resources Research*, 3(3):753–771, 1967.

[95] S. Wu. Well-posedness in sobolev spaces of the full water wave problem in 2-d. *Inventiones mathematicae*, 130(1):39–72, 1997.

[96] S. Wu. Well-posedness in sobolev spaces of the full water wave problem in 3-d. *Journal of the American Mathematical Society*, 12(2):445–495, 1999.

[97] Y. Xing and C.-W. Shu. High order well-balanced finite volume weno schemes and discontinuous galerkin methods for a class of hyperbolic systems with source terms. *Journal of Computational Physics*, 214(2):567–598, 2006.

[98] H. Yosihara. Gravity waves on the free surface of an incompressible perfect fluid of finite depth. *Publications of the Research Institute for Mathematical Sciences*, 18(1):49–96, 1982.

[99] W. Zhang and T. W. Cundy. Modeling of two-dimensional overland flow. *Water Resources Research*, 25(9):2019–2035, 1989.

[100] J. G. Zhou, D. M. Causon, D. M. Ingram, and C. G. Mingham. Numerical solutions of the shallow water equations with discontinuous bed topography. *International journal for numerical methods in fluids*, 38(8):769–788, 2002.

Mohamed Ali DEBYAOUI
Laboratoire IMATH, Université de Toulon

Contribution à la modélisation mathématique et numérique pour des modèles d'écoulement non-linéaires dispersifs en eaux peu profondes

Résumé

Cette thèse porte sur la modélisation et l'analyse mathématique de modèles asymptotiques utilisés en océanographie et décrivant la propagation des ondes longues. L'objectif de cette thèse est de construire et de justifier de nouveaux modèles asymptotiques en tenant compte de la variation de la topographie et de la section transversale. Pour ce faire, plusieurs hypothèses sont formulées sur la profondeur de l'eau et les déformations de la section transversale. La première partie de cette thèse consiste à dériver et à étudier les caractéristiques linéaires de dispersion et de shoaling des modèles asymptotiques. Dans la deuxième partie, un modèle unidimensionnel des ondes longues moyenné par section, est développé. Des équations tridimensionnelles du mouvement des fluides non visqueux et incompressibles sont d'abord intégrées sur une section transversale du canal, ce qui donne les équations de type SGN. Le nouveau modèle est donc adéquat pour décrire des ondes fortement non linéaires et faiblement dispersives le long d'un canal de section transversale arbitraire et non uniforme. Plus précisément, le nouveau modèle étend le modèle de Saint-Venant moyenné par section et généralise les équations de Serre-Green-Naghdi à toute section. Ce nouveau modèle a été reformulé d'une manière plus appropriée pour la résolution numérique en conservant le même ordre de précision que l'original et en améliorant ses propriétés de dispersion. Enfin, nous présentons quelques simulations numériques pour étudier l'influence du changement de section sur la propagation d'une onde solitaire. La dernière partie de cette thèse est consacrée à la simulation numérique du modèle SGN avec une nouvelle reformulation.

Mots clés : Équations aux dérivées partielles, Modélisation mathématique des écoulements à surface libre, Écoulement en canal ouvert, Fluide incompressible, Analyse asymptotique, Lagrangien, Dispersif, Non-Linéaire, Volumes Finis, Saint-Venant, Boussinesq, Serre-Green-Naghdi.

Contribution to mathematical and numerical modeling for non-linear dispersive shallow water flow models

Abstract

This work focuses on the modeling and mathematical analysis of asymptotic models used in oceanography describing long wave propagation. This thesis aims to derive and justify new asymptotic models taking into account the variation in topography and cross-section. To do so, several hypotheses are formulated on water depth and cross-sectional deformations. The first part of this thesis consists in deriving and studying the linear dispersion and shoaling characteristics of the asymptotic models. In the second part, a one-dimensional model of section-averaged long waves is developed. Three-dimensional equations of motion of non-viscous and incompressible fluids are first integrated over a cross-section of the channel, resulting in the SGN-type equations. Therefore, the new model is adequate to describe fully non-linear and weakly dispersive waves along a channel of an arbitrary and non-uniform cross-section. Specifically, the new model extends the Saint-Venant model to cross-section mean and generalizes the Serre-Green-Naghdi equations to any cross-section. This new model has been reformulated in a way more appropriate for numerical resolution by maintaining the same order of accuracy as the original and improving its properties of dispersion. Finally, we present some numerical simulations to study the influence of the change of section on the propagation of a solitary wave. The last part of this thesis is devoted to the numerical simulation of the SGN model with a new reformulation.

Keywords: Partial differential equations, Mathematical modeling of free surface flows, Open channel flow, Incompressible Fluid, Asymptotic Analysis, Lagrangian, Dispersive, Non-Linear, Finit Volumes, Saint-Venant, Boussinesq, Serre-Green-Naghdi.